

# **Exploring Delta Amino Acids in the Design of New Peptide Foldamers and Biomaterials**

**A thesis  
Submitted in partial fulfillment of the requirements  
Of the degree of  
Doctor of Philosophy**

**By  
Rahi Masoom Reja  
(ID No. 20122029)**

**Research Supervisor: Prof. Hosahudya N. Gopi**



**Indian Institute of Science Education and Research, Pune**

**2019**

*Dedicated to*  
*Family, Friends and Teachers*



# **CERTIFICATE**

This is to certify that the work incorporated in the thesis entitled “**Exploring Delta Amino Acids in the Design of New Peptide Foldamers and Biomaterials**” submitted by **Rahi Masoom Reja (ID No. 20122029)** carried out by the candidate at the Indian Institute of Science Education and Research (IISER), Pune, under my supervision. The work presented here or any part of it has not been included in any other thesis submitted previously for the award of any degree or diploma from any other University or Institution.

Date:

**Prof. Hosahudya N. Gopi**

(Research Supervisor)

Professor, Department of Chemistry,  
IISER-Pune

Pune-411008, India

# **DECLARATION**

I declare that this written submission represents my ideas in my own words and where others' ideas have been included, I have adequately cited and referenced the original sources. I also declare that I have adhered to all principles of academic honesty and integrity and have not misrepresented or fabricated or falsified any idea/data/fact/source in my submission. I understand that violation of the above will be cause for disciplinary action by the Institute and can also evoke penal action from the sources which have thus not been properly cited or from whom proper permission has not been taken when needed.

Date:

**Rahi Masoom Reja**

**ID No. 20122029**

Research Fellow

Department of Chemistry, IISER-  
Pune

Pune-411008

## Acknowledgement

First I would like to thank my supervisor Prof. Hosahudya N. Gopi for his unconditional support throughout five years to conduct my research. He is prolific and brilliant chemist. He is by far the hardest working person I know. His commitment at work, punctuality, motivating students and constant support at their difficult times and many more qualities I always admire at. I am fortunate to work with him.

My sincere thanks to our present Director Prof. Jayant B. Udgaonkar and former Director Prof. K. N. Ganesh for providing excellent facilities and financial support during my research here at Indian Institute of Science Education and Research (IISER)-Pune. I am also thankful to the IISER-Pune for my five years research fellowship for PhD and two year fellowship during my MS times. Special thanks to Prof. Srinivas Hotha and Dr. Moneesha Fernandes for being my RAC committee members. Their valuable suggestions and critics always encouraged me to pursue in the right direction. I am highly grateful to Dr. Raghavendra Kikkeri for providing reference letters whenever I required. I would like to acknowledge Dr. Srinivasarao Raghothama and Gijo George from NMR Research Centre, Indian Institute of Science (IISc), Bangalore for building the NMR structure models, Dr. Anjali Jha from Agarkhar Research Institute (ARI), Pune for cell viability experiments, Prof. Claudia Steinem and Yeimar Portillo Castellano from Georg-August-University Göttingen, Germany for ion channel studies of cyclic peptides. I also thank Dr. Anjali Shiras and Mohsina Khan for cell image studies for Nanoscale paper. I am very much thankful to all chemistry faculties, technicians (Pooja, Swathi, Archana, Chinmay, Nitin, Deepali, Sandeep) and admin staff of IISER-Pune for their numerous support.

I am lucky to have wonderful junior and senior labmates. I would extend my sincere thanks to all of them. Dr. Anupam Bandyopadhyay, Dr. Sandip V. Jadhav and Dr. Schitanand M. Mali, Dr. Mothukuri Ganesh Kumar, Dr. Susheel Benke, Dr. Rajkumar Misra were seniors to me when I have joined in the group. During my MS time I have lucky to work with Dr. Sandip V. Jadhav and Dr. Rajkumar Misra and I learnt a lot from them. They are very helpful from the beginning of my Ph.D and I am lucky to have such colleagues. Vereesh and Puneeth are one of my best buddies to whom I always share my thoughts and they are highly motivated, hardworking. Anindita Adak, Sanjit, Sachin, Manjit, Panda, Saikat, Shouvik are really good and supportive in maintaining lab facilities and ambience of the lab. They are cheerful and full of

energy. I was highly impressed with their motivation and interest in science. We have got highly motivated undergraduate and project students Sreena, Vivek, Rajat, Abhijith, Sumeet, Ankita, Varsha, Mona, Nithun, Devendra and Manish to work in our lab as part of their summer internship or fifth year project, they keep joyful atmosphere in lab. Among them, the contribution from Sumeet, Sreena, Vivek and Rajat are great in my work of PhD. Our advisor is fortunate enough to have such enthusiastic and motivated students. Because of all these people all my five years in IISER passed just like few days.

From last five years, I am fortunate to have many good friends from IISER apart from my labmates. I thank my roommates Chetan. We have great time in two years stay at Hostel I during our MS times. I got to learn so many things from him. I am very fortunate to have all our Int-PhD -2012 batchmates Sukrut, Mukul, Chetan, Amogh, Jerrin, Hridya, Aditi, Sneha, Meghna, Abhishek, Ankita. Among them, I, Chetan, Sukrut and Mukul, all four have spent many quality times during dinner and movies. I would extend my thanks to Sahel, Somraj, Debajan, Rahul, Abdul Khuddus, Minaj, Sattwick, and seniors like Shyama, Maidul, Rejaul, Bijoy, Dhruvo, Biplab, Partha, Arunav, Chandramouli, Abhik, Madhan B, Prabhakar and many more. Further I would thank all chemistry department friends of IISER-Pune for their support and help.

I would also like to express my deepest gratitude to my family. My family has been encouraging, supportive and shown belief in me and my work. Without them I wouldn't have chance to be at IISER-Pune. My father is my role model in life. My mother and father made lot of sacrifices to raise me and my sister and brother. My elder brother and younger sister are the one who stood like a backbone to me. I never forget their support in my life time. I extend my thanks to my college teachers during my B.Sc times late Prof. Arunav Sen (AS Sir), Dr. Chandrakanta Banerjee (CKB Sir), Dr. Subhabrata Banerjee (SB Sir), Prabir Kumar Sen (PKS Sir), Dr. Arnab Halder and Dr. Chandan Adhikari who encouraged me throughout my carrier.

Finally I thank almighty Allah for giving me strength and courage to pursue what I would like to do in my life.

**Rahi Masoom Reja**

# Contents

---

Abbreviations.....	<b>i</b>
Abstract.....	<b>iv</b>
Publications.....	<b>v</b>

---

## **Chapter 1: General Introduction of Peptide Foldamers Composed of Unnatural Amino Acids**

---

1.1 Introduction.....	2
1.2. Protein Secondary Structures .....	2
1.3. Mimicking of Protein Secondary Structures.....	5
1.4. $\beta$ -Peptide Foldamers.....	5
1.5. $\gamma$ -Peptide Foldamers.....	8
1.6. Heterogeneous Foldamers Containing $\beta$ - and $\gamma$ -Amino Acids.....	10
1.7. Biologically Active Peptide Foldamers Composed of $\beta$ - and $\gamma$ - Amino Acids.....	13
1.8. Supramolecular Assemblies from Peptides Composed of $\beta$ - and $\gamma$ - Amino Acids.....	14
1.9. Foldamers Containing $\delta$ - Amino Acids.....	15
1.10. References.....	16

# Chapter 2: Engineering $\beta$ -Hairpin with Flexible $\delta$ -Amino Acids for Disruption of $\beta$ -Amyloid Aggregation

---

2.1 Introduction.....	24
2.2. Design of $\beta$ -Turns.....	25
2.3. Aim and Rationale of the Present Work .....	28
2.4. Results and Discussion.....	29
2.4.1. Design and Synthesis.....	29
2.4.2. ORTEP Diagram of Compound <b>3</b> and Peptide <b>P2</b> .....	30
2.4.3. Conformational Analysis of Peptide <b>P1</b> .....	32
2.4.4. Conformational Analysis of Peptide <b>P2</b> .....	39
2.4.5. Conformational Analysis of Peptide <b>P3</b> .....	44
2.4.6. Peptidomimetics as $\beta$ -Amyloid Aggregation Disrupting Agent.....	51
2.4.7. Thioflavin T (ThT) Fluorescence Assay.....	52
2.4.8. Transmission Electron Microscopy (TEM) Studies.....	53
2.4.9. Cell Viability Studies using MTT Assay.....	55
2.4.10. Two Dimensional $^{15}\text{N}$ - $^1\text{H}$ HSQC NMR Studies of Amyloid Disruption by Peptide <b>P3</b> .....	56
2.5. Conclusions.....	58
2.6. Experimental Section.....	59
2.6.1. Materials and Methods.....	59
2.6.2. NMR Spectroscopy.....	59



2.6.3. Synthetic Procedures.....	59
2.6.3.1. Synthesis of <i>N</i> -Boc- $\beta$ (O)- $\delta^5$ - <sup>D</sup> Pro-O <sup>t</sup> Bu.....	59
2.6.3.2. Synthesis of <i>N</i> -Fmoc- $\beta$ (O)- $\delta^5$ - <sup>D</sup> Pro-OH.....	60
2.6.3.3. Synthesis of ( <i>E</i> )- $\alpha,\beta$ -unsaturated- $\gamma^4$ -Amino Acid.....	61
2.6.3.4. Synthesis of Tripeptide BocNH-Val-Leu-Val-OH.....	61
2.6.3.5. Synthesis of Peptide <b>P1</b> .....	63
2.6.3.6. Solid Phase Synthesis of Peptides <b>P2</b> and <b>P3</b> .....	65
2.6.4. Crystallographic Information.....	65
2.6.5. Two dimensional NMR Analysis of Peptides <b>P1</b> and <b>P3</b> .....	66
2.6.6. $\beta$ -Amyloid Disruption Study.....	68
2.6.6.1. Preparation of the Soluble Aggregates of A $\beta_{1-42}$ .....	68
2.6.6.2. Thioflavin T (ThT)-Fluorescence-Monitored Kinetics of Aggregation.....	68
2.6.6.3. Disruption of the Disulfide Linkage of the Peptide <b>P3</b> .....	69
2.6.6.4. Transmission Electron Microscopy (TEM) Studies.....	69
2.6.6.5. Cell Viability Assay.....	69
2.6.6.6. Two Dimensional <sup>1</sup> H- <sup>15</sup> N HSQC NMR study of Binding of Peptide <b>P3</b> with A $\beta_{1-42}$ .....	70
2.7 Characterization Data of Synthesized Compounds and Peptides <b>P1</b> - <b>P3</b> .....	71
2.8. References.....	72
2.9. Appendix II: Characterization Data of Synthesized Compounds and Peptides <b>P1-P3</b> .....	78
2.9.1. <sup>1</sup> H and <sup>13</sup> C NMR Spectra.....	78

2.9.2. MALDI-TOF/TOF Mass Spectra.....	82
--	----

## Chapter 3: Impact of H-Bonding in Helices Composed of Flexible $\delta$ -Amino Acids

---

3.1. Introduction.....	87
3.2. Foldamers Containing Delta Amino Acids.....	87
3.3. Aim and Rationale of the Present Work.....	89
3.4. Results and Discussion.....	90
3.4.1. Design and Synthesis.....	90
3.4.2. ORTEP Diagram of Peptides <b>P1</b> , <b>P2</b> and <b>P4</b> .....	92
3.4.3. Conformational Analysis of Peptides <b>P1-P4</b> .....	95
3.4.5. Proteolytic Stability Studies of the Delta Amino Acids.....	113
3.5. Conclusions.....	115
3.6. Experimental Section.....	116
3.6.1. Materials and Methods.....	116
3.6.2. NMR Spectroscopy.....	116
3.6.3. Synthetic Procedures.....	116
3.6.3.1. Synthesis of <i>N</i> -Boc- $\beta$ (O)- $\delta^5$ Phe-O <sup>t</sup> Bu.....	116
3.6.3.2. Synthesis of the <i>N</i> -Fmoc- $\beta$ (O)- $\delta^5$ Phe-OH.....	117

3.6.3.3. Solid Phase Synthesis of Peptides <b>P1-P6</b> .....	118
3.6.4. Crystallographic Information of Peptides <b>P1, P2</b> and <b>P4</b> .....	119
3.6.5. Two Dimensional NMR Analysis of Peptide <b>P3</b> .....	120
3.6.6. Proteolytic Stability Studies of Peptides <b>P5</b> and <b>P6</b> .....	121
3.7. Characterization of Compounds.....	122
3. 8. References .....	123
3.9. Appendix III: Characterization Data of Synthesized Amino Acids and Peptides <b>P1-P6</b> .....	127
3.9.1. <sup>1</sup> H and <sup>13</sup> C NMR Spectra of Compounds.....	127
3. 9.2. High Resolution Mass Spectra (HRMS) of the Synthesized Amino Acids.....	131
3.9.3. MALDI-TOF/TOF Spectra of the Peptides <b>P1-P6</b> .....	135

## Chapter 4: Divergent Supramolecular Gelation of Backbone Modified Short Hybrid $\delta$ -Peptides

---

4.1. Introduction.....	141
4.2. Short Peptide Based Self Assembly.....	141
4.3. Diphenyl Alanine Based Peptide Self Assembly.....	142
4.4. Short Peptide Based Assembly Composed of Different Non Canonical Amino Acids.....	144
4. 5. Aim and Rationale of the Present Work.....	145

4.6. Results and Discussion.....	146
4.6.1. Design and Synthesis of Peptides <b>P1-P5</b> .....	146
4. 6.2. Gelation Study of Peptides <b>P1, P2</b> and <b>P4</b> .....	147
4.6.3. Morphology Study.....	148
4.6.4. Viscoelastic Property.....	150
4.6.5. FT-IR Spectroscopy Study.....	151
4.6.6. Contact Angle Measurement.....	152
4.6.7. Stimuli Responsive Properties of Organo and Hydrogels.....	154
4.6.8. Oil Spill Recovery by Organogel from Peptide <b>P4</b> .....	155
4.6.10. Biocompatibility Studies of the Peptide <b>P2</b> Hydrogel.....	156
4.7. Conclusions.....	158
4.8. Experimental Section.....	158
4.8.1. Materials and Methods.....	158
4.8.2. General Procedure for the Solution Phase Peptides ( <b>P1-P5</b> ) Synthesis.....	159
4.8.2.1. Synthesis of <i>N</i> -Boc- $\delta^5$ -Phe-OH.....	159
4.8.2.2. Synthesis of <i>N</i> -Boc- $\beta$ (O)- $\delta^5$ -Phe-O <sup>t</sup> Bu.....	159
4.8.2.3. Synthesis of Peptides <b>P1-P5</b> .....	160
4.8.3. Gelation Study of Peptides <b>P1, P2</b> and <b>P4</b> .....	160
4.8.4. Morphology Study of Peptides <b>P1, P2</b> and <b>P4</b> .....	161
4.8.5. Rheology Experiment.....	161

4.8.6. Oil Spill Recovery Experiment.....	161
4.8.7. Proteolytic Stability of Peptide <b>P2</b> .....	161
4.8.8. Effect of Hydrogel from Peptide <b>P2</b> on Cell Viability.....	162
4.9. Characterization of Amino Acids and Peptides <b>P1-P5</b> .....	162
4.10. References.....	166
4.11. Appendix IV: Characterization Data of Synthesized Amino Acids and Peptides <b>P1-P5</b> .....	170
4.11.1. <sup>1</sup> H and <sup>13</sup> C NMR Spectra.....	170
4.11.2. HRMS Spectra of Amino Acids and Peptides <b>P1-P5</b> .....	177

## **Chapter 5: Design and Synthesis of Novel Parallel $\delta$ -Peptide Macrocylces for Transmembrane Ion Channels**

---

5.1. Introduction.....	182
5.2. Design of the Cyclic Peptide Nanotubes (CPNs) form $\alpha$ -Amino Acids.....	183
5.3. Design of Cyclic Peptide Nanotubes (CPNs) from Non-Canonical Amino Acids.....	184
5. 4. Application of Self-Assembled Cyclic Peptide Nanotubes (CPNs).....	185
5.5. Aim and Rationale of the Present Work.....	187
5.6. Results and Discussion.....	188

5.6.1. Design and Synthesis.....	188
5.6.2. ORTEP Diagram of BocNH- $\beta$ (O)- $\delta^5$ -Val-- $\beta$ (O)- $\delta^5$ -Leu-OH and Peptide <b>CP1</b> .....	190
5.6.3. Conformational Analysis of Peptides <b>CP1-CP3</b> .....	191
5.6.4. Vesicle Leakage Assay for the Study of Transmembrane Activity of the Peptides <b>CP1</b> and <b>CP2</b> .....	195
5.7. Conclusions.....	196
5.8. Experimental Section.....	197
5.8.1. Materials and Methods.....	197
5.8.2. NMR Spectroscopy.....	197
5.8.3. General Procedure for the Solution Phase Peptides ( <b>CP1-CP3</b> ) Synthesis.....	198
5.8.3.1. Synthesis of <i>N</i> -Boc- $\delta^5$ -Leu-OH.....	198
5.8.3.2. Synthesis of <i>N</i> -Boc- $\beta$ (O)- $\delta^5$ -Phe-O <sup>t</sup> Bu.....	198
5.8.3.3. Synthesis of Cyclic Peptides <b>CP1-CP3</b> .....	199
5.8.4. Crystallographic Information.....	201
5.8.5. Preparation of Large Unilamellar Vesicles (LUVs).....	201
5.8.6. Procedure for the Vesicle Leakage Assay.....	202
5.9. Characterization of Synthesized Amino Acids and Peptides <b>CP1-CP3</b> .....	203
5.10. References.....	206

5.11. Appendix V: Characterization Data of Synthesized Amino Acids and Peptides <b>CP1-CP3</b> .....	209
5.11.1. <sup>1</sup> H and <sup>13</sup> C NMR Spectra of Compounds.....	209
5.11.2. HRMS and MALDI-TOF/TOF Spectra of Amino Acids and Peptides <b>CP1-CP3</b> .....	215
<hr/>	
Permission for Reuse of Figures from Journals .....	221

# Abbreviations

Ac<sub>2</sub>O = Acetic anhydride

ACN = Acetonitrile

AcOH = Acetic acid

Aib =  $\alpha$ -Amino isobutyric acid

A $\beta$ <sub>1-42</sub> = Amyloid Beta Peptide (1-42)

aq. = Aqueous

Bn = Benzyl

Boc = *tert*-Butoxycarbonyl

(Boc)<sub>2</sub>O = Boc anhydride

<sup>t</sup>Bu = tertiary Butyl

$\beta$ (O)- $\delta^5$ -Amino Acids =  $\beta$ -Oxy- $\delta^5$ -Amino Acids

Calcd. = Calculated

Cbz = Benzyloxycarbonyl

Cbz-Cl = Benzyl chloroformate

CCDC no. = Cambridge Crystallographic Data Centre number

CD = Circular Dichroism

COSY = **C**orrelation **S**pectroscop**Y**

CIF = Crystallographic Information File

CP = Cyclic Peptides

d $\gamma$  = dehydro gamma

DCM = Dichloromethane

DIEA = Diisopropylethyl Amine

DMF = Dimethylformamide



DMSO = Dimethylsulfoxide

EDC.HCl = N-(3-Dimethylaminopropyl)-N'-ethylcarbodiimide hydrochloride

EtOH = Ethanol

Et = Ethyl

EtOAc = Ethyl acetate

Fmoc = 9-Fluorenylmethoxycarbonyl

Fmoc-OSu = N-(9-Fluorenylmethoxycarbonyloxy) succinimide

g = gram

h = hours

HBTU = 2-(1H-benzotriazol-1-yl)-1, 1, 3, 3-tetramethyluronium hexafluorophosphate

H-bond = Hydrogen bond

HOBT = Hydroxybenzotriazole

HCl = Hydrochloric acid

HPTS = 8-Hydroxypyrene-1,3,6-Trisulfonic Acid

LAH = Lithium Aluminium Hydride

LUV = Large Unilammellar Vesicles

M = Molar

MALDI-TOF/TOF = Matrix-Assisted Laser Desorption/Ionization-Time of Flight

MBHA = Methyl bezydrylamine

Me = Methyl

MeOH = Methanol

mg = Milligram

min = Minutes

$\mu$ L = Micro liter

mL = Milliliter

mM = Millimolar

mmol = millimoles

MS = Mass Spectroscopy

N = Normal

NHS = N-hydroxysuccinimide

NMP = N-methyl pyrrolidone

NMR = Nuclear Magnetic Resonance

NOE = Nuclear Overhauser Effect

ORTEP = Oak Ridge Thermal-Ellipsoid Plot Program

PG = Protecting Group

ppm = Parts per million

Py = Pyridine

R<sub>f</sub> = Retention factor

R<sub>t</sub> = Retention time

ROESY = **R**otating-frame nuclear **O**verhauser**E**ffect correlation**S**pectroscop**Y**

RP- HPLC = Reversed Phase-High Performance Liquid Chromatography

RT = Room Temperature

FE-SEM = Field Emission Scanning Electronic Microscopy

TFA = Trifluoroacetic acid

THF = Tetrahydrofuran

TOCSY = **T**Otal**C**orrelation**S**pectroscop**Y**

TEM = Transmission Electron Microscopy

## Abstract

Over the last two decades, backbone homologated  $\alpha$ -amino acids such as  $\beta$ - and  $\gamma$ -amino acids have been extensively explored as building blocks to design various types of functional foldamers. In contrast to the  $\beta$ - and  $\gamma$ -peptides, foldamers constituted with  $\delta$ -amino acids have been less explored. This is probably due to the difficulties in the synthesis of enantiopure  $\delta$ -amino acids as well as issues related to the solubility of  $\delta$ -peptide foldamers. Instructively,  $\delta$ -amino acids can be used as mimics of  $\alpha$ -dipeptides. In this context, we have designed new  $\delta$ -amino acids encompassing “O” atom in the backbone,  $\beta(\text{O})$ - $\delta^5$ -amino acids, and explored their utility in the design of novel foldamers and biomaterials. In contrast to the  $\delta$ -peptides with complete carbon backbone,  $\delta$ -peptides with  $\beta(\text{O})$ - $\delta^5$ -amino acids have showed better solubility in organic solvents. We have utilized these  $\delta$ -amino acids to induce single residue  $\beta$ -turns. We have examined solution and single crystal conformations of  $\beta$ -hairpin consisting of single residue  $\delta$ -amino acid  $\beta$ -turns. Further, we have demonstrated the disruption of  $\beta$ -amyloid aggregation through designed amphiphilic  $\beta$ -hairpin models. The A $\beta$ -amyloid disruption was studied in solution using various spectroscopic and microscopic techniques. Along with reverse turns, we have also utilized the  $\delta$ -amino acids to construct hybrid peptide helical foldamers. As the amino acid is mimic of  $\alpha$ -dipeptide, we further examined the proteolytic stability of peptides composed these amino acids against various proteases. Furthermore, we have utilized these  $\delta$ -amino acids to construct a new class of cyclic peptide macrocycles. Instructively, some of these macrocycles self-assembled into polar tubular assembly in single crystals. We have examined the transmembrane ion channel activity of these cyclic peptides using vesicle leakage assay and their electrophysiological characterization in the transmembrane ion channels are under investigation. Along with the utilization of these amino acids in the peptide design, we have also examined the supramolecular gelation properties of short hybrid peptides composed of backbone modified  $\delta$ -amino acids. Overall, the basic conformational properties of  $\delta$ -amino acids presented in this thesis can be further utilized to construct new functional foldamers as well as functional biomaterials.

# Publications

1. Structural Investigation of Hybrid Peptide Foldamers Composed of  $\alpha$ -Dipeptide Equivalent  $\beta$ -Oxy- $\delta^5$ -amino Acids. **Rahi M. Reja**, Vivek Kumar, Gijo George, Rajat Patel, DRGKoppalu R. Puneeth Kumar, Srinivasarao Raghothama and Hosahudya N. Gopi. *Chem.-Eur. J.* Accepted Article **2020** (10.1002/chem.201904780)
2. Divergent Supramolecular Gelation of Backbone Modified Short Hybrid  $\delta$ -Peptides. **Rahi M. Reja**, Rajat Patel, Vivek Kumar, Anjali Jha and Hosahudya N. Gopi. *Biomacromolecules* **2019**, *20*, 1254-1262.
3. Engineering Two-Helix Motifs through NDI Linker: A Modular Approach for Charge Transferable Conductive Foldamers Design. **Rahi M. Reja**, Rajkumar Misra and Hosahudya N. Gopi. *ChemNanoMat*. **2019**, *5*, 51–54.
4. Chemoselective Nitrile Oxide–Alkyne 1,3-Dipolar Cycloaddition Reactions from Nitroalkane-Tethered Peptides. **Rahi M. Reja**, Sreena Sunny and Hosahudya N. Gopi. *Org. Lett.* **2017**, *19*, 3572-3575.
5. pH sensitive coiled coils: a strategy for enhanced liposomal drug delivery. **Rahi M. Reja**, Mohsina Khan, Sumeet K Singh, Rajkumar Misra, Anjali Shiras and Hosahudya N. Gopi. *Nanoscale* **2016**, *8*, 5139–5145.
6. Rajkumar Misra, Gijo George, **Rahi M. Reja**, Sanjit Dey, Srinivasarao Raghothama and Hosahudya N. Gopi. Structural Insight into Hybrid Peptide  $\epsilon$ -Helices. *Chem. Commun.* **2020**, *56*, 2171-2173.
7. Exploring structural features of folded peptide architectures in the construction of nanomaterials. Rajkumar Misra, **Rahi M. Reja**, Lagumaddepalli V. Narendra, Gijo George, Srinivasarao Raghothama and Hosahudya N. Gopi. *Chem. Commun.* **2016**, *52*, 9597-9600.
8. Artificial  $\beta$ -Double Helices from Achiral  $\gamma$ -Peptides. Rajkumar Misra, Sanjit Dey, **Rahi M. Reja** and Hosahudya N. Gopi. *Angew. Chem. Int. Ed.* **2018**, *57*, 1057–1061.
9.  $\gamma$ -Amino acid mutated  $\alpha$ -coiled coils as mild thermal triggers for liposome delivery. Sandip V. Jadhav, Sumeet K. Singh, **Rahi M. Reja** and Hosahudya N. Gopi. *Chem. Commun.* **2013**, *49*, 11065-11067.
10. Engineering  $\beta$ -Hairpin with Flexible  $\delta$ -Amino Acids for Disruption of  $\beta$ -Amyloid Aggregation. **Rahi M. Reja**, Vivek Kumar, Gijo George, Anjali Jha, Srinivasarao Raghothama and Hosahudya N. Gopi. *Manuscript under preparation*.

## *Chapter 1*

# **General Introduction of Peptide Foldamers Composed of Unnatural Amino Acids**

## 1.1. Introduction

Proteins are the most important bio-molecules in all living system.<sup>1</sup> With the help of the three dimensional structure, proteins carry out all biologically important events in the living system.<sup>2</sup> Using 20 ribosomal amino acids, nature has made the myriad of proteins with definite 3D structures and functions. Protein structures are mainly described at four levels as shown in Figure 1.1. The primary structure represents the sequence of the amino acids. The primary structure then folds into definite secondary structures. The secondary structures can be further

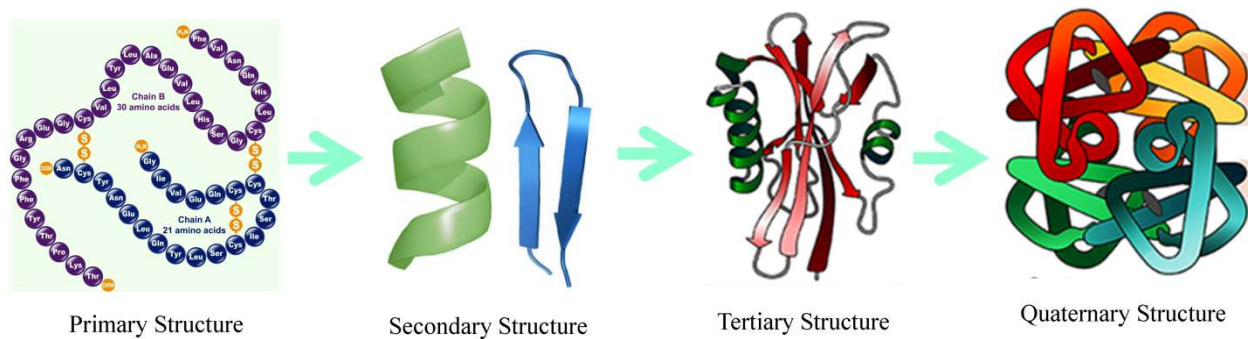


**Figure 1.1:** Four levels of protein structure (tertiary structure PDB code 1OYH and quaternary structure represents hemoglobin structure).

classified into  $\beta$ -sheets, helices, and turns. These protein secondary structures are further connected by the loosely structured loops that leads to the super secondary structures such as  $\beta$ -hairpins ( $\beta$ - $\beta$  motifs), coiled-coils, helix-turn-helix,  $\beta$ - $\alpha$ - $\beta$  motifs,  $\beta$ -meanders, Greek key motifs etc. Tertiary structure of protein explains the overall structure of single polypeptide chain resulting from interactions of amino acid side chains and secondary structural elements. The quaternary structure defines the spatial arrangement of two or more polypeptide chains in specific oligomer complex which is accompanied by a variety of non-covalent interactions and disulfide cross linkages. Protein secondary structures play a vital role in overall protein folding and peptide based drug design.

## 1.2. Protein Secondary Structures

Protein secondary structures are classified mainly into helices,  $\beta$ -sheets and reverse turns. In their pioneering work by Linus Pauling and colleagues first described the  $\alpha$ -helix and  $\beta$ -sheet

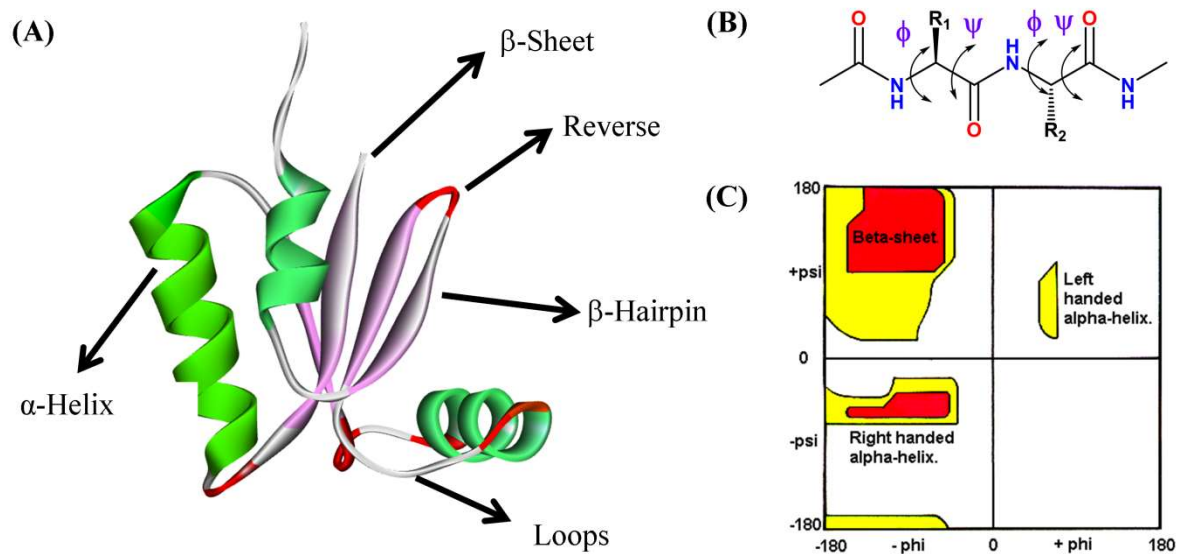


**Figure 1.2:** (A) Different protein secondary structural elements shown in a protein by ribbon model (PDB code: 1H75) (B) Torsional angles  $\phi$  and  $\psi$  on peptide backbone composed of  $\alpha$ -amino acids (C) Classical Ramachandran plot and the allowed region for torsional angles of different secondary structures.

structures.<sup>2</sup> These secondary structures are characterized by the well-defined pattern of hydrogen bond pseudocycles between the main chain NH and CO groups. The loop region which connects two adjacent anti-parallel  $\beta$ -strands are called as reverse turns. In their seminal work, G. N. Ramachandran and colleagues<sup>3</sup> described the sterically allowed stable conformations of polypeptide secondary structures using two degrees of torsional freedom  $\phi$  and  $\psi$  (Figure 1.2C). Brief descriptions regarding secondary structures are given below.

**Helices:** Based on the involvement of H-bond pseudocycles and number of residues per turn, helices are mainly classified into four distinct categories such as  $2.2_7$  ( $\gamma$ -helix),  $3_{10}$ ,  $3.6_{13}$  ( $\alpha$ -helix) and  $4.4_{16}$  ( $\pi$ )-helices. Among them,  $\alpha$ -helix is most predominant in proteins. In 1951, Linus Pauling proposed the  $\alpha$ -helix structure, which consists of 3.6 residues per turn and 13-atoms are involved in the H-bond pseudocycle. General nomenclature of the  $\alpha$ -helix is  $3.6_{13}$ -P-helix with average torsion angles  $\phi = -60^\circ$  and  $\psi = -45^\circ$ . Unlike  $\alpha$ -helix,  $3_{10}$ -helix is rarely present in proteins. It mainly exists at the terminal of the  $\alpha$ -helix in the protein structures. The average  $\phi$  and  $\psi$  values of  $3_{10}$ -P-helix are  $-49^\circ$  and  $-26^\circ$  respectively. The  $3_{10}$ -helix contains three residues per turn and

10-atom H-bond pseudocycles. Similarly,  $\pi$ -helix is denoted by  $4.4_{16}$ -P-helix ( $\phi = -55^\circ$ ,  $\psi = -70^\circ$ ) and  $\gamma$ -helix as  $2.2_7$  helix ( $\phi = -70^\circ$ ,  $\psi = 70^\circ$ ).

**$\beta$ -Sheets:**  $\beta$ -Pleated sheets are the second major structural elements found in proteins. They are generally 5 to 10 residues long with fully extended conformation. The torsion angles of  $\phi$  and  $\psi$  values are found to be within the broad structurally allowed region in the upper left quadrant of Ramachandran Map.<sup>3</sup> The first  $\beta$ -sheet structure was proposed by William Astbury in 1930.<sup>4</sup> However, in 1951, Linus Pauling and Robert Corey refined the  $\beta$ -sheet structure.<sup>5</sup> Depending upon the directionality of the  $\beta$ -strands arranged in  $\beta$ -pleated sheets, they are classified into (i) parallel  $\beta$ -sheets and (ii) anti-parallel  $\beta$ -sheets (Figure 1.3).  $\beta$ -Sheets usually exhibit a right-handed twist, which is mainly favored by the intrastrand non-bonded interactions and interstrand geometric constrain. But at the tertiary structure of proteins, the  $\beta$ -sheets are oriented  $\sim 30^\circ$  angles to each other in their  $\beta$ -sheet structure.

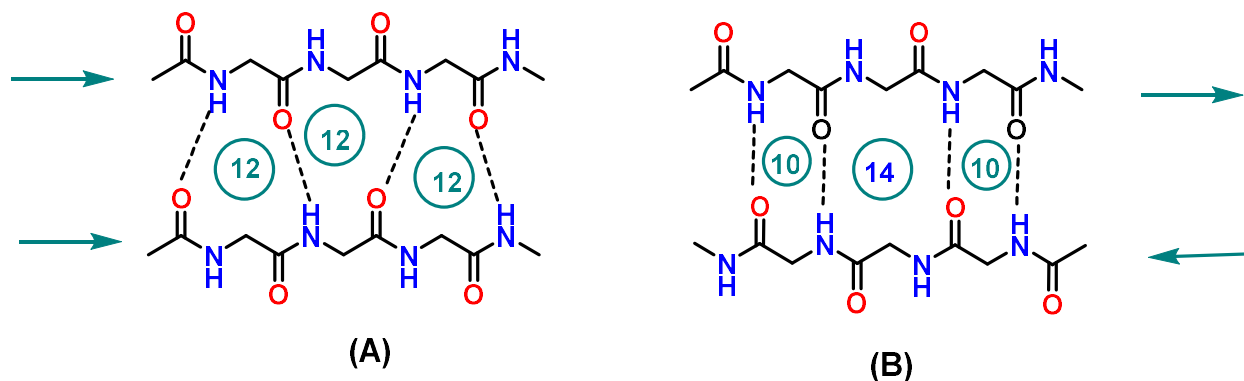


**Figure 1.3:** H-bonding and directionality of  $\beta$ -sheets shown in (A) parallel  $\beta$ -sheets and (B) anti-parallel  $\beta$ -sheets.

**Reverse Turns:** Reverse turns are also considered one of the important secondary structures of proteins. Reverse turns are generally classified based on the number of amino acid residues involved in inducing the reverse directionality of the polypeptide chain. They are classified as  $\pi$ -turn (6 amino acids),  $\alpha$ -turn (5 amino acids),  $\beta$ -turn (4 amino acids),  $\gamma$ -turn (3 amino acids),  $\delta$ -turn (2 amino acids). Among them,  $\beta$ -turns are predominantly occurring in the protein structures. Depending on the dihedral angles  $\phi$  and  $\psi$  of  $i+1$  and  $i+2$  residues,  $\beta$ -turns are further classified into type I, II and III as well as their mirror images type I', II' and III' turns respectively.<sup>6</sup>



### 1.3. Mimicking of Protein Secondary Structures

The relationship between structure and function of proteins has attracted significant attention over the years to design protein mimetics using unnatural building blocks.<sup>1</sup> Great attention has been paid over the past several decades to design folded architectures from sterically constrained  $\alpha$ -amino acids templates.<sup>7</sup> These *de novo* design of protein secondary structural elements are not only useful in our understanding of overall protein folding and their function, but also provides an excellent opportunity to peptide based drug design. Besides the  $\alpha$ -amino acid, a variety of unnatural amino acids and organic templates have been explored as building blocks in the design of protein secondary structures. In addition to the various unnatural amino acids and organic templates, the backbone homologated  $\beta$ - and  $\gamma$ -amino acid have also been well explored in the design of protein structure mimetics.<sup>8</sup>

### 1.4. $\beta$ -Peptide Foldamers

The term “Foldamers” was coined by Prof. Samuel H. Gellman and he stated that “*any oligomer which can adopt a rigid conformation in solution.*”<sup>8a</sup> Foldamers can adopt any specific structure or geometry. In the literature various foldameric building blocks were used to design protein secondary structure mimetics. Among them  $\beta$ -amino acids have been extensively utilized for the construction of different protein secondary structure elements. Some of the  $\beta$ - amino acids utilized in the construction of protein secondary structure are shown in the Figure 1.4. In their seminal work, Seebach<sup>9</sup> and Gellman<sup>10</sup> reported utilization of acyclic chiral and cyclic  $\beta$ -amino acids, respectively in the construction of a variety of folded architectures. Gellman and colleagues used cyclic *trans*-2-amino cyclopentanecarboxylic acid (ACPC) and *trans*-2-aminocyclohexanecarboxylic acid (ACHC), respectively and reported oligomers of cyclic  $\beta$ -amino acids ACPC and ACHC are prompted to form 12- and 14-helical conformations, respectively. In continuation, Sharma and co-workers reported the 10/12 or 12/10 mixed helical structures from carbo- $\beta$ -amino acid oligomers.<sup>11</sup> Further, Atkins<sup>12</sup> and Fulop<sup>13</sup> groups have used various cyclic amino acids to construct  $\beta$ -peptide foldamers.

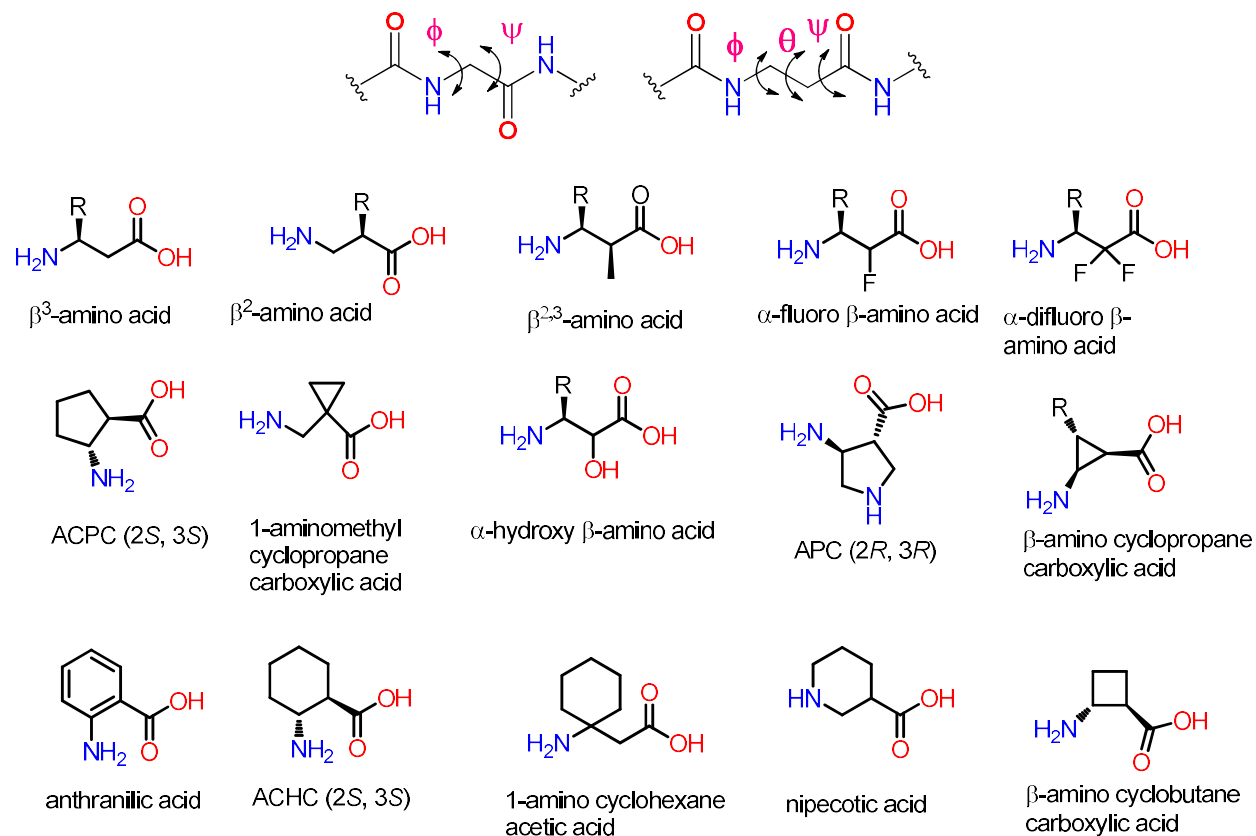


**Figure 1.4:** Chemical structure of  $\beta$ -amino acids utilized for foldamers design.

The definite folded architectures derived from the  $\beta$ -peptides suggested that folding is not unique to proteins. The folding of  $\beta$ - and higher homologue peptides is not only helpful in understanding the complex protein folding, but also serve as excellent candidates in medicinal chemistry and drug discovery. Depending upon the substitution on the backbone  $\beta$ -amino acids are classified mainly into two categories such as  $\beta^2$ - and  $\beta^3$ -amino acids. Another advantage of  $\beta$ -amino acids over the  $\alpha$ -amino acids is that as they are proteolytically stable against different proteases and have been utilized for the intracellular drug delivery.<sup>14</sup> Secondary structure formed by the acyclic and cyclic  $\beta$ -amino acids are classified mainly as helices, sheet and turns. In contrast to the  $\alpha$ -peptides,  $\beta$ -peptide displayed helices with different hydrogen bonding pseudocycles. Different types of helices observed in the  $\beta$ -peptide foldamers are shown in the Figure 1.5. Among the various

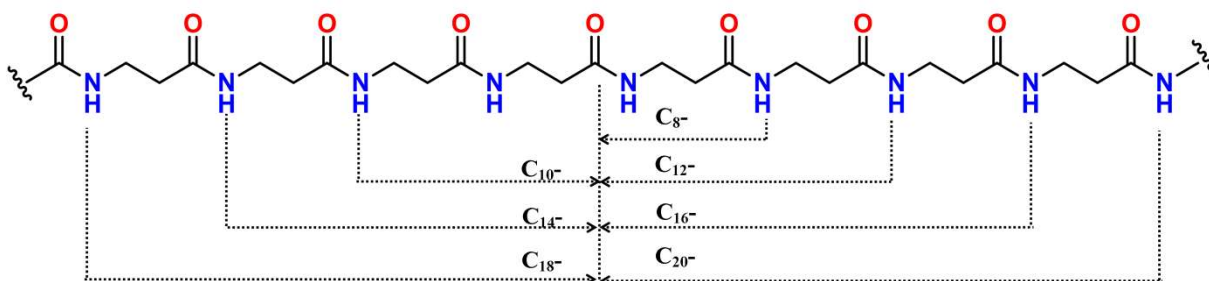


**Figure 1.5:** Possible H-bonding pattern in the oligomer of  $\beta$ -peptide by quantum mechanical calculation.

types of helices  $C_8$ ,  $C_{10}$ ,  $C_{12}$ ,  $C_{14}$  are well characterized from the  $\beta$ -peptide foldamers.<sup>15</sup> These helices have different H-bonding polarity with respect to N and C-terminal. Both  $C_8$  and  $C_{12}$  helices showed hydrogen bond direction ( $C \leftarrow N$ ) similar to  $\alpha$ -helix, while  $C_{10}$  and  $C_{14}$  helices showed the opposite ( $N \leftarrow C$ ) hydrogen bonding direction. Apart from the helical structures parallel and antiparallel sheets and  $\beta$ -hairpin structures have also been reported from the  $\beta$ -amino acid oligomers. In contrast to the 14-helical conformations of cyclic  $\beta$ -amino acids with six membered ring constraint (*trans*-2-aminocyclohexane carboxylic acid)<sup>16</sup> and acyclic  $\beta$ -amino acids ( $\beta^3$ - and  $\beta^2$ -amino acids),<sup>9b</sup> the homooligomers of cyclic  $\beta$ -amino acids with four (*trans*-2-aminocyclobutane carboxylic acid)<sup>12</sup>, five (*trans*-2-aminocyclopentane carboxylic acid and its derivatives)<sup>17</sup> membered ring constraint and bicycle [3.3.1] heptane skeleton<sup>18</sup> displayed the stable 12-helical conformations. Further, Balaram and colleagues reported incorporation of synthetic  $\beta$ -amino acids for the construction of helices and  $\beta$ -hairpins.<sup>19</sup>  $\beta$ -Hairpin<sup>19a</sup> and three stranded<sup>19c</sup>  $\beta$ -sheets have been studied by incorporating  $\beta$ -Phe residues at opposite faces of anti-parallel  $\beta$ -strands using  $^D$ Pro-Gly<sup>19a,19b</sup> at the turn position. The major difference in the  $\beta$ -sheets is the directionality of hydrogen bonds. In case of  $\alpha$ -peptides, they produce hydrogen bonds that are alternate in direction which results in an apolar  $\beta$ -sheet, whereas in the case of  $\beta$ -peptides they produce polar sheet where the hydrogen bonds are in the same direction. Introduction of additional methylene group in the backbone of  $\beta$ -amino acid residues

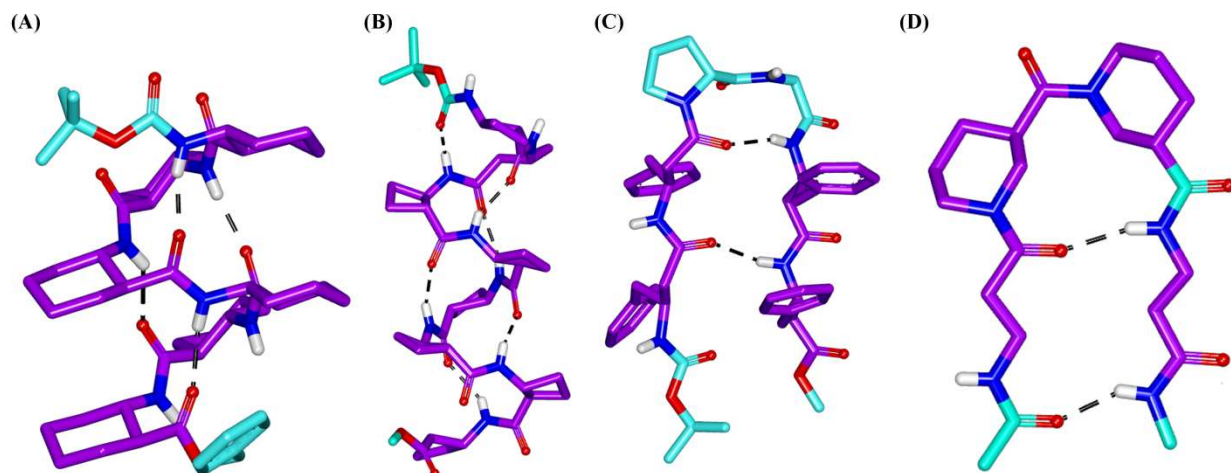


**Figure 1.6:** Crystal structure from of (A) *trans*-ACHA ( $C_{14}$ -helix) (B) cyclobutane  $\beta$ -amino acid ( $C_{12}$ -helix).  $\beta$ -hairpin conformation constructed from  $\beta$ -amino acids containing (C)  $\alpha,\beta$ -disubstituted  $\beta$ -amino acids and (D)  $\beta^3$ -amino acids. (Magenta color represented the  $\beta$ -amino acids). Crystal structures were generated from the ref no (A) 10a, (B) 12, (C) 19a and (D) 10d respectively.

leading the introduction of additional torsion angle freedom  $\theta$  ( $C^\beta$ - $C^\alpha$ ) along with  $\phi$  ( $N$ - $C^\beta$ ) and  $\psi$  ( $C^\alpha$ -CO). It is quite surprising to observe the formation of stable higher ordered structures from  $\beta$ -peptides even after introducing additional backbone rotational freedom.

### 1.5. $\gamma$ -Peptide Foldamers

$\gamma$ -Amino acids are double homologated  $\alpha$ -amino acids. It has two extra backbone torsion angles  $\theta_1$  ( $C^\beta$ - $C^\alpha$ ) and  $\theta_2$  ( $C^\gamma$ - $C^\beta$ ) along with  $\phi$  ( $N$ - $C^\beta$ ) and  $\psi$  ( $C^\alpha$ -CO) compared to  $\alpha$ -amino acids. Due to two additional backbone atoms, it is expected higher structural diversity from the  $\gamma$ -peptides. Seebach pointed out that ***“the structural diversity of  $\gamma$ -amino acids and  $\gamma$ -peptides havenot been elucidated nearly as well as that of  $\beta$ -peptides: it is expected to be richer”***.<sup>20</sup> The group of Seebach<sup>21</sup> and Hanessian<sup>22</sup> reported the stable right handed 14-helical conformations from the oligomers of  $\gamma$ -amino acids thorough NMR studies. In addition, Hoffman and colleagues reported wide range of helical structures from  $\gamma$ -peptides by *ab initio* theoretical calculations.<sup>23</sup> They reported that among the all possible helices,  $C_{14}$ - and  $C_9$ - helices are most stable structures. The predicted  $C_9$ -helices structure was later experimentally proved by the group of Sharma and co-workers from alternating C-linked carbo- $\gamma^4$ -amino acid and  $\gamma$ -aminobutyric acid (GABA).<sup>24</sup> In their seminal work, Balaram and colleagues reported  $C_9$

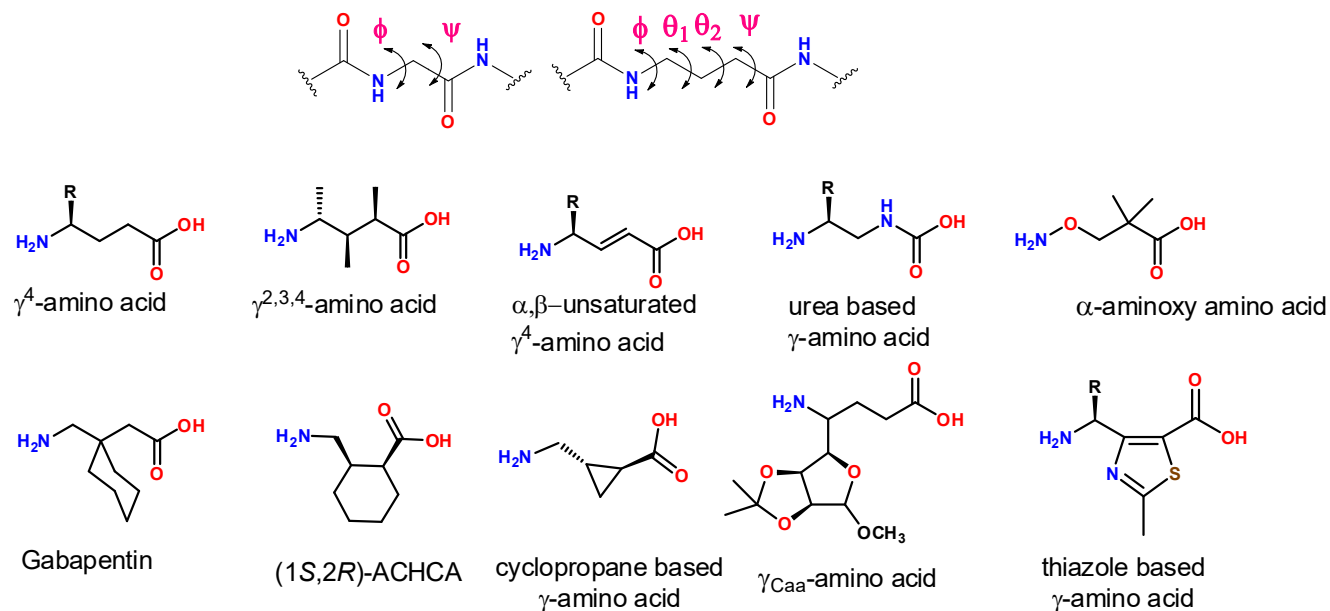


**Figure 1.7:** Chemical structure of  $\gamma$ -amino acids utilized for foldamers design.

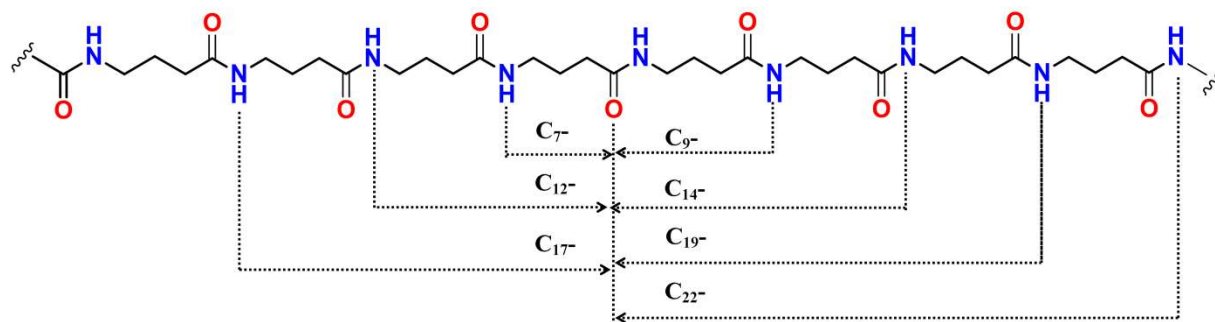


**Figure 1.8:** Possible H-bonding pattern in the oligomer of  $\gamma$ -peptide foldamer.

helical conformations from the oligomers gabapentin (3, 3-dialkyl- $\gamma$ -amino acid) in single crystals. The  $C_9$  helical structure is stabilized by the H-bonds between the  $i$  and  $i + 2$  residues.<sup>25</sup> Apart from the gabapentin, Balaram and colleagues reported  $C_{14}$  helical conformation from the oligomer of  $\gamma^4$ -amino acids having proteinogenic side chains ( $\gamma^4$ -Val,  $\gamma^4$ -Leu,  $\gamma^4$ -Ile) in single crystals.<sup>26</sup> Gellman and co-workers reported the stable  $C_{14}$  helices from the cyclic  $\gamma$ -amino acids.<sup>27,28</sup> Furthermore, Smith and colleagues reported synthesis and conformational analysis of

cyclopropane based  $\gamma$ -amino acids.<sup>29</sup> They showed that oligomer of this  $\gamma$ -amino acids showed parallel type  $\beta$ -sheet

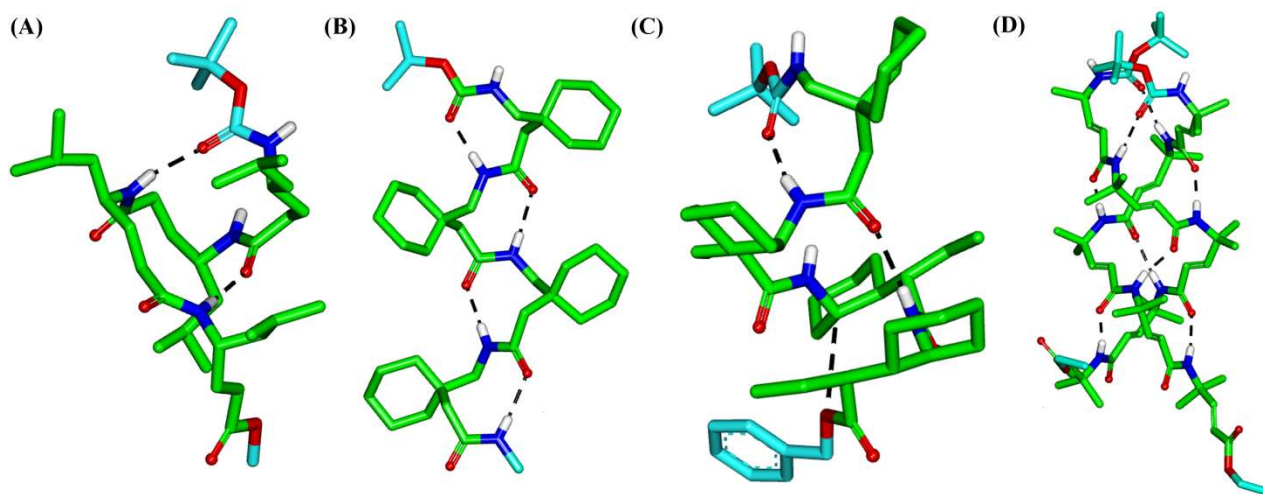


**Figure 1.9:** Crystal structure of (A)  $C_{14}$ -helix of  $\gamma^4$ -peptide oligomer (B)  $C_9$ -helix of gabapentin oligomers (C)  $C_{14}$  helical conformations of homooligomers of cyclic  $\gamma$ -amino acid (D) artificial  $\beta$ -double helices from homooligomer of (*E*)- $\alpha,\beta$ -unsaturated- $\gamma^{4,4}$ -amino acids. (Green color represents  $\gamma$ -amino acids). Crystal structures were generated from the ref no (A) 26, (B) 25, (C) 27 and (D) 74 respectively.

structures and the structure stabilized by bifurcated hydrogen-bonds between the carbonyl oxygen with the amide NH group and one CH of the cyclopropane ring in solid state. Further they utilised this amino acids as non peptidic reverse turn for the design of  $\beta$ -hairpins.<sup>29</sup> In addition,  $\gamma^{2,3}$ -*trans*-dioxolane-constrained homooligomers have been explored to design peptide foldamers.<sup>30</sup> Apart from the cyclic  $\gamma$ -amino acids, backbone containing oxygen and nitrogen atom also have been explored to design various functional foldamers. Yang and colleagues reported that  $C_8$  helical conformations from  $\alpha$ -aminoxy peptides.<sup>31</sup> Further, Guichard and colleagues utilised the oligourea based peptide foldamer by replacing  $\gamma^3$ -carbon in the  $\gamma$ -peptide backbone with NH.<sup>32</sup> In a recent study Millard and colleagues reported the formation of  $C_9$  helices from the homooligomers of 4-amino-(methyl)-1,3-thiazole-5-carboxylic acids (ATCs).<sup>33</sup>

## 1.6. Heterogeneous Foldamers Containing $\beta$ - and $\gamma$ -Amino Acids

In recent years, peptide foldamers with heterogeneous backbone gained much more momentum over the homogeneous backbone counterparts. This is because various types of helices with

different H-bonding pattern can be derived through proper mixing of different types of amino acids. In their pioneering work, Balaram and co-workers reported hybrid peptides by inserting  $\beta$ -amino acids in the host  $\alpha$ -peptides.<sup>34</sup> Hofmann and colleagues predicted various types helices available to  $\alpha,\beta$ -hybrid peptides by vigorous quantum mechanical calculation.<sup>35</sup> They proposed that the possible helices can be generated from  $\alpha,\beta$ -hybrid peptide are 9-, 11/9-, 9/11-, 11-, 12/13-, 15/14-, 16/18- and 18/16- helices., Sharma and co-workers reported 11/9-helical conformation with alternating hydrogen bonding direction from  $\alpha,\beta$ - sequence consisting of  $\alpha$ - and  $\beta^3$ -amino acids.<sup>36,37</sup> In an unique study, the group of Gellman reported the conformation of short  $\alpha, \beta$ -hybrid peptides composed of backbone constrained *trans*-ACPC amino acids (*trans*-2-aminocyclopentane carboxylic acid) and Aib residues through crystallography.<sup>38</sup> They showed the conversion of 11-helices into 14/15 helices by replacing terminal Aib residues with alanine, which suggested that little energy difference between the two helix types. Furthermore

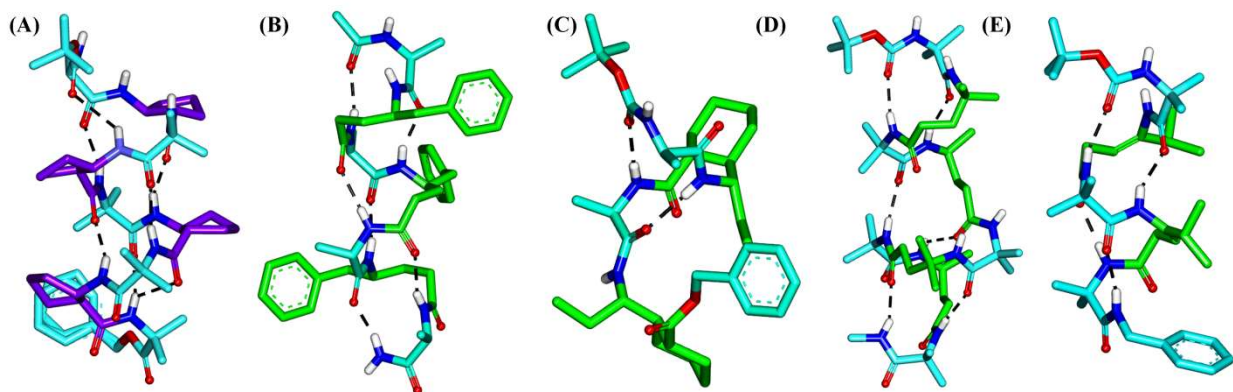


**Figure 1.10:** Crystal structure of (A) 14/15-helix from  $\alpha,\beta$ -hybrid peptide BocNH-Ala-(ACPC-Aib)<sub>3</sub>-ACPC-OBn (B) C<sub>12</sub>-helix from  $\alpha,\gamma^4$ -hybrid peptide Ac-(Ala- $\gamma^4$ Phe)<sub>3</sub>-Ala-NH<sub>2</sub> (C) 12/10-helix from BocNH-(<sup>D</sup>Ala-APCH)<sub>2</sub>-OBn (D) 12/15/17-helix from achiral  $\alpha,\gamma^{4,4}$ -hybrid peptide BocNH-Aib-(Aic-Aib)<sub>4</sub>-OMe (E) C<sub>12</sub>-helix from  $\alpha,\gamma^4$ -hybrid peptide BocNH-[Aib-(Z)- $\beta,\gamma$ -unsaturated  $\gamma^4$ Val]<sub>2</sub>-Aib-OBn.(Magenta color represented the  $\beta$ -amino acids and green color represents  $\gamma$ -amino acids). Crystal structures were generated from the ref no (A) 38a, (B) 43b, (C) 45c, (D) 48 and (E) 50 respectively.

C<sub>11/11/12</sub> and C<sub>10/11/11</sub>-helix formation in 1:2 and 2:1 from  $\alpha,\beta$ -hybrid peptides were demonstrated by Gellman and co-workers.<sup>39</sup> Fülöp and colleagues reported the effect of the stereochemical patterns in the folding of  $\alpha,\beta$ -hybrid peptides.<sup>40</sup> In addition, Gellman and colleagues reported the quaternary structure type helical bundles from the oligomers consisting of  $-\beta-\beta-\alpha-\beta-\beta$  and  $\alpha-\alpha-\alpha-$

$\beta$ - $\alpha$ - $\alpha$ - $\beta$  repeats.<sup>41</sup> Along with mixed  $\alpha$ -,  $\beta$ - hybrid peptides, the structural properties of  $\alpha$ , $\gamma$ -hybrid peptides have also been examined in the literature. Hofmann and colleagues predicted the possible helical conformation from the hybrid peptide composed of 1:1 alternating  $\alpha$ - and  $\gamma$ -amino acids.<sup>42</sup> They proposed that 12-helix is the most stable helix followed by 12/10- or 18/20-helices. Further, Balaram and co-workers reported formation of 12 helix from  $\alpha$ , $\gamma$ -hybrid consisting of 1:1 Aib and Gabapentin residue.<sup>43a</sup> Stable C<sub>12</sub>-helix structure was also observed in hybrid peptide with 1:1 of  $\alpha$ -and  $\gamma^4$ -amino acids.<sup>43b</sup> The structure is stabilised by the intramolecular hydrogen bonding between  $i$  and  $i+3$  residues. Several 12/10-helices were also studied from  $\alpha$ , $\gamma$ -hybrid peptides composed of L-Ala and  $\gamma$ -C<sub>aa</sub> (C-linked carbo- $\gamma$ -amino acid) by Sharma and colleagues.<sup>44</sup> Gellman's group further demonstrated the design, synthesis and characterisation of different  $\alpha/\gamma$ -peptides containing sterically constrained cyclic  $\gamma$ -amino acids.<sup>45</sup> Apart from the crystallographic characterisation, they also showed the stable 12-helix structures in aqueous buffer by NMR study.<sup>46</sup> In addition, Balaram and colleagues utilised  $\alpha/\gamma$ -peptide for the stable reverse turn in  $\beta$ -hairpin conformation.<sup>47</sup> In recent study by Misra *et al* reported co-existence of 12- and 15/17-helices from achiral  $\alpha/\gamma$ - hybrid peptide.<sup>48</sup> But when the Aib residue was replaced by the  $\alpha$ -amino acids, the 12-helix is transformed into 12/10-mixed helical structure.<sup>49</sup> Further, Veeresh *et al* showed the formation of stable C<sub>12</sub> helix from  $\alpha$ ,  $\gamma$ -hybrid peptide from the unstructured peptide by base mediated  $\alpha,\beta \rightarrow \beta,\gamma$  double-bond migration.<sup>50</sup> Apart from the  $\alpha$ ,  $\beta$ - and  $\alpha$ ,  $\gamma$ -hybrid peptides, only few reports are available in conformation properties of  $\beta/\gamma$ - peptides. The hydrogen bonding pattern in the  $\beta/\gamma$ - peptides are shown in Figure 1.11. Further Sharma and Kunwar reported mixed 11/13 helical conformation from the  $\beta/\gamma$ -peptides consisting of C-linked carbo- $\beta$ - and  $\gamma$ -amino acids in solution.<sup>51</sup> Furthermore, Balaram and colleagues reported the 13-helix structure from a short  $\beta$ ,  $\gamma$ -hybrid peptide.<sup>52</sup> Gellman and colleagues demonstrated the 13-helix from  $\beta,\gamma$ -hybrid peptides.<sup>53</sup> The helical parameters in 13-helix from are similar to helical parameters as that of  $\alpha$ -helix.  $\beta,\gamma$ -hybrid peptide gives a great opportunity to mimic the helical parameters of the naturally occurring  $\alpha$ -helices. In addition, 9/8-ribbon structure from  $\beta,\gamma$ -hybrid peptide with stereo chemically constrained  $\beta$ -amino acids and 13-helix from the unconstrained  $\gamma^4$ -amino acids were studied by Aitken and colleagues.<sup>54</sup>



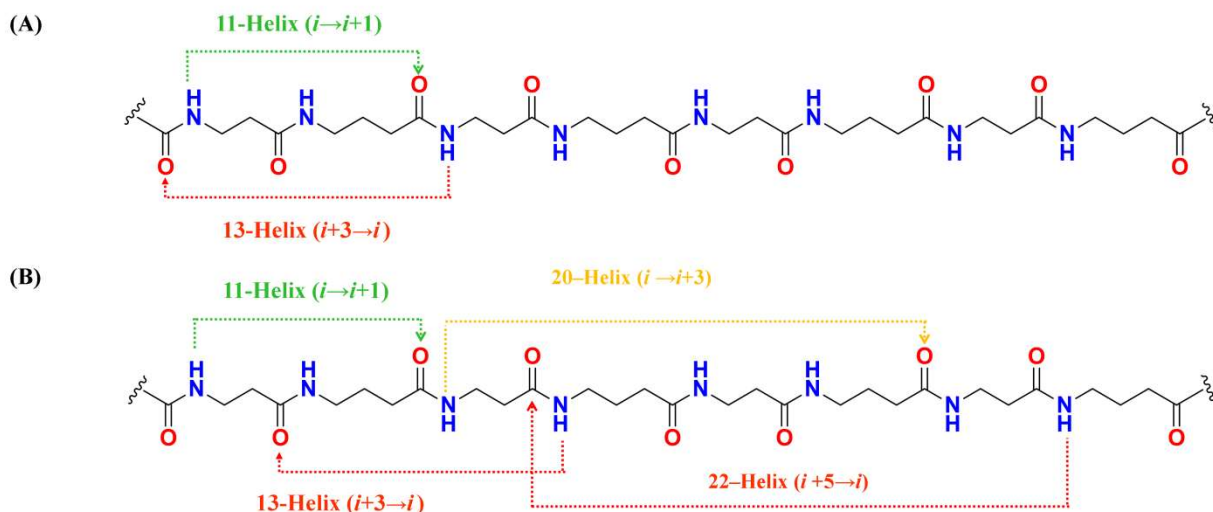


**Figure 1.11:** Possible H-bonding pattern in  $\beta$ ,  $\gamma$ -hybrid peptide by quantum mechanical calculations.

### 1.7. Biologically Active Peptide Foldamers Composed of $\beta$ - and $\gamma$ - Amino Acids

Due to their proteolytic stability and their readily folding ability into definite structures,  $\beta$ -, $\gamma$ - and the  $\alpha\beta$ -, $\alpha\gamma$ -hybrid peptide foldamers have attracted considerable attention from the fields of medicinal chemistry and chemical biology.<sup>55</sup> Gellman and colleagues reported amphiphilic cationic 14-helical peptide from  $\beta$ -amino acids and showed their potent activity and specificity towards the bacteria.<sup>56</sup> Apart from homooligomers from  $\beta$ -amino acids, they also demonstrated amphiphilic  $\alpha$ ,  $\beta$ -hybrid peptides and showed potent antibacterial activity against various Gram-negative and Gram-positive bacteria.<sup>57</sup> Further Schepartz and co-workers designed p53 mimetics from the  $\beta^3$ -peptides and utilised them as inhibitors for p53-MDM2 interactions.<sup>58</sup> They also reported design and synthesis of inhibitors for HIV-1 gp41-mediated fusion.<sup>59</sup> In addition,  $\alpha$ ,  $\beta$ -hybrid peptides have also been explored for the design of inhibitors against the Bak/Bcl-xL interactions.<sup>60</sup> Foldamers derived from  $\gamma$ -peptide and their analogous have showed several potential biological application although it was not explored like  $\beta$ -peptide foldamers. Peptide composed of different  $\gamma$ -amino acids such as  $\gamma^2$ -,  $\gamma^3$ -,  $\gamma^4$ -,  $\gamma^{2,3,4}$ - showed proteolytic stability against 15 proteolytic enzymes and no degradation was observed after 48 h.<sup>8b</sup> Small  $\gamma$ -peptides show submicro molar affinity towards several different type of human somatostatin receptors.<sup>61</sup>

Apart from this, oligonucleotide analogues derived from  $\gamma$ -peptides and  $\gamma/\varepsilon$ -peptides strongly bind to the DNA or RNA.<sup>62</sup> Further, *N*-functionalized hexamers of *cis*- $\gamma$ -amino proline have also been explored for their cellular uptake.<sup>63</sup> Potent antimicrobial properties short  $\alpha,\gamma$ -hybrid peptides<sup>64,65</sup> have also been examined.

### 1.8. Supramolecular Assemblies from Peptides Composed of $\beta$ - and $\gamma$ - Amino Acids

Apart from the biologically active peptide composed  $\beta$ -,  $\gamma$ - amino acids, these peptide have also been explored to design different supramolecular assemblies. In their seminal work, Gellman and co-workers demonstrated formation of tetrameric and hexameric helix bundles from 14-helical  $\beta$ -peptide.<sup>66</sup> In addition, they have also reported quaternary bundles from  $\alpha$ ,  $\beta$ -hybrid peptides in solution as well as in crystalline state through hydrophobic and ion pair interactions.<sup>67</sup> Ghadiri and co-workers reported polar cyclic peptide nanotubes (CPNs) from  $\beta$ -peptides by extensive intermolecular hydrogen bonding interactions.<sup>68</sup> They further showed the channel forming ability of these CPNs by liposome based proton transport assay and single channel conductance measurement experiments. Fülöp and his colleagues reported formation of supramolecular vesicles and ribbon like structures form  $\beta$ -hexapeptides with 10/12-helical structures.<sup>69</sup> In a recent studies by Lee and co-workers reported various supramolecular nano architectures form  $\beta$ -peptides. In addition, the groups of Perlmutter and Ortuno reported the self-assembled fibers and gelation from peptides compose of *N*-acetylated  $\beta$ -tri- and hexapeptides and cyclobutane  $\beta$ -amino acids respectively.<sup>70</sup> Along with the  $\beta$ -peptides,  $\gamma$ -peptides have also been well explored in the literature to design different supramolecular assemblies. Jadhav *et al* reported hollow nanotube formation from  $\alpha,\gamma^4$ -hybrid peptide foldamers and further they utilized these nanotubes for biomineralization of silver ions to silver nanowires.<sup>71</sup> Granja and co-workers demonstrated the utilization of cyclic peptide nanotubular structures from  $\alpha,\gamma$ -peptides for transmembrane ion channels.<sup>72</sup> Apart from nanotubularassemblies, self-assembled vesicular structures were also derived from the  $\gamma$ -peptide foldamers.<sup>73</sup> In continuation, Jadhav *et al* reported the supramolecular organogels from the oligomers of  $\gamma^{4,4}$ -amino acids,<sup>74</sup> however the  $\alpha,\beta$ -unsaturated  $\gamma^{4,4}$ -amino acids adopts stable  $\beta$ -double helical structure both in solid and solution state.<sup>75</sup> Furthermore, short  $\alpha,\gamma^4$ -hybrid peptides have been used as templates to construct metal-helix frameworks.<sup>76</sup>

## 1.9. Foldamers Containing $\delta$ -Amino Acids

Compared to  $\beta$ - and  $\gamma$ -amino acids, peptides composed of  $\delta$ -amino acid are scarcely discussed in the literature. Nevertheless, Hofmann and colleagues theoretically proposed the different types helices available to the homooligomers of  $\delta$ -amino acids. They proposed that 10-helix (10-membered hydrogen bonding) is the most stable helix followed by 14, 16 and 8 membered hydrogen bonded helices.<sup>77</sup> Along with the helical structures, they also reported the possible  $\beta$ -turn conformation from  $\delta$ -amino acid constituents. The groups of Chakraborty and Sharma reported different hybrid helices from pyranose- or furanose-based carboamino and furan based

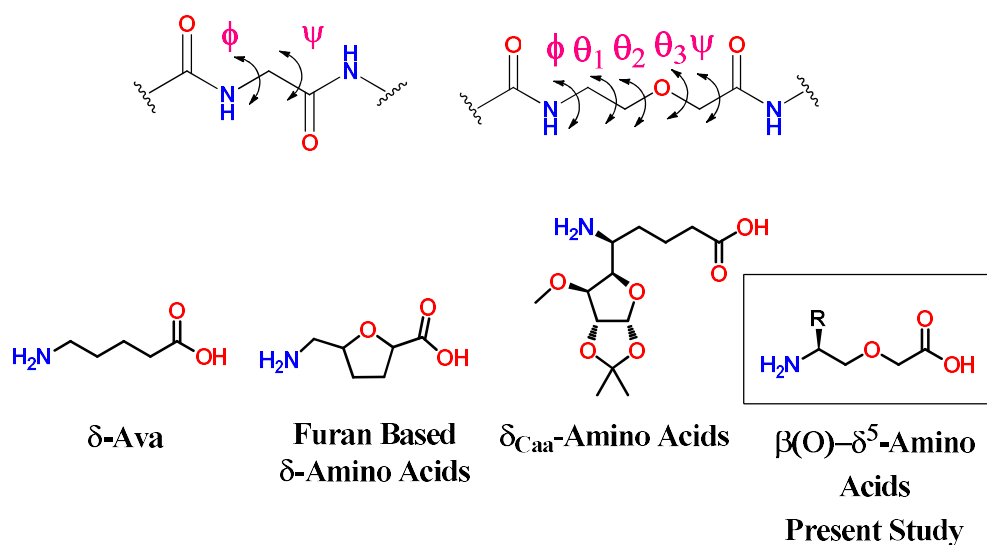


**Figure 1.12:** Chemical structure of  $\delta$ -amino acids utilized for design of peptide foldamers.

$\delta$ -amino acids. Chakraborty and co-workers used constrained furanoid sugar amino acids to design different reverse turns in  $\beta$ -hairpins.<sup>78</sup> Further, Sharma and co-workers showed the formation of 11/13 mixed helices from the  $\alpha/\delta$  hybrid peptides through NMR as well as theoretical calculations.<sup>79</sup> Apart from the pyranose and furanose based  $\delta$ -amino acids, Huc and co-workers showed the helical

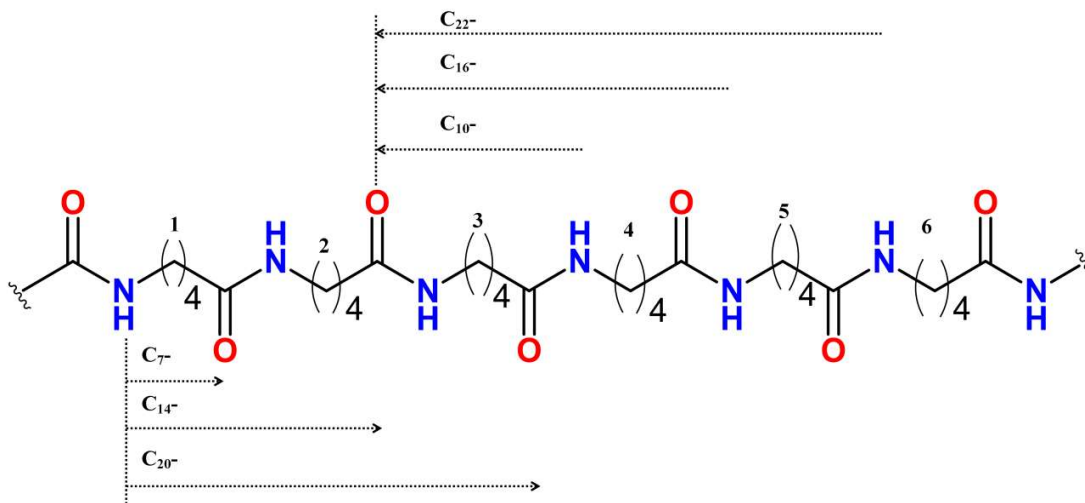


**Figure 1.13:** Possible H-bonding pattern in homo oligomers of  $\delta$ -peptide by quantum mechanical calculations.

structures from the quinolone based  $\delta$ -amino acids in single crystals.<sup>80</sup> Furthermore polar cyclic peptide nanotubes (CPNs) were also generated from cyclic tripeptide of  $\alpha,\beta$ -unsaturated  $\delta$ -amino acid residue with *trans* geometry of the vinyl group.<sup>81</sup> In addition, Balaram and co-workers showed the stability of the helices by replacing Gly-Gly residue with  $\delta$ -aminovaleric acid ( $\delta$ -Ava).<sup>82</sup> More importantly  $\delta$ -amino acids serve as surrogates of  $\alpha$ -dipeptides. This thesis is mainly focusing on the synthesis and exploration of new  $\beta(O)$ - $\delta^5$ -amino acids (where the central amide bond in  $\alpha$ -dipeptide is replaced  $O^\beta-C^\gamma$  bond) towards the design of different functional foldamers and biomaterials.

## 1.10. References

1. Linderstrom-Lang, K. U.; Schellman, J. A. (1959), *The Enzymes*, (P. D. Boyer, Ed.), Vol. 1, 2<sup>nd</sup> ed., pp. 443-510. Academic Press, New York.
2. Pauling, L.; Corey, R. B.; Branson, H. R. *Proc. Nat. Acad. Sci. USA*. **1951**, *37*, 205.
3. Ramachandran, G. N.; Sasisekaran, V. *Adv. Protein Chem.* **1968**, *23*, 283.
4. Astbury, W.; T.; Woods, H. J. *Nature* **1931**, *127*, 663.
5. Pauling, L.; Corey, R. B. *Proc. Nat. Acad. Sci. USA*. **1951**, *37*, 729.
6. Venkatachalam, C. M. *Biopolymers* **1968**, *6*, 1425.

7. a) Marshall, G. R.; Bosshard, H. E. *Circ. Res.* **1972**, *31*, 143. b) Ramachandran, G. N.; Chandrasekaran, R. *Progress in Peptide Research*. Lande, S. Ed.; Gordon & Breach: New York, 1972; Vol. II (Proceedings of the Second American Peptide Symposium, Cleveland, 1970), p 195. c) Toniolo, C.; Benedetti, E. *ISI Atlas Sci. Biochem.* **1988**, *1*, 225. d) Bosch, R.; Schmitt, H.; Jung, G.; Winter, W. *Biopolymers* **1985**, *24*, 961. e) Toniolo, C.; Benedetti, E. *Trends Biochem. Sci.* **1991**, *16*, 350. f) Karle, I. L.; Balaram, P. *Biochemistry* **1990**, *29*, 6747. g) Marshall, G. R.; Hodgkin, E. E.; Langs, D. A.; Smith, G. D.; Zabrocki, J.; Leplawy, M. T. *Proc. Natl. Acad. Sci. U.S.A.* **1990**, *87*, 487. h) Karle, I. L. *Acc. Chem. Res.* **1999**, *32*, 693. i) Kaul, R.; Balaram, P. *Bioorg. Med. Chem.* **1999**, *7*, 105. j) Balaram, P. *J. Pept. Res.* **1999**, *54*, 195. k) Venkatraman, J.; Shankaramma, S. C.; Balaram, P. *Chem. Rev.* **2001**, *101*, 3131.
8. a) Gellman, S. H. *Acc. Chem. Res.* **1998**, *31*, 173. b) Frackenpohl, J.; Arvidsson, P. I.; Schreiber, J. V.; Seebach, D. *ChemBioChem* **2001**, *2*, 445. c) Goodman, C. M.; Choi, S.; Shandler, S.; DeGrado, W.F. *Nat. Chem. Biol.* **2007**, *3*, 252.
9. a) Hintermann, T.; Gademann, K.; Jaun, B.; Seebach, D. *Helv. Chim. Acta*, **1998**, *81*, 983. b) Seebach, D.; Beck, A. K.; Bierbaum, D. J. *Chem. Biodiv.* **2004**, *1*, 1111.
10. a) Appella, D. H.; Christianson, L. A.; Karle, I. L.; Powell, D. R.; Gellman, S. H. *J. Am. Chem. Soc.* **1996**, *118*, 13071. b) Appella, D. H.; Christianson, L. A.; Karle, I. L.; Powell, D. R.; Gellman, S. H. *J. Am. Chem. Soc.*, **1999**, *121*, 6206. c) Appella, D. H.; Christianson, L. A.; Klein, D. A.; Richards, M. A.; Powell, D. R.; Gellman, S. H. *J. Am. Chem. Soc.* **1999**, *121*, 7574. d) Krauthauser, S.; Christianson, L. A.; Powell, D. R.; Gellman, S. H. *J. Am. Chem. Soc.* **1997**, *119*, 11719.
11. a) Sharma, G. V. M.; Reddy, R.; Krishna, P. R.; Ravi Sankar, A.; Narsimulu, K.; Kumar, S. K.; Jayaprakash, P.; Jagannadh, B.; Kunwar, A. C. *J. Am. Chem. Soc.*, **2003**, *125*, 13670. b) Sharma, G. V. M.; Chandramouli, N.; Choudhary, M.; Nagendar, P.; Ramakrishna, K. V. S.; Kunwar, A. C.; Schramm, P.; Hofmann, H. -J. *J. Am. Chem. Soc.* **2009**, *131*, 17335.
12. Fernandes, C.; Faure, S.; Pereira, E.; Thery, V.; Declerck, V.; Guillot, R.; Aitken, D. J. *Org. Lett.* **2010**, *12*, 3606.
13. a) Fulop, F.; Forro, E.; Toth, G. K. *Org. Lett.* **2004**, *6*, 4239. b) Martinek, T. A.; Fulop, F. *Chem. Soc. Rev.* **2012**, *41*, 687.

14. a) Gopi, H. N.; Ravindra, G.; Pal, P. P.; Pattanaik, P.; Balaram, H.; Balaram, P. *FEBS Lett.* **2003**, *535*, 175. b) Frackenpohl, J.; Arvidsson, P. I.; Schreiber, J. V.; Seebach, D. *ChemBioChem*, **2001**, *2*, 445. c) Hook, D. F.; Bindschädler, P.; Mahajan, Y. R.; Sebesta, R.; Kast, P.; Seebach, D. *Chem. Biodiv.* **2005**, *2*, 591.
15. Cheng, R.P.; Gellman, S. H.; DeGrado, W. F. *Chem. Rev.* **2001**, *101*, 3219.
16. Choi, S. H.; Guzei, I. A.; Spencer, L. C.; Gellman, S. H. *J. Am. Chem. Soc.* **2010**, *132*, 13879.
17. Mandity, I. M.; Fulop, L.; Vass, E.; Toth, G. K.; Martinek, T. A.; Fulop, F. *Org. Lett.* **2010**, *12*, 5584.
18. Kwon, S.; Jeon, A.; Yoo, S. H.; Chung, I. S.; Lee, H.-S. *Angew. Chem. Int. Ed.* **2010**, *49*, 8232.
19. a) Karle, I. L.; Gopi, H. N.; Balaram, P. *Proc. Nat. Acad. Sci. USA.* **2001**, *98*, 7. b) Vasudev, P. G.; Chatterjee, S.; Shamala, N.; Balaram, P. *Chem. Rev.* **2011**, *111*, 657. c) Sonti, R.; Gopi, H. N.; Muddegowda, U.; Ragothama, S.; Balaram, P. *Chem. Eur. J.* **2013**, *19*, 5955. d) Aravinda, S.; Shamala, N.; Rajkishore, R.; Gopi, H. N.; Balaram, P. *Angew. Chem. Int. Ed.* **2002**, *20*, 3863.
20. Seebach, D.; Hook, D. F.; Glattli, A. *Biopolymers (Peptide Science)* **2006**, *84*, 23.
21. Hintermann, T.; Gademann, K.; Seebach, D. *Helv. Chim. Acta.* **1998**, *81*, 893.
22. Hanessian, S.; Luo, X.; Schaum, R.; Michnick, S. *J. Am. Chem. Soc.* **1998**, *120*, 8569.
23. Baldauf, C.; Gunther, R.; Hofmann, H. -J. *J. Org. Chem.* **2006**, *71*, 1200.
24. Sharma, G. V. M.; Jayaprakash, P.; Narsimulu, K.; Sankar, A. R.; Reddy, K. R.; Kunwar, A. *C. Angew. Chem. Int. Ed.* **2006**, *45*, 2944.
25. Vasudev, P. G.; Shamala, N.; Ananda, K.; Balaram, P. *Angew. Chem., Int. Ed.* **2005**, *44*, 4972.
26. Basuroy, K.; Dinesh, B.; Reddy, M. B. M.; Chandrappa, S.; Ragothama, S.; Shamala, N.; Balaram, P. *Org. Lett.* **2013**, *15*, 4866.
27. Guo, L.; Zhang, W.; Reidenbach, A. G.; Giuliano, M.W.; Guzei, I. A.; Spencer, L.C.; Gellman, S. H. *Angew. Chem. Int. Ed.* **2011**, *50*, 5843.
28. Seebach, D.; Brenner, M.; Rueping, M.; Schweizer, B.; Jaun, B. *Chem. Commun.* **2001**, 207
29. Khurram, M.; Qureshi, N.; Smith, M. D. *Chem. Commun.* **2006**, 5006

30. Kothari, A.; Khurram, M.; Qureshi, N.; Beck, E. M.; Smith, M. D. *Chem. Commun.* **2007**, 2814.
31. a) Lee, X.; Yang, D. *Chem. Commun.* **2006**, 3367. b) Chen, F.; Zhu, N.-Y.; Yang, D. *J. Am. Chem. Soc.* **2004**, *126*, 15980.
32. Pendem, N.; Nelli, Y. R.; Douat, C.; Fischer, L.; Laguerre, M.; Ennifar, E.; Kauffman, B.; Guichard, G. *Angew. Chem. Int. Ed.* **2013**, *52*, 4147.
33. Mathieu, L.; Legrand, B.; Deng, C.; Vezenkov, L.; Wenger, E.; Didierjean, C.; Amblard, M.; Averlant-Petit, M. C.; Masurier, N.; Lisowski, V.; Martinez, J.; Maillard, L. T. *Angew. Chem. Int. Ed.* **2013**, *52*, 6006.
34. a) Karle, I. L.; Pramanik, A.; Banerjee, A.; Bhattacharjya, S.; Balaram, P. *J. Am. Chem. Soc.* **1997**, *119*, 9087 b) Roy, R. S.; Karle, I. L.; Raghothama, S.; Balaram, P. *Proc. Natl. Acad. Sci. USA.* **2004**, *101*, 16478.
35. Baldauf, C.; Günther, R.; Hofmann, H.-J. *Peptide Science.* **2006**, *84*, 408.
36. Srinivasulu, G.; Kumar, S. K.; Sharma, G. V. M.; Kunwar, A. C. *J. Org. Chem.* **2006**, *71*, 8395.
37. Jagadeesh, B.; Prabhakar, A.; Sarma, G. D.; Chandrasekhar, S.; Chandrashekar, G.; Reddy, M. S.; Jagannadh. B. *Chem. Commun.* **2007**, 371.
38. a) Choi, S. H.; Guzei, I. A.; Gellman, S. H. *J. Am. Chem. Soc.* **2007**, *129*, 13780 b) Schmitt, M. A.; Choi, S. H.; Guzei, I. A.; Gellman, S. H. *J. Am. Chem. Soc.* **2005**, *127*, 13130.
39. Schmitt, M. A.; Choi, S. H.; Guzei, I. A.; Gellman, S. H. *J. Am. Chem. Soc.* **2006**, *128*, 4538
40. Mándity, I. M.; Weber, E.; Martinek, T. A.; Olajos, G.; Tóth, G. K.; Vass, E.; Fülöp, F. *Angew. Chem., Int. Ed.* **2009**, *48*, 2171.
41. a) Giuliano, M. W.; Horne, W. S.; Gellman, S. H. *J. Am. Chem. Soc.* **2009**, *131*, 9860. b) Horne, W. S.; Price, J. L.; Keck, J. L.; Gellman, S. H. *J. Am. Chem. Soc.* **2007**, *129*, 4178.
42. Baldauf, C.; Gunther, R.; Hofmann, H.-J. *J. Org. Chem.* **2006**, *71*, 1200
43. a) Ananda, K.; Vasudev, P.G.; Sengupta, A.; Raja, K.M.P.; Shamala N.; Balaram, P. *J. Am. Chem. Soc.* **2005**, *127*, 168. b) Jadhav, S. V.; Bandyopadhyay, A.; Gopi, H. N. *Org. Biomol. Chem.* **2013**, *11*, 509.
44. Sharma, G. V. M.; Jadhav, V. B.; Ramakrishna, K. V. S.; Jayaprakash, P.; Narsimulu, K.; Subash, V.; Kunwar, A. C. *J. Am. Chem. Soc.* **2006**, *128*, 14657.

45. a) Guo, L.; Chi, Y.; Almeida, A. M.; Guzei, I. A.; Parker, B. K.; Gellman, S. H. *J. Am. Chem. Soc.* **2009**, *131*, 16018. b) Guo, L.; Zhang, W.; Guzei, I. A.; Spencer, L. C.; Samuel H. Gellman, S. H. *Org. Lett.* **2012**, *14*, 2582. c) Giuliano, M. W.; Maynard, S. J.; Almeida, A. M.; Guo, L.; Guzei, I. A.; Spencer, L. C.; Gellman, S. H. *J. Am. Chem. Soc.* **2014**, *136*, 15046.
46. Fisher, B. F.; Gellman, S.H. *J. Am. Chem. Soc.* **2016**, *138*, 10766.
47. Chatterjee, S.; Vasudev, P. G.; Raghothama, S.; Ramakrishnan, C.; Shamala, N.; Balaram, P. *J. Am. Chem. Soc.* **2009**, *131*, 5956.
48. Misra, R.; Saseendran, A.; George, G.; Veeresh, K.; Raja, K. M. P.; Raghothama, S.; Hofmann, H.-J.; Gopi, H. N. *Chem. Eur. J.* **2017**, *23*, 3764
49. Misra, R.; Raja, K. M. P.; Hofmann, H. -J.; Gopi, H. N. *Chem. Eur. J.* **2017**, *23*, 16644.
50. Veeresh, K.; Gopi, H. N. *Org. Lett.* **2019**, *21*, 4500.
51. Sharma, G. V. M. Jadhav, V. B.; Ramakrishna, K. V. S.; Jayaprakash, P.; Narsimulu, K.; Subash, V.; Kunwar, A. C.; *J. Am. Chem. Soc.* **2006**, *128* , 14657.
52. Vasudev, P. G.; Ananda, K.; Chatterjee, S.; Aravinda, S.; Shamala, N.; Balaram, P. *J. Am. Chem. Soc.* **2007**, *129*, 4039.
53. Shin, Y.-H.; Mortenson, D. E.; Satyshur, K. A.; Forest, K. T.; Gellman, S. H. *J. Am. Chem. Soc.* **2013**, *135*, 8149.
54. a) Grison, C. M.; Robin, S.; Aitken, D. J. *Chem. Commun.* **2016**, *52*, 7802. b) Grison, C. M.; Robinab, S.; Aitken D. J. *Chem. Commun.* **2015**, *51*, 16233.
55. a) English, E. P.; Chumanov, R. S.; Gellman, S. H.; Compton, T. *J. Biol. Chem.* **2006**, *281*, 2661. b) Imamura, Y.; Watanabe, N.; Umezawa, N.; Iwatsubo, T.; Kato, N.; Tomita, T.; Higuchi, t.; *J. Am. Chem. Soc.* **2009**, *131*, 7353. c) Horne, W. S.; Price, J. L.; Gellman, S. H. *Proc. Natl. Acad. Sci. U.S.A.* **2008**, *105*, 9151. d) Hook, D. F.; Bindschadler, P.; Mahajan, Y. R.; Sebesta, R.; Kast, P.; Seebach, D. *Chem. Biodiv.* **2005**, *2*, 591. (e) Rueping, M.; Mahajan, Y.; Sauer, M.; Seebach, D. *ChemBioChem* **2002**, *3*, 257.
56. Porter, E. A.; Weisblum, B.; Gellman, S. H. *J. Am. Chem. Soc.* **2002**, *124*, 7324.
57. Schmitt, M. A.; Weisblum, B.; Gellman, S. H. *J. Am. Chem. Soc.* **2007**, *129*, 417.



58. a) Kritzer, J. A.; Hodsdon, M. E.; Schepartz, A. *J. Am. Chem. Soc.* **2005**, *127*, 4118. b) Kritzer, J. A.; Lear, J. D.; Hodsdon, M. E.; Schepartz, A. *J. Am. Chem. Soc.* **2004**, *126*, 9468.
59. Stephens, O. M.; Kim, S.; Welch, B. D.; Hodsdon, M. E.; Kay, M. S.; Schepartz, A. *J. Am. Chem. Soc.* **2005**, *127*, 13126.
60. Sadowsky, J. D.; Fairlie, W. D. Hadley, E. B. Lee, H.-S. Umezawa, N.; Nikolovska-Coleska Z.; Wang, S.; Huang, D. C. S.; Tomita, Y.; Gellman, S. H. *J. Am. Chem. Soc.* **2007**, *129*, 139.
61. Seebach, D.; Schaeffer, L.; Brenner, M.; Hoyer, D. *Angew. Chem. Int. Ed.* **2003**, *42*, 776.
62. Roviello, G. N.; Musumeci, D.; Pedone, C.; Bucci, E. M. *Amino Acids*, **2010**, *38*, 103.
63. Farrera-Sinfreu, J.; Giralt, E.; Castel, S.; Albericio, F.; Royo, M. *J. Am. Chem. Soc.* **2005**, *127*, 9459.
64. Claudon, P.; Violette, A.; Lamour, K.; Decossas, M.; Fournel, S.; Heurtault, B.; Godet, J.; Mély, Y.; Jamart-Grégoire, B.; Averlant-Petit, M. -C.; Briand, J, -P.; Duportail, J.; Monteil, H.; Guichard, G. *Angew. Chem. Int. Ed.* **2010**, *49*, 333.
65. Benke, S. N.; Thulasiram, H. V.; Gopi, H. N. *ChemMedChem* **2017**, *12*, 1610.
66. Raguse, T. L.; Lai, J. R.; LePlae, P. R.; Gellman, S. H. *Org. Lett.* **2001**, *3*, 3963
67. Horne, W. S.; Price, J. L.; Keck, J. L.; Gellman, S. H. *J. Am. Chem. Soc.* **2007**, *129*, 4178.
68. Clark, T. D.; Buehler, L. K.; Ghadiri, M. R. *J. Am. Chem. Soc.* **1998**, *120*, 651.
69. a) Martinek, T.A.; Hetenyi, A.; Fulop, L.; Mandity, I.M.; Toth, G. K., Dekany, I., Fulop, F. *Angew. Chem. Int. Ed.* **2006**, *45*, 2396. b) Hetényi, A.; Mándity, I. M.; Martinek, T.A.; Tóth, G. K.; Fülöp, F. *J. Am. Chem. Soc.* **2005**, *127*, 547. c) Mándity, I. M.; Fülöp, L.; Vass, E.; Tóth, G. K.; Martinek, T. A.; Fülöp, F. *Org. Lett.* **2010**, *12*, 5584.
70. a) Yoo, S. H.; Lee, S. H. *Acc. Chem. Soc. Res.* **2017**, *50*, 832. b) Kwon, S.; Shin, H.S.; Gong, J.; Eom, J. H.; Jeon, A.; Yoo, S. H.; Chung, I. S.; Cho, S. J.; Lee, H. S. *J. Am. Chem. Soc.* **2011**, *133*, 17618. c) Kwon, S.; Jeon, A.; Yoo, S.H.; Chung, I. S.; Lee, H. S. *Angew. Chem. Int. Ed.* **2010**, *49*, 8232.
71. Jadhav, S. V.; Misra, R.; Gopi, H. N. *Chem. Eur. J.* **2014**, *20*, 16523.
72. Montenegro, J.; Ghadiri, R. M.; Granja, J. R. *Acc. Chem. Res.* **2013**, *46*, 2955.
73. Misra, R.; Reja, R. M.; Narendra, L. V.; George, G.; Raghothama, S.; Gopi, H. N. *Chem. Commun.* **2016**, *52*, 9597.

74. Jadhav, S. V.; Gopi, H. N. *Chem. Commun.* **2013**, *49*, 9181.
75. Misra, R.; Dey, S.; Reja, R. M.; Gopi, H. N. *Angew. Chem. Int. Ed.* **2018**, *57*, 1057.
76. Misra, R.; Saseendran, A.; Dey, S.; Reja, R. M.; Gopi, H. N. *Angew. Chem. Int. Ed.* **2019**, *58*, 2251.
77. Baldauf, C.; Gunther, R.; Hofmann, H.-J. *J. Org. Chem.* **2004**, *69*, 6214.
78. a) Chakraborty, T. K.; Roy, S.; Kumar, S. K.; Kunwar, A. C. *Tetrahedron Lett.* **2005**, *46*, 3065. b) Chakraborty, T. K.; Roy, S.; Koley, D.; Dutta, S. K.; Kunwar, A. C. *J. Org. Chem.* **2006**, *71*, 6240. c) Chakraborty, T. K.; Arora, A.; Roy, S.; Kumar, N.; Maiti, S. *J. Med. Chem.* **2007**, *50*, 5539. d) Siriwardena, A.; Pulukuri, K. K.; Kandiyal, P. S.; Roy, S.; Bande, O.; Ghosh, S.; Fernandez, J. M. G.; Martin, F. A.; Ghigo, J.-M.; Beloin, C.; Ito, K.; Woods, R. J.; Ampapathi, R. S.; Chakraborty, T. K. *Angew. Chem. Int. Ed.* **2013**, *52*, 10221.
79. Sharma, G. V. M.; Babu, B. S.; Ramakrishna, K. V. S.; Nagendar, P.; Kunwar, A. C.; Schramm, P.; Baldauf, C.; Hofmann, H.-J. *Chem. Eur. J.* **2009**, *15*, 5552.
80. Jiang, H.; Léger, J. M.; Huc, I. *J. Am. Chem. Soc.* **2003**, *125*, 3448.
81. Gauthier, D.; Baillargeon, P.; Drouin, M.; Dory, Y. L. *Angew. Chem. Int. Ed.* **2001**, *40*, 4635.
82. Banerjee, A.; Pramanik, A.; Bhattacharjya, S.; Balaram, P. *Biopolymers* **1996**, *39*, 769.

## *Chapter 2*

# **Engineering $\beta$ -Hairpin with Flexible $\delta$ - Amino Acids for Disruption of $\beta$ -Amyloid Aggregation**

## 2.1. Introduction

Functions of protein are intrinsically linked to their specific three dimensional structures.<sup>1</sup> Hypothetical dissection three dimensional structure of proteins leads to the three different types of secondary structure elements, such as helices,  $\beta$ -sheet and reverse turn along with loosely structure loops. Reverse turns changes the direction of the polypeptide chains. Among the reverse turns,  $\beta$ -turns are most prevalent in the proteins. Compared to  $\beta$ -sheets and  $\alpha$ -helices, it is difficult to design reverse turns because of their non-periodic nature and structure heterogeneity.<sup>2</sup> Besides the natural  $\beta$ -turn inducing motif, different groups have been extensively utilized different amino acids and organic template based reverse turn to design variety of  $\beta$ -hairpin mimetics.<sup>3</sup> The  $\beta$ -hairpin structure motif constitutes of binding epitopes of various proteins and play a significant role in molecular recognition. High resolution structures revealed that turns are present in different antibody-peptide complexes.<sup>4</sup> This complex structure are entirely consistent with the recognition motif which is derived from the structure activity relationship of different peptide hormones such as bradykinin,<sup>5a,5b</sup> angiotensin II,<sup>5c,5d</sup> somatostatin,<sup>5e,5f</sup> RGD (Arg-Gly-Asp)<sup>5g,5h</sup> sequence etc. In addition,  $\beta$ -hairpin structural motifs with different reverse turn motifs are part of a large family of cationic antimicrobial peptides such as mammalian defensin, tachyplesins, protegrins etc (Figure 2.1E). These peptides show broad spectrum antimicrobial activity against different Gram positive and Gram negative bacteria.<sup>6</sup> Apart from the antimicrobial activity of the  $\beta$ -hairpin, different  $\beta$ -hairpins scaffolds were also been explored to mimic the structural similarity of epitope and cytokine receptor.<sup>7</sup> In this context, Robinson and colleagues reported  $\beta$ -hairpin peptidomimetics containing <sup>D</sup>Pro-<sup>L</sup>Pro as reverse turn which binds with HDM2 protein and inhibits the interaction of p53-HDM2 interactions (Figure 2.1B).<sup>7f</sup> Apart from the biological importance different  $\beta$ -hairpins are also used as asymmetric catalyst for different organic transformation reactions because of its properties in tunability and modality.<sup>8</sup> The group of Miller and co-workers extensively utilized varieties of  $\beta$ -turn mimetic catalysts to establish mechanism-based phosphorylation, conjugate

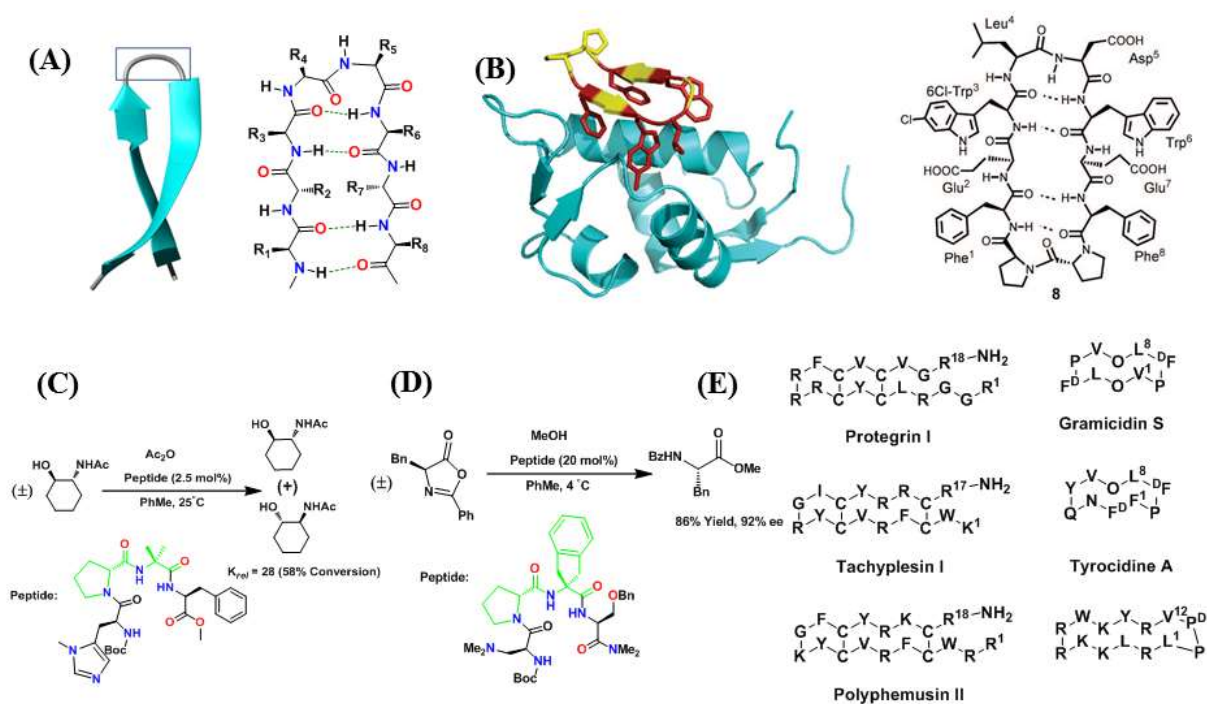


**Figure 2.1:** (A) Schematic representation of  $\beta$ -hairpin and reverse turn. (B) Binding of designed  $\beta$ -hairpin with HDM2 (PDB Code: 2AXI) (C) and (D) Asymmetric catalyst reactions by designed  $\beta$ -turn (E) Naturally occurring antimicrobial  $\beta$ -hairpins. Figure 2.1B was reproduced with permission from ref 3a.

addition, asymmetric acylation, asymmetric C-C bond formation and site specific reaction (Figure 2.1C).<sup>8a-8c</sup> In addition different  $\beta$ -hairpins are also used for design self-assembled materials such as hydrogels. These hydrogels are further used for the tissue culture, drug delivery system and different biotechnological application.<sup>9</sup> Thus  $\beta$ -hairpin is one of the important structural motif that displayed widespread applications in biology, medicinal chemistry as well as in biotechnology. These widespread applications of  $\beta$ -hairpins has attracted synthetic chemists and structural biologist to design stable  $\beta$ -turns and  $\beta$ -hairpins using different natural and non-natural amino acids.

## 2.2. Design of $\beta$ -Turns

In case of hairpin structure, two antiparallel  $\beta$ -strand are connected by a segment of reverse turn residues. Depending upon the hydrogen bonding pattern these reverse turns can be classified into different classes. The analysis of the various high resolution protein structures suggested that  $\beta$ -

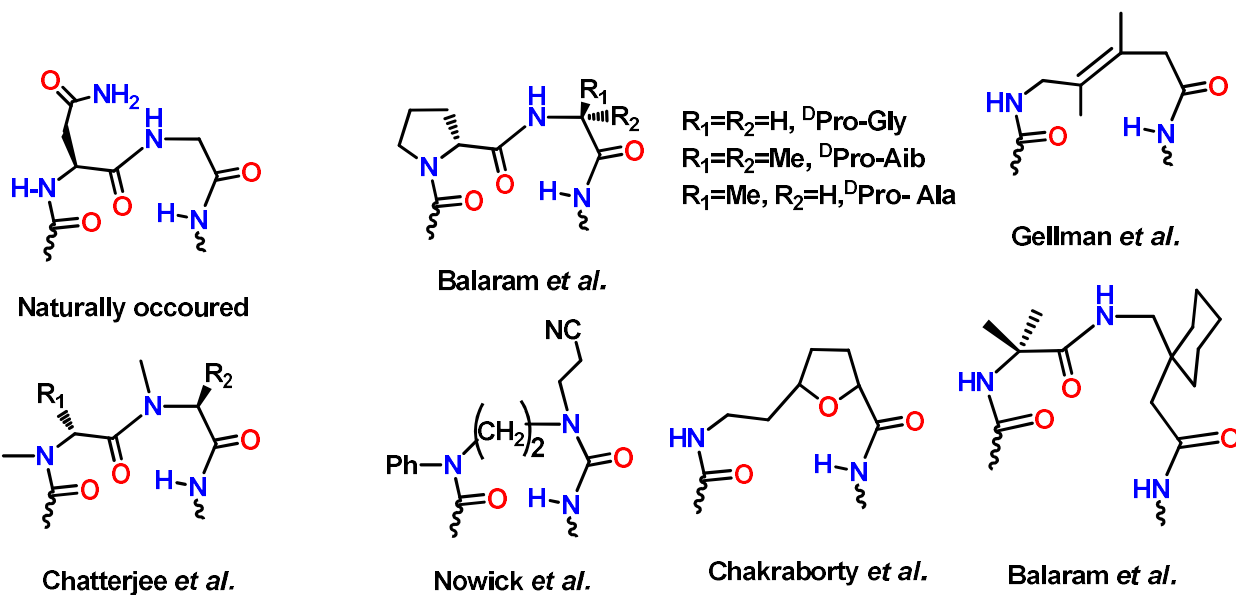
turns are the most predominant reverse turns. A  $\beta$ -turn consists of four residues and designated as  $i, i+1, i+2, i+3$  where the polypeptide chain changes its direction about  $180^\circ$ . Mainly, the  $\beta$ -turn structures are further classified into various types such as type I, type II, type I' type II' etc based on the torsion angles of residues  $i+1$  and  $i+2$ . The list torsion angles of different types of  $\beta$ -turns are shown in Table 2.1.

**Table 2.1:** List of different  $\beta$ -turns and their torsion angles

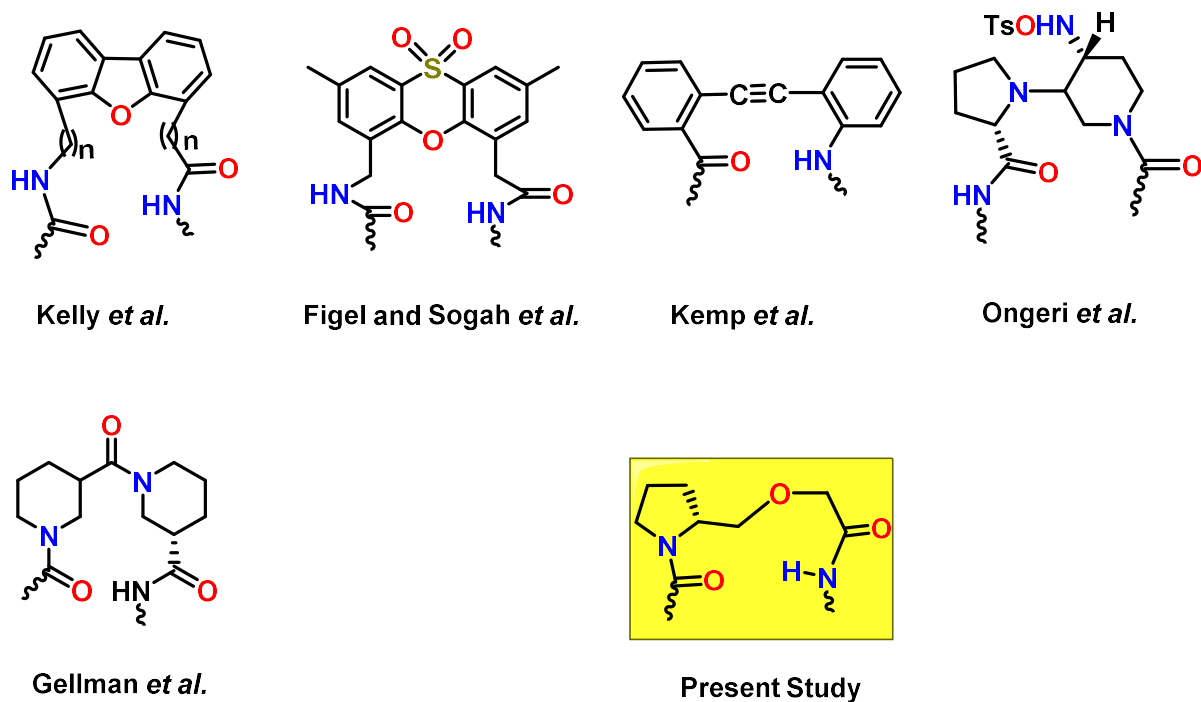
Type	$\Phi_{i+1} (^\circ)$	$\Psi_{i+1}(^\circ)$	$\Phi_{i+2}(^\circ)$	$\Psi_{i+2}(^\circ)$
I	-60	-30	-90	0
II	-60	120	80	0
I'	60	30	90	0
II'	60	-120	-80	0

Among them type I  $\beta$ -turns are common in protein structures. These turns are play an important role in various types of biological process including protein-protein, protein-peptide, protein-DNA interaction, biomolecular recognition, phosphorylation, glycosylation and hydroxylation.<sup>10</sup> Extensive efforts have been made over the last few decades in the design of artificial  $\beta$ -turns. These  $\beta$ -turns not only provides insight towards understanding the higher order bimolecular structures but also they can be useful in designing drug like functional epitopes. In this context, various types of  $\beta$ -turns such as  $^D\text{Pro-XX}$  (where XX is Gly, Pro, Aib), Aib- $^D\text{Ala}$  etc have been developed to stabilize  $\beta$ -hairpin conformations.<sup>11</sup> Besides designing  $^D\text{Pro-XX}$  (XX= Gly, Aib, Pro, Ala etc.) as a  $\beta$ -turn segment, Balaram and co-workers further expanded the  $\beta$ -turn mimetics using  $^D\text{Pro-Xaa}$  (Xaa=  $\beta$ -,  $\gamma$ -, and  $\delta$ - amino acid) dipeptide template. They have shown that peptides with  $\alpha, \beta$ - and  $\alpha, \gamma$ - residues at the turn can adopt  $\beta$ -hairpin structures in polar protic solvent.<sup>12</sup> Besides the peptides, different organic template and building blocks have also been reported as  $\beta$ -turn mimetics. Kemp and colleagues demonstrated the 2,2'-substituted tolan as  $\beta$ -turn mimetic.<sup>13</sup> Further, Figel and Sogah studied the reverse turn inducing properties of 4-phenoxathiin derivatives.<sup>14</sup> Kelly and co-workers have examined the ability of dibenzofuran-based amino

### Amino acid based template as reverse turn:



### Organic Template Based Reverse Turn



acids as reverse turns.<sup>15</sup> Further, Gellman and co-workers have showed utility of tetra substituted alkenes in inducing  $\beta$ -turns.<sup>16</sup> Borggraeve and co-workers have designed amino(oxo)piperidinecarboxylate scaffolds as reverse turns.<sup>17</sup> Nowick and colleagues showed urea derivatives and 5-amino-2-methoxybenzoic acids as  $\beta$ -turns.<sup>18</sup>

### 2.3. Aim and Rationale of the Present Work

From the last few years, we have been interested in the utilization of various non natural amino acids for the design of different functional peptide foldamers.<sup>19</sup> Recently we showed the utilization of  $\alpha,\beta$ -unsaturated- $\gamma$ -amino acid in the design of  $\beta$ -hairpin and three stranded  $\beta$ -hairpin using <sup>D</sup>Pro-Gly as a  $\beta$ -turn-inducing segment.<sup>20</sup> Through extensive theoretical studies Hoffman and co-workers proposed that  $\delta$ -amino acids can be used as  $\beta$ -turn segment to design  $\beta$ -hairpins.<sup>21</sup> The amide bond between  $i+1$  and  $i+2$  will be replaced by the  $C^\beta-C^\gamma$  bond in  $\delta$ -amino acid mediated  $\beta$ -turns. Motivated by the theoretical predictions, we sought to investigate whether or not  $\beta(O)-\delta^5$ -amino acids can be used as single residue  $\beta$ -turn to design  $\beta$ -hairpins. Furthermore, we sought to investigate the disruption of A $\beta$  (1-42) amyloid aggregation of Alzheimer's disease using designed  $\beta$ -hairpins.

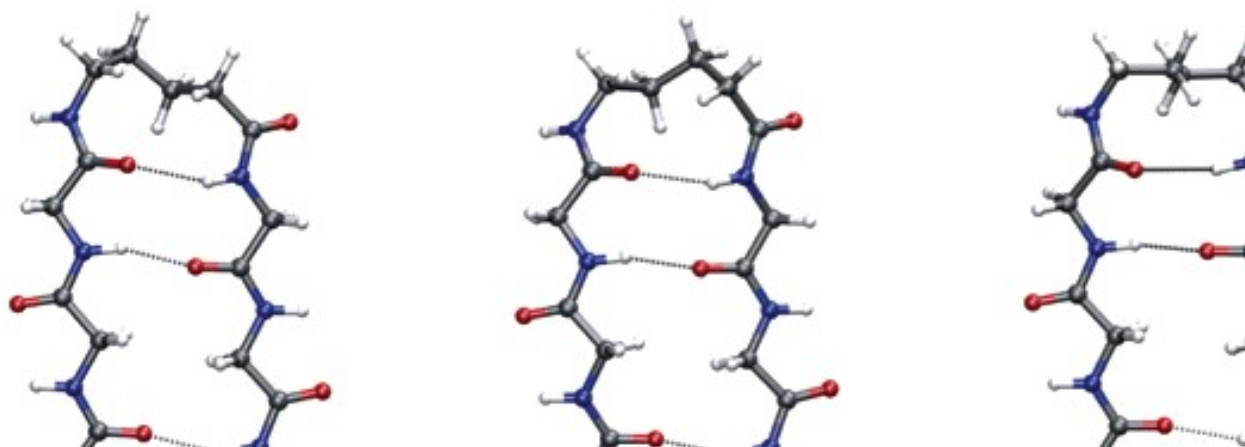


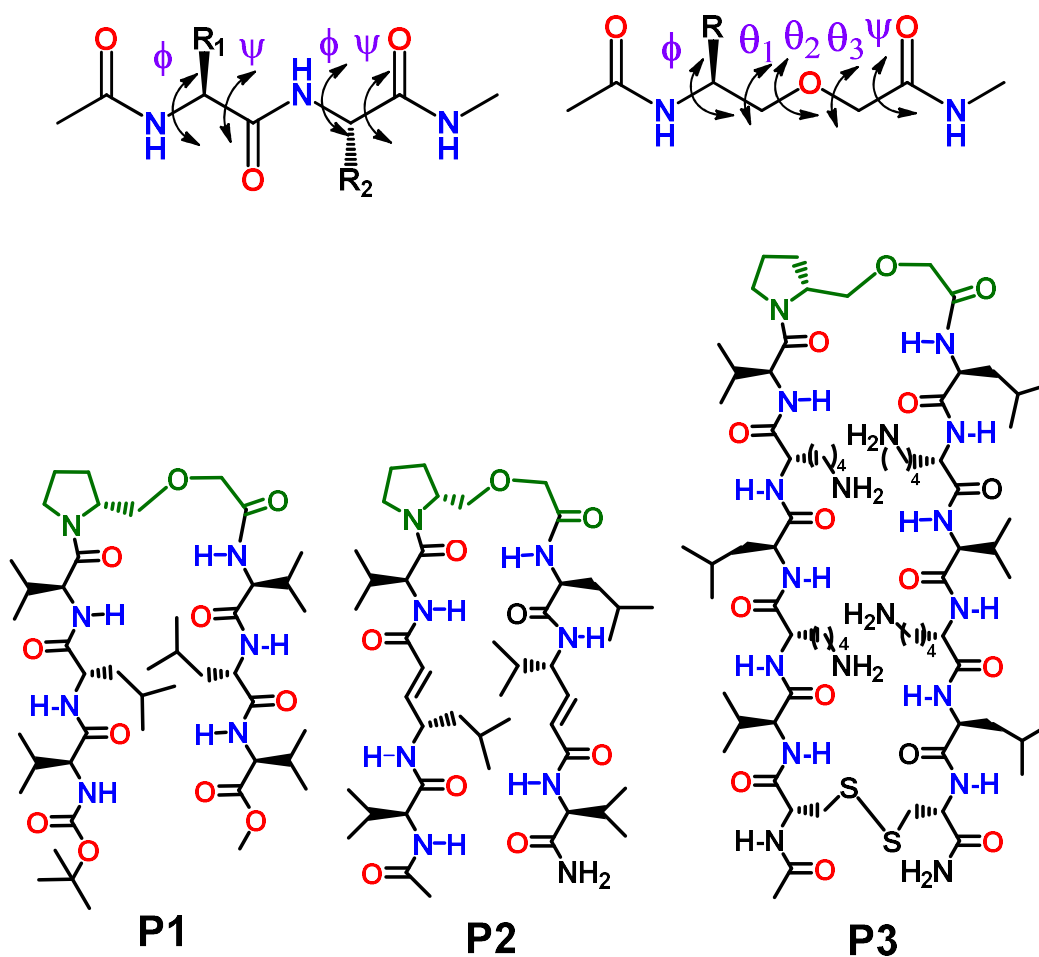
**Figure 2.2:** Formation of  $\beta$ -hairpins composed of  $\delta$ -amino acids as single residue  $\beta$ -turn. Figure was reproduced with permission from ref 21.



## 2.4. Results and Discussion

### 2.4.1. Design and Synthesis

To understand whether or not  $\delta$ -amino acids can be used as  $\beta$ -turns, we have synthesized  $\beta(O)$ - $\delta^5$ -D-Pro-OH starting from the *N*-Boc protected (D)-proline alcohol. Reaction between *N*-Boc protected amino alcohol and *tert*-butyl bromo acetate in the presence of base leads to the formation of *tert*-butyl ester of *N*-Boc protected  $\beta(O)$ - $\delta^5$ -D-Pro-OH. The acid labile Boc-group and *tert*-butyl esters were removed using TFA and the free amine was further protected with either Fmoc- or Boc- groups.



**Scheme 2.1:** Sequences of peptides under investigations.

The Fmoc- $\beta(\text{O})\text{-}\delta^5\text{-}^{\text{D}}\text{Pro-OH}$  was used in the solid phase synthesis, while Boc- $\beta(\text{O})\text{-}\delta^5\text{-}^{\text{D}}\text{Pro}$  was used in the solution phase peptide synthesis. The synthesis of the  $\beta(\text{O})\text{-}\delta^5\text{-}^{\text{D}}\text{Pro-OH}$  is shown in the experimental section. The single crystal conformation of Fmoc- $\beta(\text{O})\text{-}\delta^5\text{-}^{\text{D}}\text{Pro-OH}$  is shown in the Figure 2.3. Using  $\beta(\text{O})\text{-}\delta^5\text{-}^{\text{D}}\text{Pro}$ , we have designed and synthesized three peptides **P1-P3**. The sequences of these peptides are shown in the Scheme 2.1. Peptide **P1** was synthesized by the conventional solution phase condensation strategy using EDC.HCl/HOBt as a coupling reagent. Peptides **P2** and **P3** were synthesized by conventional manual solid phase peptide synthesis on Rinak Amide resin on 0.2 mmol scale. Fmoc- group was deprotected using 20% piperidine in DMF. All peptide couplings were carried out using HBTU/HOBt as coupling reagent, DIEA as base in NMP solvent. For disulfide formation in peptide **P3**, the crude peptide **P3** was dissolved in  $\text{NH}_4\text{CO}_3$  buffer (20 mM, pH 7.4, peptide concentration 2 mM) and stirred for about 24 h in an open flask. Insoluble material was separated by centrifugation and the supernatant solution lyophilized and purified on reverse phase HPLC using C18 column by ACN/ $\text{H}_2\text{O}$  system. The hydrophobic peptides **P1** and **P2** were purified on reverse phase HPLC using C18 column by MeOH/ $\text{H}_2\text{O}$  system.

#### 2.4.2. ORTEP Diagram of Compound 3 and Peptide P2

##### Compound 3 (FmocNH- $\beta(\text{O})\text{-}\delta^5\text{-}^{\text{D}}\text{Pro-OH}$ )

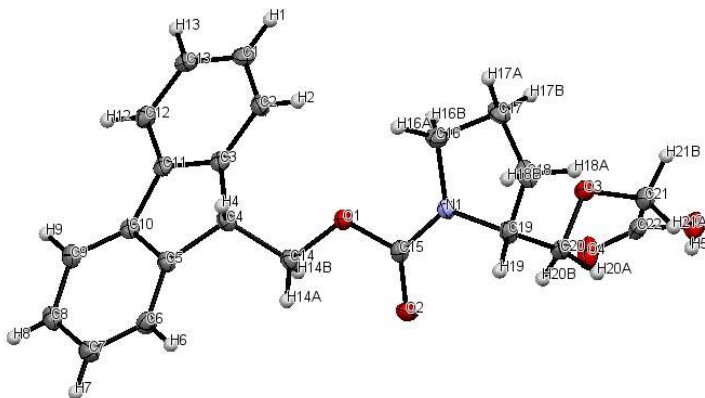


**Figure 2.3:** ORTEP diagram of compound 3. Ellipsoids are drawn at 50% probability. (CCDC No 1950179)

## Peptide P2:

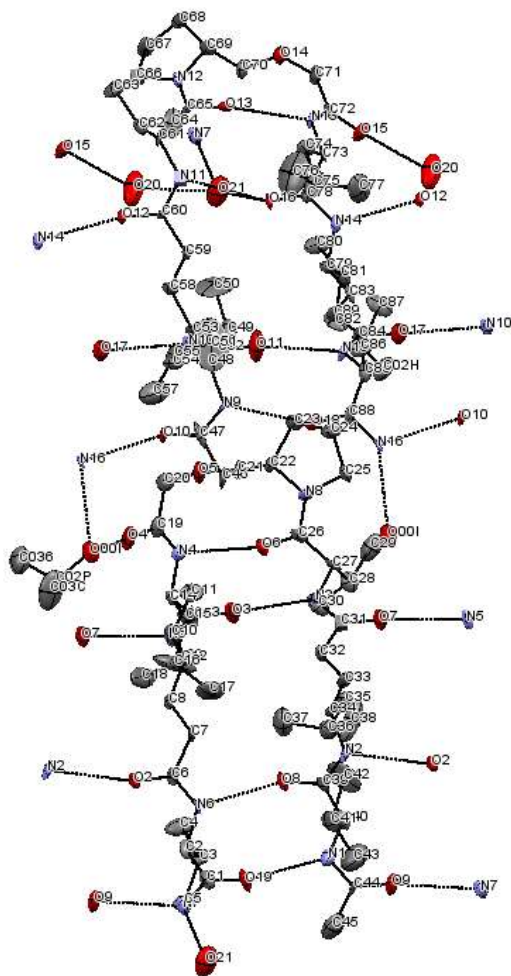


**Figure 2.4:** ORTEP diagram of peptide **P2**. H-bonds are shown in dotted lines. H-atoms are omitted for clarity. Ellipsoids are drawn at 50% probability. (CCDC No 1950178)

### 2.4.3. Conformational Analysis of Peptide P1

To know the conformational analysis of the peptides, peptide **P1** was subjected for 2D NMR analysis in CDCl<sub>3</sub> (3 mM). The <sup>1</sup>H NMR of the peptide **P1** revealed a well dispersed NH and C<sup>α</sup>H region suggesting a well-defined secondary structure in solution. Fully assigned <sup>1</sup>H NMR spectrum of peptide **P1** is shown in the Figure 2.5. The amino acid type and sequential connectivity of the residues were established using ROESY and TOCSY spectra. The fully assigned partial ROESY spectrum depicting NH↔NH interactions and NH↔C<sup>α</sup>H interactions are shown in the Figure 2.6 and Figure 2.7, respectively. The NMR analysis revealed the medium NH(3)↔NH(5), weakNH(1)↔NH(7) and strong NH(2)↔C<sup>α</sup>H(1), NH(3)↔C<sup>α</sup>H(2), NH(6)↔C<sup>α</sup>H(5), NH(7)↔C<sup>α</sup>H(6), NH(5)↔C<sup>α</sup>H(4), C<sup>α</sup>H(2)↔C<sup>α</sup>H(6) interactions. Key NOEs

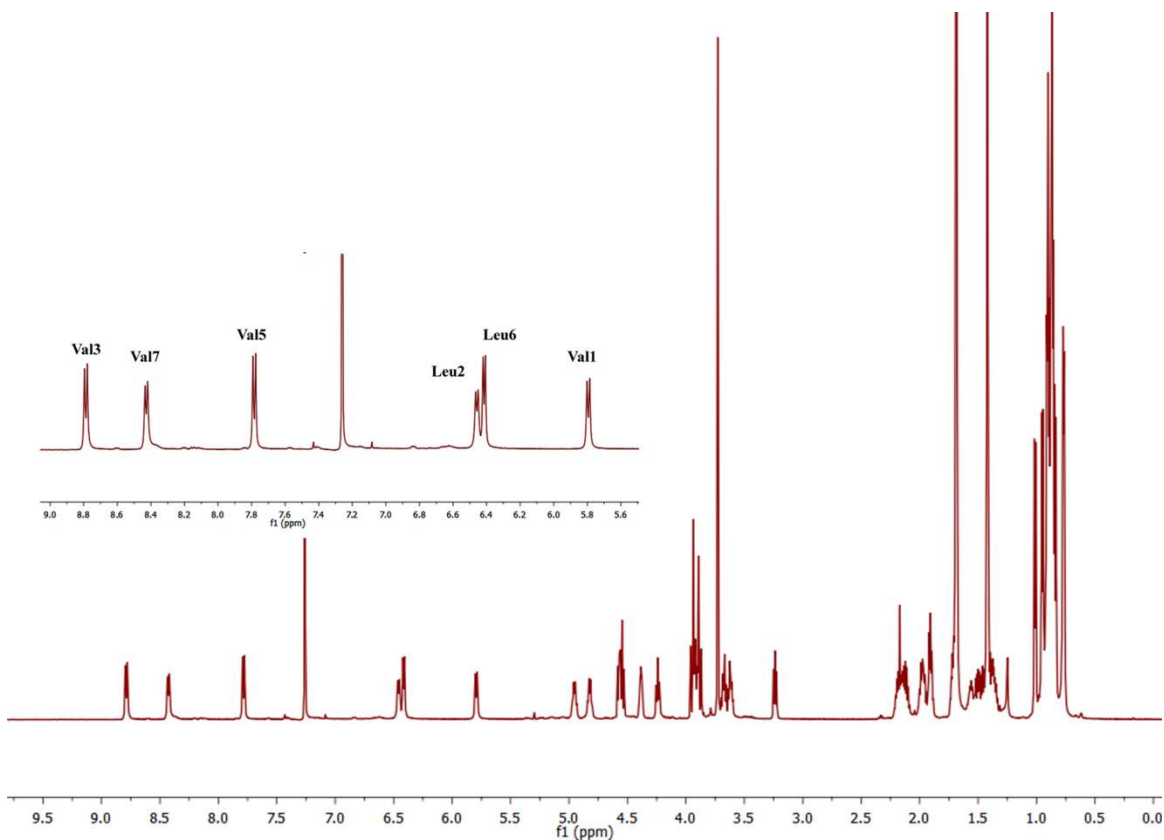


**Figure 2.5:** Full <sup>1</sup>H NMR spectra of peptide **P1** in CDCl<sub>3</sub> (3mM). NHs region is shown in insert.

are tabulated in the Table 2.2. Further, we subjected peptide **P1** for the temperature dependent NMR to understand the involvement of amide NH groups in the H-bonding. Experimental results suggested that the change in chemical shift of NH(5) is very negligible compared to other NHs. (Figure 2.9 and 2.10), indicating that the turn is stabilized by the 10 membered H-bond between CO(3)---NH(5). Further, the DMSO-*d*<sub>6</sub> titration in CDCl<sub>3</sub> indicates NH(1), NH(3), NH(5) and NH(7) are involved in the intramolecular H-bond and stabilized the overall hairpin structure (See Figure 2.11). Using the distance restraints from ROESY, the solution conformation of **P1** was generated. The ensemble of NMR structures resulting from the restrained MD simulations on the basis of the NOE and H-bond constrain is shown in Figure 2.12. The peptide adopted  $\beta$ -hairpin conformation in solution. Overall, this structural analysis suggested that  $\beta$ (O)- $\delta^5$ -<sup>D</sup>Pro can stabilize the  $\beta$ -hairpin conformation in peptides with 10 member hydrogen bond pseudocycle similar to <sup>D</sup>Pro-Gly dipeptide. The list of the average torsion angles of the newly designed reverse turns are given in the Table 2.4. The torsion angles observed in are consistent with the value reported by Hofmann and colleagues for unsubstituted  $\delta$ - amino acids.<sup>21</sup>

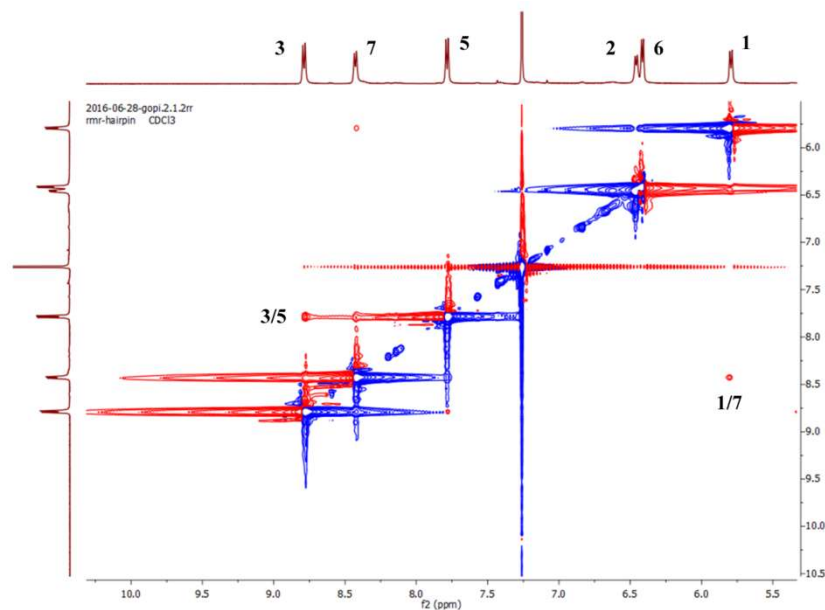


**Figure 2.6:** Partial ROESY spectrum of peptide **P1** (3mM) in CDCl<sub>3</sub> showing NH $\leftrightarrow$ NH interactions.

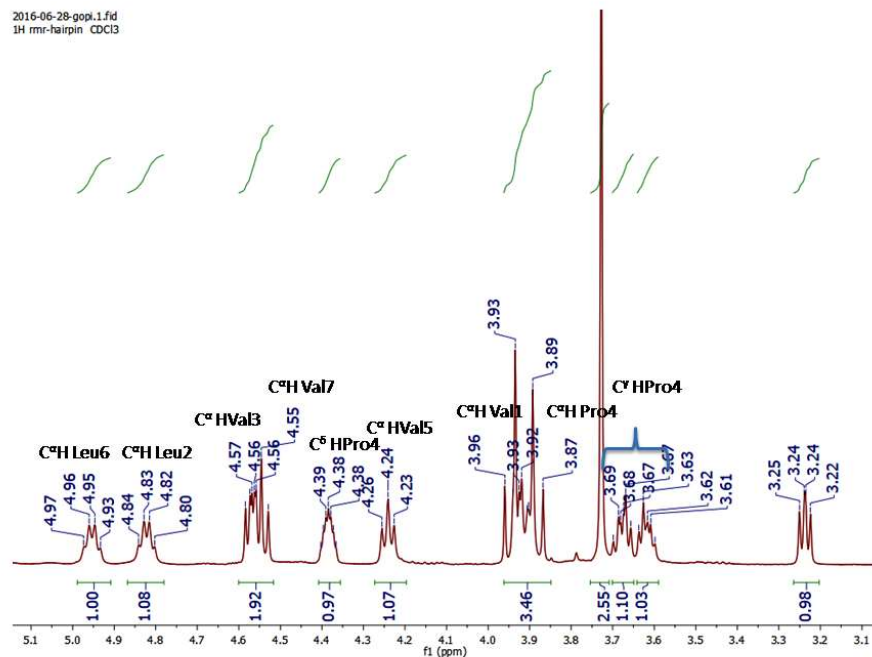


**Figure 2.7:** Partial  $^1\text{H}$  NMR of peptide **P1** ( $\text{C}^\alpha\text{H}$ ,  $\text{C}^\beta\text{H}$ ,  $\text{C}^\gamma\text{H}$  region).

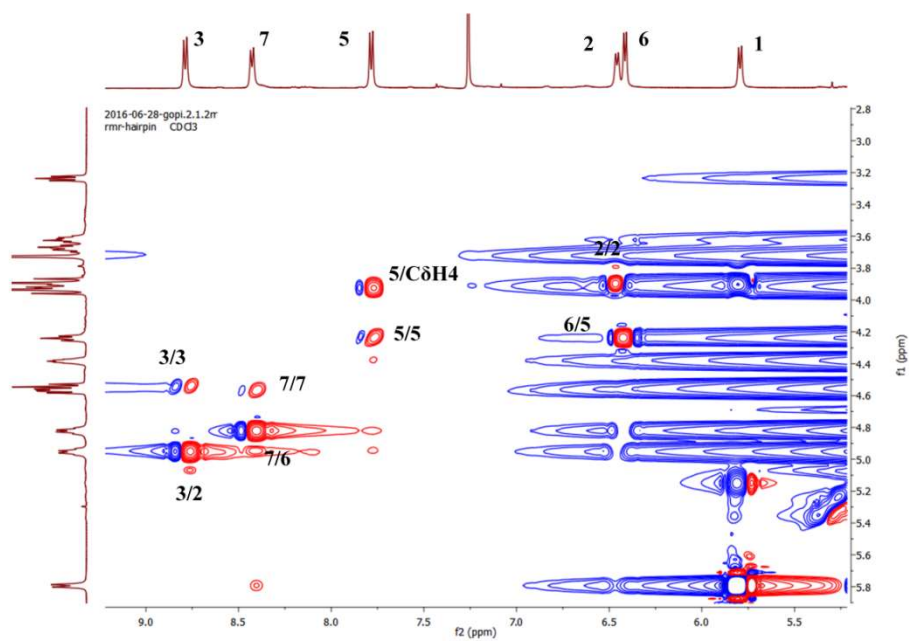


**Figure 2.8:** Partial ROESY spectrum of peptide **P1** (3mM) in  $\text{CDCl}_3$  showing  $\text{NH} \leftrightarrow \text{C}^\alpha\text{H}$ ,  $\text{NH} \leftrightarrow \text{C}^\beta\text{H}$ ,  $\text{NH} \leftrightarrow \text{C}^\delta\text{H}$  interactions.

**Table 2.2:** Key NOEs observed for peptide **P1**

<b>Residue</b>	<b>H-atom</b>	<b>Residue</b>	<b>H-atom</b>	<b>NOE Observed</b>
Val3	NH	Val5	NH	Medium
Val1	NH	Val7	NH	Weak
Leu2	NH	Val1	C <sup>α</sup> H	Strong
Val3	NH	Leu2	C <sup>α</sup> H	Strong
Leu6	NH	Val5	C <sup>α</sup> H	Strong
Val7	NH	Leu6	C <sup>α</sup> H	Strong
Val5	NH	δPro4	C <sup>δ</sup> H	Weak
Leu2	NH	Leu2	C <sup>α</sup> H	Medium
Val3	NH	Val3	C <sup>α</sup> H	Medium
Val5	NH	Val5	C <sup>α</sup> H	Medium
Leu6	NH	Leu6	C <sup>α</sup> H	Medium
Val7	NH	Val7	C <sup>α</sup> H	Medium
Leu6	C <sup>α</sup> H	Leu2	C <sup>α</sup> H	Strong

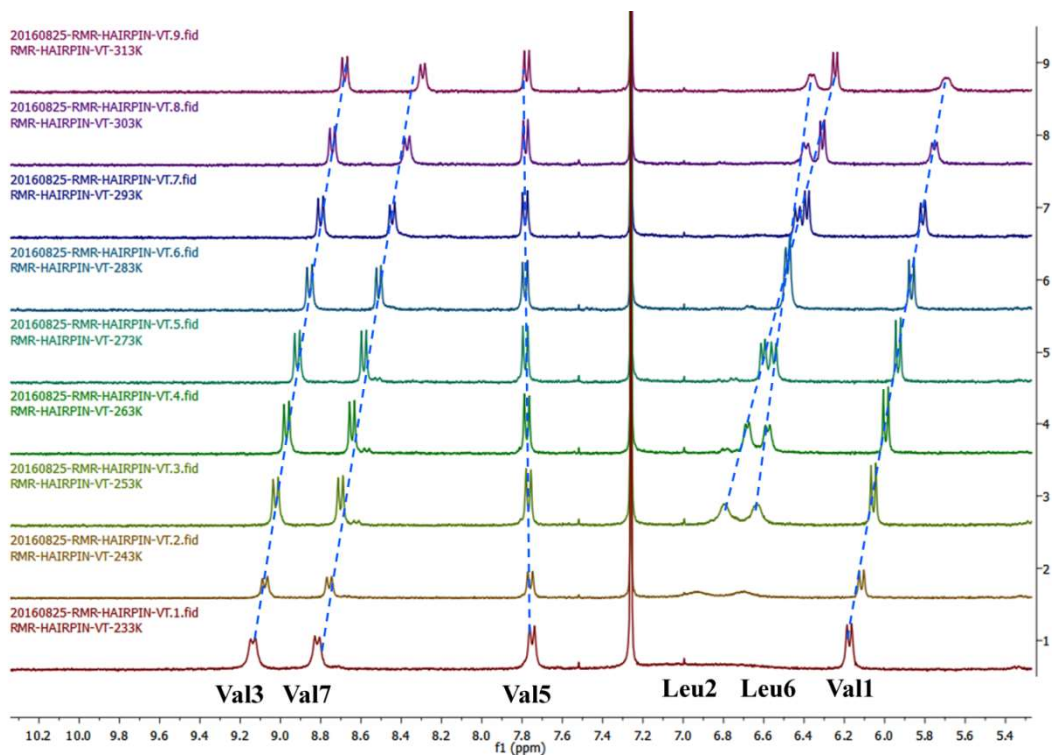


Figure 2.9: Temp dependent  $^1\text{H}$ NMR spectra (NH region) of peptide **P1** from 233 K to 313 K.

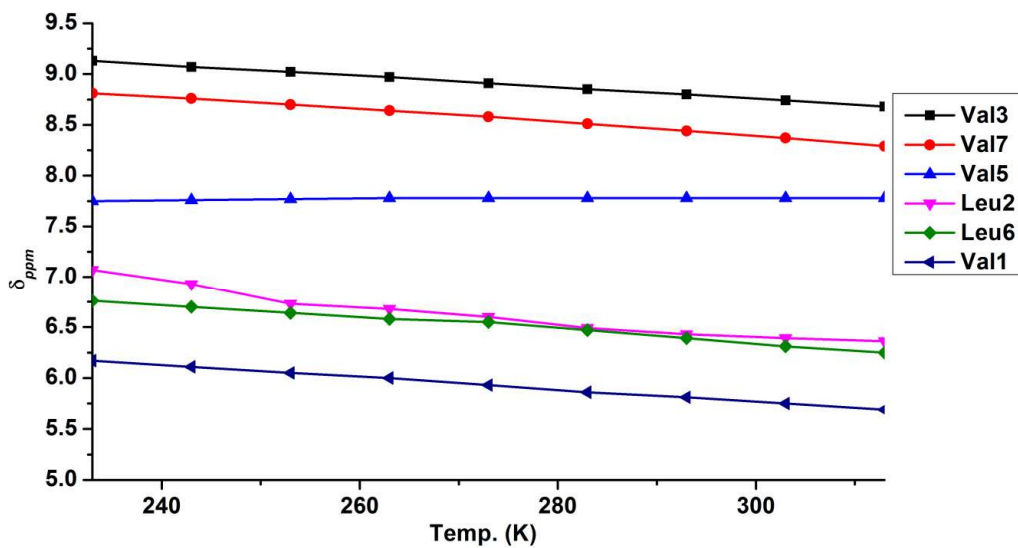
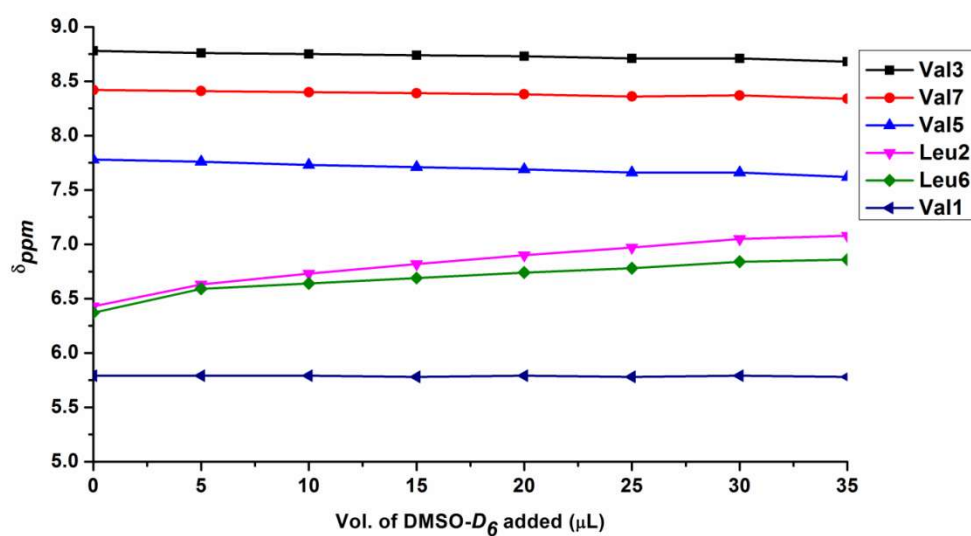


Figure 2.10: Plot of Temp vs chemical shift ( $\delta_{ppm}$ ) for peptide **P1** in  $\text{CDCl}_3$



**Table 2.3:** Calculation of  $d\delta/dT$  for peptide **P1**

Residue	233K	243K	253K	263K	273K	283K	293K	303K	313K	$d\delta/dT(\text{ppb})$
Val3	9.13	9.07	9.02	8.97	8.91	8.85	8.80	8.74	8.68	5.6
Val7	8.81	8.76	8.70	8.64	8.58	8.51	8.44	8.37	8.29	6.5
Val5	7.75	7.76	7.77	7.78	7.78	7.78	7.78	7.78	7.78	0.3
Leu2	7.07	6.93	6.79	6.68	6.60	6.49	6.43	6.39	6.36	8.8
Leu6	6.76	6.70	6.64	6.58	6.55	6.47	6.39	6.31	6.25	6.3
Val1	6.17	6.11	6.05	6.00	5.93	5.86	5.81	5.75	5.69	6.0



**Figure 2.11:** Plot of chemical shift ( $\delta_{ppm}$ ) vs vol. of  $\text{DMSO-}d_6$  for peptide **P1** in  $\text{CDCl}_3$ .

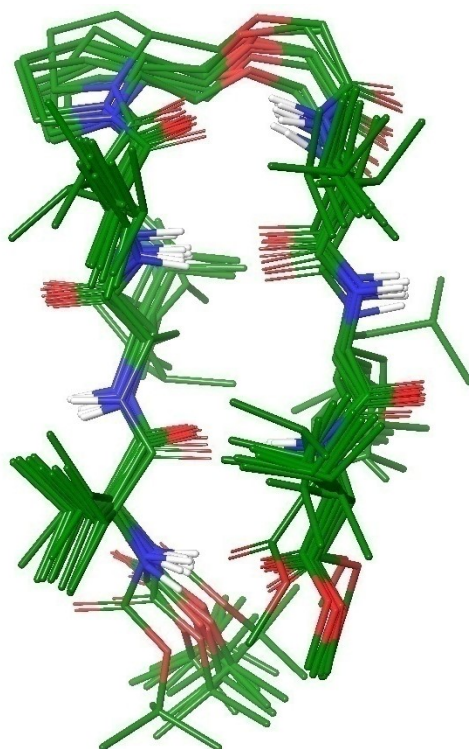


**Figure 2.12:** Superimposed NMR structures form peptide **P1** in  $\text{CDCl}_3$  solvent.

**Table 2.4:** Torsion angles for  $\beta(\text{O})\text{-}\delta^5$ -amino acid measured from the minimized conformation of structure **P1**

StructureP1	$\phi(\text{deg})$	$\theta_1(\text{deg})$	$\theta_2(\text{deg})$	$\theta_3(\text{deg})$	$\Psi(\text{deg})$
1	50.61	-103.29	-175.30	-79.89	-25.64
2	51.35	-107.73	-175.83	-81.23	-24.21
3	52.37	-108.01	-176.17	-80.30	-23.55
4	46.62	-96.50	-171.19	-76.76	-25.35
5	57.69	-87.95	177.78	-124.88	-6.35
6	68.25	-126.64	176.34	-81.12	-15.28
7	51.58	-108.02	-177.17	-87.24	-20.60

8	50.53	-109.79	-178.11	-89.40	-18.18
9	43.49	-92.71	-172.58	-72.21	-35.56
10	49.61	-109.38	-175.39	-82.44	-20.75
Range	43 to 69	-127 to -87	178 to -171	-125 to -72	-36 to -6
Average	52.21	-105.00	-176.76	-85.55	-21.55

#### 2.4.4. Conformational Analysis of Peptide P2

Recently, we demonstrated single crystal conformations of  $\beta$ -hairpins and three-stranded  $\beta$ -sheets by incorporating  $\beta$ -sheet promoting  $\alpha,\beta$ -unsaturated  $\gamma$ -amino acids.<sup>20a, 20b</sup> As unsaturated amino acids restrict the rotational freedom, which promote the molecules to take stable conformations and eventually leads to help in getting the single crystals. Single crystal conformation helps to understand the unambiguous conformations of peptides. As peptide **P1** did not give the single crystals even after several attempts, we designed peptide **P2** by incorporating  $\alpha,\beta$ -unsaturated  $\gamma$ -amino acids along the opposite face of  $\beta$ -strands. The sequence of the peptide **P2** is shown in the Scheme 2.1. The details synthetic procedure of *E*-vinylogous amino acids are given in the experimental section. As anticipated, **P2** gave X-ray quality single crystal from the slow evaporation of aqueous methanol/IPA solution. The X-ray diffraction structure of **P2** is shown in Figure 2.13A. The peptide **P2** adopts perfect  $\beta$  hairpin with 10-membered hydrogen bond pseudo cycle in the turn segment. Instructively, the structure was stabilized by the four intramolecular H-bonds between the anti-parallel  $\beta$ -strands. All the exposed NH (d $\gamma$ Leu2 NH and d $\gamma$ Val6) and carbonyls are involved in the intermolecular H bonding with other parallelly positioned  $\beta$ -hairpins in the crystal packing. The packing of the  $\beta$ -hairpin in the single crystals is shown in Figure 2.14. The reported torsion angles for a  $\beta$ -II' turn are  $\phi_{i+1}=60$ ,  $\psi_{i+1}=-120$ ,  $\phi_{i+2}=-80$  and  $\psi_{i+2}=0$ . However, as the amide bond between  $i+1$  and  $i+2$  was replaced by O <sup>$\beta$</sup> -C <sup>$\gamma$</sup>  in peptide **P2** in the turn segment. Peptide **P2** displayed the torsion angles  $\phi = 69$ ,  $\theta_1 = -129$ ,  $\theta_2 = 175$ ,  $\theta_3 = -96$

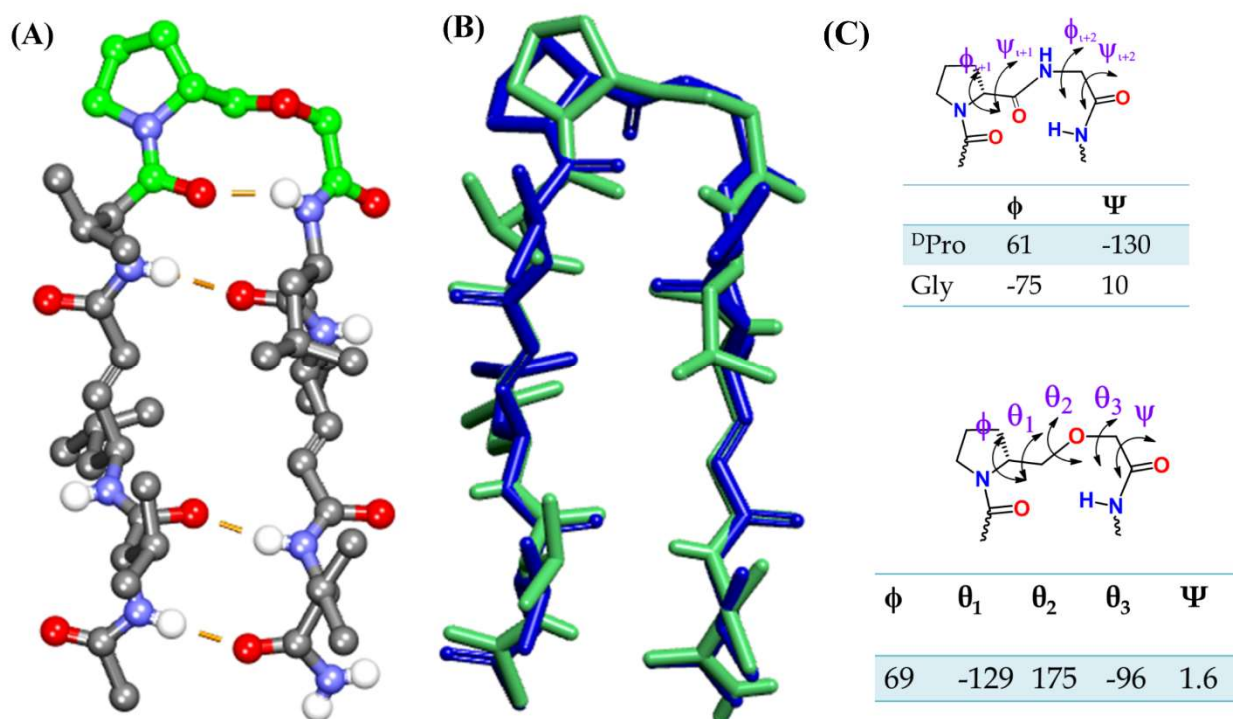


**Figure 2.13:** (A) X-ray structure of peptide **P2** (B) Overlay of X-ray structure of peptide **P2** with  $\beta$ -hairpin having <sup>D</sup>Pro-Gly as reverse turn. (C) Backbone torsion angles of <sup>D</sup>Pro-Gly and  $\beta(O)$ - $\delta^5$ -<sup>D</sup>Pro  $\beta$ -turn in  $\beta$ -hairpin.

and  $\psi = 1.6$ . The torsion angles displayed by the peptide are consistent with the torsion angles of  $\beta$ -II' turn. The superimposition of the backbone conformations of peptide **P2** with the earlier reported  $\beta$ -hairpin<sup>20a</sup> with <sup>D</sup>Pro-Gly in the turn segment is shown in Figure 13B. Instructively, the backbone conformation of the  $\beta$ -turn of peptide **P2** is well correlated with the  $\beta$ -II' turn observed in the  $\beta$ -hairpin containing <sup>D</sup>Pro-Gly. The torsion angles of  $\beta$ -turn having <sup>D</sup>Pro-Gly and  $\beta(O)$ - $\delta^5$ -<sup>D</sup>Pro are shown in Figure 2.13C. Full list of the all torsion angles and the H-bond parameters are shown in Table 2.5 and 2.6 respectively. Further structural analysis of the peptide **P2** revealed that all the  $\alpha$ -amino acids in the anti-parallel  $\beta$ -strand adopted extended conformation. Both (*E*)-vinylogous amino acids *dy*Leu(2) ( $\phi = -116$ ,  $\theta_1 = 120$ ,  $\theta_2 = -179$  and  $\psi = 172$ ) and *dy*Val(6) ( $\phi = -126$ ,  $\theta_1 = 111$ ,  $\theta_2 = -172$  and  $\psi = 176$ ) were nicely accommodated into the  $\beta$ -sheets with a very similar characteristic backbone conformations.<sup>20a</sup>

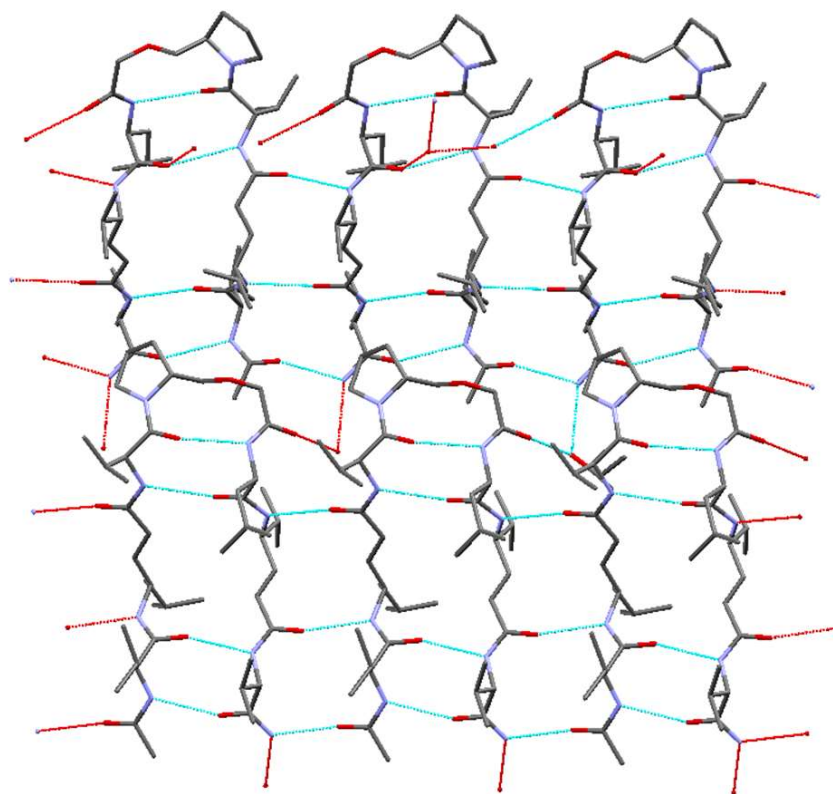


**Figure 2.14:** Lateral assembly of peptide **P2** through intermolecular H bonds.

### Torsion Angles and H-Bond Parameters of Peptide P2

**Table 2.5:** Torsion angles parameters of **P2**:

Peptide **P2** contains two molecules in the asymmetric unit.

#### Molecule A

Peptide P2	$\phi$ (deg)	$\theta_1$ (deg)	$\theta_2$ (deg)	$\theta_3$ (deg)	$\Psi$ (deg)
Val1	-101.3				112.0

dγLeu2	-116.9	117.2	-178.6		164.9
Val 3	-157.0				136.5
β(O)-δ <sup>5</sup> -DPro 4	69.27	-129.4	174.7	-96.4	-0.65
Leu5	-77.1				125.1
dγVal6	-126.3	101.2	-170.3		177.1
Val7	-124.3				120.8

**Molecule B**

<b>Peptide P2</b>	<b>φ(deg)</b>	<b>θ<sub>1</sub> (deg)</b>	<b>θ<sub>2</sub> (deg)</b>	<b>θ<sub>3</sub> (deg)</b>	<b>Ψ (deg)</b>
Val1	-127.2				132.3
dγLeu2	-114.7	122.4	-179.8		179.6
Val 3	-157.9				131.9
β(O)-δ <sup>5</sup> -DPro 4	63.5	-127.1	174.7	-88.30	-8.8
Leu5	-81.4				124.2
dγVal6	-126.1	120.5	-173.9		174.1
Val7	-130.1				123.8

**Table 2.6:** Hydrogen bond parameters of **P2**:

Peptide **P2** contains two molecules in the asymmetric unit.

**Intramolecular H-bonds**

**Molecule A**

<b>Donor(D)</b>	<b>Acceptor(A)</b>	<b>D....A(Å)</b>	<b>DH....A(Å)</b>	<b>NH....O(deg)</b>
N9	O18	2.89	2.07	160.6
N11	O16	3.04	2.26	150.2
N13	O13	2.90	2.17	141.6
N15	O11	2.84	2.01	161.2

**Molecule B**

<b>Donor(D)</b>	<b>Acceptor(A)</b>	<b>D....A(Å)</b>	<b>DH....A(Å)</b>	<b>NH....O(deg)</b>
N1	O19	2.86	2.05	158.3
N4	O3	2.97	2.17	154.1
N5	O6	2.90	2.17	141.8
N6	O8	2.85	2.00	169.6

## Intermolecular H-bonds

### Molecule A

Donor(D)	Acceptor(A)	D...A(Å)	DH...A(Å)	NH...O(deg)
N14	O12	2.84	1.94	175.6
N10	O17	2.83	2.26	155.3
N16	O10	2.88	2.02	171.2

### Molecule B

Donor(D)	Acceptor(A)	D...A(Å)	DH...A(Å)	NH...O(deg)
N7	O9	2.88	2.02	178.2
N2	O2	2.87	2.05	161.3
N5	O7	2.94	2.11	166.9

### 2.4.5. Conformational Analysis of Peptide P3

Peptide **P3** was designed to understand the whether or not  $\beta(\text{O})\text{-}\delta^5\text{-}^{\text{D}}\text{Pro}$  can adopt  $\beta$ -turn conformation in aqueous solution. Both **P1** and **P2** are hydrophobic peptides and their conformation were determined in organic solvent and X-ray crystallography respectively. Peptide **P3** did not give well resolved  $^1\text{H}$  NMR spectrum in water, however CD data suggested that the peptide **P3** adopted  $\beta$ -hairpin conformation in  $1\times\text{PBS}$  buffer at pH 7.4.(Figure **2.15**). To understand it's molecular conformation in solution, we subjected peptide **P3** for the 2D NMR analysis in  $\text{CD}_3\text{OH}$  (3 mM). In contrast to water, the peptide gave well dispersed NHs and  $\text{C}^\alpha\text{Hs}$  in  $^1\text{H}$  NMR spectrum in  $\text{CD}_3\text{OH}$ , suggesting that peptide **P3** adopted a well-defined



conformation in protic solvent. The amino acid type and sequential connectivity of the residues were established using

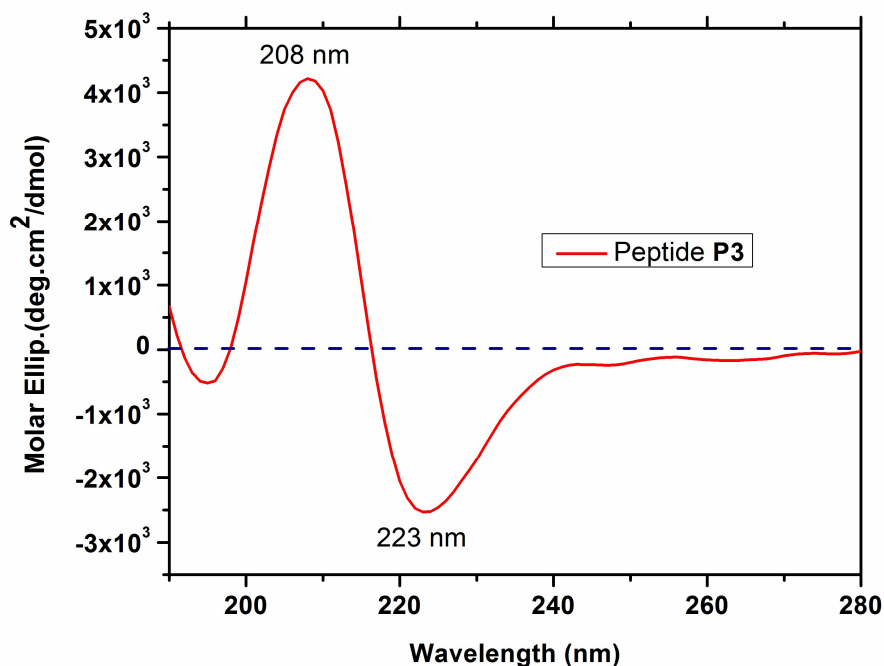


**Figure 2.15:** CD Spectra of peptide **P3** at conc. of 1mg/mL in 1×PBS buffer at pH 7.4.

ROESY and TOCSY spectrum. The analysis of the ROESY spectrum revealed the sequential strong  $\text{NH}(i+1) \leftrightarrow \text{C}^\alpha\text{H}(i)$  interactions. To understand the intra and intermolecular interactions, we subjected the peptide to temperature dependent NMR. The temperature dependent variations in the chemical shifts of amide NH are shown in the Figure 2.19 and 2.20. Results suggested that the change in the chemical shift of NHs (Val2, Leu4, Val6, Leu8, Val10, Leu12) which are involving in H-bonding with opposite strand are small compared to the NHs are involving in intermolecular H-bonding. No cross-strand  $\text{NH} \leftrightarrow \text{NH}$  NOEs were observed, however we have observed cross-strand  $\text{C}^\alpha\text{H}(1) \leftrightarrow \text{C}^\alpha\text{H}(13)$  and characteristic  $\text{C}^\alpha\text{H}(6) \leftrightarrow \text{C}^\alpha\text{H}(7)$  NOEs at the turn segment. The analysis of 2D NMR and the temperature dependent NMR supports the stable  $\beta$ -hairpin formation. Based on NOEs observed in the ROESY spectrum the solution conformation of **P3** was generated. The ensemble of NMR structures resulting from the restrained MD simulations on the basis of the NOE and H-bond data is shown in Figure 2.21. The structural analysis indicates that  $\beta(\text{O})\text{-}\delta^5\text{-DPro}$  stabilized the  $\beta$ -hairpin structure in the

solution. The list of the average torsion angles of the newly designed reverse turns are given in the Table 2.8. The torsion angles of the  $\beta(\text{O})\text{-}\delta^5$ -amino acids are consistent with the peptide **P1**. Overall, we have demonstrated that  $\beta(\text{O})\text{-}\delta^5\text{-}^{\text{D}}\text{Pro}$  can be used as a single residue  $\beta$ -turn. Results suggested that we do not need a central amide bond to induce the  $\beta$ -turns. Irrespective of the central amide bond,  $\beta(\text{O})\text{-}\delta^5$ -amino acid displayed very similar torsion values as that of the type II'  $\beta$ -turns. The studies can be further extended to replace other dipeptide  $\beta$ -turns by  $\beta(\text{O})\text{-}\delta^5$ -amino acids.

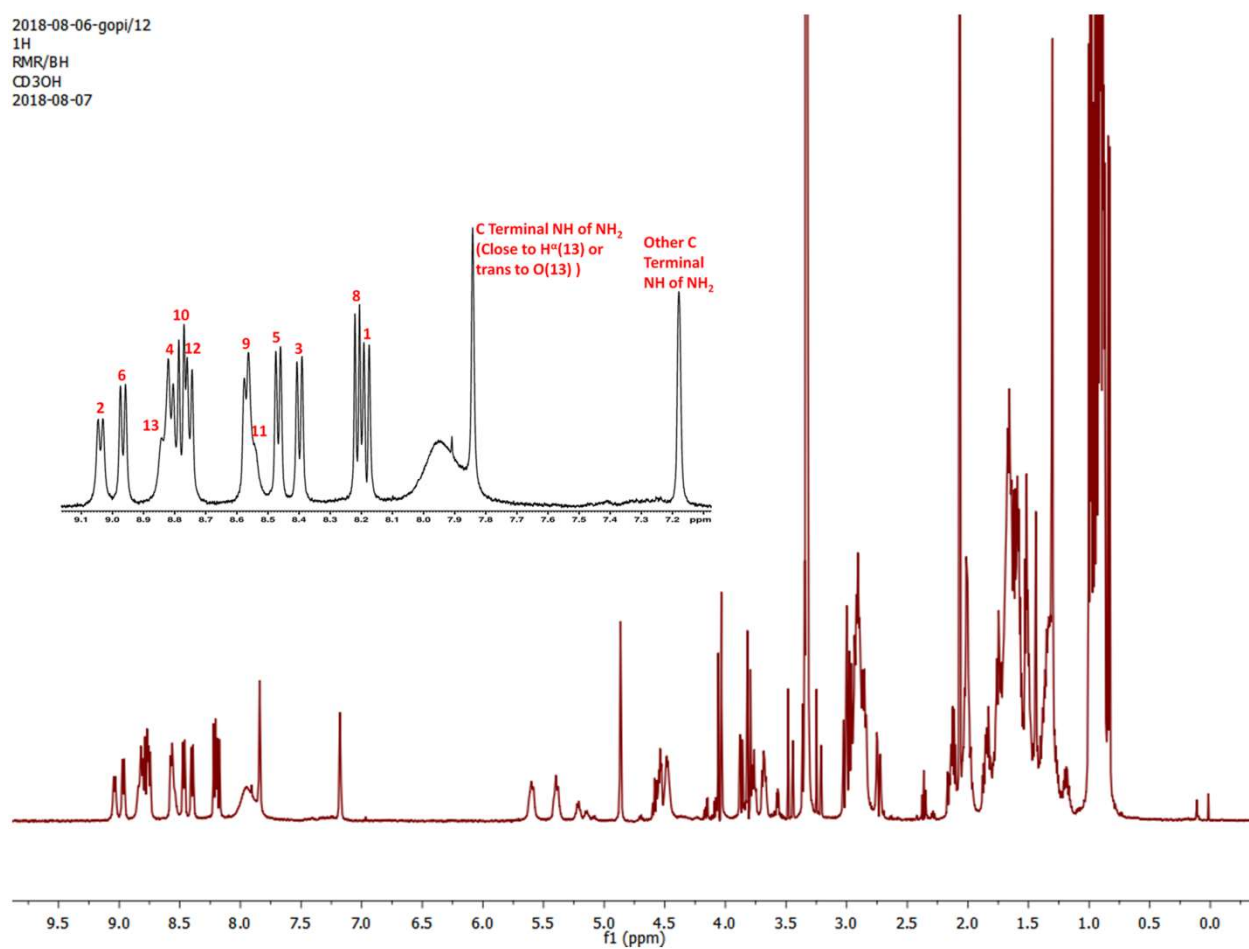


**Figure 2.16:** Full  $^1\text{H}$  NMR spectra of peptide **P3** in  $\text{CD}_3\text{OH}$  (3mM). NHs region is shown in insert.

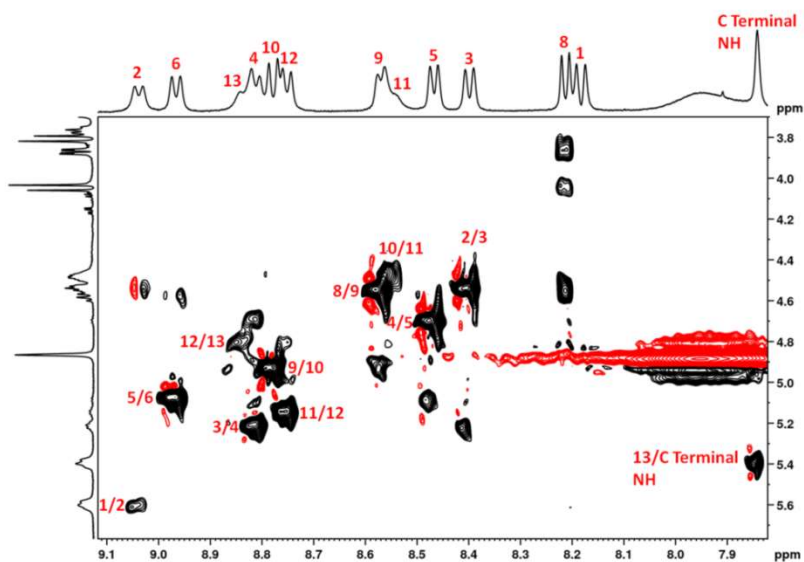


**Figure 2.17:** Partial ROESY spectrum of peptide **P3** (3mM) in CD<sub>3</sub>OH showing NH↔C<sup>α</sup>H interaction.

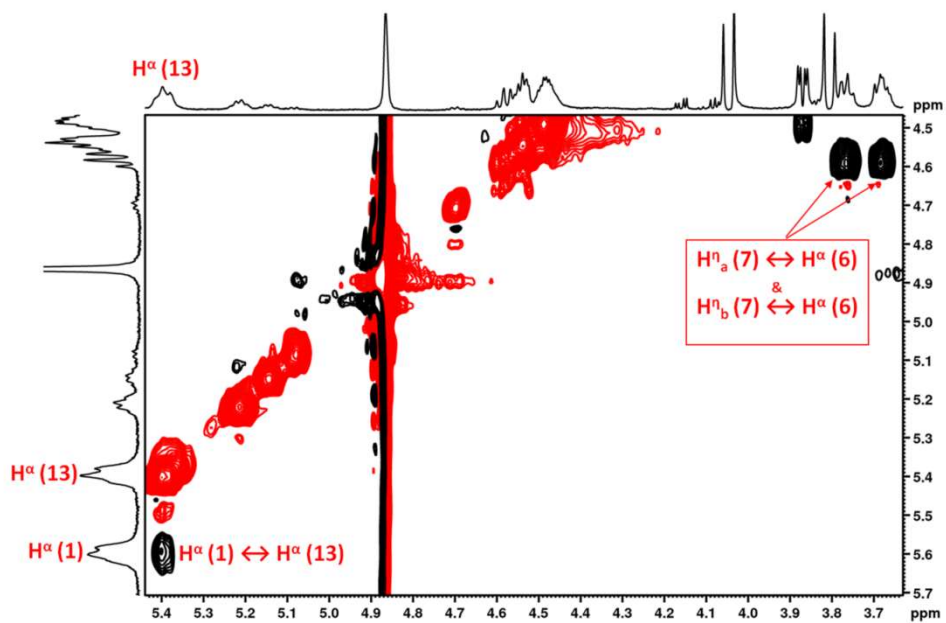


**Figure 2.18:** Partial ROESY spectrum of peptide **P3** (3mM) in CD<sub>3</sub>OH showing C<sup>α</sup>H(1)↔C<sup>α</sup>H (13), C<sup>η</sup>H(7)↔C<sup>α</sup>H(6) interaction.

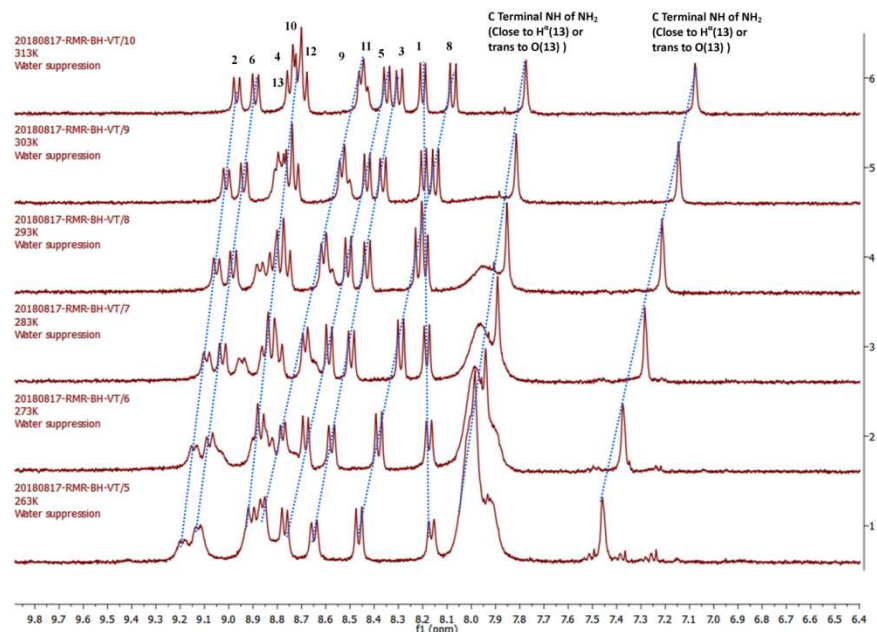


Figure 2.19: Temp dependent  $^1\text{H}$ NMR spectra (NH region) of peptide **P3** from 263 K to 313 K.

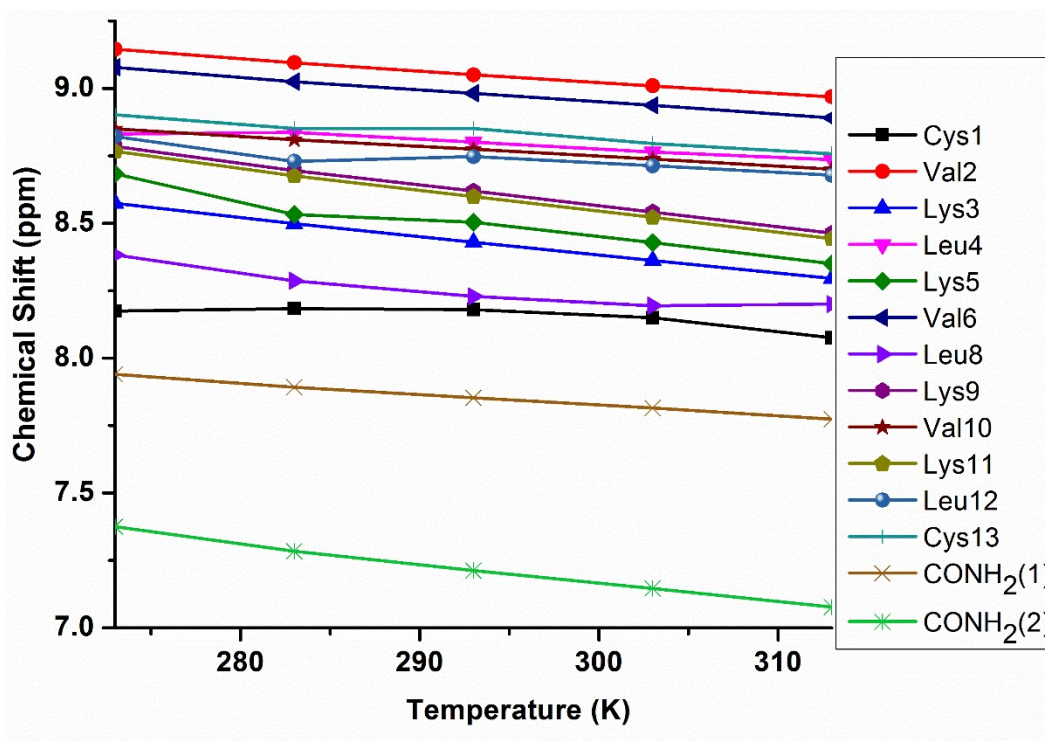
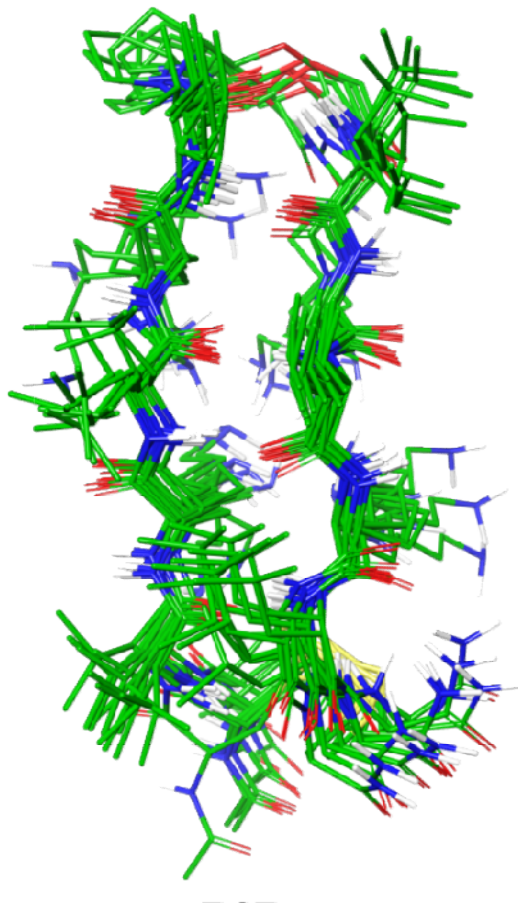


Figure 2.20: Plot of Temp. vs chemical shift ( $\delta_{ppm}$ ) for peptide **P3** in  $\text{CD}_3\text{OH}$ .

**Table 2.7:** Key NOEs used for the structure calculation of peptide **P3**

<b>Residue</b>	<b>H-atom</b>	<b>Residue</b>	<b>H-atom</b>	<b>NOE Observed</b>
<b>Cys1</b>	C <sup>α</sup> H	Val2	NH	Medium
<b>Val2</b>	C <sup>α</sup> H	Lys3	NH	Strong
<b>Lys3</b>	C <sup>α</sup> H	Leu4	NH	Strong
<b>Leu4</b>	C <sup>α</sup> H	Lys5	NH	Strong
<b>Lys5</b>	C <sup>α</sup> H	Val6	NH	Strong
<b>Leu8</b>	C <sup>α</sup> H	Lys9	NH	Strong
<b>Lys9</b>	C <sup>α</sup> H	Val10	NH	Strong
<b>Val10</b>	C <sup>α</sup> H	Lys11	NH	Strong
<b>Lys11</b>	C <sup>α</sup> H	Leu12	NH	Strong
<b>Leu12</b>	C <sup>α</sup> H	Cys13	NH	Medium
<b>Cys13</b>	C <sup>α</sup> H	Cys13	NH(C-terminal)	Strong
<b>Val2</b>	C <sup>α</sup> H	Val2	NH	Weak
<b>Lys3</b>	C <sup>α</sup> H	Lys3	NH	Medium
<b>Cys1</b>	C <sup>α</sup> H	Cys13	C <sup>α</sup> H	Strong
<b>Val6</b>	C <sup>α</sup> H	β(O)-δ <sup>5</sup> -D <sup>2</sup> Pro(7)	C <sup>α</sup> H	Strong



**Figure 2.21:** Superimposed NMR structures form peptide **P3** in CD<sub>3</sub>OH solvent.

**Table 2.8:** Torsion angles for  $\beta(\text{O})\text{-}\delta^5$ -amino acid measured from the minimized conformation of structure **P3**

Structure P3	$\phi$ (deg)	$\theta_1$ (deg)	$\theta_2$ (deg)	$\theta_3$ (deg)	$\Psi$ (deg)
<b>1</b>	68.66	-118.84	177.25	-80.78	-28.90
<b>2</b>	68.58	-113.12	179.86	-81.11	-21.07
<b>3</b>	44.95	-95.29	-171.90	-75.00	-27.89
<b>4</b>	52.65	-117.22	-176.83	-92.41	-5.59

<b>5</b>	54.16	-108.33	179.25	-90.68	-23.25
<b>6</b>	51.94	-104.33	-177.54	-94.16	-18.40
<b>7</b>	51.67	-100.89	-175.26	-77.64	-29.25
<b>8</b>	66.74	-114.48	-178.20	-82.93	-20.15
<b>9</b>	66.92	-104.48	-177.99	-78.94	-26.14
<b>10</b>	70.21	-124.50	177.73	-83.60	-19.36
<b>Range</b>	44 to 71	-125 to -95	177 to -171	-95 to -75	-30 to -5
<b>Average</b>	59.65	-110.15	-178.36	-83.72	-22.00

#### 2.4.6. Peptidomimetics as $\beta$ -Amyloid Aggregation Disrupting Agent

Teplow and co-workers examined the ability of  $\beta$ -hairpin secondary structures derived from  $\theta$ -defensins as inhibitor of amyloid- $\beta$  aggregation.<sup>22</sup> Recently, Ongerer and co-workers studied the ability of designed  $\beta$ -hairpin mimetics as amyloid- $\beta$  inhibitors.<sup>23</sup> Recently we have also demonstrated the inhibition of amyloid- $\beta$  aggregation using designed  $\beta$ -hairpin consisting of <sup>D</sup>Pro-Gly in  $\beta$ -turn segment.<sup>24</sup> Alzheimer's disease is the most commonly occurred neurodegenerative disorder and it is a major global health concern.<sup>25</sup> Deposition of insoluble amyloid fibrils formed mainly by 42-residue containing protein amyloid- $\beta$  ( $A\beta_{1-42}$ ) in the extra cellular portion of the cerebral causes Alzheimer diseases.<sup>26</sup> The mechanism suggest that the soluble  $A\beta$  peptide formed after proteolytic degradation of the amyloid precursor protein (APP) self-aggregates into fibrils.<sup>27</sup> The soluble oligomers of the  $A\beta$  peptide are found to be initially toxic to the cells.  $\beta$ -sheet breaker peptide (BSBP) using peptides and small molecules were extensively used to test for therapeutic value.<sup>28-33</sup> As many  $\beta$ -hairpins have been shown to inhibit the  $\beta$ -amyloid aggregation, we sought to examine the anti amyloidogenic properties our  $\beta$ -hairpin **P3**.

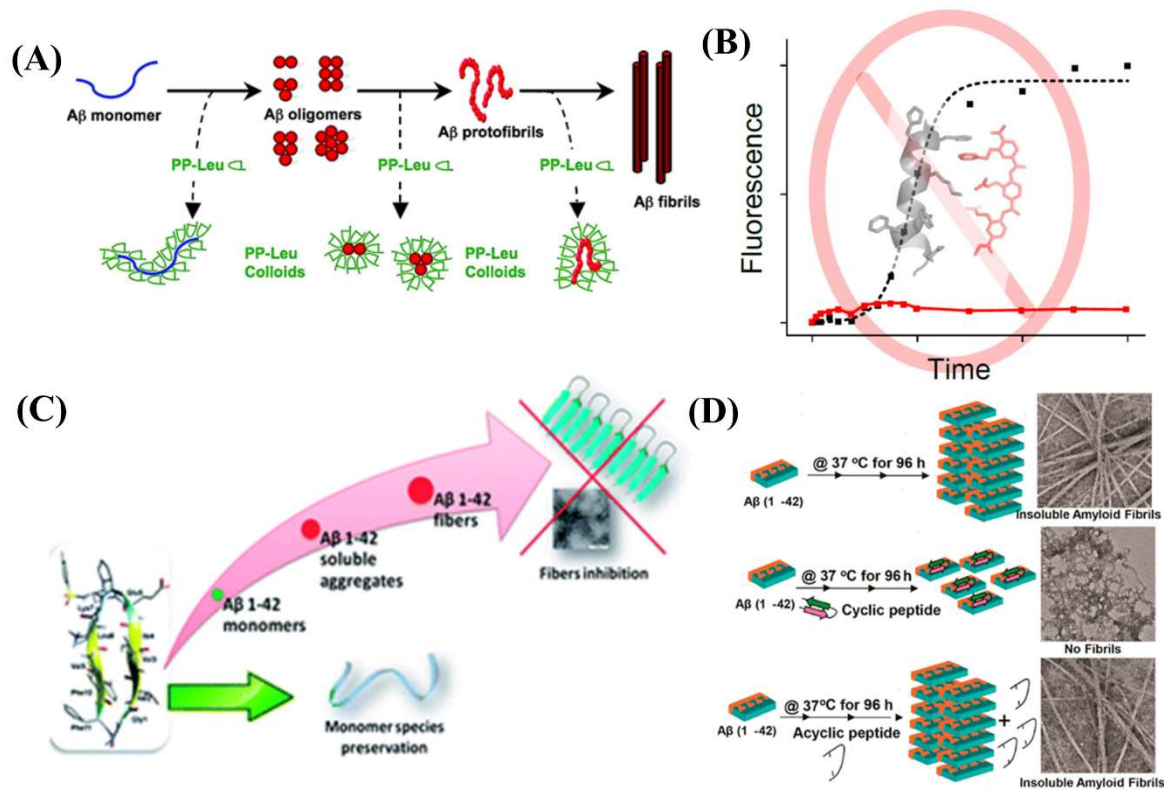


**Figure 2.22:** Disruption of  $\beta$ -amyloid from (A) designed  $\beta$ -hairpin from  $\theta$ -defensin with  $^D\text{Pro}^L\text{Pro}$  as  $\beta$ -turn (B) helical peptidomimetics (C)  $\beta$ -hairpins with piperidine-pyrrolidine scaffolds as  $\beta$ -turn (D) disulphided bridged  $\beta$ -hairpins as  $^D\text{Pro}^L\text{Gly}$  as  $\beta$ -turn. Figure 2.22A, 2.22B, 2.22C and 2.22D was reproduced with permission from references no. 22, 34, 23 and 24 respectively.

#### 2.4.7. Thioflavin T (ThT) Fluorescence Assay

We examined the anti amyloidogenic property of the peptide **P3** through fluorescence assay using known marker ThioflavinT (ThT). The intensity of fluorescence emission was used to monitor the process of the formation/inhibition of  $\beta$ -amyloid fibrils. We first studied the inhibition effect of the peptide **P3** on the soluble protofibril step of  $\text{A}\beta_{1-42}$  aggregation process. The soluble protofibrillar aggregates of  $\text{A}\beta_{1-42}$  was prepared by incubation of  $100\ \mu\text{M}$  protein at  $37\ ^\circ\text{C}$  for 24 h at pH 7.4. Due to the binding to  $\beta$ -sheet-rich region of  $\text{A}\beta_{1-42}$  amyloid aggregates, Thioflavine - T displays dramatic enhancement in the fluorescence emission intensity at 480 nm. But when the proto fibrillar aggregates of  $\text{A}\beta_{1-42}$  was co incubated with peptide **P3** at 1:10 ratio, a drastic decrease in the fluorescence intensity of ThT was observed. No enhanced fluorescence emission



intensity was observed when ThT was incubated with peptide **P3** alone, indicating that peptide **P3** alone is not having aggregating properties as A $\beta$ -amyloid peptides. These results are shown in the Figure 2.23. The analysis of the results suggested that ~40% decrease in ThT fluorescence emission intensity was observed at molar ratio of 1:10 of A $\beta$ <sub>1-42</sub> and peptide **P3**, respectively.

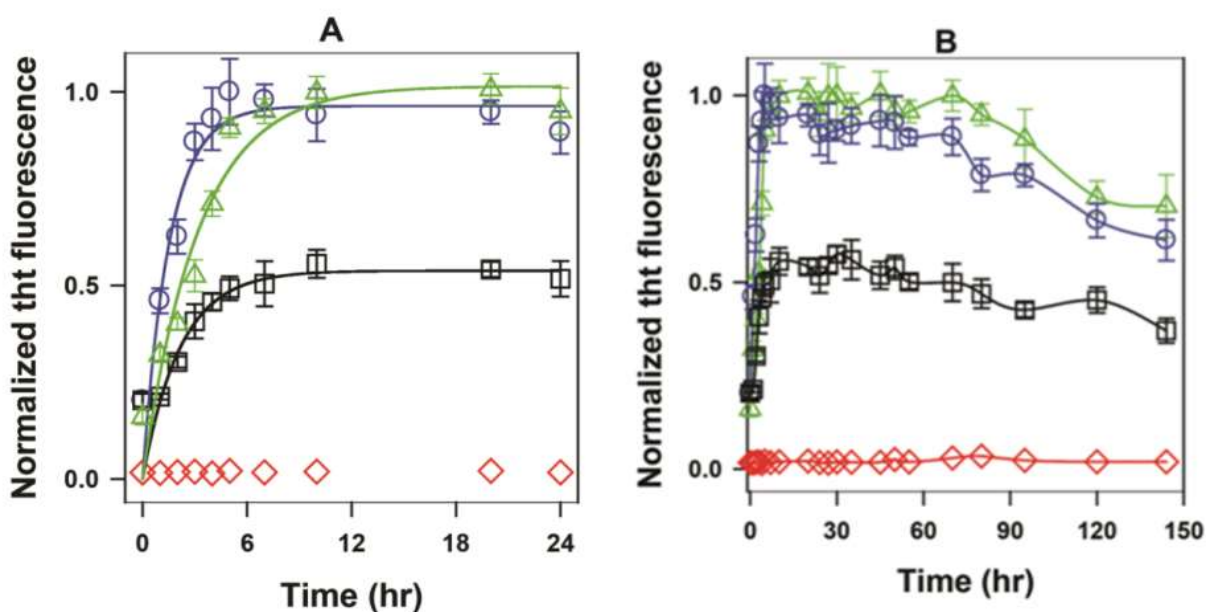


**Figure 2.23:** Thioflavin T (ThT) fluorescence assay of aggregation of A $\beta$ <sub>1-42</sub> upon treatment with different concentration of peptide **P3**. Aggregation process of A $\beta$ <sub>1-42</sub> was monitored in the absence and in the presence of peptide **P3** for (A) 24 h (B) 148 h. (i) 25  $\mu$ M A $\beta$ <sub>1-42</sub> only (violet circles) (ii) 25  $\mu$ M A $\beta$ <sub>1-42</sub> + 250  $\mu$ M peptide **P3** (black square), (iii) 25  $\mu$ M A $\beta$ <sub>1-42</sub> + 250  $\mu$ M disulphide reduced peptide **P3** (green triangle) (iv) 250  $\mu$ M peptide **P3** alone (red diamonds).

#### 2. 4.8. Transmission Electron Microscopy (TEM) Studies

The morphology of the  $\beta$ -amyloid fibrils alone and co incubated with peptide **P3** (1:10) was analyzed by the transmission electron microscopy (TEM). The TEM images are shown

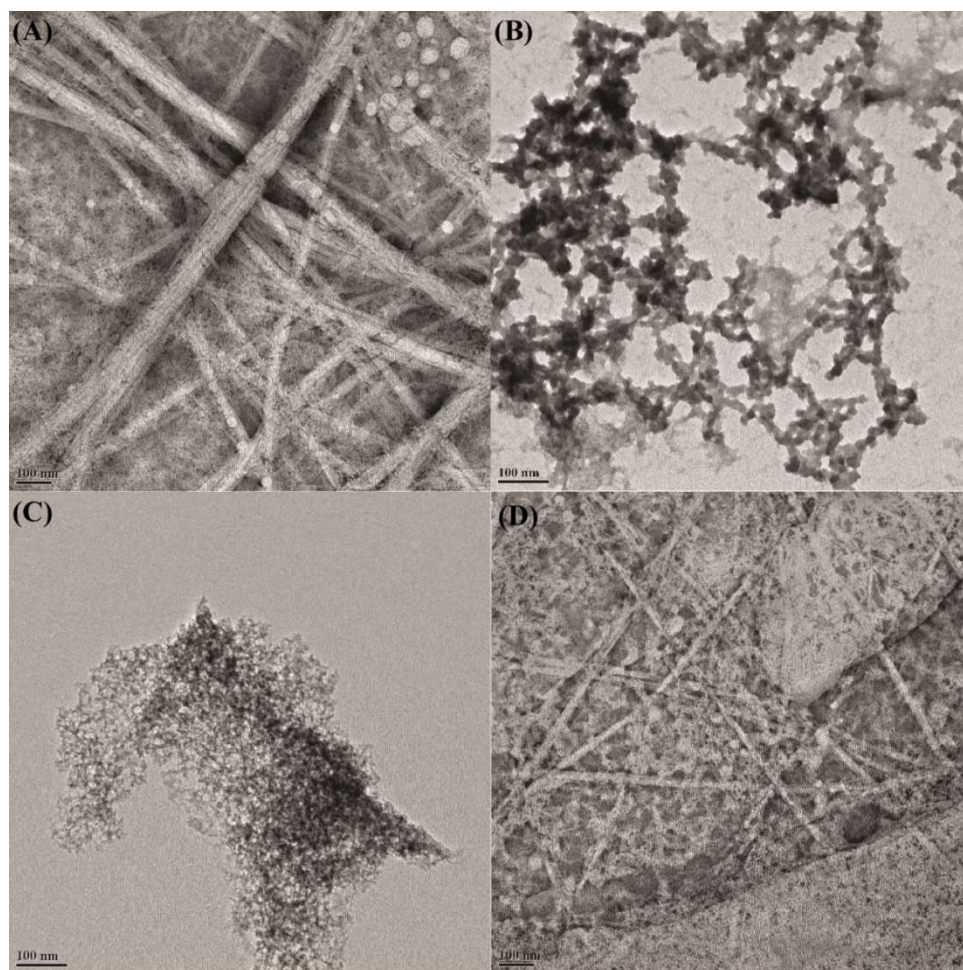


**Figure 2.24:** Effect of peptide **P3** on the morphology of  $A\beta_{1-42}$  fibrils. (A) 25 $\mu$ M of  $A\beta_{1-42}$  fibrils (B) 25 $\mu$ M of  $A\beta_{1-42}$  + 250  $\mu$ M peptide **P3** (C) 250 $\mu$ M of peptide **P3** (D) 25 $\mu$ M of  $A\beta_{1-42}$  + 250  $\mu$ M disulphide reduced peptide **P3**. Scale bar for the all images (A)-(D) is 100 nm.

in Figure 2.24. The formation of fibrils from the soluble  $A\beta_{1-42}$  was confirmed by the presence of twisted morphology and unbranched threadlike structures (Figure 2.24A). When the protofibrils of  $A\beta_{1-42}$  were co incubated with peptide **P3** (1:10) at 37 °C for about 96 h, no formation of fibrils of  $A\beta_{1-42}$  were observed (Figure 2.24B). In addition, no fibrillar morphology of peptide **P3** alone was observed. These results indicate that peptide **P3** inhibits the formation of ordered aggregates from the soluble  $A\beta_{1-42}$ . Further, we have examined role  $\beta$ -hairpin structure of **P3** is in the disruption of  $A\beta_{1-42}$  fibrils. To understand the  $\beta$ -hairpin and its amyloid disrupting activities, we break the disulfides using DTT and subjected acyclic peptide to inhibit the  $A\beta$ -amyloid aggregation under identical conditions. The TEM analysis suggested that acyclic peptide

not effective in inhibiting the A $\beta$ -amyloid aggregation. In addition, ThT assay also suggested the lack of inhibitory activities of acyclic peptide. These results suggested that the structure of  $\beta$ -hairpin is important for the inhibition of A $\beta$ -amyloid aggregation.

#### 2.4.9. Cell Viability Studies using MTT Assay

As the resulted soluble aggregates which are formed during the different pathways of amyloid peptide, are toxic to the neuronal cells, we sought to investigate the effect of the peptide **P3** on the soluble aggregates of A $\beta_{1-42}$  towards the neuronal cells by the MTT assay using SH-SY5Y human neuroblastoma cell lines. The results are shown in Figure 2.25. The results revealed that due to the cytotoxicity of the soluble aggregates decrease the relative cell viability to around ~30%. However, when A $\beta_{1-42}$  was incubated with peptide **P3** at 1:10 molar ratio, the relative cell viability increases to ~80%. Whereas, loss of cell viability was observed in acyclic form of peptide **P3**. But peptide **P3** alone up to 250  $\mu$ M was found to be not toxic to SH-SY5Y cell lines. These results suggested that peptide **P3** can inhibit the aggregation of A $\beta_{1-42}$  *in vitro*.

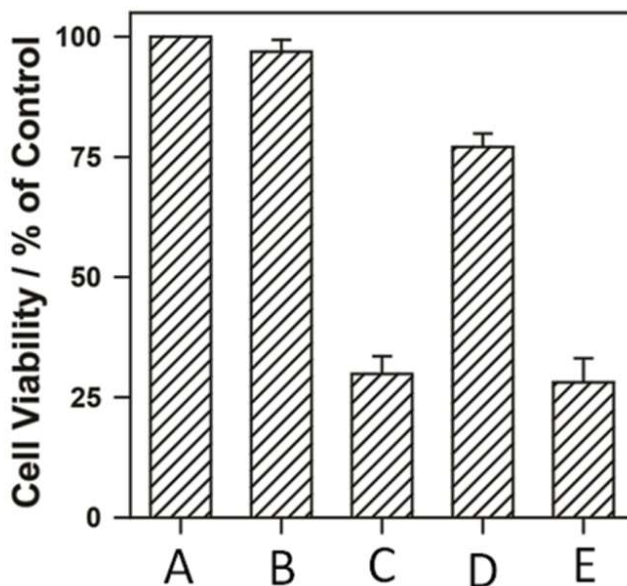


**Figure 2.25:** Effect of peptide **P3** on SH-SY5Y human neuroblastoma cell lines. (A) Cell only (B) 250  $\mu$ M of peptide **P3** alone (C) 10  $\mu$ M of A $\beta_{1-42}$  (D) 10  $\mu$ M of A $\beta_{1-42}$  + 100  $\mu$ M peptide **P3** (E) 10  $\mu$ M of A $\beta_{1-42}$  + 100  $\mu$ M disulphide reduced peptide **P3**.

#### 2.4.10. Two Dimensional $^{15}\text{N}$ - $^1\text{H}$ HSQC NMR Studies of Amyloid Disruption by Peptide P3

As  $\beta$ -hairpin shown the excellent  $\beta$ -amyloid inhibition activity, we sought examine whether any changes in the structural properties of  $\text{A}\beta_{1-42}$ . To understand the structural reorganization  $\text{A}\beta_{1-42}$  upon binding of peptide **P3**, we subjected **P3** and soluble  $\text{A}\beta_{1-42}$  to two dimensional  $^{15}\text{N}$ - $^1\text{H}$  HSQC NMR. We used uniformly  $^{15}\text{N}$  labeled  $\text{A}\beta_{1-42}$  for the studies. First  $^{15}\text{N}$ - $^1\text{H}$  NMR spectrum of  $\text{A}\beta_{1-42}$  (40  $\mu\text{M}$ ) were recorded in 20 mM NaPi at pH 7.4. Fully assigned  $^{15}\text{N}$ - $^1\text{H}$  NMR spectrum of  $\text{A}\beta_{1-42}$  is shown in the Figure 2.26. Then solution of peptide **P3** was added to  $\text{A}\beta_{1-42}$  at a ratio of 1:10 ( $\text{A}\beta_{1-42}$ : **P3**) in NaPi and HSQC was recorded again. The  $^1\text{H}$ - $^{15}\text{N}$  HSQC NMR of  $\text{A}\beta_{1-42}$ + peptide **P3** (1:10) HSQC spectrum is shown in the Figure 2.27. All the contours of both the spectra was assigned and change in the chemical shift for all the residues were calculated. The overlay of  $\text{A}\beta_{1-42}$  HSQC spectrum over the mixture of **P3** and  $\text{A}\beta_{1-42}$  spectrum is shown in the Figure 2.28. The analysis of the results of the HSQC experiments revealed that changes in their chemical shift observed for residues Glu3 to Val24 (Figure 2.29).

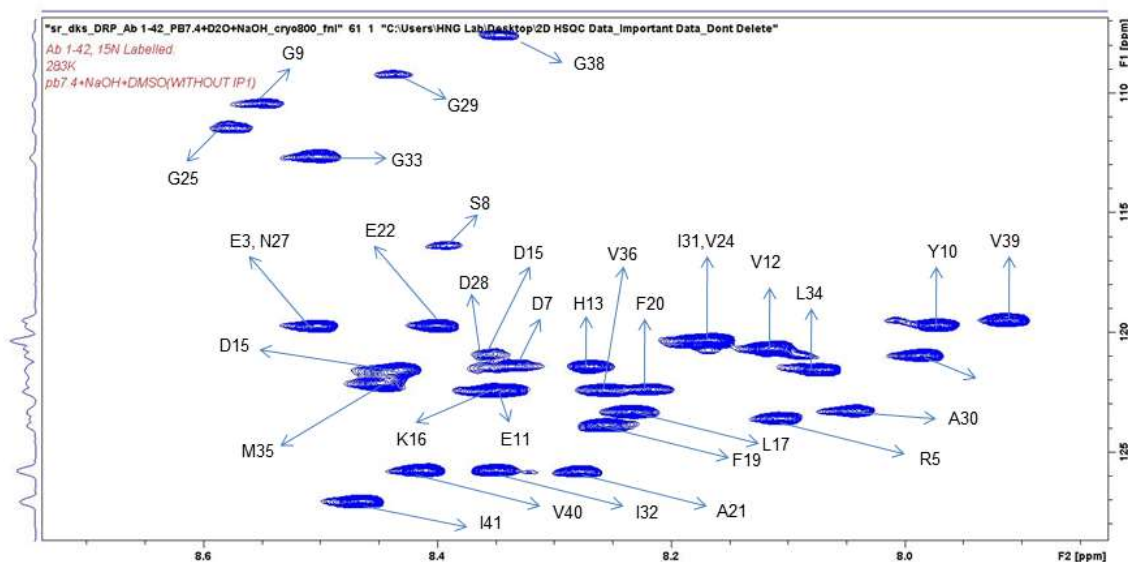
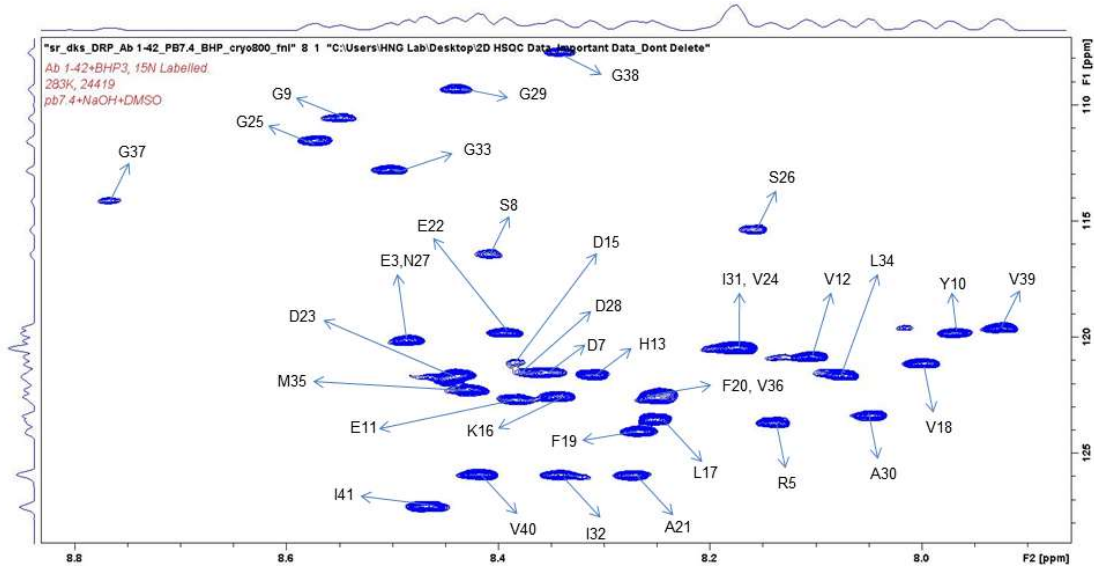
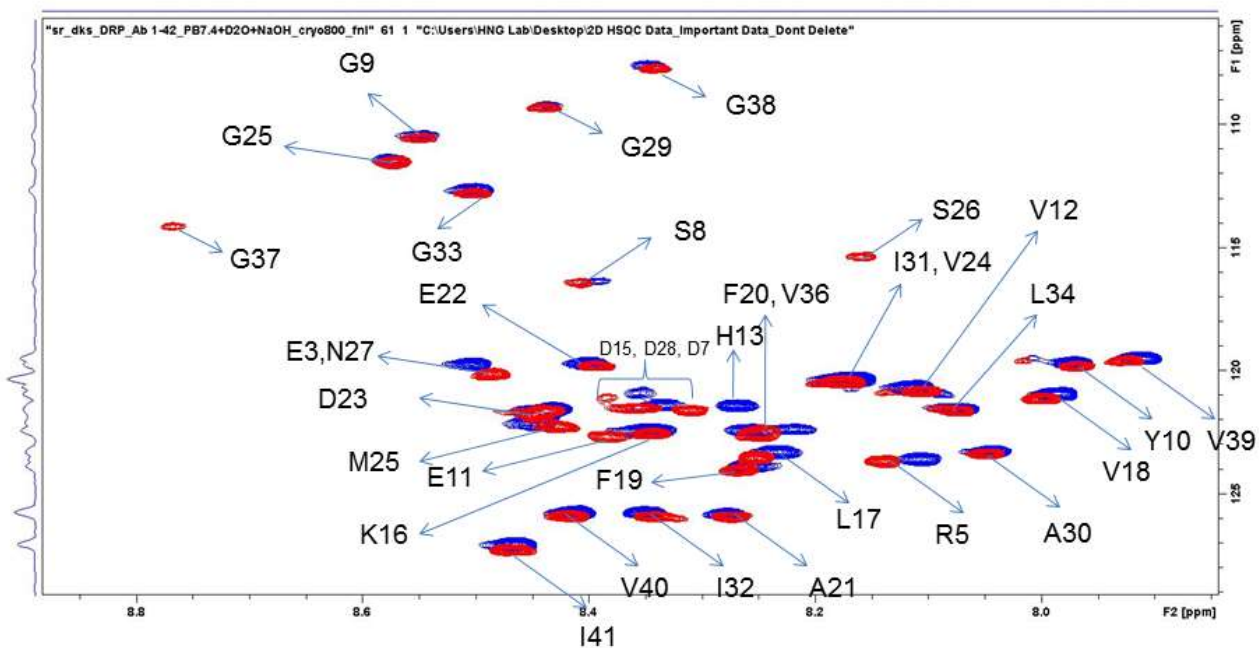


Figure 2.26:  $^1\text{H}$ - $^{15}\text{N}$  HSQC NMR of 40  $\mu\text{M}$  of  $\text{A}\beta_{1-42}$  in 20mM NaPi buffer at pH 7.4.



**Figure 2.27:**  $^1\text{H}$ - $^{15}\text{N}$  HSQC NMR of  $\text{A}\beta_{1-42}$  peptide **P3** (1:10) in 20mM NaPi buffer at pH 7.4



**Figure 2.28:** Overlay  $^1\text{H}$ - $^{15}\text{N}$  HSQC NMR spectra of  $\text{A}\beta_{1-42}$  (40  $\mu\text{M}$ ) and  $\text{A}\beta_{1-42}$  + **P3** (1:10) in 20 mMNaPi buffer at pH 7.4. Blue contour represents the  $\text{A}\beta_{1-42}$  only and red contour represents  $\text{A}\beta_{1-42}$  + **P3**

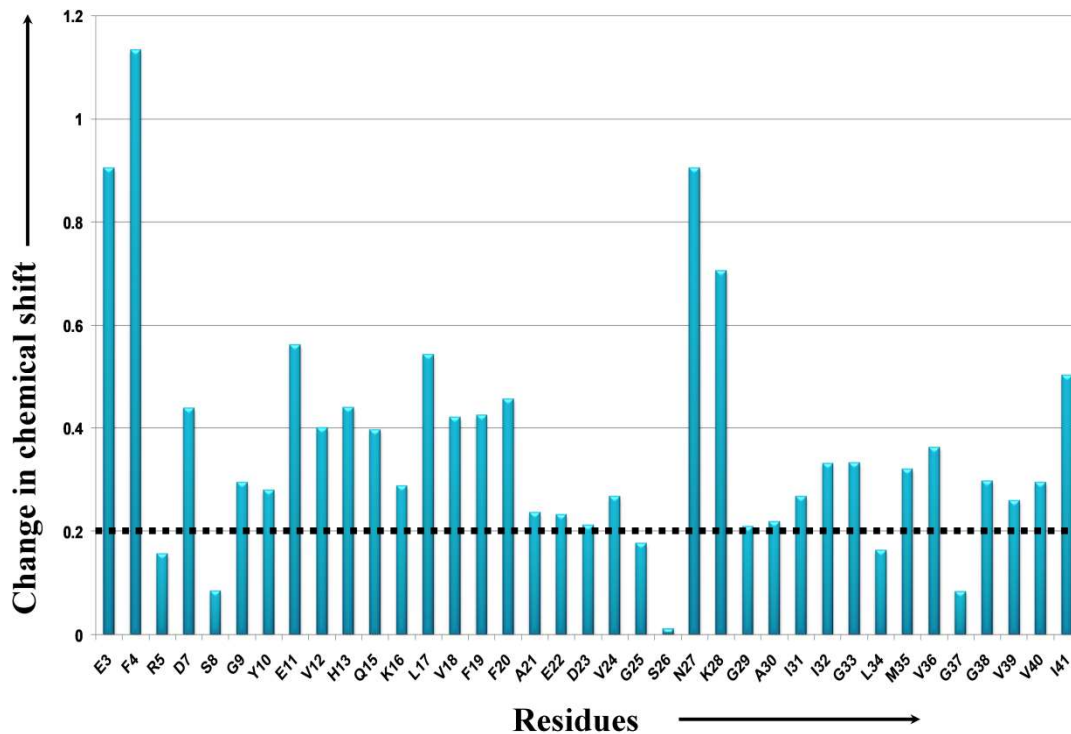


**Figure 2.29:** The changes in the chemical shift perturbation of  $A\beta_{1-42}$  induces by peptide **P3**. The dotted line represents the minimum change in the chemical shift for  $A\beta_{1-42}$ .

## 2.5. Conclusions

In summary, we describe the utilization of novel  $\beta(O)-\delta^5$ -amino acid single residue  $\beta$ -turn mimetics in the design of  $\beta$ -hairpin. Both NMR and single crystal structure shows that the  $\beta$ -turn is stabilized by ten membered hydrogen bond pseudocycle. Further the single crystal analysis also suggested that the  $\beta(O)-\delta^5$ -amino acid adopted type II'  $\beta$ -turn similar to the  $^D$ Pro-Gly. Further, we studied ability the amphiphilic  $\beta$ -hairpin as  $A\beta_{1-42}$  amyloid aggregation inhibitor. Peptide **P3** effectively inhibit  $A\beta_{1-42}$  amyloid aggregation *in vitro*. Further, the two dimensional HSQC NMR studies suggested the conformational changes of residues from Glu3 to Ser24 of  $A\beta_{1-42}$  was observed upon binding with amphiphilic  $\beta$ -hairpin. In addition, we showed enhanced cell viability of neuroblastoma cells by the designed  $\beta$ -hairpin. Overall, these studies reported here can be opened up a new avenue for the design of  $\beta$ -turn and  $\beta$ -hairpin mimetics for different therapeutic applications.

## 2.6. Experimental Section

### 2.6.1. Materials and Methods

All the reagents including amino acids were purchased from the commercial sources. DCM and MeOH were purchased from the commercial sources and distilled before to use. Column chromatography was performed on silica gel (120-200 mesh). Final peptides were purified by reverse phase HPLC.  $^1\text{H}$  (400 MHz) and  $^{13}\text{C}$  (100 MHz) NMR spectra were used to record the NMR spectra on respectively using the residual solvent signal as internal standards ( $\text{CDCl}_3$ ). Chemical shifts ( $\delta$ ) reported in parts per million (ppm) and coupling constants (J) reported in Hz. Mass of pure peptides was confirmed by MALDI-TOF /TOF.

### 2.6.2. NMR Spectroscopy

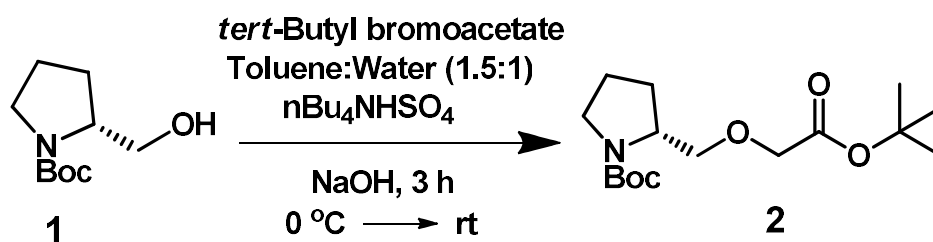
All NMR studies were carried out by using either 400 or 600 MHz spectrometer. Resonance assignments were obtained by TOCSY and ROESY analysis. All two-dimensional data were collected in phase-sensitive mode by using the time-proportional phase incrimination (TPPI) method. Sets of 1024 and 512 data points were used in the  $t_2$  and  $t_1$  dimensions respectively. For TOCSY and ROESY analysis, 32 and 72 transients were collected, respectively. A spectral width of 600MHz was used in both dimensions. A spin-lock time of 200 and 250 ms were used to obtain ROESY spectra. Zero-filling was carried out to finally yield a data set of  $2\text{ K} \times 1\text{ K}$ . A shifted square-sine-bell window was used before processing. All the HSQC NMR experiment were carried out using 800MHz NMR instrument and the change in the chemical shift perturbation value was calculated from the reported literature.<sup>34</sup>

### 2.6.3. Synthetic Procedures

#### 2.6.3.1. Synthesis of *N*-Boc- $\beta$ (O)- $\delta^5$ - $^{\text{D}}$ Pro-O<sup>t</sup>Bu

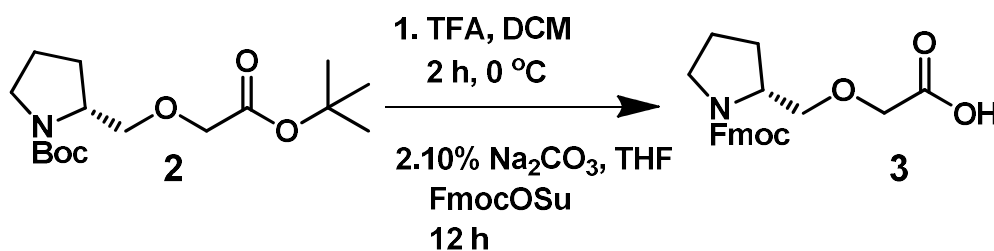
*N*-Boc- $\beta$ (O)- $\delta^5$ - $^{\text{D}}$ Pro-O<sup>t</sup>Bu was synthesized by the reported protocol from *N*-Boc-amino alcohol.<sup>17</sup> Briefly, to the solution containing 10 mL of water and 10 mL of toluene, sodium hydroxide (10g, 250 mmol) was dissolved in ice-cold condition. Thereafter, *tert*-butyl bromoacetate (2.2 mL, 15 mmol) was added slowly to the biphasic reaction mixture at room temperature. After that, the solution containing *N*-Boc- $^{\text{D}}$ Proline alanine alcohol (2.1 g, 10 mmol)

in toluene (10 mL) was added slowly to the reaction mixture at 0 °C. Then the reaction mixture was stirred for about 3 h and at room temperature. After completion of reaction (confirmed by TLC), the organic layer was extracted with diethyl ether (30 mL×2). The combined organic layer was washed with brine (30 mL×2) and dried over anhydrous sodium sulfate. The solvent was evaporated under reduced pressure to get white gummy product. The crude product of *N*-Boc-β(O)-δ<sup>5</sup>-D<sup>D</sup>Pro-O<sup>t</sup>Bu was purified by column chromatography using EtOAc/hexane solvent system.



### 2.6.3.2. Synthesis of *N*-Fmoc-β(O)-δ<sup>5</sup>-D<sup>D</sup>Pro-OH

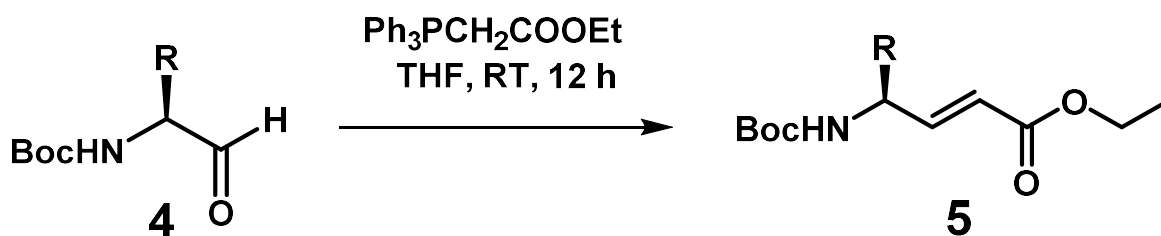
Compound **2** (3.15 g, 10 mmol) was dissolved in 15 mL of TFA/DCM (1:1) mixture at 0 °C. To this solution 500μL of H<sub>2</sub>O was added. Then the reaction mixture was kept for about 2 h at RT. After completion of the reaction (confirmed by TLC), the TFA was evaporated completely under *vacuum*. Then the free amine was protected with Fmoc and used for the solid phase peptide synthesis.





### 2.6.3.3. Synthesis of (*E*)- $\alpha,\beta$ -unsaturated- $\gamma^4$ -Amino Acid

(*E*)- $\alpha,\beta$ -unsaturated- $\gamma^4$ -amino acids were synthesized from the reported protocol.<sup>35</sup> Briefly Boc-amino aldehyde (5mmol) was dissolved in 30 mL of dry THF. Ethyl ester Wittig ylide (7.5 mmol) was to this solution at RT. After that the reaction mixture was stirred for about 5 h at RT. Completion of reaction was confirmed by TLC. After completion, reaction mixture was quenched with 50mL of 2N NH<sub>4</sub>Cl solution. The product was extracted with EtOAc (3  $\times$  40 mL). Then the combined organic layer was washed with brine (3  $\times$  30 mL) and dried over anhydrous Na<sub>2</sub>SO<sub>4</sub>. Then the combined organic layer was concentrated under reduced pressure to give crude product, which was further purified on silica gel column chromatography using EtOAc/Pet-ether to get pure ethyl ester of Boc-protected (*E*)- $\alpha,\beta$ -unsaturated- $\gamma^4$ -amino acids.

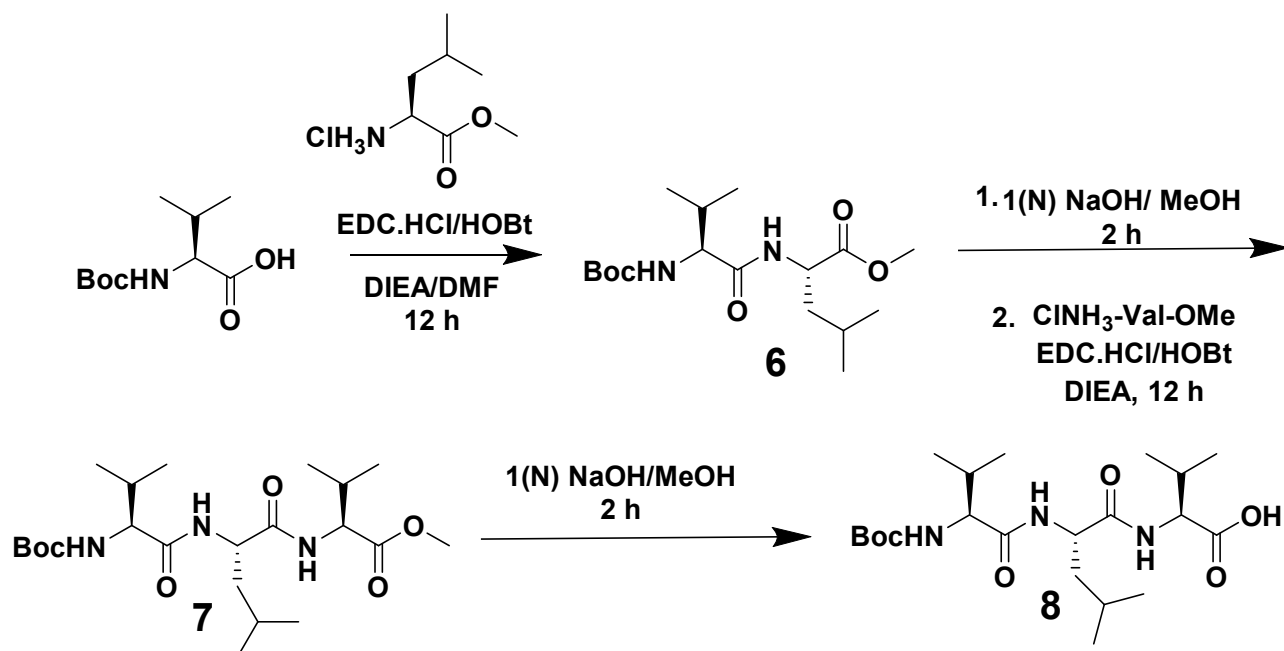


### 2.6.3.4. Synthesis of Tripeptide BocNH-Val-Leu-Val-OH

BocNH-Val-OH (1.08 g, 5 mmol) was dissolved in 3 mL of DMF under N<sub>2</sub> atmosphere. To this solution EDC.HCl (960 mg, 5 mmol), HOBT (675 mg, 5 mmol) and DIEA (1.74 mL, 10 mmol) was added at 0 °C. Then the reaction mixture was stirred for about 15 min. After that ClH<sub>3</sub>N-Leu-OMe (1.36g, 5.5 mmol) was added to the reaction mixture and stirred for about 12 h. After completion of the reaction (confirmed by TLC), 15 mL of brine solution was added to the reaction mixture and the compound was extracted with EtOAc (3  $\times$  20 mL). The combined organic layer was washed with 10% HCl (3  $\times$  20 mL), 10% Na<sub>2</sub>CO<sub>3</sub> (3  $\times$  20 mL) and brine (3  $\times$  20 mL) respectively. Then the combined organic layer was dried over anhydrous Na<sub>2</sub>SO<sub>4</sub>. After

that the combined organic layer was evaporated under reduced pressure to get the dipeptide BocNH-Val-Leu-OMe. After that the dipeptide was hydrolysed using 1N NaOH in MeOH. Then the dipeptide acid BocNH-Val-Leu-OH (1.03 g, 3 mmol) was dissolved in 3 mL of DMF under N<sub>2</sub> atmosphere. To this solution EDC.HCl (576 mg, 3 mmol), HOBt (405 mg, 3 mmol) and DIEA (1mL, 6 mmol) was added at 0 °C. Then the reaction mixture was stirred for about 15 min. After that ClH<sub>3</sub>N-Val-OMe (772 mg, 3.3 mmol) was added to the reaction mixture and stirred for about 12 h. After completion of the reaction, 15 mL of brine solution was added to the reaction mixture and the compound was extracted with EtOAc (3 × 20 mL). The combined organic layer was washed with 10% HCl (3 × 20 mL), 10% Na<sub>2</sub>CO<sub>3</sub> (3 × 20 mL) and brine (3 × 20 mL) respectively. Then the combined organic layer was dried over anhydrous Na<sub>2</sub>SO<sub>4</sub>. After that the combined organic layer was evaporated under reduced pressure to get the Tripeptide BocNH-Val-Leu-Val-OMe. The crude compound was purified by column chromatography using EA/Hexane solvent system to get pure compound **7**. Yield: 580.5 mg (50%).

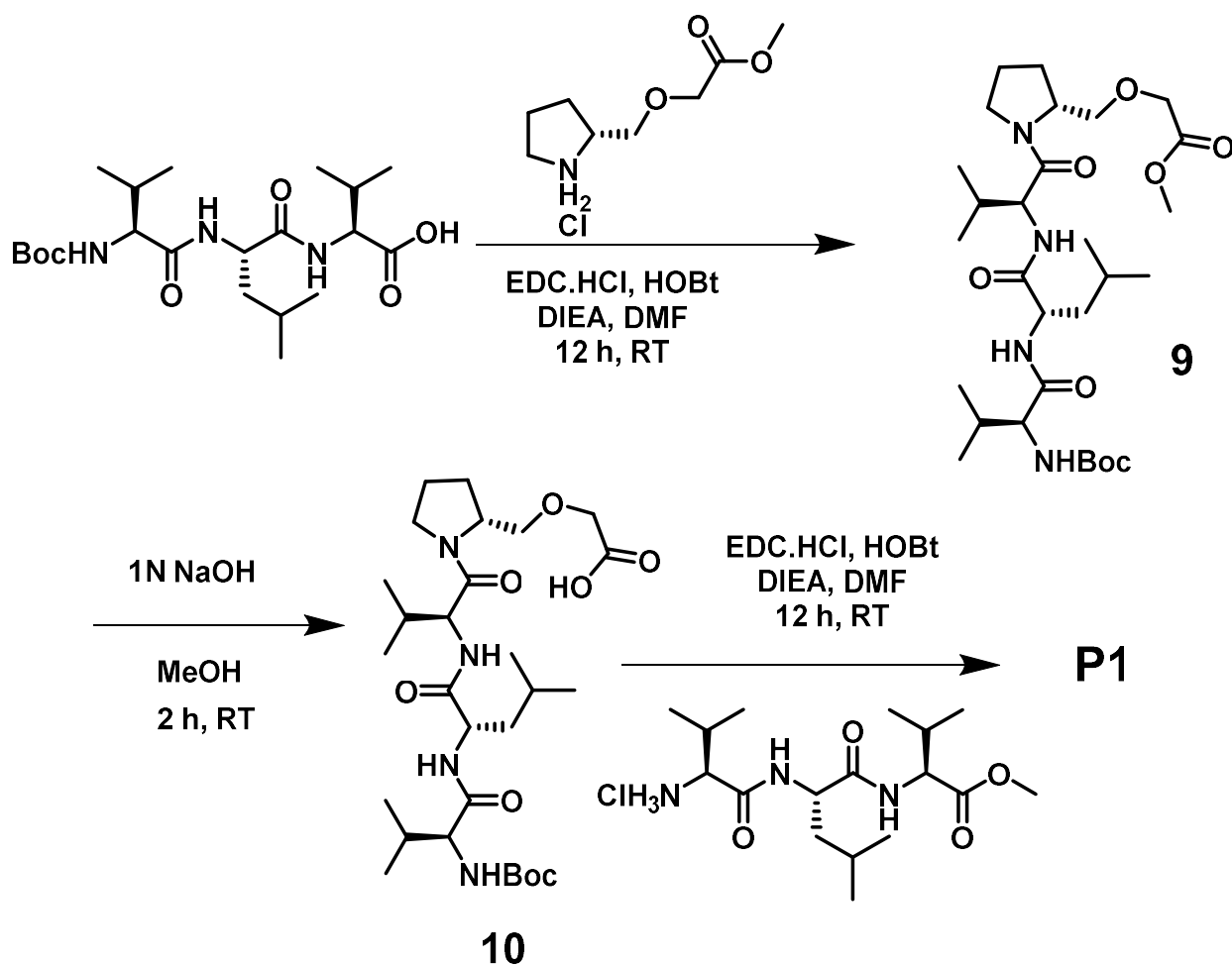
After that the tripeptide BocNH-Val-Leu-Val-OMe (886 mg, 2 mmol) was dissolved in 10 mL of MeOH. To this solution 5 mL of 1N NaOH was added. Then the reaction mixture was stirred for 1 h. After completion of the reaction (confirmed by TLC), MeOH was evaporated under *vacuum*. Then the reaction mixture was acidified with 10% HCl and extracted with EtOAc (3 × 20 mL). The combined organic layer was brine (3 × 20 mL). Then the combined organic layer was dried over anhydrous Na<sub>2</sub>SO<sub>4</sub>. After that the combined organic layer was evaporated under reduced pressure to get the tripeptide BocNH-Val-Leu-Val-OH (Compound **8**). The compound **8** was used without further purifications. Crude yield: 560 mg (75%).



### 2.6.3.5. Synthesis of Peptide P1

Tripeptide BocNH-Val-Leu-Val-OH (858 mg, 2 mmol) was dissolved in 4 mL DMF at 0 °C under  $\text{N}_2$  atmosphere. To this solution EDC.HCl (384 mg, 2mmol), HOBt (270 mg, 2 mmol) and DIEA (697.2 $\mu\text{L}$ , 4mmol) was added at 0 °C. Then the reaction mixture was stirred for 15 min. After that  $\text{ClH}_3\text{N}-\delta^{\text{D}}\text{Pro-OMe}$  (363 mg, 0.5 mmol) was added to the reaction mixture and stirred for about 12 h. After completion of the reaction, 15 mL of brine solution was added to the reaction mixture and the compound was extracted with EtOAc (3  $\times$  20 mL). The combined organic layer was washed with 10% HCl (3  $\times$  20 mL), 10%  $\text{Na}_2\text{CO}_3$  (3  $\times$  20 mL) and brine (3  $\times$  20 mL) respectively. Then the combined organic layer was dried over anhydrous  $\text{Na}_2\text{SO}_4$ . After that the combined organic layer was evaporated under reduced pressure to get the crude compound. Then the tetra peptide BocNH-Val-Leu-Val- $\beta(\text{O})-\delta^5\text{-}^{\text{D}}\text{Pro-OMe}$  was hydrolysed using 1N NaOH in MeOH. Then the tetra peptide BocNH-Val-Leu-Val- $\delta^5\text{-}^{\text{D}}\text{Pro-OH}$  (570 mg, 1 mmol) was dissolved in 4 mL DMF at 0 °C under  $\text{N}_2$  atmosphere. To this solution EDC.HCl (192 mg, 1mmol) and HOBt (192 mg, 1mmol) and DIEA (348.6  $\mu\text{L}$ , 2mmol) was added at 0 °C. Then the reaction mixture was stirred for 15 min. After that  $\text{ClH}_3\text{N-Val-Leu-Val-OMe}$  (417 mg, 1.1mmol) was added to the reaction mixture and stirred for about 12 h. After completion of the reaction, 15 mL of brine solution was added to the reaction mixture and the compound was

extracted with EtOAc (3 × 20 mL). The combined organic layer was washed with 10% HCl (3 × 20 mL), 10% Na<sub>2</sub>CO<sub>3</sub> (3 × 20 mL) and brine (3 × 20 mL) respectively. Then the combined organic layer was dried over anhydrous Na<sub>2</sub>SO<sub>4</sub>. After that the combined organic layer was evaporated under reduced pressure to get the crude compound. The crude compound was dissolved in HPLC grade MeOH and purified by reverse phase HPLC using C18 column using MeOH/Water gradient system. MALDI TOF/TOF m/z calculated for C<sub>60</sub>H<sub>90</sub>N<sub>10</sub>O<sub>14</sub> [M+Na<sup>+</sup>] 1197.6536 and observed 1197.6510.



### 2.6.3.6. Solid Phase Synthesis of Peptides P2 and P3

The *N*-acetylated peptides were synthesized using MBHA Knorr amide resin on a 0.2 mmol scale using manual solid phase synthesis protocol. The synthesis was carried out in NMP solvent by a standard Fmoc protocol using HBTU/HOBt as coupling reagent. Fmoc deprotection was accomplished by a solution of 20% piperidine in DMF. *N*-acetylation of the peptides was carried out using acetic anhydride/pyridine (1:9) mixture in DMF solvent. Acidic cleavage from the resin was achieved by treatment of the resin with a mixture of trifluoroacetic acid (TFA)/triisopropylsilane/water (90:5:5, 2 h). The resin was extracted with additional 5 mL of TFA and the combined extracts were concentrated under *vacuum*. The crude peptide was then precipitated in cold diethyl ether (30 mL) and isolated by centrifugation and decantation of the ether. The precipitate was re-dissolved and lyophilized to get a fine white solid. Further the crude peptide **P2** were dissolved in MeOH and purified by RP-HPLC on C18 column using MeOH/H<sub>2</sub>O system.

The peptide **P3** was synthesized using above mentioned protocol. For disulfide formation, crude peptide **P3** was dissolved in NH<sub>4</sub>CO<sub>3</sub> buffer (20 mM, pH 7.4, peptide concentration 2mM) and stirred for 12 h in an open flask. Insoluble material was separated by centrifugation and the supernatant solution lyophilized and purified by reverse phase HPLC on a C18 column using ACN/H<sub>2</sub>O (with 0.1% TFA) gradient system.

### 2.6.4. Crystallographic Information

#### Compound 3 (FmocNH-β(O)-δ<sup>5</sup>-D<sup>15</sup>Pro-OH) (CCDC No 1950179)

Crystals of compound **3** were grown by slow evaporation from a solution of aqueous methanol. A single crystal (0.1 × 0.05 × 0.03 mm) was mounted on loop with a small amount of the paraffin oil. The X-ray data were collected at 100K temperature on a Bruker APEX(II) DUO CCD diffractometer using Cu Kα radiation ( $\lambda = 1.54178\text{\AA}$ ),  $\omega$ -scans ( $2\theta = 72.59$ ), for a total of 9464 independent reflections. Space group P2<sub>1</sub>2<sub>1</sub>2<sub>1</sub>, a= 5.6414(4), b= 14.5190(10), c= 22.8300(15),  $\alpha=90$ ,  $\beta=90$ ,  $\gamma=90$ , V = 1869.95 Å<sup>3</sup>, orthorhombic, Z = 2 for chemical formula C<sub>22</sub>H<sub>23</sub>N O<sub>5</sub>, with one molecules in asymmetric unit;  $\rho_{\text{calcd}} = 1.355 \text{ g cm}^{-3}$ ,  $\mu = 0.788 \text{ mm}^{-1}$ , F(000)

= 808.0. The structure was obtained by direct methods using SHELXS-97. The final R value was 0.0811 (wR2 = 0.0925) 3634 observed reflections ( $F_0 \geq 4\sigma(|F_0|)$ ) and 691 variables, S = 1.054.

### **Peptide P2 (CCDC No 1950178)**

Crystals of peptide **P2** were grown by slow evaporation from a solution of methanol/IPA. A single crystal ( $0.15 \times 0.02 \times 0.05$  mm) was mounted on loop with a small amount of the paraffin oil. The X-ray data were collected at 100K temperature on a Bruker APEX(II) DUO CCD diffractometer using Mo K $\alpha$  radiation ( $\lambda = 0.71073$  Å),  $\omega$ -scans ( $2\theta = 56.77$ ), for a total of 84907 independent reflections. Space group P2<sub>1</sub>, a= 9.615(2), b= 21.245(5), c= 26.618(6),  $\alpha=90$ ,  $\beta=94.807$ ,  $\gamma=90$ , V = 5418.15Å<sup>3</sup>, monoclinic, Z = 2 for chemical formula C<sub>93</sub> H<sub>163</sub> N<sub>16</sub> O<sub>21</sub>, with two molecules in asymmetric unit;  $\rho_{\text{calcd}} = 1.129$  gcm<sup>-3</sup>,  $\mu = 0.080$  mm<sup>-1</sup>, F(000) = 2002.0. The structure was obtained by direct methods using SHELXS-97. The final R value was 0.1736 (wR2 = 0.4048) 26947 observed reflections ( $F_0 \geq 4\sigma(|F_0|)$ ) and 1199 variables, S = 1.901.

### **2.6.5. Two dimensional NMR Analysis of Peptides P1 and P3**

Hydrophilic peptide **P3**:

Solution state structure calculation of peptide **P2** and **P3**:

Strong  $\leq 2.5$  Å

Medium  $\leq 3.5$  Å

Weak  $\leq 5$  Å

Structure calculation was done using a simulated annealing protocol in vacuum using DESMOND and OPLS 2005 force field with NOE and hydrogen bonding constraints. A peptide molecule was kept in orthorhombic simulation cell. Upper limit for distance was kept at 2.5Å, 3.5 Å and 5 Å for strong, medium and weak NOEs respectively. All the lower distance limits were taken to be 1.8 Å. A force constant of 1KCal/Mol was used for all the constraints. NOE

potentials (appropriate for treating ambiguous NOE assignments) used are having the following form,

$$E_{\text{NOE}} = fc * (\text{lower} - d)^2, \text{ if } d < \text{lower};$$

$$E_{\text{NOE}} = 0, \text{ if } \text{lower} \leq d \leq \text{upper};$$

$$E_{\text{NOE}} = fc * (\text{upper} - d)^2, \text{ if } \text{upper} < d \leq \text{upper} + \text{sigma};$$

$$E_{\text{NOE}} = fc * (a + \text{beta} * (d - \text{upper}) + c / (d - \text{upper})), \text{ if } d > \text{upper} + \text{sigma};$$

where  $d$  is the distance and  $fc$  is the force constant.

Values of  $\text{sigma}$  and  $\text{beta}$  used in the calculation are 0.5 and 1.5 respectively. The values  $a$  and  $c$  are determined automatically such that potential is continuous and differential everywhere.

Before production run simulation, a default NVT relaxation was done as implemented in DESMOND. NVT ensemble was used for the production run simulation. Nose-Hoover Chain thermostat with a relaxation time of 1ps was used. A RESPA integrator was used in which a time step of 1 fs was used for all the bonded interactions, near non-bonded interactions and far non-bonded interaction. A cutoff of 9 Å was used for short range electrostatic interactions. A smooth particle mesh ewald method was used for treating long range electrostatic interactions. Simulated annealing was done in 6 stages. First stage consist simulation for 10 ps at 10 K. In the second stage, temperature was linearly increased to 3000 K till 3000 ps. In the third stage, temperature was linearly decreased to 1500 K till 6000 ps. In the fourth stage, temperature was linearly decreased to 1000 K till 8000 ps. In the fifth stage, temperature was linearly decreased to 600 k till 11200 ps. In the sixth stage, temperature was linearly decreased to 300 K till 16000 ps and maintained at 300 k till 17000 ps. Examination of the trajectory of simulation shows the occurrence of 4 types of hairpin structures (Structure A, B, C and D) defined by the main chain dihedral angles of the delta amino acid. The lowest energy structures were taken from each type and minimized using a steepest descent method using a convergence gradient threshold of 0.05 kcal/mol/Å.

## 2.6.6. $\beta$ -Amyloid Disruption Study

### 2.6.6.1. Preparation of the Soluble Aggregates of $A\beta_{1-42}$

First commercially available  $A\beta_{1-42}$  peptides were dissolved at a concentration of 1mg/mL in 1,1,1,3,3,3-hexafluoro-2-propanol (HFIP). After that HFIP solution containing  $A\beta_{1-42}$  peptides was kept overnight in laminar flow to evaporated HFIP. Final traces of HFIP was evaporated by the lyophilization of the sample. After that the lyophilized sample of  $A\beta_{1-42}$  peptides were kept at  $-80\text{ }^{\circ}\text{C}$  for further use. Final stock solution of monomeric  $A\beta_{1-42}$  were made at a concentration of 2 mM by dissolving the lyophilized  $A\beta_{1-42}$  in dimethyl sulfoxide (DMSO). After that it was sonicated in a bath sonicator for 1 min. Then the aggregates of  $A\beta_{1-42}$  were prepared by diluting the stock solution to 100 $\mu\text{M}$  with 10 mM NaPi (Sodium Phosphate) buffer at pH 7.4 and then it was incubated in a dry bath at  $37\text{ }^{\circ}\text{C}$ . These incubated aggregates of  $A\beta_{1-42}$  treated with peptide **P3** were by diluting the mixture of  $A\beta_{1-42}$  and peptide **P3** at ratio with 1:10 with 10 mM NaPi buffer at pH 7.4. In this mixture the concentration of  $A\beta_{1-42}$  was kept at 25 $\mu\text{M}$ . This was further incubated in a dry bath at  $37\text{ }^{\circ}\text{C}$ , and the final pH was maintained at 7.4.

### 2.6.6.2. Thioflavin T (ThT)-Fluorescence-Monitored Kinetics of Aggregation

Thioflavin T (ThT) fluorescence experiments were carried out as earlier reported protocol.<sup>25</sup> A fresh stock solution containing 400  $\mu\text{M}$  ThT in 10 mM NaPi buffer at pH 7.4 was prepared. An aliquot of 25 $\mu\text{L}$  of  $A\beta_{1-42}$  was added to the 40  $\mu\text{L}$  of the ThT assay solution in NaPi buffer at pH 7.4 in such way so that the final concentration of  $A\beta_{1-42}$  and ThT will be 25  $\mu\text{M}$  and 20  $\mu\text{M}$ , respectively. For the inhibition of  $A\beta_{1-42}$  oligomerisation assay, peptide **P3** (127  $\mu\text{L}$ ) from their stock solutions was added to the wells which containing 20 $\mu\text{L}$  of  $A\beta_{1-42}$  and 40 $\mu\text{L}$  of ThT. The final concentration of peptide **P3** was kept at 250  $\mu\text{M}$  along with 25 $\mu\text{M}$   $A\beta_{1-42}$  and 20 Mm ThT in the wells. All the experiments were carried out at pH 7.4. The plate was incubated at  $37\text{ }^{\circ}\text{C}$  and fluorescence readings were recorded over a time period of 144 h at  $37\text{ }^{\circ}\text{C}$  with gently shaking for 45 s prior to each reading to get more homogeneous results. All the measurements were carried out as triplicate independents. Then all the obtained recorded values were averaged, and background measurements for NaPi buffer containing only ThT were subtracted.



### 2.6.6.3. Disruption of the Disulfide Linkage of the Peptide P3

The disulfide linkage of the peptide **P3** was reduced using DTT by reported protocol.<sup>35</sup> Disulfide-reduced peptide **P3** was obtained by incubating of peptide **P3**+ DTT solution at 37 °C for 12 h. The final peptide **P3** and DTT concentrations were kept at 250 μM and 0.5 mM respectively. After this, the combine solution was used for co-incubation with 25μMAβ<sub>1-42</sub> at 37 °C and the aggregation kinetics for Aβ<sub>1-42</sub> was monitored by the ThT assay as described earlier.

### 2.6.6.4. Transmission Electron Microscopy (TEM) Studies

First 25 μM of Aβ<sub>1-42</sub> was incubated (i) alone (ii) in the presence of 250 μM peptide **P3**, and (iii) in the presence of 250μM disulfide-reduced peptide **P3** in water (0.22 μm filtered) for 96 h at 37 °C. Then aliquots of 1 μL each sample was taken and diluted to 10-fold. After that sample was spotted on individual carbon-coated 200mesh copper grids and air-dried for 24 h. Then, all the coated grids were stained with 2% uranium acetate in Milli-Q water and examined under an electron microscope.

### 2.6.6.5. Cell Viability Assay

Cell viability assay was carried by reported protocol<sup>25</sup> using human neuroblastoma SH-SY5Y cell lines. Briefly, the cells were seeded using 96- well plate at a density of 100 cells/plate in DMEM/F12 medium which contains 10% (v/v) FBS and 100U/mL penicillin. Further the cells were humidified by using 5% (v/v) CO<sub>2</sub>/air at 37 °C for 24 h. After that, the medium was replaced with the solution which contains 10 μM Aβ<sub>1-42</sub> aggregates. To study the cell viability effect of peptide **P3**, cells were incubated with by combinedly with 10 μM Aβ<sub>1-42</sub> and 100 μM peptide **P3** aggregated at 37 °C for about 12 h. To study the effect of disulfide-reduced peptide **P3** on the toxicity of Aβ<sub>1-42</sub> aggregates, cells were incubated with 10 μM Aβ<sub>1-42</sub> and 100 μM disulfide-reduced peptide **P3** aggregated solution for period of 12 h at 37 °C. For the study of cell viability of peptide **P3** alone, cells were incubated with 250 μM of peptide **P3** for period at 37 °C for 12 h. The plates contain all the samples were incubated in humidified 5% (v/v) CO<sub>2</sub>/air at 37 °C for 24 h. After that MTT, a final concentration of 0.5 mg/mL was added to the wells and then again incubated for about 4 h at 37 °C in a CO<sub>2</sub> incubator. After that, the supernatant from each well was removed, and 200μL of DMSO was added to the cells, which resulted in the

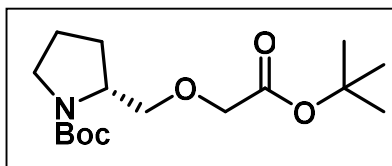
formation of crystals. Then the crystal containing solution was incubated in a humidified CO<sub>2</sub> incubator for about 20 mins and the absorbance was recorded at 570 nm using a microplate reader. All the cell viability was compared to the control cells without any peptide **P3** treatment.

#### **2.6.6.6. Two Dimensional <sup>1</sup>H-<sup>15</sup>N HSQC NMR study of Binding of Peptide P3 with Aβ<sub>1-42</sub>**

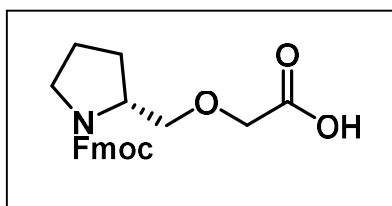
Two dimensional <sup>1</sup>H-<sup>15</sup>N HSQC NMR study was carried out on 800 MHz NMR Bruker instrument with cryoprobe by reported protocol<sup>34</sup> and the uniformly labeled <sup>15</sup>N Aβ<sub>1-42</sub> were purchased from rPeptide (Bogart, GA). First, the labeled Aβ<sub>1-42</sub> was dissolved in HFIP and allowed to evaporate. After complete evaporation of HFIP, Aβ<sub>1-42</sub> was lyophilized. Then labeled Aβ<sub>1-42</sub> at concentration of 40 μM was dissolved in 20 mM NaPi buffer at pH 7.4 containing 10 μL of 1(N) NaOH and 10 μL of DMSO. Thereafter that HSQC NMR of uniformly labeled Aβ<sub>1-42</sub> was recorded at 7 °C. Binding studies of peptide **P3** with Aβ<sub>1-42</sub> was carried at the concentration ratio of 1:10 (Aβ<sub>1-42</sub>:**P3**). The dilution effect was corrected at the time of calculation of <sup>1</sup>H and <sup>15</sup>N chemical shift. For two dimensional HSQC NMR experiments, data for the <sup>1</sup>H and <sup>15</sup>N frequencies were acquired using 1024 and 512 points, respectively. Further Bruker Topspin software was used for the process of NMR spectra and analyzing the data. Resonance assignments (both <sup>1</sup>H and <sup>15</sup>N) of all of the residues were determined according to a previously published method.<sup>32</sup> The combined perturbation in the chemical shifts for both of the resonances (<sup>1</sup>H-<sup>15</sup>N) was determined using the following equation:

$$\Delta_{\text{ppm}} = [(5*\Delta^1\text{H})^2 + (\Delta^{15}\text{N})^2]^{1/2}$$

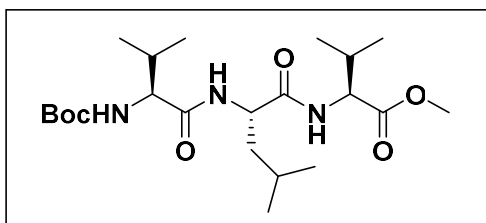
## 2.7. Characterization Data of Synthesized Compounds and Peptides P1-P3



$^1\text{H}$  NMR (400 MHz, Chloroform-*d*)  $\delta$  3.96 (bs, 2H), 3.61 (bs, 1H), 3.33 (bs, H), 2.08 – 2.04 (m, 2H), 1.92 (bs, 2H), 1.83-1.77 (m, 1H), 1.63 (s, 0H), 1.47 (s, 3H), 1.41 (d,  $J = 4.2$  Hz, 0H).  $^{13}\text{C}$  NMR (100 MHz, Chloroform-*d*)  $\delta$  169.59, 154.50, 81.46, 79.18, 72.27, 71.74, 69.03, 56.38, 28.56, 28.15, 23.81, 22.90. HRMS  $m/z$  calculated value for  $\text{C}_{16}\text{H}_{29}\text{NO}_5$  is  $[\text{M}+\text{Na}^+]$  338.1943 and observed 338.1942



$^1\text{H}$  NMR (400 MHz, Chloroform-*d*)  $\delta$  7.76 (d,  $J = 8$  Hz, 2H), 7.59 (d,  $J = 8$  Hz, 2H), 7.39 (t,  $J = 8$  Hz, 2 H), 7.31 (t,  $J = 8$  Hz, 2 H), 4.61 (bs, 1H), 4.38 – 4.42 (m, 2H), 4.22 (bs, 1H), 4.12 (bs, 2H), 3.32-3.3 (m, 2H), 1.91 (bs, 4H).  $^{13}\text{C}$  NMR (100 MHz, Chloroform-*d*)  $\delta$  173.35 , 144.12 , 141.46 , 127.82 , 127.18 , 125.16 , 120.08 , 72.88 , 68.59 , 67.46 , 57.05 , 47.42 , 46.92 , 28.61 , 28.00 , 23.96. MALDI/TOF-TOF  $m/z$  calculated value for  $\text{C}_{22}\text{H}_{23}\text{NO}_5$  is  $[\text{M}+\text{Na}^+]$  404.14 and observed 404.14



$^1\text{H}$  NMR (400 MHz, Chloroform-*d*)  $\delta$  6.72 (d,  $J = 8$  Hz, 1H), 6.58 (d,  $J = 8$  Hz, 1H), 4.97 (d,  $J = 8$  Hz, 1H), 4.44 – 4.53 (m, 2H), 4.08 – 4.14 (m, 1H), 3.72 (s, 3H), 2.10 – 2.19 (m, 1H), 1.59 – 1.70 (m, 4H), 1.42 (s, 9H), 0.87 – 0.92 (m, 18H).  $^{13}\text{C}$  NMR (101 MHz, Chloroform-*d*)  $\delta$  172.87, 172.21, 171.79, 155.8, 57.26, 52.24, 51.89, 41.03, 40.73, 31.30, 28.40, 24.83, 24.71, 23.03, 22.14, 19.06, 17.85. MALDI/TOF-TOF  $m/z$  calculated value for  $\text{C}_{22}\text{H}_{41}\text{N}_3\text{O}_6$  is  $[\text{M}+\text{Na}^+]$  466.28 and observed 466.30

## 2.8. References

1. a) Dill, K. A.; MacCallum, J. L. *Science* **2012**, *338*, 1042. b) Dill, K. A. *Biochemistry* **1990**, *29*, 7133. c) Hess, G. P.; Rupley, J. A. *Annu. Rev. Biochem.* **1971**, *40*, 1013. d) DeGrado, W. F.; Summa, C. M.; Pavone, V.; Nastri, F.; Lombardi, A. *Annu. Rev. Biochem.* **1999**, *68*, 779.
2. a) Chou, P. Y.; Fasman, G. D. *J. Mol. Biol.* **1977**, *115*, 135. b) Smith, J. A.; Pease, L. G. *CRC Crit. Rev. Biochem.* **1980**, *8*, 315. c) Rose, G. D.; Gierasch, L. M.; Smith, J. A. *Adv. Protein Chem.* **1985**, *37*, 1.
3. a) Robinson, J. A. *Acc. Chem. Res.* **2008**, *41*, 1278. b) References mentioned in ref no 11-18.
4. a) Stanfield, R. L.; Fieser, T. M.; Lerner, R. A.; Wilson, I. A. *Science* **1990**, *248*, 712. b) Rini, J. M.; Schulze-Gahmen, U.; Wilson, I. A. *Science* **1992**, *255*, 959. c) Garcia, K. C.; Ronco, P. M.; Veroust, P. J.; Brunger, A. T.; Amzel, L. M. *Science* **1992**, *257*, 502.
5. a) Kyle, D. J.; Blake, P. R.; Smithwick, D.; Green, L. M.; Martin, J. A. *J. Med. Chem.* **1993**, *36*, 1450. b) Thurieau, C.; Félétou, M.; Hennig, P.; Raimbaud, E.; Canet, E.; Fauchère, J.-L. *J. Med. Chem.* **1996**, *39*, 2095. c) Plucinska, K.; Kataoka, T.; Yodo, M.; Cody, W. L.; He, J. X.; Humblet, C.; Lu, G. H.; Lunney, E.; Major, T. C. *J. Med. Chem.* **1993**, *36*, 1902. d) Nikiforovich, G. V.; Marshall, G. R. *Biochem. Biophys. Res. Commun.* **1993**, *195*, 222. e) Nutt, R. F.; Veber, D. F.; Saperstein, R. *J. Am. Chem. Soc.* **1980**, *102*, 6539. f) Brady, S. F.; Paleveda, W. J., Jr.; Arison, B. H.; Saperstein, R.;

- Brady, E. J.; Raynor, K.; Reisine, T.; Veber, D. F.; Freidinger, R. M. *Tetrahedron* **1993**, *49*, 3449. g) Bach, A. C., II; Espina, J. R.; Jackson, S. A.; Stouten, P. F. W.; Duke, J. L.; Mousa, S. A.; DeGrado, W. F. *J. Am. Chem. Soc.* **1996**, *118*, 293. h) Haubner, R.; Schmitt, W.; Holzemann, G.; Goodman, S. L.; Jonczyk, A.; Kessler, H. *J. Am. Chem. Soc.* **1996**, *118*, 7881.
6. a) Cole, A. M.; Wang, W.; Waring, A. J.; Lehrer, R. I. *Curr. Protein Pept. Sci.* **2004**, *5*, 373. b) Brogden, K. A. *Nat. Rev. Microbiol.* **2005**, *3*, 238.
7. a) Russell, S. J.; Cochran, A. G. *J. Am. Chem. Soc.* **2000**, *122*, 12600. b) Jager, M.; Dendle, M.; Fuller, A. A.; Kelly, J. W. *Protein Sci.* **2007**, *16*, 2306. c) Favre, M.; Moehle, K.; Jiang, L.; Bfeiffer, B.; Robinson, J. A. *J. Am. Chem. Soc.* **1999**, *121*, 2679. d) Jiang, L.; Moehle, K.; Dhanapal, B.; Obrecht, D.; Robinson, J. A. *Helv. Chim. Acta*, **2001**, *83*, 3097. e) Fasan, R.; Dias, R. L. A.; Moehle, K.; Zerbe, O.; Obrecht, D.; Mittl, P. R. E.; Grutter, M. G.; Robinson, J. A. *ChemBioChem* **2006**, *7*, 515.
8. a) Metrano, A. J.; Miller, S. J. *Acc. Chem. Res.* **2019**, *52*, 199. b) Yan, X. C.; Anthony J. Metrano, A. J.; Robertson, M. J.; Abascal, N. C.; Tirado-Rives, J.; Miller, S. J.; Jorgensen, J. L. *ACS Catal.* **2018**, *8*, 9968. c) Metrano, A. J.; Abascal, N. C.; Mercado, B. Q.; Paulson, E. K.; Hurlley, A. E.; Miller, S. J. *J. Am. Chem. Soc.* **2017**, *139*, 492. d) Copeland, G. T.; Jarvo, E. R.; Miller, S. J. *J. Org. Chem.* **1998**, *63*, 6784. e) Metrano, A. J.; Miller, S. J. *J. Org. Chem.* **2014**, *79*, 1542. f) Schnitzer, T.; Wennemers, H. *J. Am. Chem. Soc.*, **2017**, *139*, 15356. g) Kastl, R.; Wennemers, H. *Angew. Chem. Int. Ed.* **2013**, *52*, 7228.
9. a) Majumder, P.; Baxa, U.; Walsh, S. T. R.; Schneider, J. P. *Angew. Chem. Int. Ed.* **2018**, *57*, 15040. b) Shi, J.; Fichman, G.; Schneider, J. P. *Angew. Chem. Int. Ed.* **2018**, *57*, 11188. c) Schloss, A. C.; Williams, D. M.; Regan, L. J. *Adv. Exp. Med. Biol.* **2016**, *940*, 167. d) Lindsey, S.; Piatt, J. H.; Worthington, P.; Sönmez, C.; Satheye, S.; Schneider, J. P.; Pochan, D. J.; Langhans, S. A. *Biomacromolecules* **2015**, *169*, 2672. e) Worthington, P.; Langhans, S.; Pochan, D. *Adv. Drug. Deliv. Rev.* **2017**, *110*, 127. f) Salick, D. A.; Kretsinger, J. K.; Pochan, D. J.; Schneider, J. P. *J. Am. Chem. Soc.* **2007**, *129*, 14793.

10. a) Somers, W. S.; Phillips, S. E. *Nature* **1992**, 359, 387. b) Puglisi, J. D.; Chyen, L.; Blanchard, S.; Frankel, A. D. *Science* **1995**, 270, 1200. c) Derrick, J. P.; Wigley, D. B.; *Nature* **1992**, 359, 752. d) Mattern, R.; Tran, T.; Goodman, M. J. *J. Med. Chem.* **1998**, 41, 2686. e) Rose, G. D.; Gierasch, L. M.; Smith, J. A. *Adv. Protein Chem.* **1985**, 37, 1. f) Varani, G. *Acc. Chem. Res.* **1997**, 30, 189. g) J. A. Robinson, *Chimia* **2007**, 61, 84.
11. a) Gellman, S. H. *Curr. Opin. Chem. Biol.* **1998**, 2, 717. b) Venkatraman, J.; Shankaramma, S. C.; Balaram, P. *Chem. Rev.* **2001**, 101, 3131. c) Haque, T. S.; Little, J. C.; Gellman, S. H. *J. Am. Chem. Soc.* **1994**, 116, 4105. d) Karle, I. L.; Awasthi, S. K.; Balaram, P. *Proc. Natl. Acad. Sci. U.S.A.* **1996**, 93, 8189. e) Ramirez-Alvarado, M.; Blanco, F. J.; Serrano, L. *Nat. Struct. Biol.* **1996**, 3, 604. f) Aravinda, S.; Shamala, N.; Rajkishore, R.; Gopi, H. N.; Balaram, P. *Angew. Chem., Int. Ed.* **2002**, 41, 3863.
12. a) Rai, R.; Vasudev, P. G.; Ananda, K.; Raghothama, S.; Shamala, N.; Karle, I. L.; Balaram, P. *Chem.-Eur. J.* **2007**, 13, 5917. b) Venkatraman, J.; Shankaramma, S. C.; Balaram, P. *Chem. Rev.* **2001**, 101, 3131.
13. a) Kemp, D. S.; Li, Z. Q. *Tetrahedron Lett.* **1995**, 36, 4175. b) Kemp, D. S.; Li, Z. Q. *Tetrahedron Lett.* **1995**, 36, 4179.
14. a) Feigel, M. J. *J. Am. Chem. Soc.* **1986**, 108, 181. b) Wagner, G.; Feigel, M. *Tetrahedron* **1993**, 49, 10831. c) Brandmeier, V.; Sauer, W. H. B.; Feigel, M. *Helv. Chim. Acta* **1994**, 77, 70. d) Winningham, M. J.; Sogah, D. Y. *J. Am. Chem. Soc.* **1994**, 116, 11173.
15. a) Diaz, H.; Espina, J. R.; Kelly, J. W. *J. Am. Chem. Soc.* **1992**, 114, 8316. b) Diaz, H.; Kelly, J. W. *Tetrahedron Lett.* **1991**, 32, 5725. c) Tsang, K. Y.; Diaz, H.; Graciani, N.; Kelly, J. W. *J. Am. Chem. Soc.* **1994**, 116, 3988. d) Diaz, H.; Tsang, K. Y.; Choo, D.; Espina, J. R.; Kelly, J. W. *J. Am. Chem. Soc.* **1993**, 115, 3790.
16. a) Gardner, R. R.; Liang, G.-B.; Gellman, S. H. *J. Am. Chem. Soc.* **1999**, 121, 1806. b) Gardner, R. R.; Liang, G.-B.; Gellman, S. H. *J. Am. Chem. Soc.* **1995**, 117, 3280.
17. a) Verbist, B. M. P.; Borggraave, W. M. D.; Toppet, S.; Compennolle, F.; Hoornaert, G. J. *Eur. J. Org. Chem.* **2005**, 2841. b) Rombouts, R.; Borggraave, W. M. D.; Delaere, D.;

- Froeyen, M.; Toppet, S. M.; Compernelle, F.; Hoornaert, G. J. *Eur. J. Org. Chem.* **2003**, 1868. c) Borggraeve, W. M. D.; Rombouts, F. J. R.; dEychen, E. V. V.; Toppet Hoornaert, S. M. G. J. *Tetrahedron Lett.* **2001**, 42, 5693.
18. a) Nowick, J. S.; Powell, N. A.; Martinez, E. J.; Smith, E. M.; Noronha, G. *J. Org. Chem.* **1992**, 57, 3763. b) Nowick, J. S.; Smith, E. M.; Noronha, G. *J. Org. Chem.* **1995**, 60, 7386. c) Smith, E. M.; Holmes, L.; Shaka, A. J.; Nowick, J. S. *J. Org. Chem.* **1997**, 62, 7906. d) Junquera, E.; Nowick, J. S. *J. Org. Chem.* **1999**, 64, 2527. e) Nowick, J. S.; Lam, K. S.; Khasanova, T. V.; Kemnitzer, W. E.; Maitra, Mee, H.T.; Liu, R. *J. Am. Chem. Soc.* **2002**, 124, 4972. f) Michael, D.; Nowick, J. S. *J. Am. Chem. Soc.* **2004**, 126, 3062.
19. a) Misra, R.; Dey, S.; Reja, R. M.; Gopi, H. N. *Angew. Chem. Int. Ed.* **2018**, 57, 1057. b) Jadhav, S. J.; Bandyopadhyay, A.; Gopi, H. N. *Org. Biomol. Chem.* **2013**, 11, 509. c) Kumar, M. G.; Thombare, V. J.; Katariya, M. M.; Veeresh, K.; Raja, K. M. P.; Gopi, H. N. *Angew. Chem. Int. Ed.* **2016**, 55, 7847. d) Kumar, M. G.; Gopi, H. N. *Org. Lett.* **2015**, 17, 4738.
20. a) Bandyopadhyay, A.; Mali, S. M.; Lunawat, P.; Raja, K. M. P.; Gopi, H. N. *Org. Lett.* **2011**, 13, 4482. b) Bandyopadhyay, A.; Misra, R.; Gopi, H. N. *Chem. Commun.* **2016**, 52, 4938. c) Kumar, M. G.; Mali, S. M.; Raja, K. M. P.; Gopi, H. N. *Org. Lett.* **2015**, 17, 230.
21. Baldauf, C.; Gunther, R.; Hofmann, H.-J. *J. Org. Chem.* **2004**, 69, 6214.
22. Yusof, Y.; Tan, D. T. C.; Arjomandi, O. K.; Schenk, G.; McGeary, R. P. *Bioorg. Med. Chem. Lett.* **2016**, 26, 1589.
23. Yamin, G.; Ruchala, P.; Teplow, D. B. *Biochemistry* **2009**, 48, 11329.
24. Pellegrino, S.; Tonali, N.; Erba, E.; Kaffy, J.; Taverna, M.; Contini, A.; Taylor, M.; Allsop, D.; Gelmia, M. L.; Ongeri, S. *Chem. Sci.* **2017**, 8, 1295.
25. Jha, A.; Kumar, M. G.; Gopi, H. N.; Paknikar, K. M. *Langmuir* **2018**, 34, 1591.

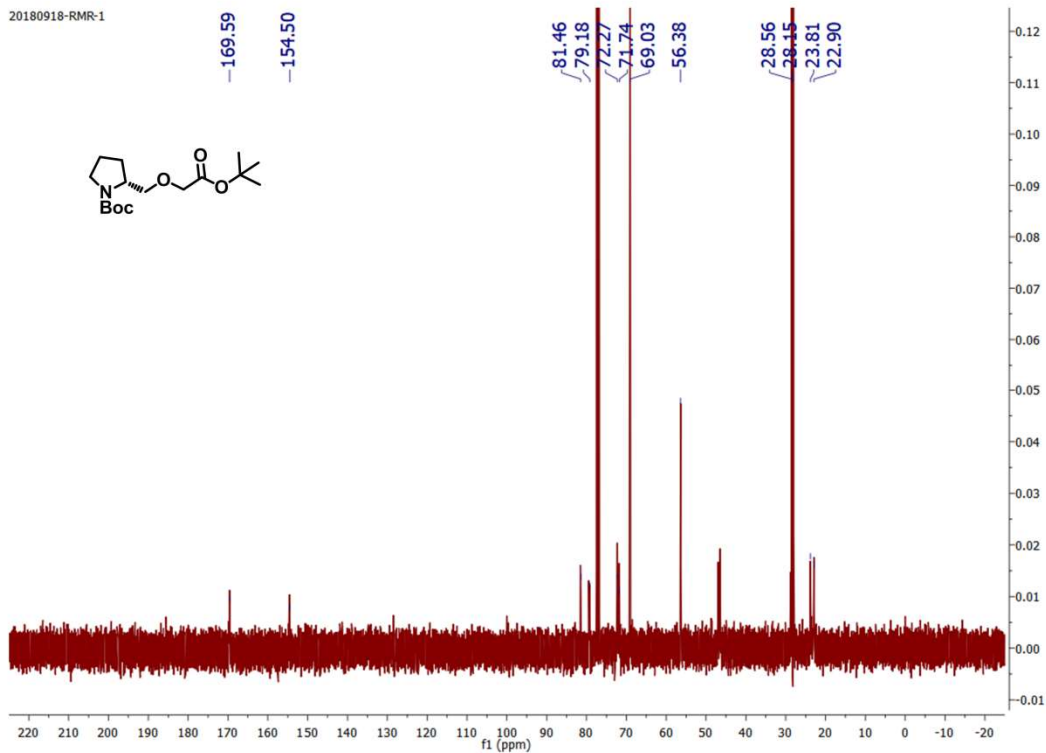
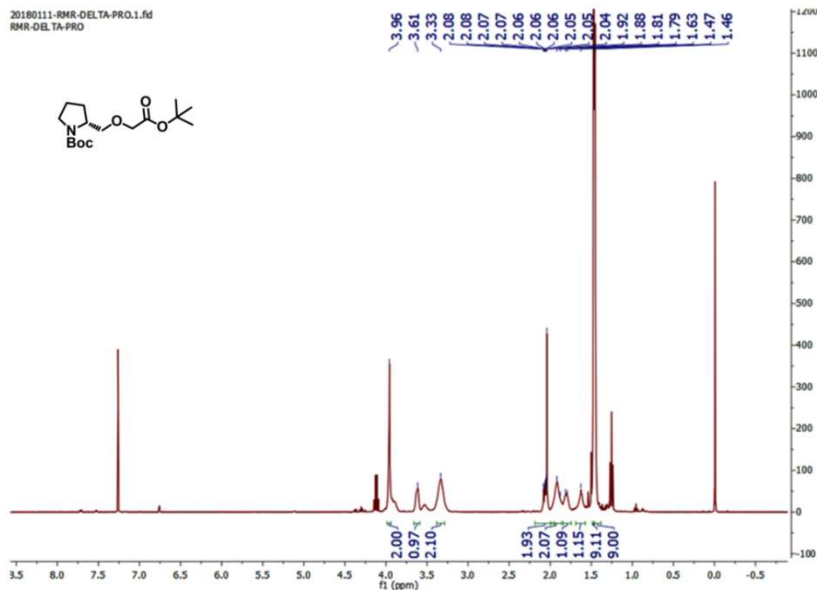
26. a) Jakob-Roetne, R.; Jacobsen, H. *Angew. Chem. Int. Ed.* **2009**, *48*, 3030. b) Chiti, F.; Dobson, C. M. J. *Annu. Rev. Biochem.* **2006**, *75*, 333. c) Stefani, M.; Dobson, C. M. J. *Mol. Med.* **2003**, *81*, 678. d) Ties, W.; Bleiler, L. 2012 Alzheimer's disease facts and figures. *Alzheimer's & dementia: the journal of the Alzheimer's Association* *8*, 131 (2012) e) *World Alzheimer Report*, 2010, <http://www.alz.co.uk/research/worldreport/>
27. a) Cohen, F. E.; Kelly, J. W. *Nature* **2003**, *426*, 905. b) Masliah, E. *Nature* **2008**, *451*, 638. c) Goedert, M.; Spillantini, M. G. A. *Science* **2006**, *314*, 777. d) Haas, C.; Selkoe, D. J. *Nat. Rev. Mol. Cell Biol.* **2007**, *8*, 101. e) Hardy, J.; Selkoe, D. J. *Science* **2002**, *297*, 353. f) Hardy, J. A.; Higgins, G. A. *Science* **1992**, *256*, 184.
28. a) Benilova, I.; Karran, E.; Strooper, B. D. *Nature Neurosci.* **2012**, *15*, 349.
29. a) Takahashi, T.; Mihara, H. *Acc. Chem. Res.* **2008**, *41*, 1309. b) Kreutzer, A. G.; Nowick, J. S. *Acc. Chem. Res.* **2018**, *51*, 706. c) Rajasekhar, K.; Chakrabarti, M.; Govindaraju, T. *Chem. Commun.* **2015**, *51*, 13434. d) Adessi, C.; Soto, C. *Drug Dev. Res.* **2002**, *56*, 184. e) Paul, A.; Nadimpally, K. C.; Mondal, T.; Thalluri, K.; Mandal, B. *Chem. Commun.* **2015**, *51*, 2245.
30. a) Tjernberg, L. O.; Naslund, J.; Lindqvist, F.; Johansson, J.; Karlstrom, A. R.; Thyberg, J.; Terenius, L.; Nordstedt, C. *J. Biol. Chem.* **1996**, *271*, 8545. b) Austen, B. M.; Paleologou, K. E.; Ali, S. A.; Qureshi, M. M; Allsop, D.; El-Agnaf, O. M. *Biochemistry* **2008**, *47*, 1984.
31. a) Soto, C.; Kindy, M. S.; Baumann, M.; Frangione, B. *Biochem. Biophys. Res. Commun.* **1996**, *226*, 672. b) Martin-Jones, Z.; Chen, D.; Gilbertson, S.; Schein, C.; Kaye, R.; Soto, C. *Ann. Neurol.* **2008**, *64*, S48.
32. a) Poduslo, J. F.; Curran, G. L.; Kumar, A.; Frangione, B.; Soto, C. *J. Neurobiol.* **1999**, *39*, 371. b) Adessi, C.; Soto, C. *Curr. Med. Chem.* **2002**, *9*, 963. c) Funke, S. A.; Willbold, D. *Curr. Pharm. Des.* **2012**, *18*, 755.
33. a) Chalifour, R. J.; McLaughlin, R. W.; Lavoie, L.; Morissette, C.; Tremblay, N.; Boule, M.; Sarazin, P.; Stea, D.; Lacombe, D.; Tremblay, P.; Gervais, F. *J. Biol. Chem.* **2003**,



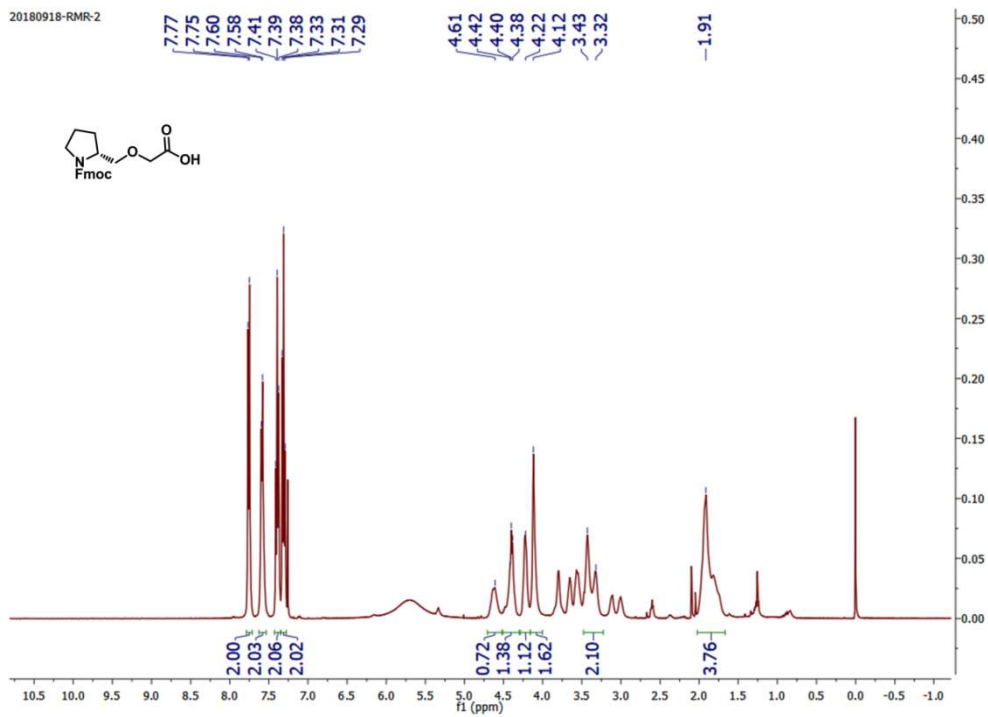
- 278, 34874. b) Sinopoli, A.; Giuffrida, A.; Tomasello, M. F.; Giuffrida, M.; Leone, M. L.; Attanasio, F.; Caraci, F.; De Bona, P.; Naletova, I.; Saviano, M.; Copani, A.; Pappalardo, G.; Rizzarelli, E. *ChemBioChem* **2016**, *17*, 1541.
34. a) Kumar, S.; Hamilton, A. D. *J. Am. Chem. Soc.* **2017**, *139*, 5744. b) Kumar, S.; Henning-Knechtel, A.; Chehade, I.; Magzoub, M.; Hamilton, A. D. *J. Am. Chem. Soc.* **2017**, *47*, 17098.
35. Mali, S. M.; Bandyopadhyay, A.; Jadhav, S. V.; Kumar, M. G.; Gopi, H. N. *Org. Biomol. Chem.* **2011**, *9*, 6566.

## 2.9. Appendix II: Characterization Data of Synthesized Compounds and Peptides P1-P3

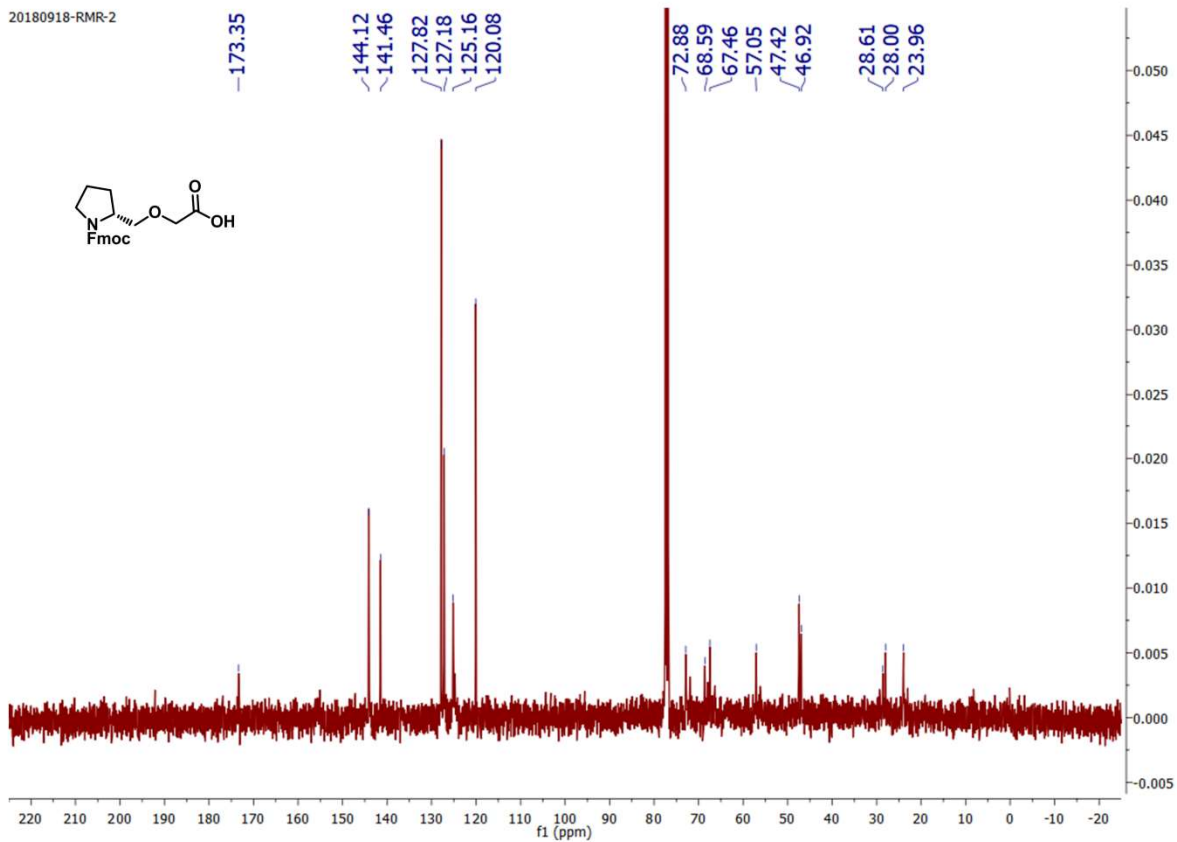
### 2.9.1. $^1\text{H}$ and $^{13}\text{C}$ NMR Spectra

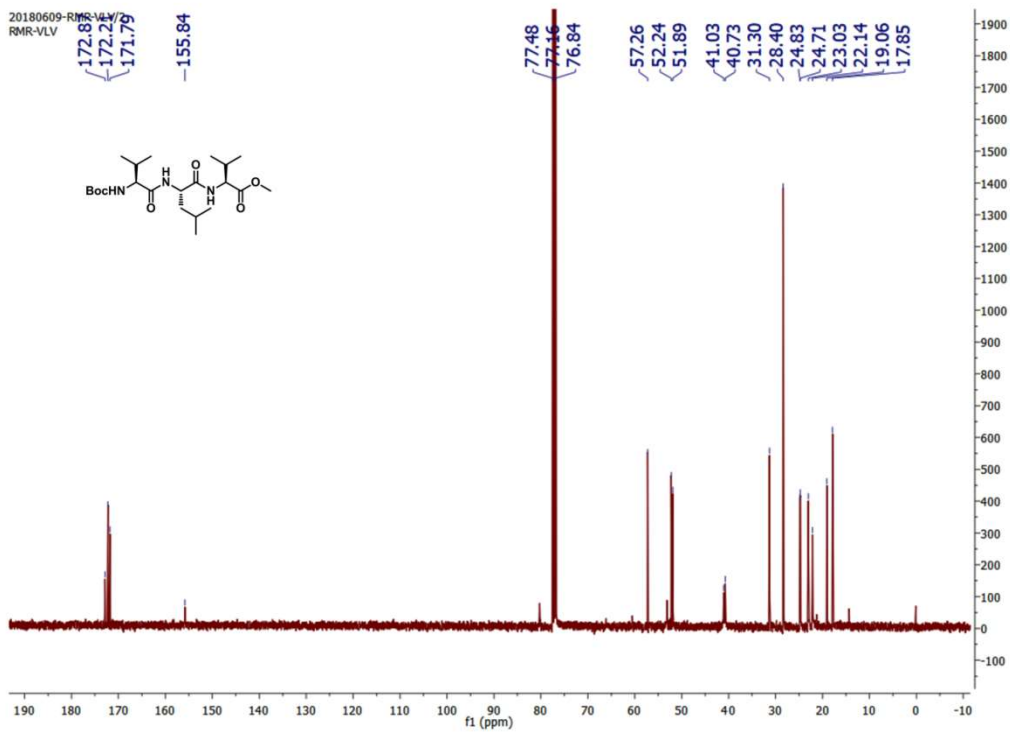
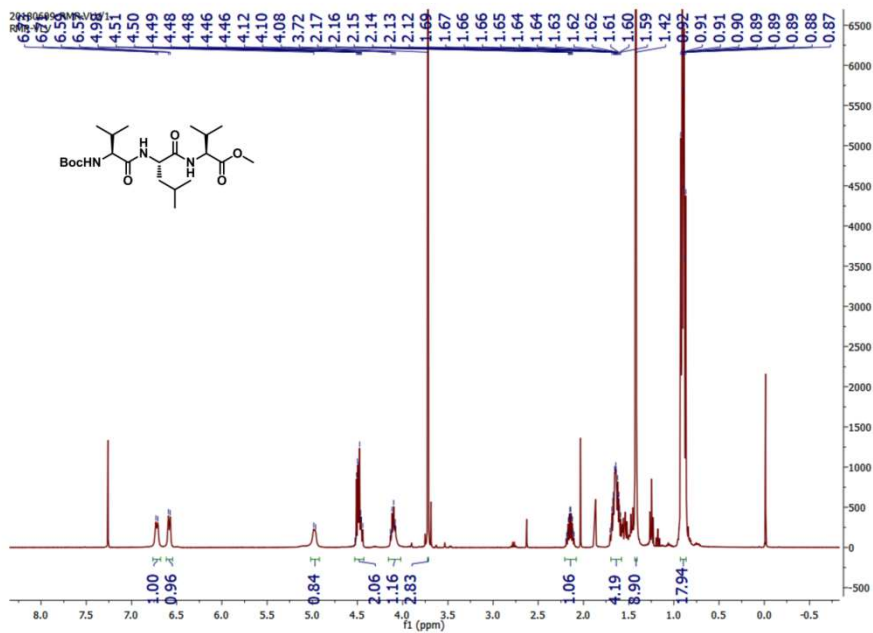


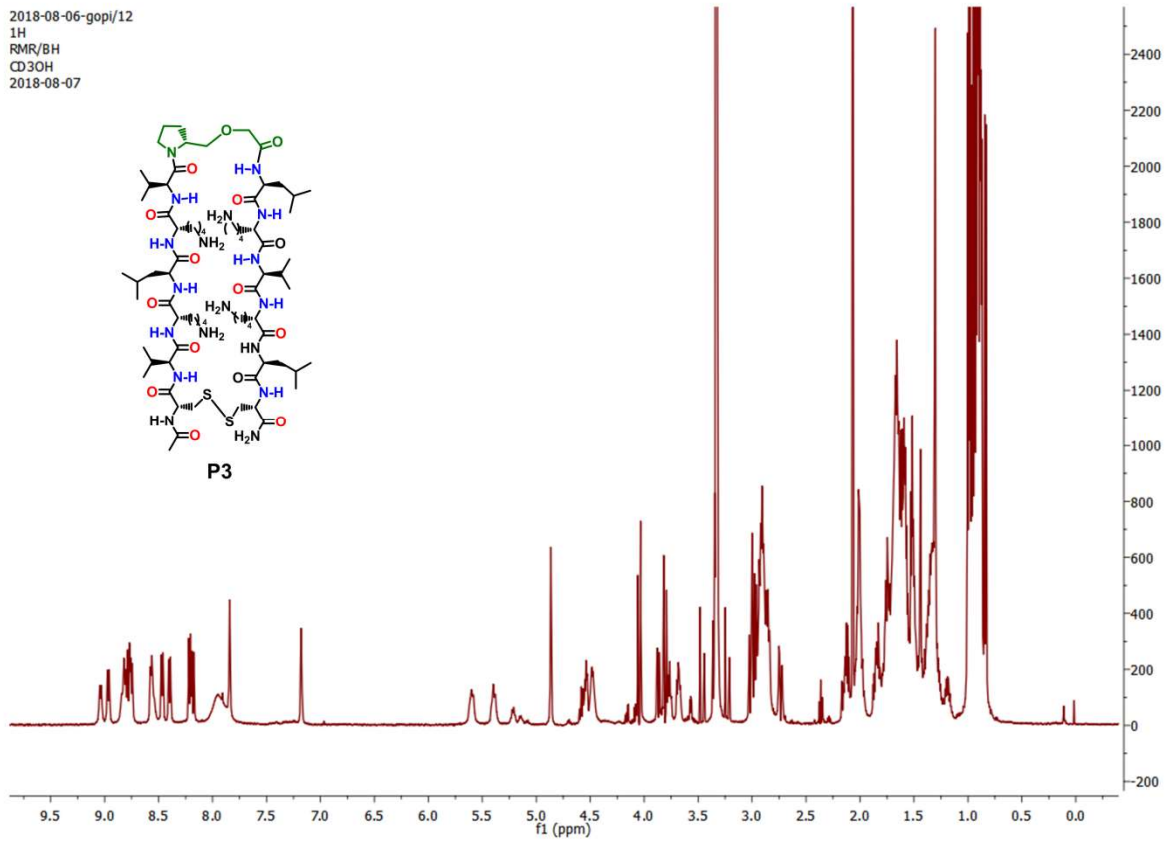
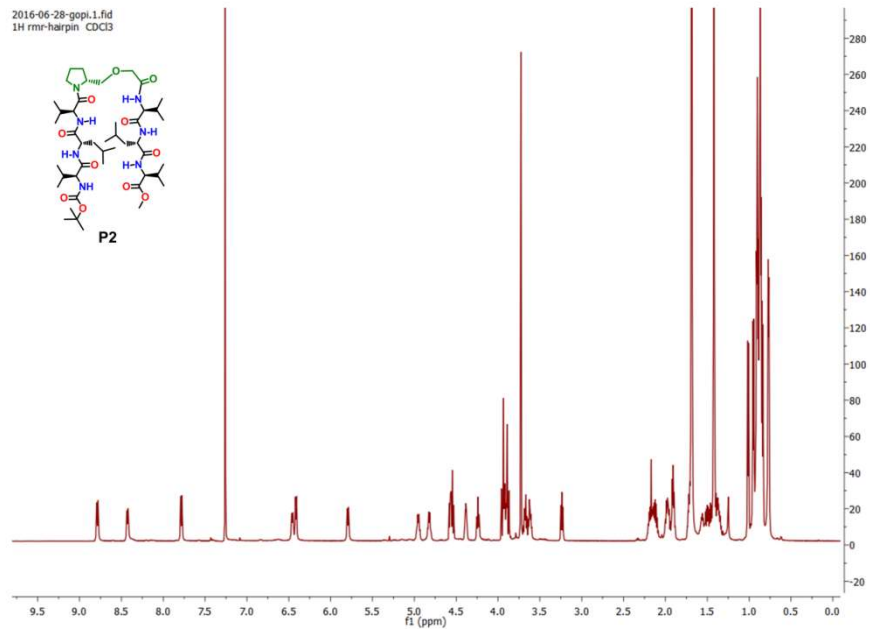
20180918-RMR-2



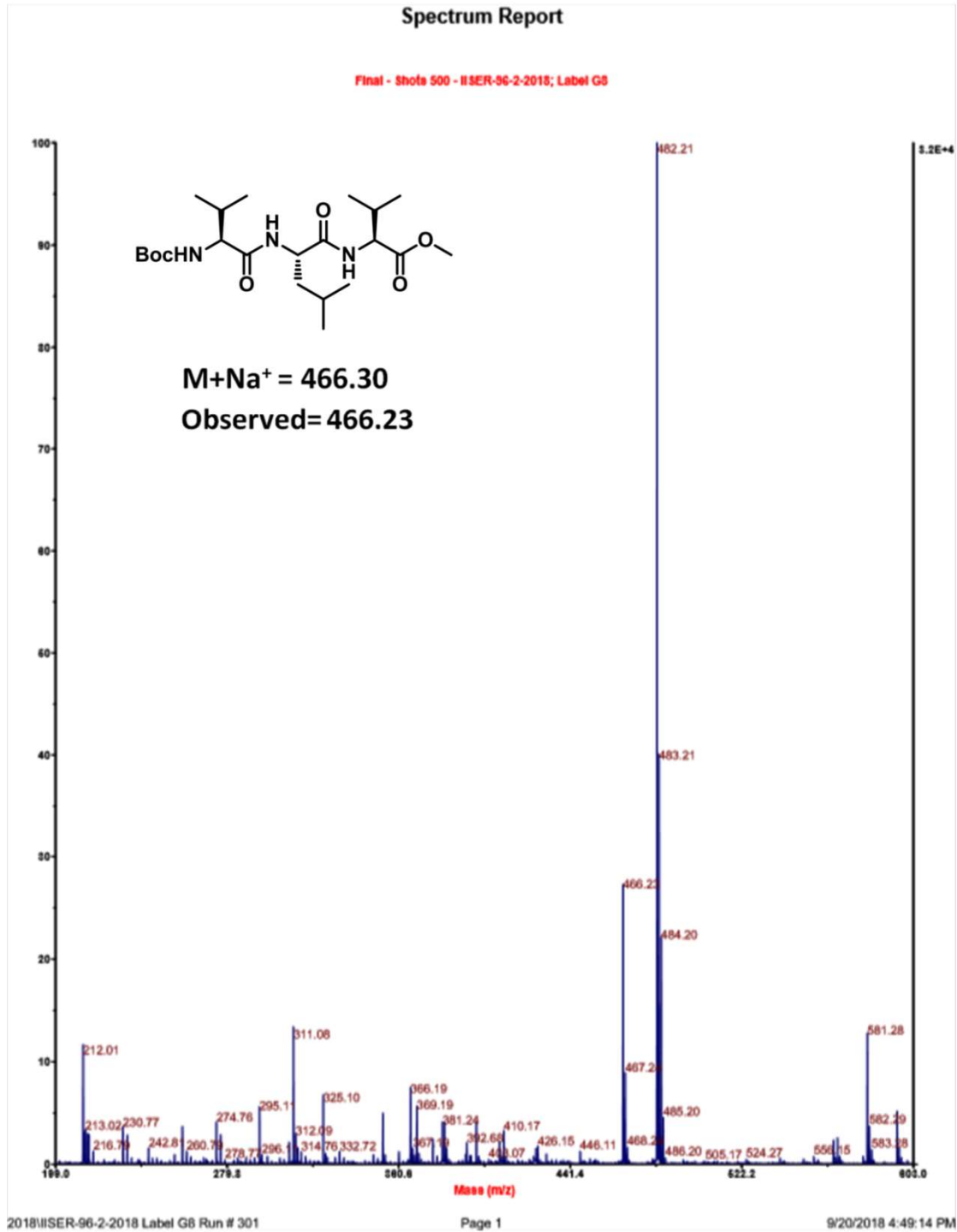
20180918-RMR-2





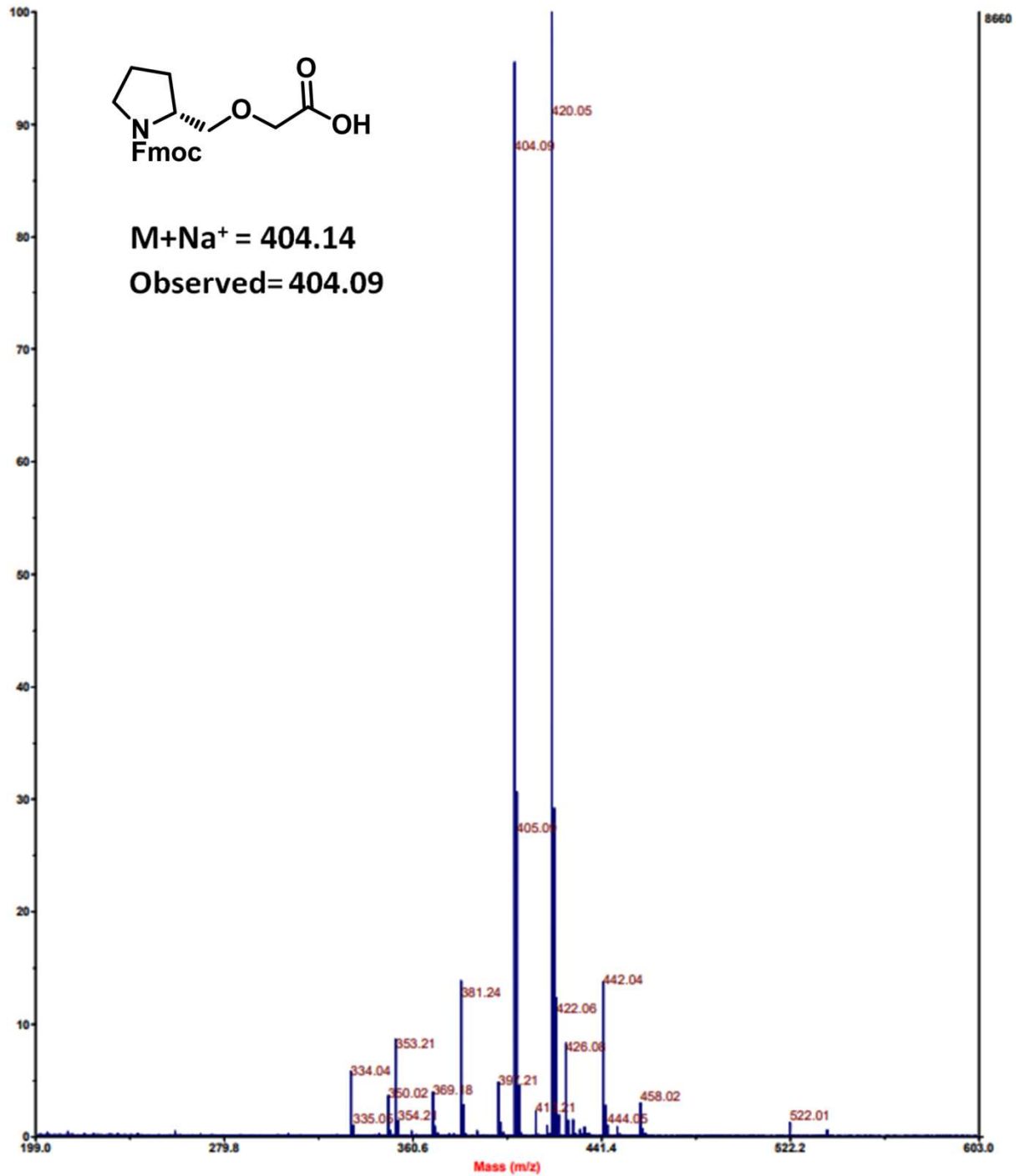


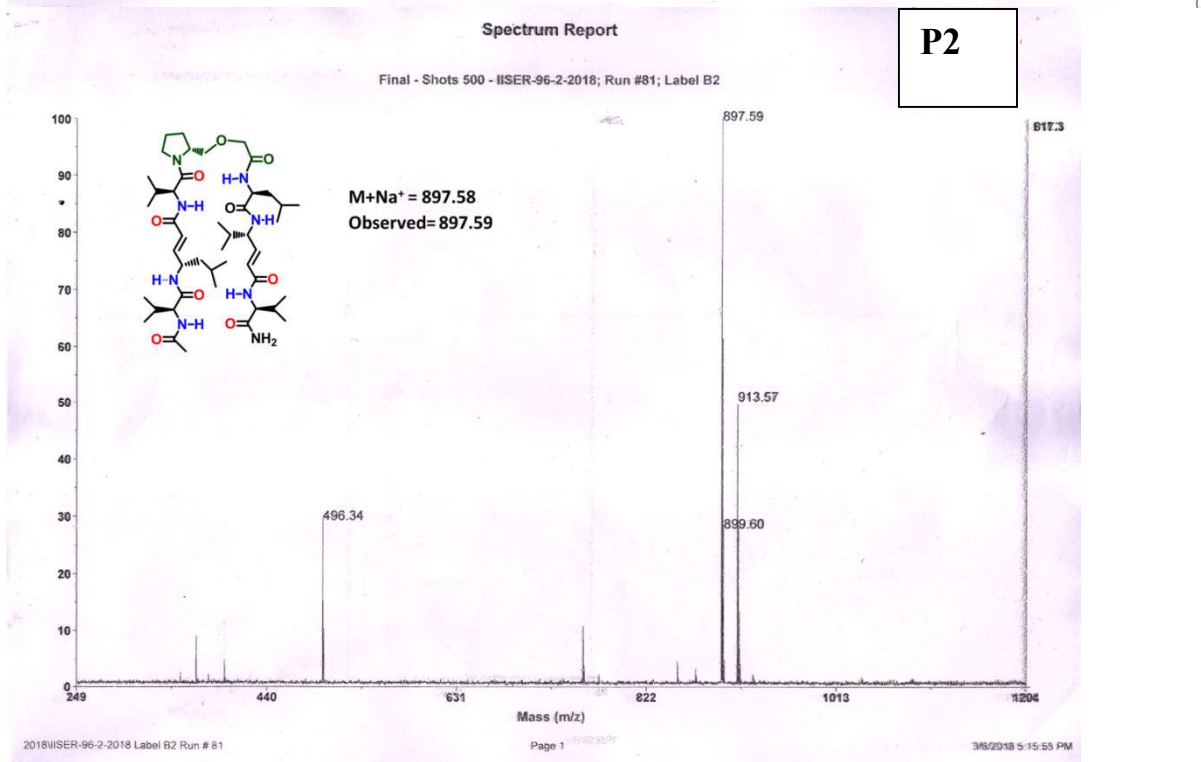
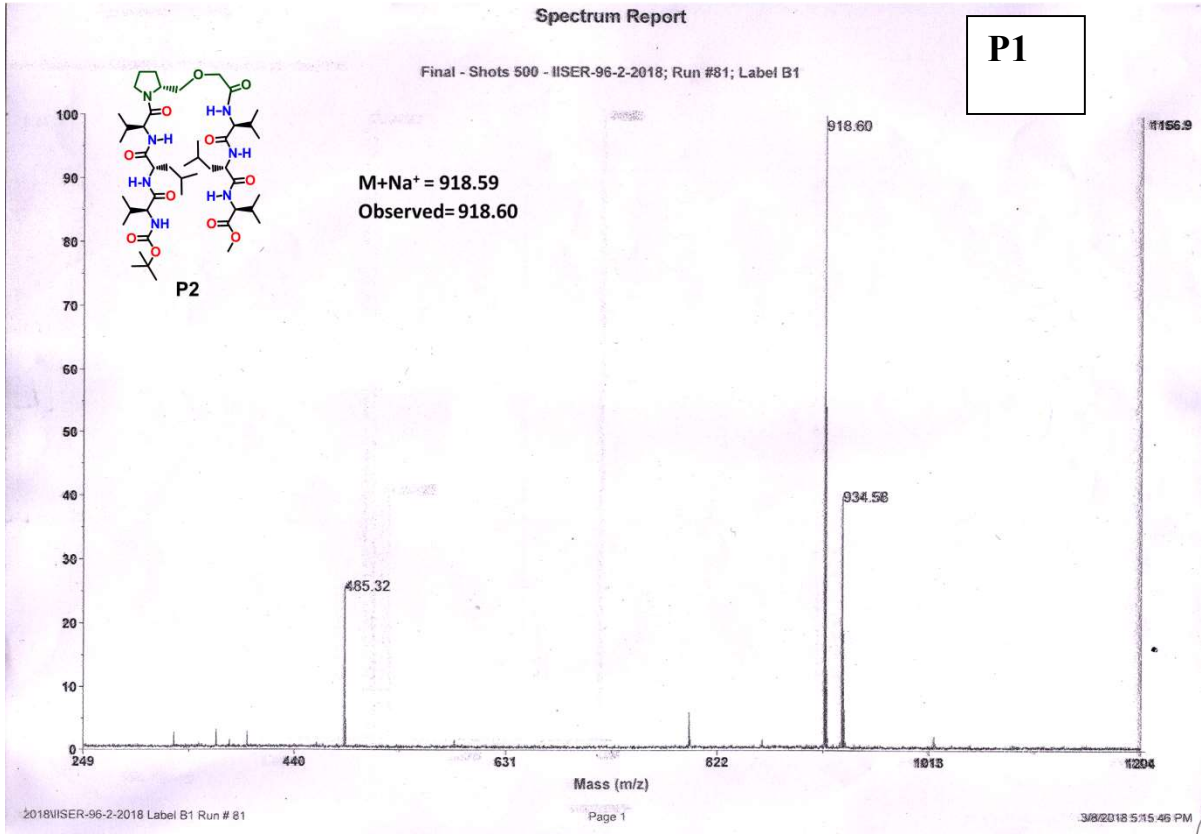
## 2.9.2. MALDI-TOF/TOF Mass Spectra



# Spectrum Report

Final - Shots 500 - IISER-96-2-2018; Label G6



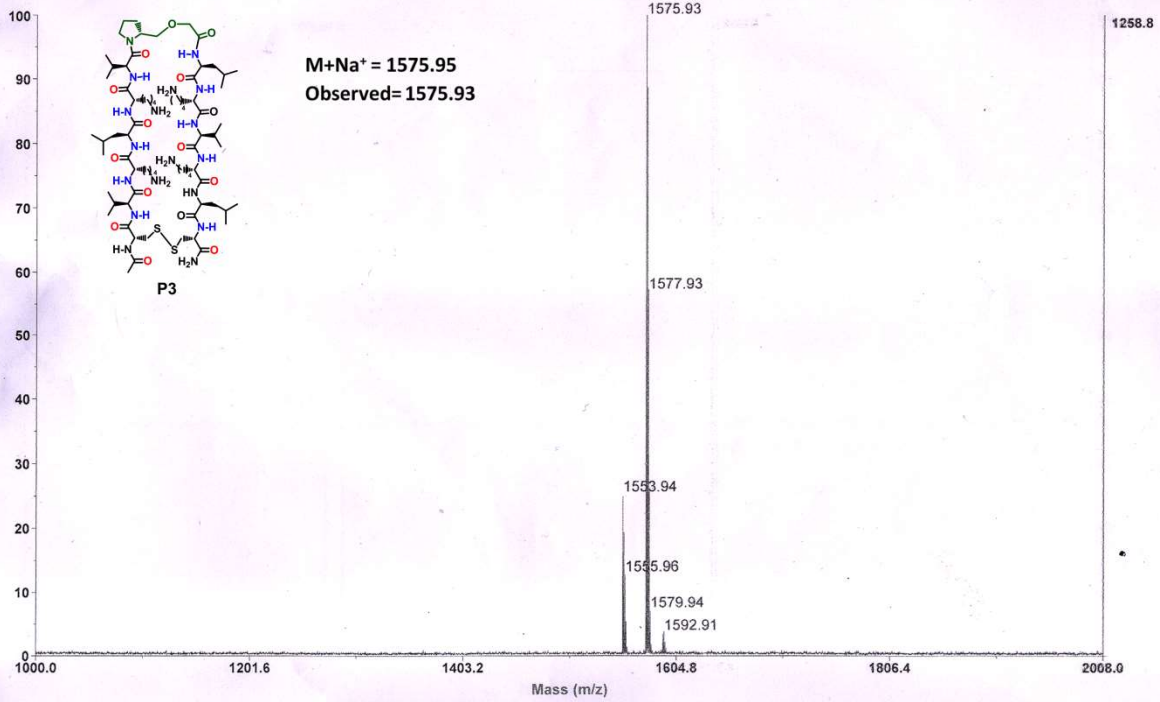




Spectrum Report

Final - Shots 500 - IISER-96-2-2018; Label B4

**P3**



## *Chapter 3*

# **Impact of H-Bonding in Helices Composed of Flexible $\delta$ -Amino Acids**

### 3.1. Introduction

The conformation of any folded polypeptide chain consisting of  $\alpha$ -amino acids is mainly governed by the three torsion angles of  $\phi, \psi$  and  $\omega$ .<sup>1</sup> Using this 3-Dimensional compact structure, proteins carry out different diversified function in biological process.<sup>2</sup> The non-bonded interactions have a great role for the determining the stereochemistry of the polypeptide along with the torsion angles which lie within the allowed region of the Ramachandran Map.<sup>3</sup> The peptide bond ( $\omega$ ) is generally restricted to *trans* geometry ( $\omega = 180^\circ$ ). But in case of peptide bonds preceding prolyl residue *cis* conformations ( $\omega = 0^\circ$ ) is observed with a higher propensity.<sup>4</sup> The backbone hydrogen bonding interaction between CO and NH leads to the formation of the different secondary structure like helices, sheet and turns. But due to the proteolytic degradation of peptide composed of  $\alpha$ -amino acids are suffered from the poor efficacy and short half-life.<sup>5</sup> To overcome these limitations people come up with different type of modification such as incorporation of non-natural amino acids, N-methylation, cyclization etc.<sup>6</sup> In addition to the modifications of  $\alpha$ -amino acids, extensive efforts have also been made over the last two decades in synthesise and utilization of various types of backbone homologated non-natural amino acids such as  $\beta, \gamma, \delta, \epsilon$  etc. and examined their folding properties. Surprisingly, the oligomers of these  $\beta, \gamma$ - and higher homologue amino acids are spontaneously fold into definite structures similar to protein structures termed as “Foldamers”.<sup>7</sup> Importantly, in addition to the homooligomers, the mixed sequences containing  $\alpha$ -amino acids and higher homologue  $\beta$ - and  $\gamma$ -amino acids also fold into definite structures. This type of molecular chimera in peptide foldamers are great interest due to the improved pharmacological properties and efficacy.<sup>8</sup>

### 3.2. Foldamers Containing Delta Amino Acids

Over the years homologated amino acids such as  $\beta, \gamma, \delta, \epsilon$  have been extensively explored to mimic the protein secondary structures.<sup>7</sup> Among the secondary structures, the  $\alpha$ -helix is one of the most predominant protein secondary structure. In their pioneering work, the groups of Seebach<sup>7e</sup> and Gellman<sup>7a-7c</sup> showed the design of different types of helices from various types of  $\beta$ -amino acids. The spontaneous folding of  $\beta$ -peptides in the helices, motivated to examine folding properties of the homooligomers of  $\gamma$ -, and higher homologue amino acids as well as

other artificial building blocks.<sup>9</sup> In addition to the homooligomers, different types of hybrid peptides composed of mixed sequences containing more than one type of amino acids are also studied to broaden the peptide foldamer research. In this context, the folding properties of mixed  $\alpha/\beta^{10a-10f}$ ,  $\alpha/\gamma^{10g-10j}$  and  $\beta/\gamma^{10k-10m}$  sequences containing various backbone modified amino acids have been studied

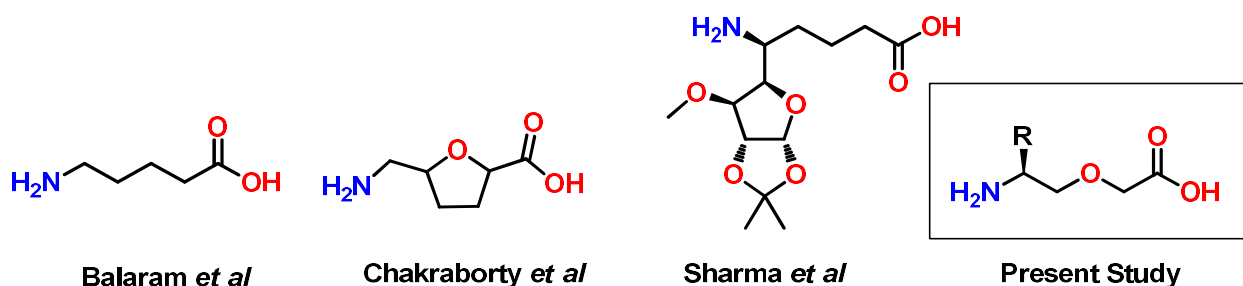


**Figure 3.1:** Chemical structure of different  $\delta$ -amino acid available in the literature.

for mimicking of native protein structure. Though the folding properties of  $\beta$ - and  $\gamma$ - and their mixed have been extensively examined, however, peptides composed of  $\delta$ -amino acid are scarcely discussed in the literature. Nevertheless, Hofmann *et al* theoretically proposed the ability of different helices from the homooligomers from  $\delta$ -amino acids.<sup>11</sup> Based on the computational calculations, they proposed that helices having 10-membered hydrogen bonding are most stable followed by 14, 16 and 8 membered hydrogen bonded oligomers. The groups of Chakraborty and Sharma have reported different hybrid helices from pyranose- or furanose-based carboamino and furan based  $\delta$ -amino acids. Chakraborty and co-workers used constrained furanoid sugar amino acids to design different reverse turns in  $\beta$ -hairpins.<sup>12a,12b</sup> Further they examined the ability of cyclic oligomers from furan amino acids as antimicrobial candidates and also to G-quadruplex.<sup>12c</sup> In a recent study by Sharma and colleagues reported the  $\alpha/\delta$  hybrid peptides composed of sugar amino acids. Through both solution and theoretical calculations, they proved that  $\alpha/\delta$  hybrid peptides composed of sugar amino acids prefer to adopt 11/13 mixed helices.<sup>13</sup> Apart from the pyranose and furanose based  $\delta$ -amino acids, Huc and co-workers showed helical folding form quinolone based  $\delta$ -amino acids in single crystals.<sup>14</sup> In addition, Balam and co-workers examined the stability of the  $\alpha$ -helices by replacing Gly-Gly residue of bovine pancreatic trypsin inhibitor with  $\delta$ -aminovaleric acid ( $\delta$ -Ava).<sup>15</sup> Where the amide bond is

replaced by the  $C^\beta-C^\gamma$  bond. The different types of  $\delta$ -amino acids studied in the literature is shown in the Figure 3.1.

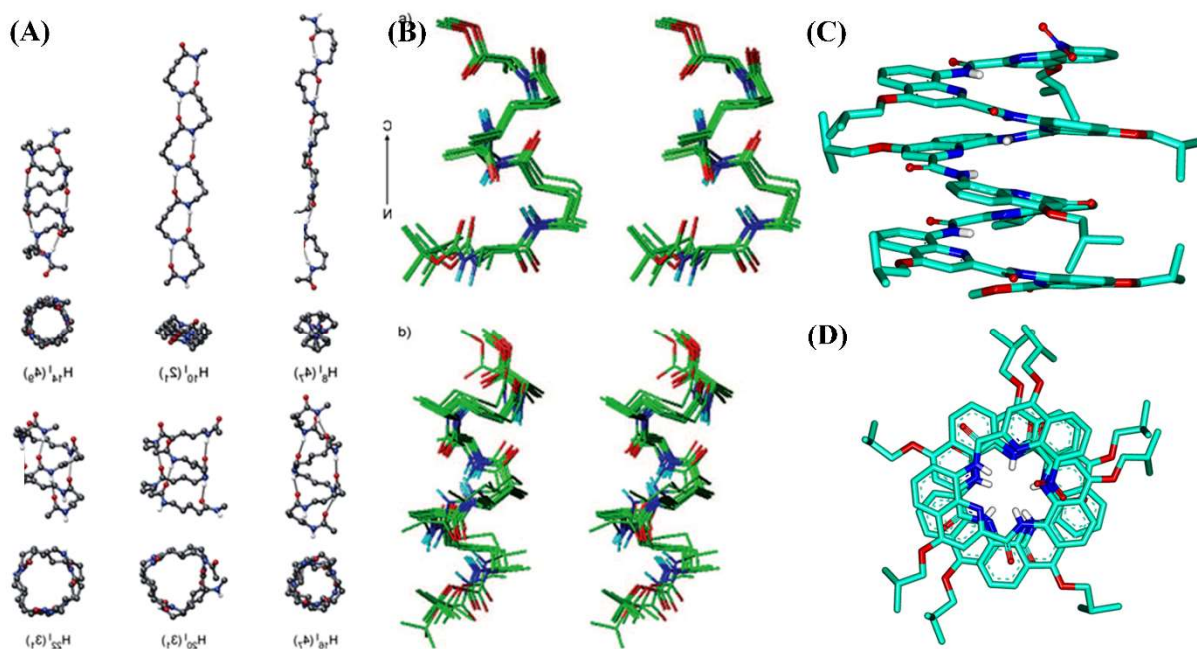


**Figure 3.2:** (A) Theoretical calculation for folding ability of oligomers from  $\delta$ -amino acids. (B) Formation of mixed helices from  $\alpha/\delta_{Caa}$  hybrid peptide. (C) and (D) X-ray crystal structure of helical folding from quinolone based aromatic  $\delta$ -amino acids and top-view respectively. Figure 3.2A and 3.2D were reproduced with permission from ref 11 and 13 respectively. Crystal structure shown in (C) and (D) was generated from the CIF available in ref no. 14.

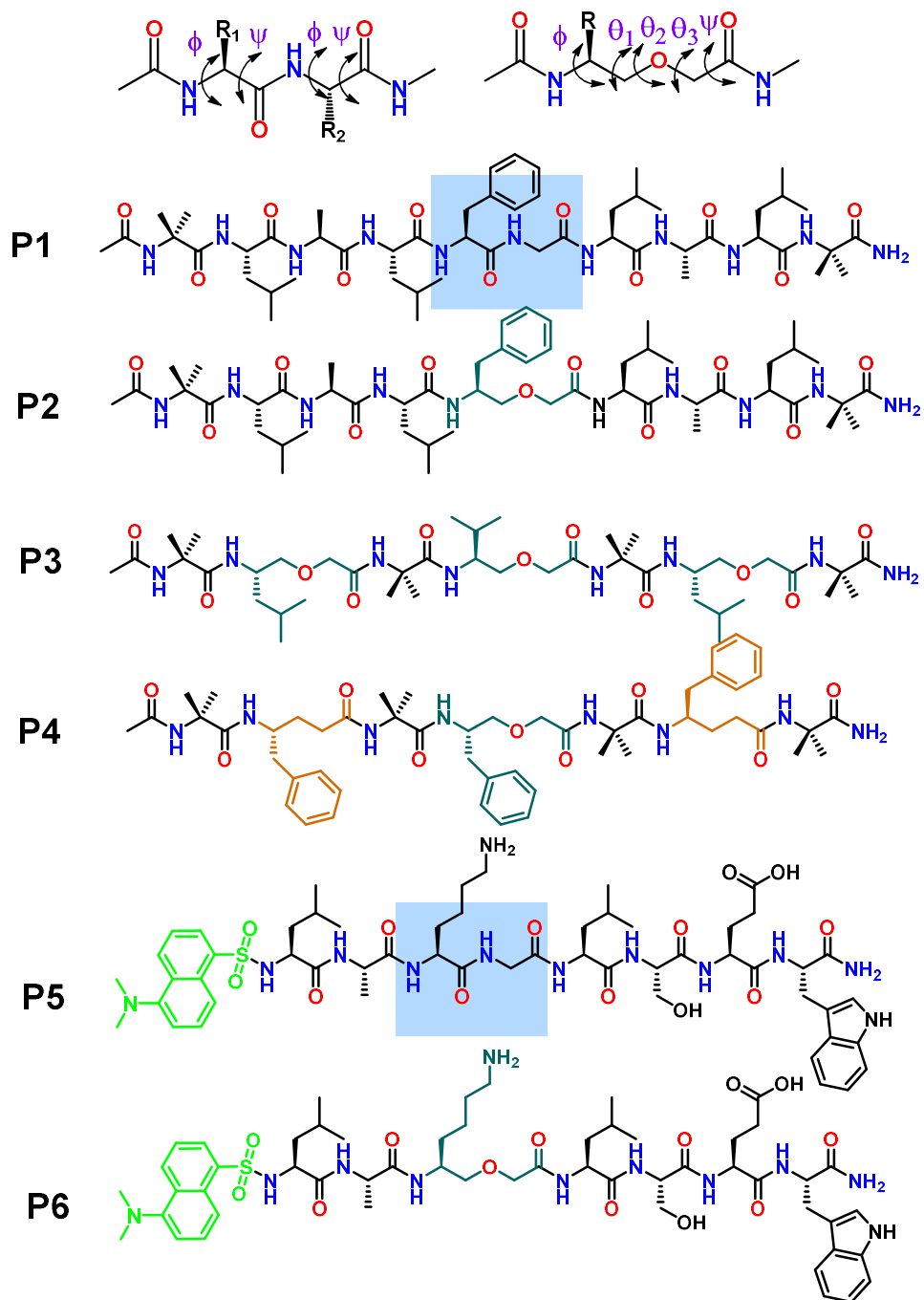
### 3.3. Aim and Rationale of the Present Work

Foldamers consisting of proteogenic side chain containing  $\delta^5$ -amino acids are not well explored due to the difficulties in the synthesis of the  $\delta^5$ -amino acid. As we are interested in design of different folded peptides from the non-ribosomal amino acids such as  $\gamma$ -,  $\alpha,\beta$ -unsaturated amino  $\gamma$ -acids.<sup>16</sup> Recently we showed stable  $C_{12}$  helices from  $\alpha, \gamma^4$  hybrid peptide<sup>16a-16d</sup> and structural dimorphism from achiral  $\alpha, \gamma^4$  hybrid peptide in single crystals.<sup>16f</sup> As the  $\delta^5$ -amino acids are surrogates of  $\alpha$ -dipeptide, we sought to investigate the folding of  $\beta(O)$ - $\delta^5$ -amino acid towards different folded structure as a guest in host  $\alpha$ -peptide and hybrid peptide sequences.

### 3.4. Results and Discussion

#### 3.4.1. Design and Synthesis

The sequences of peptides under investigations are shown in Scheme **3.1**. The  $\beta(\text{O})\text{-}\delta^5$ -amino acid was synthesized by the reported protocol from Boc protected amino alcohol.<sup>17</sup> All peptides were synthesized by the conventional solid phase peptide synthesis strategy on Rink Amide resin on 0.2 mmol scale and purified by RP-HPLC using MeOH/H<sub>2</sub>O system. Peptide **P1** is a control  $\alpha$ -helical peptide. In peptide **P2**, we replaced Phe-Gly dipeptide by  $\beta(\text{O})\text{-}\delta^5$ -Phe in the  $\alpha$ -helix. To understand whether  $\alpha,\delta$ - hybrid peptides with 1:1 alternating  $\alpha$ - and  $\delta$ -amino acids can give 13-helix similar to the  $\alpha$ -peptides, we designed peptide **P3**. Further, to understand the versatility  $\beta(\text{O})\text{-}\delta^5$ -amino acid, we have designed peptide **P4** by incorporating  $\beta(\text{O})\text{-}\delta^5$ -amino acid as a guest in the sequences of  $\alpha,\gamma$ -hybrid peptide. The  $\alpha,\gamma^4$  hybrid peptides are known to form stable C<sub>12</sub>-helix.<sup>16a-16d</sup> As the  $\beta(\text{O})\text{-}\delta^5$ -amino acids is mimic of  $\alpha$ -dipeptide composed of  $\alpha$ -amino acids, we designed peptide **P5** and **P6** consisting of Tryptophan and Dansyl group understand their stability towards proteases.



**Scheme 3.1:** Sequences of peptides under investigations.





## Peptide P2:

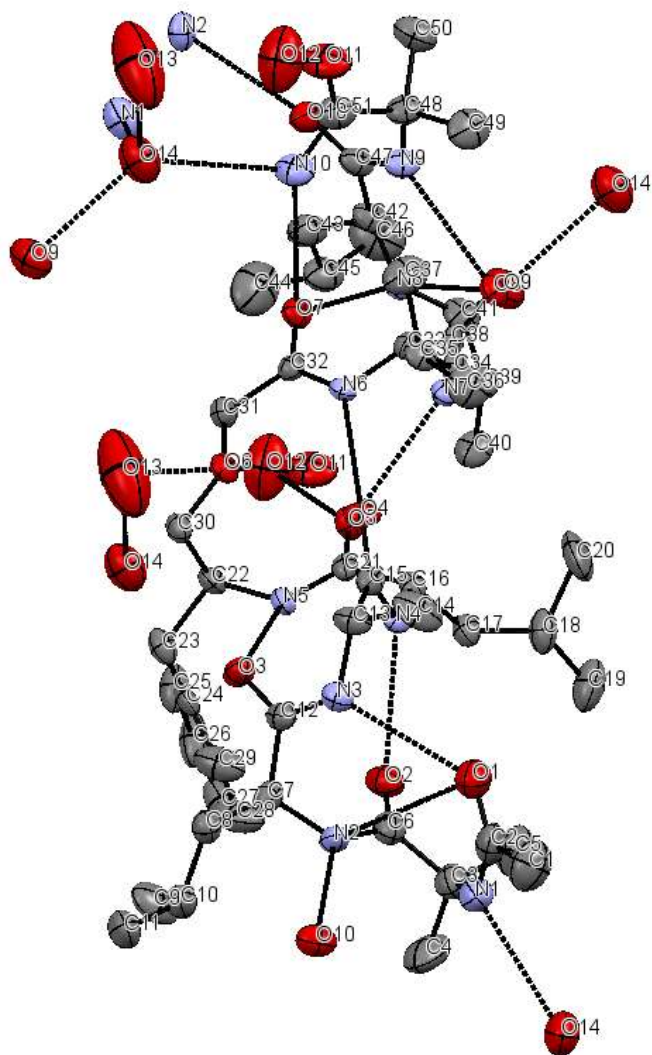


**Figure 3.4:** ORTEP diagram of peptide **P2**. H-bonds are shown in dotted lines. H-atoms are omitted for clarity. Ellipsoids are drawn at 50% probability (CCDC No 1919644)



### 3.4.3. Conformational Analysis of Peptides P1-P4

#### Peptide P1

The X-ray diffraction quality single crystals of the control  $\alpha$ -helix **P1** were grown from slow evaporation of aqueous methanol solution and its single crystal structure is shown in the Figure **3.6A**. The helical structure is stabilized by six hydrogen bonds. Except the terminal Aib all NHs and carbonyls are involved in 13-membered H-bond form ( $i$ ) $\leftarrow$ ( $i+4$ ). The average H---O distance:  $2\pm 0.2$  Å, N---O distance:  $2.9\pm 0.1$ Å. The average value of the torsion angles  $\phi = -50\pm 20$  and  $\psi = -50\pm 20$ . Full set of torsion angle values and hydrogen bonding parameters are given in Table **3.1** and **3.2**. Like in many designed peptides containing Aib residues, the terminal residue is not participated in the canonical helix.<sup>18</sup> The peptide **P1** adopted  $\alpha$ -helix conformation in single crystals.

**Table 3.1:** Torsion angles of peptide **P1**

Peptide **P1** contains two molecules in the asymmetric unit.

Molecule **A** in the asymmetric unit

Peptide P1	$\phi$ (deg)	$\Psi$ (deg)
Aib 1	-52.27	-50.04
Leu2	-70.47	-35.81
Ala3	-60.99	-48.43
Leu4	-67.03	-38.53
Phe5	-53.82	-48.39
Gly6	-65.69	-40.61
Leu7	-64.06	-33.23
Ala8	-70.49	-16.35

Leu9	-97.91	-57.86
Aib10	57.03	43.57

Molecule **B** in the asymmetric unit

Peptide P2	$\phi$ (deg)	$\Psi$ (deg)
Aib 1	-53.89	-50.04
Leu2	-70.11	-36.11
Ala3	-60.99	-47.74
Leu4	-68.44	-38.18
Phe5	-55.65	-46.57
Gly6	-67.78	-39.03
Leu7	-64.09	-34.56
Ala8	-68.72	-15.92
Leu9	-99.39	-58.14
Aib10	56.79	-137.07

**Table 3.2:** H-bonding parameters of peptide **P1**

Molecule **A** in the asymmetric unit

Intermolecular H-bonding

<b>Donor(D)</b>	<b>Acceptor(A)</b>	<b>D...A(Å)</b>	<b>DH...A(Å)</b>	<b>NH...O(deg)</b>
N4	O1	2.939	2.086	171.31
N5	O2	2.815	1.980	163.57
N6	O3	3.017	2.195	159.90
N7	O4	3.034	2.194	165.22
N8	O5	2.969	2.105	147.48
N10	O7	2.969	2.155	156.03

Intermolecular H-bonding

<b>Donor(D)</b>	<b>Acceptor(A)</b>	<b>D...A(Å)</b>	<b>DH...A(Å)</b>	<b>NH...O(deg)</b>
N1	O9	2.824	1.973	160.90
N2	O10	2.825	2.073	145.57
N11	O24	2.985	2.173	168.59

Molecule **B** in the asymmetric unit

Intermolecular H-bonding

<b>Donor(D)</b>	<b>Acceptor(A)</b>	<b>D...A(Å)</b>	<b>DH...A(Å)</b>	<b>NH...O(deg)</b>
N15	O12	2.943	2.093	169.64

N16	O13	2.818	1.982	163.82
N17	O14	3.003	2.189	158.05
N18	O15	3.032	2.195	165.11
N19	O16	2.965	2.077	151.87
N21	O18	2.965	2.141	160.54

#### Intermolecular H-bonding

Donor(D)	Acceptor(A)	D....A(Å)	DH....A(Å)	NH....O(deg)
N12	O20	2.823	1.976	165.03
N13	O21	2.987	2.098	145.16

### Peptide P2

To understand the effect of the incorporation of the  $\beta(\text{O})\text{-}\delta^5$ -amino acids on the structures of the  $\alpha$ -helices, we have synthesized peptide **P2** where the central dipeptide Phe-Gly was replaced by the  $\beta(\text{O})\text{-}\delta^5$ -Phe. The conformation of  $\beta(\text{O})\text{-}\delta^5$ -amino acid can be represented by the backbone torsion angles  $\phi(\text{N-C}^\delta)$ ,  $\theta_1(\text{C}^\delta\text{-C}^\gamma)$ ,  $\theta_2(\text{C}^\gamma\text{-O}^\beta)$ ,  $\theta_3(\text{O}^\beta\text{-C}^\alpha)$  and  $\psi(\text{C}^\alpha\text{-C=O})$  (Scheme 3.1). The X-ray diffraction quality single crystals of peptide **P2** were obtained from the slow evaporation of aqueous methanol and gave a helical structure as shown in the Figure 3.6B. The peptide adopted an uncommon 10/13/16-helix (Figure 3.6B). The helical structure was stabilized by seven intramolecular hydrogen bonds. Interestingly, the first three hydrogen bonds are 10-membered pseudocycles between the residues  $i$  and  $i+3$  residues. The residues  $\text{Ac}(1)\text{CO} \leftarrow \text{HNAib}(3)$ ,  $\text{Aib}(1)\text{CO} \leftarrow \text{NHLeu}(4)$  and  $\text{Leu}(2)\text{CO}(i) \leftarrow \text{NH}\delta^5\text{-Phe}(5) (i+3)$  are involved in the 10 membered H-bonds. The next two H-bonds are involving 13-membered pseudocycles. The residues  $\text{Ala}(3)\text{CO} (i) \leftarrow \text{HNLeu}(6)(i+3)$  and  $\text{Leu}(4)\text{CO}(i) \leftarrow \text{NHAla}(7) (i+3)$ . The last three hydrogen

bonds are two 10 membered  $\delta^5\text{Phe}(5)\text{CO}(i)\leftarrow\text{HNLeu}(8)(i+3)$  and between  $\text{Leu}(6)\text{CO}(i)\leftarrow\text{NHAib}(9)(i+3)$ . The terminal amide NH are involved 16 membered hydrogen bond between  $\text{Leu}(6)\text{CO}(i)\leftarrow\text{CONH}_2$ . It is interesting to note

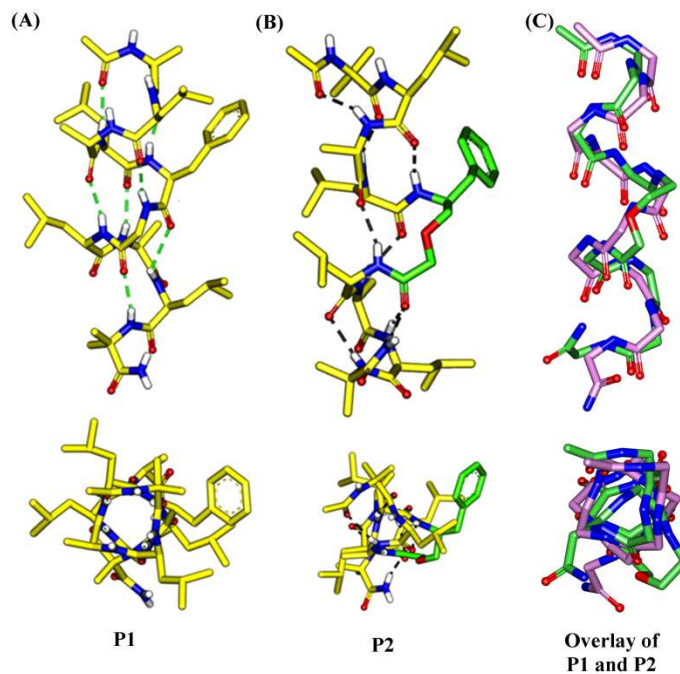


**Figure 3.6:** X-ray structure of peptide (A) **P1** and (B) **P2**.  $\beta(\text{O})\text{-}\delta^5\text{-Phe}$  are shown in green colour (C) The overlay structure of **P1** and **P2** were shown (magenta and green colour represents peptide **P1** and **P2** respectively).

that except the terminal H-bond, both 10 and 13-membered H-bonds in the peptide **P2** are stabilized by the residues between  $i\leftarrow i+3$ . The torsion angles of amino acid residues in **P2** are tabulated and given in Table 3.3. The torsion angles of the  $\beta(\text{O})\text{-}\delta^5\text{-Phe}$  were found to be  $\phi = -92.56$ ,  $\theta_1 = 52.95$ ,  $\theta_2 = 79.20$ ,  $\theta_3 = -158.37$  and  $\psi = 7.12$ . The torsion angles of other residues were found to be very similar to that of the residues **P1**. In comparison to the **P1**, incorporation of the  $\beta(\text{O})\text{-}\delta^5\text{-amino}$  acid leads to disruption in the H-bonding pattern in **P2**. The first three residues in **P2** adopted  $3_{10}$ -helical conformation, while in **P1** they adopted  $\alpha$ -helix conformation. These results also suggested the small energy difference between the two helix types. Probably, the lack of the one H-bond indeed disturbed the H-bonding pattern throughout the helix in **P1**. The overlay structure of peptides **P1** and **P2** was shown in Figure 3.6C. It is evident from the Figure

3.6C that the helical pore of peptide **P2** was little narrow compared to peptide **P1** due to incorporation of  $\beta(O)\text{-}\delta^5\text{-Phe}$  amino acid in place of Phe-Gly dipeptide residue.

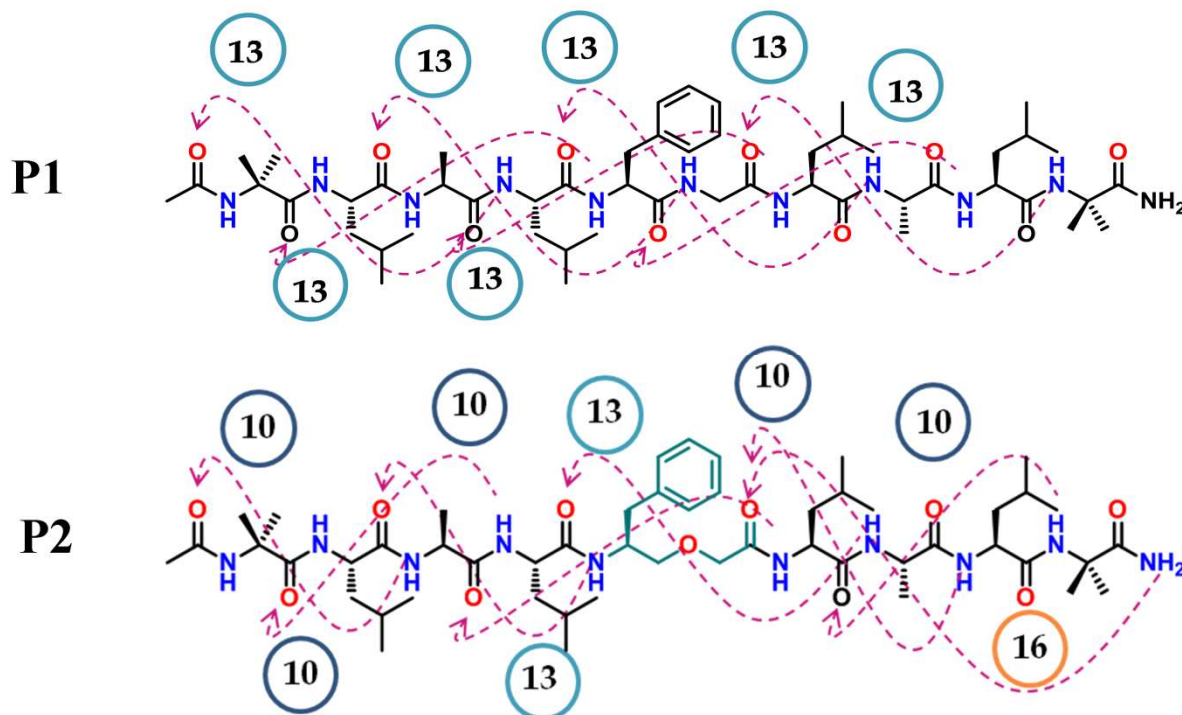


**Figure 3.7:** H-bonding pattern in peptide **P1** and **P2**

**Table 3.3:** Torsion angles of peptide **P2**

Peptide P1	$\phi$ (deg)	$\theta_1$ (deg)	$\theta_2$ (deg)	$\theta_3$ (deg)	$\Psi$ (deg)
Aib 1	-49.43				-47.43
Leu2	-66.23				-22.02
Ala 3	-62.08				-24.78
Leu4	-74.69				-17.30



$\beta(\text{O})-\delta^5\text{-Phe 5}$	-92.56	52.95	79.20	-159.37	7.12
Leu6	-64.25				-21.70
Ala7	-60.35				-20.47
Leu8	-120.78				34.73
Aib9	66.68				19.37

**Table 4:** H-bonding parameters of peptide **P2**

Intermolecular H-bonding

<b>Donor(D)</b>	<b>Acceptor(A)</b>	<b>D....A(Å)</b>	<b>DH....A(Å)</b>	<b>NH....O(deg)</b>
N3	O1	2.945	2.203	144.46
N4	O2	3.024	2.293	151.70
N5	O3	3.017	2.329	137.19
N6	O4	2.938	2.160	159.96
N7	O5	2.986	2.143	166.22
N8	O7	2.948	2.148	154.52
N9	O8	3.017	2.198	159.03
N10	O7	2.957	2.154	155.29

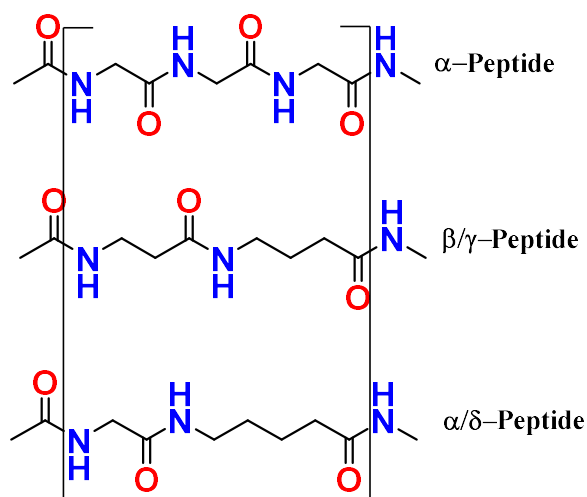
Intermolecular H-Bonding

<b>Donor(D)</b>	<b>Acceptor(A)</b>	<b>D....A(Å)</b>	<b>DH....A(Å)</b>	<b>NH....O(deg)</b>
-----------------	--------------------	------------------	-------------------	---------------------

N1	O14	3.032	2.294	143.88
N2	O10	3.005	2.293	163.80

### Peptide P3

Recently, Gellman and colleagues demonstrated the 13-membered H-bonds stabilized  $\beta,\gamma$ -hybrid helices.<sup>10k-10m</sup> Hofmann and colleagues have theoretically predicted the formation of 13-helix from the  $\beta,\gamma$ -hybrid peptides.<sup>19</sup> In addition to the  $\beta,\gamma$ -hybrid helices,  $\alpha,\delta$ -hybrid peptides are also expected to adopt 13-helix conformation. As the length of  $\beta\gamma$ - and  $\alpha\delta$ -hybrid peptides are similar it is expected  $\alpha,\delta$ -hybrid peptides can also form 13-helix. The structural details of  $\alpha$ -peptides,  $\beta,\gamma$ - and  $\alpha,\delta$ -hybrid peptides are shown in Scheme 2. In order to understand 1:1 alternating  $\alpha,\delta$ -hybrid The 13/11- hydrogen bonding pattern of  $\alpha,\delta$ - hybrid peptides also more stable compared to the other hybrid peptide mixed helices.<sup>13</sup> It is also known in the literature that the energy difference between 13/11-helices and 13-helices with all hydrogen bonds in the backward direction is small.<sup>13</sup> Whether  $\alpha/\delta$ - hybrid peptides can adopt 13-helix conformation similar to  $\alpha$ -helix, peptide **P3** was designed and synthesized. The peptide **P3** did not give X-ray quality single crystal. Therefore, the



**Scheme 3.2:** Schematic representation of structural analogy of  $\alpha$ -,  $\beta/\gamma$ - and  $\alpha/\delta$ - peptides

conformation of the peptide **P3** was analyzed by the 2D NMR analysis. The  $^1\text{H}$  NMR of the peptide **P3** in  $\text{CDCl}_3$  (3 mM) revealed the well dispersed NH and  $\text{C}^\delta\text{H}$  suggesting a well-defined secondary structure in solution. The amino acid types and sequential connectivity of the residues **P3** were established using TOCSY and ROESY spectra. The analysis of ROESY spectrum revealed the sequential NOEs between the  $\text{NH}(i) \leftrightarrow \text{NH}(i+1)$ . Among them medium  $\text{NH}(3) \leftrightarrow \text{NH}(4)$ ,  $\text{NH}(5) \leftrightarrow \text{NH}(6)$  and weak  $\text{NH}(1) \leftrightarrow \text{NH}(2)$ ,  $\text{NH}(2) \leftrightarrow \text{NH}(3)$  were observed. In addition to the  $\text{NH} \leftrightarrow \text{NH}$  NOEs,  $\text{NH}(3) \leftrightarrow \text{C}^\delta\text{H}(2)$  and  $\text{NH}(7) \leftrightarrow \text{C}^\delta\text{H}(6)$  were also observed. Further,  $\text{DMSO-}d_6$  titration in  $\text{CDCl}_3$  indicates that only NH of Aib1 is solvent exposed. Using the distance restraints from ROESY, the solution conformation of **P3** was generated. The ensemble of NMR structures resulting from the restrained MD simulations on the basis of the NOE data and H-bond constraints is shown in Figure 3.12. In contrast to the expected 13-helix, peptide **P3** adopted 13/11-helix conformation in solution. The structure is stabilized by

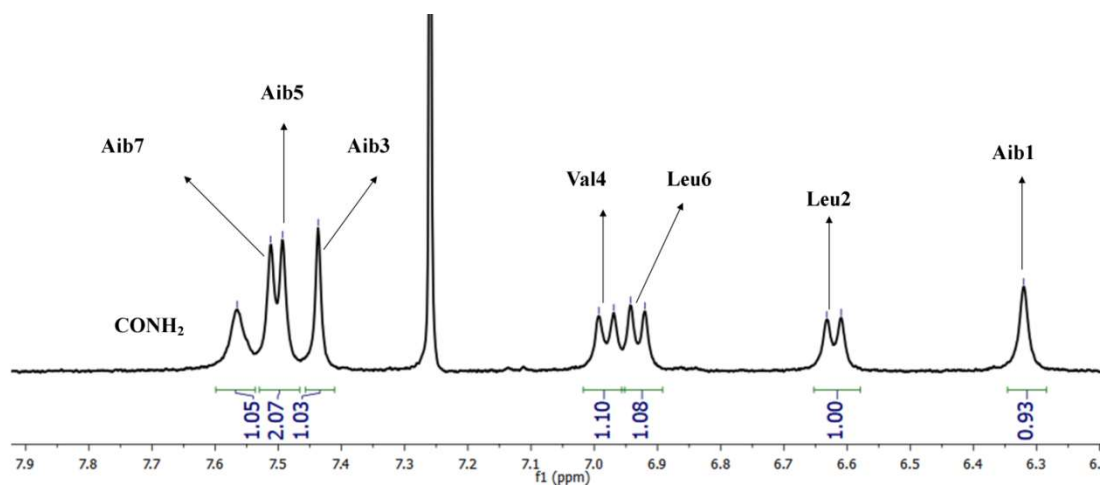


**Figure 3.8:** Partial  $^1\text{H}$  NMR of peptide **P3** (NH region)

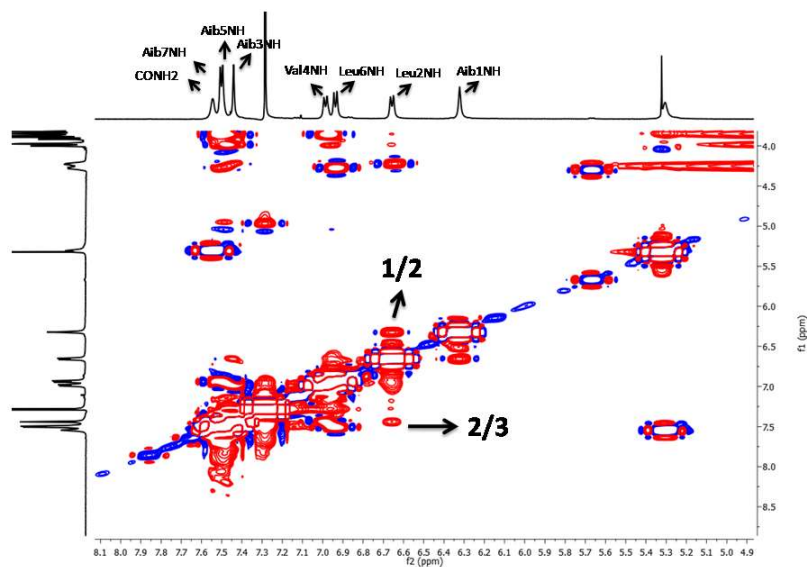


**Figure 3.9:** Partial ROESY spectrum of peptide P3 (3mM) in CDCl<sub>3</sub> showing NH↔NH interaction.

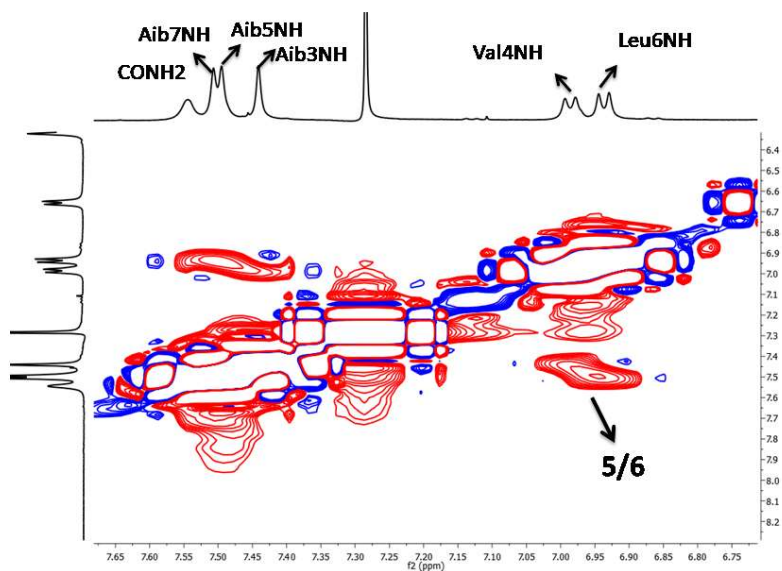


**Figure 3.10:** Partial ROESY spectrum of peptide P3 (3mM) in CDCl<sub>3</sub> showing NH↔NH interaction.

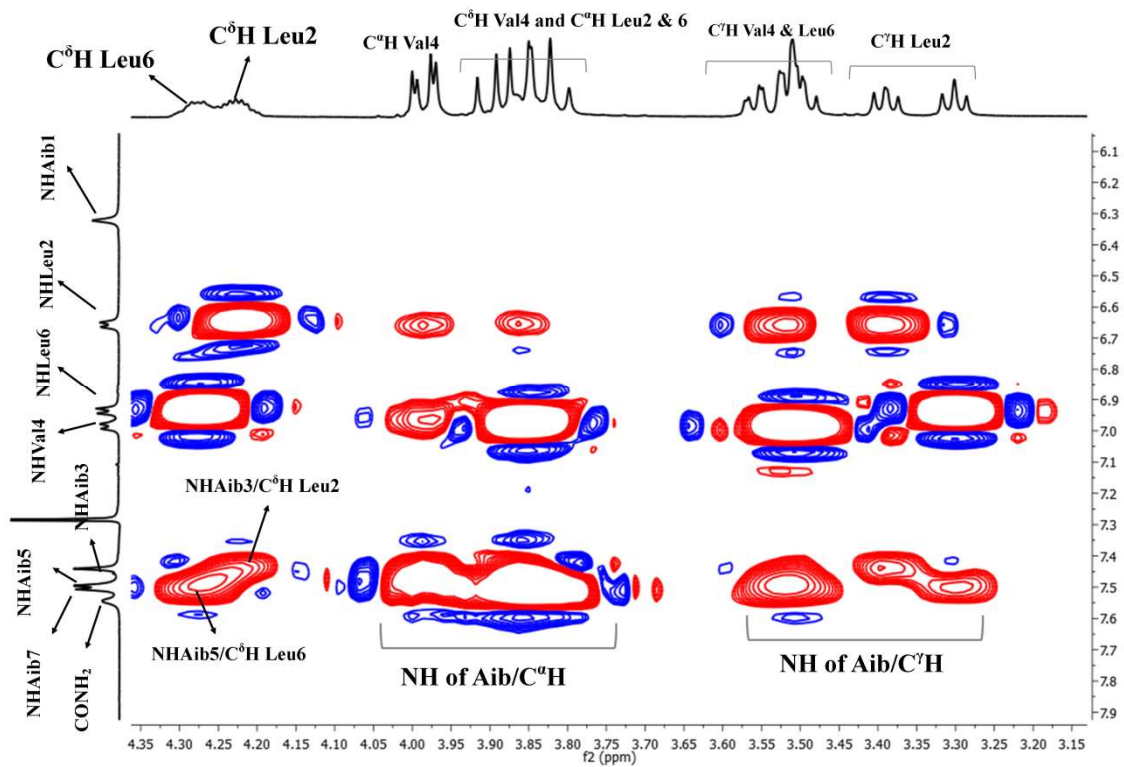


**Figure 3.11:** Partial ROESY spectrum of peptide **P3** (3mM) in CDCl<sub>3</sub> showing NH↔C<sup>α</sup>H, NH↔C<sup>γ</sup>H, NH↔C<sup>δ</sup>H interaction.

**Table 3.5:** NOEs used for the structure calculation of peptide **P3**

Residue	Atom	Residue	Atom	NOE
Aib1	NH	β(O)-δ <sup>5</sup> Leu2	NH	Weak
β(O)-δ <sup>5</sup> Leu2	NH	Aib3	NH	Weak
Aib3	NH	β(O)-δ <sup>5</sup> Val4	NH	Medium
Aib5	NH	β(O)-δ <sup>5</sup> Leu6	NH	Medium
β(O)-δ <sup>5</sup> Leu2	C <sup>δ</sup> H	Aib3	NH	Weak

$\beta(\text{O})\text{-}\delta^5\text{Leu6}$	$\text{C}^\alpha\text{H}$	Aib7	NH	Weak
--	---------------------------	------	----	------

**Table 3.6:** Calculation of  $d\delta/dT$  of peptide **P3**

<b>NH Residue</b>	<b>263K</b>	<b>273K</b>	<b>283K</b>	<b>293K</b>	<b>303K</b>	<b>313K</b>	<b><math>d\delta/dT</math> (ppb)</b>
CONH <sub>2</sub>	8.0	7.86	7.71	7.57	7.43	7.36	12.8
Aib7	7.75	7.69	7.60	7.51	7.43	7.36	7.8
Aib5	7.72	7.65	7.57	7.49	7.43	7.32	8
Aib3	7.69	7.59	7.50	7.44	7.38	7.32	7.4
$\beta(\text{O})\text{-}\delta^5\text{Val4}$	7.71	7.15	7.05	6.98	6.94	6.91	16
$\beta(\text{O})\text{-}\delta^5\text{Leu6}$	7.15	7.07	6.99	6.93	6.89	6.85	6
$\beta(\text{O})\text{-}\delta^5\text{Leu2}$	6.60	6.58	6.59	6.62	6.65	6.68	1.6
Aib1	6.80	6.62	6.44	6.32	6.23	6.16	12.8

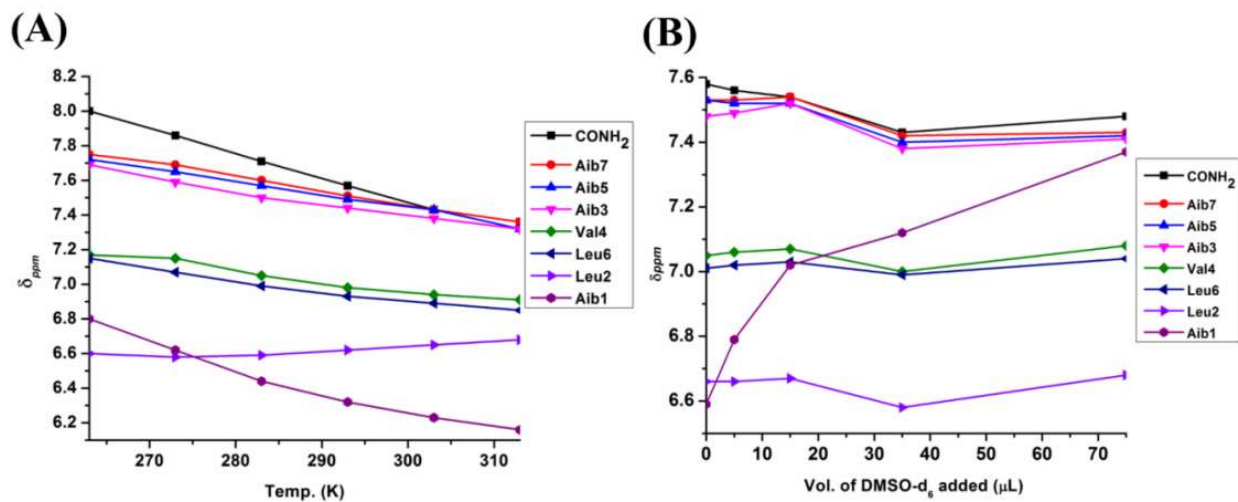


**Figure 3.12:** (A) Plot of  $\delta_{ppm}$  Vs Temp (K) of peptide **P3** in  $CDCl_3$  (B) DMSO- $d_6$  titration of peptide **P3** in  $CDCl_3$ .

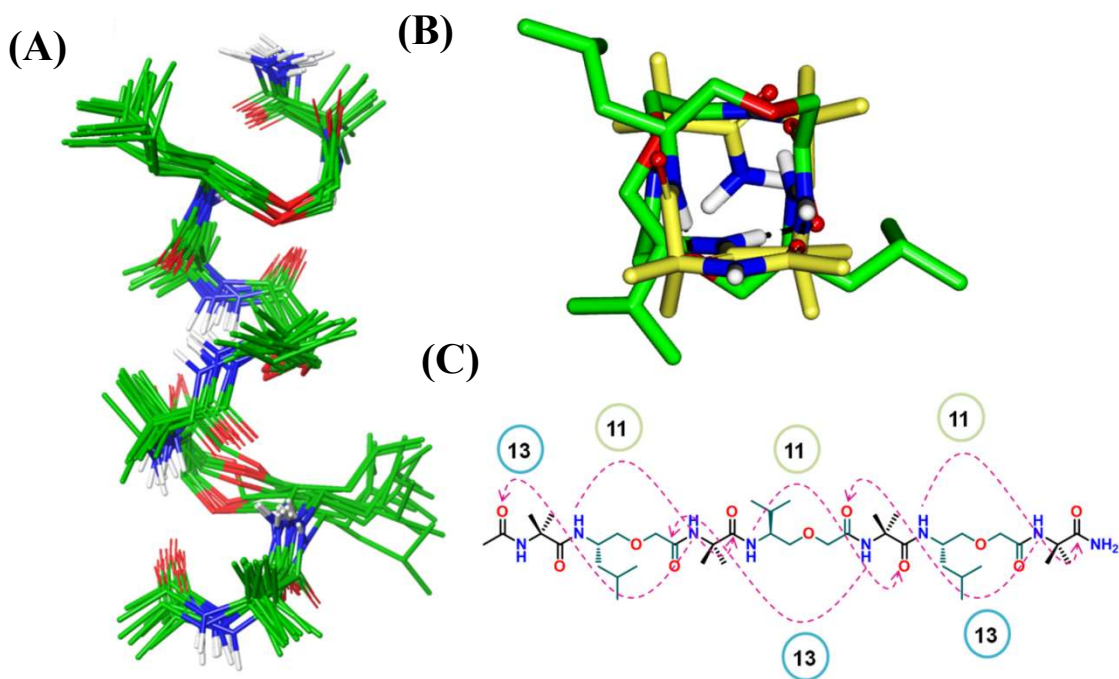


**Figure 3.12:** (A) Solution conformation of peptide **P3** (B) Top view of peptide **P3** (C) H-bonding pattern in peptide **P3** in solution.

**Table 3.7:** Torsion angles (in degree) measured from the minimized lowest energy conformation of peptide **P3** from simulation:

Peptide P3	$\phi$ (deg)	$\theta_1$ (deg)	$\theta_2$ (deg)	$\theta_3$ (deg)	$\Psi$ (deg)
Aib 1	-59.60				104.16
$\beta$ (O)- $\delta^5$ Leu2	60.92	42.49	99.90	-82.42	-57.53
Aib3	-66.16				113.80
$\beta$ (O)- $\delta^5$ Val4	62.80	47.16	96.20	-88.33	-56.26
Aib5	-67.28				108.65
$\beta$ (O)- $\delta^5$ Leu6	57.33	39.17	100.88	-73.85	-63.55
Aib7	-71.38				70.10

alternating intramolecular  $i \rightarrow i+3$  and  $i \rightarrow i-1$  mixed H-bonds. Surprisingly, the H-bonds observed in the peptide **P3** displayed opposite directionality. The 13-membered H-bonds are realized between  $i \rightarrow i+3$ , while 11-membered H-bonds are realized between  $i \rightarrow i-1$  residues. Similar type of mixed helices are also observed in the  $\alpha, \beta$ - and  $\alpha, \gamma$ -hybrid peptides,<sup>20</sup> however we have not observed this type of mixed H-bonding directionality in case of peptide **P2**.

### Peptide P4

To know whether same effect can be also possible in hybrid helices, we incorporate  $\beta$ (O)- $\delta^5$ -amino acid in known stable  $C_{12}$ - $\alpha, \gamma^4$ -hybrid helix.<sup>16a-16d</sup> The X-ray diffraction quality crystals of peptide **P4** are obtained from the aqueous methanol solution. The crystal structure revealed that  $\beta$ (O)- $\delta^5$ -amino acid is well accommodated in the helical structure. The helical structure is stabilized by six intramolecular hydrogen bonds. Among them the  $\gamma$ -residue are involved in 12 membered hydrogen bonding between  $(i) \leftarrow (i+3)$ . The average H----O distance:  $2.1 \pm 0.1$  Å, N----O distance:  $3 \pm 0.1$  Å. The average torsion angle value of the  $\gamma$  residue is  $\phi = -130 \pm 20$ ,  $\theta_1(N-C^\gamma-$



$C^\beta-C^\alpha=55\pm 1$ ,  $\theta_2(C^\gamma-C^\beta-C^\alpha-C)=58\pm 1$  and  $\psi = -120\pm 10$ . The stereochemical analysis of  $\gamma^4$ -Phe residues peptide indicates that they adopted *gauche+*, *gauche+* ( $g^+$ ,  $g^+$ ,  $\theta_1 \approx \theta_2 \approx 60^\circ$ ) local conformations about the  $C^\beta-C^\gamma$  and  $C^\alpha-C^\beta$  bonds which are concurrent with the reported value.<sup>16a-16c</sup> But the  $\beta(O)-\delta^5$ -Phe is involved in the 13 membered hydrogen bond with  $(i)\leftarrow-(i+3)$ . The peptide displayed the H-bonding pattern of 12 and 13-membered H-bonds. The torsion angles of the  $\beta(O)-\delta^5$ -Phe are  $\phi = -107.17$ ,  $\theta_1 = 61.88$ ,  $\theta_2 = 79.95$ ,  $\theta_3 = -154.25$  and  $\psi = 1.88$ . The stereochemical analysis shows that the backbone torsions are *gauche+*, *gauche+* and *extended*. (The full set of torsion angle values are given in Table 8) Which are concurrent with the backbone torsion value of  $\beta(O)-\delta^5$ -amino acid residue in peptide **P2**. The backbone torsion angles for  $\delta$ -amino acid in the peptide **P2**, **P3** and **P4** are given in the Table 3.10.

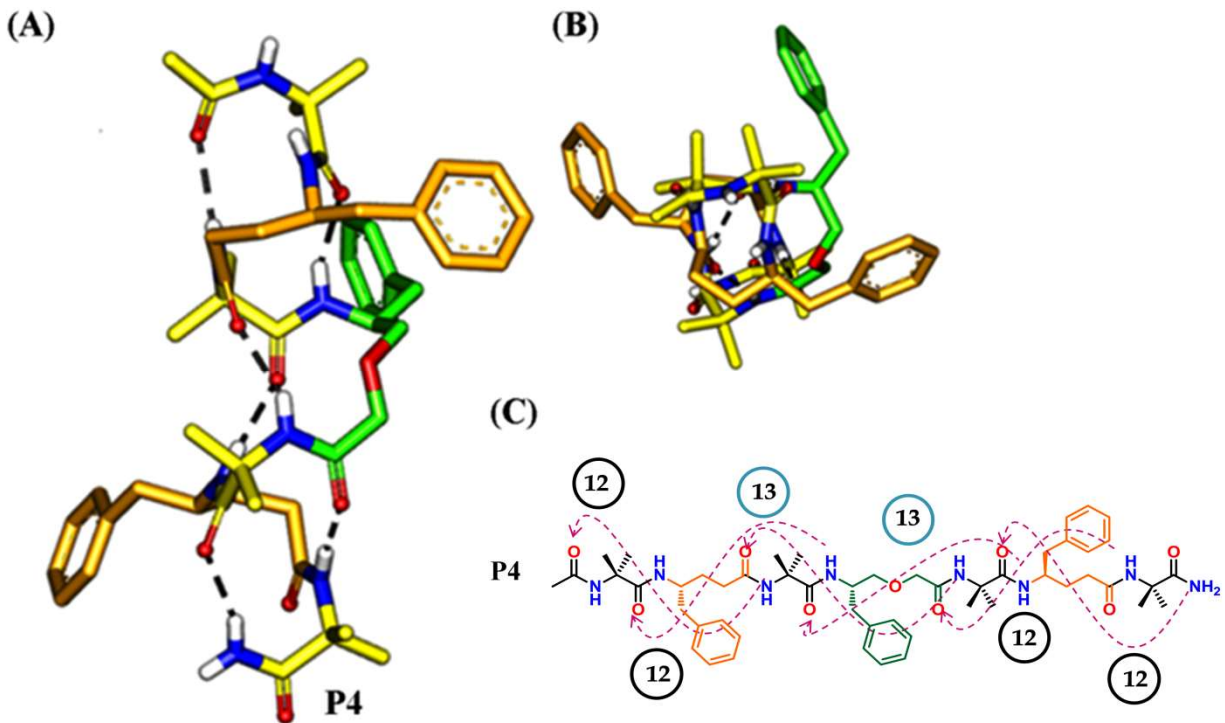


**Figure 3.13:** (A) X-ray crystal structure of peptide **P4**. (B) Top view of crystal structure of peptide **P4**. (C) H-bonding pattern observed in peptide **P4**.  $\gamma^4$ - and  $\beta(O)-\delta^5$ -Amino acids are represented by golden yellow and green colour respectively.

**Table 3.8:** Torsion angles of peptide **P3**

Peptide **P4** contains two molecules in the asymmetric unit.

Molecule **A** in the asymmetric unit

Peptide P4	$\phi$ (deg)	$\theta_1$ (deg)	$\theta_2$ (deg)	$\theta_3$ (deg)	$\Psi$ (deg)
Aib 1	-64.56				-35.45
$\gamma$ Phe2	-124.29	49.81	64.31		-122.03
Aib3	-56.95				-47.07
$\beta$ (O)- $\delta^5$ -Phe 4	-102.27	62.44	86.63	-148.13	-0.73
Aib5	-54.31				-47.13
$\gamma$ Phe6	-148.86	53.20	63.18		-113.78
Aib7	-54.54				-49.30

Molecule **B** in the asymmetric unit

Peptide P4	$\phi$ (deg)	$\theta_1$ (deg)	$\theta_2$ (deg)	$\theta_3$ (deg)	$\Psi$ (deg)
Aib 1	-64.33				-29.90
$\gamma$ Phe2	-123.69	56.29	57.94		-125.34
Aib3	-50.50				-52.72
$\beta$ (O)- $\delta^5$ -Phe 4	-107.17	61.88	79.95	-154.26	1.88

Aib5	-59.69				-39.61
$\gamma$ Phe6	-143.85	54.19	58.74		-112.13
Aib7	-53.66				-53.02

**Table 3.9:** H-bonding parameters in peptide **P4**

Peptide **P4** contains two molecules in the asymmetric unit.

Molecule **A** in the asymmetric unit

Intermolecular H-bonding

<b>Donor(D)</b>	<b>Acceptor(A)</b>	<b>D...A(Å)</b>	<b>DH...A(Å)</b>	<b>NH...O(deg)</b>
N4	O2	2.826	2.015	156.98
N5	O3	2.971	2.197	149.68
N6	O6	2.905	2.059	167.49
N7	O4	3.043	2.232	157.05
N8	O7	2.985	2.159	161.12

Intermolecular H-bonding

<b>Donor(D)</b>	<b>Acceptor(A)</b>	<b>D...A(Å)</b>	<b>DH...A(Å)</b>	<b>NH...O(deg)</b>
N2	O9	2.932	2.159	149.32
N1	O8	2.902	2.056	167.50

Molecule **B** in the asymmetric unit

Intermolecular H-bonding

Donor(D)	Acceptor(A)	D...A(Å)	DH...A(Å)	NH...O(deg)
N12	O11	2.891	2.080	157.02
N14	O14	2.837	2.012	160.44
N33	O12	2.935	2.099	163.68
N13	O30	3.095	2.257	164.61
N11	O10	2.909	2.059	169.74

Intermolecular H-bonding

Donor(D)	Acceptor(A)	D...A(Å)	DH...A(Å)	NH...O(deg)
N10	O17	2.855	2.087	148.16
N9	O16	2.940	2.108	163.36

**Table 3.10:** Backbone torsion angles for  $\delta$ -amino acids

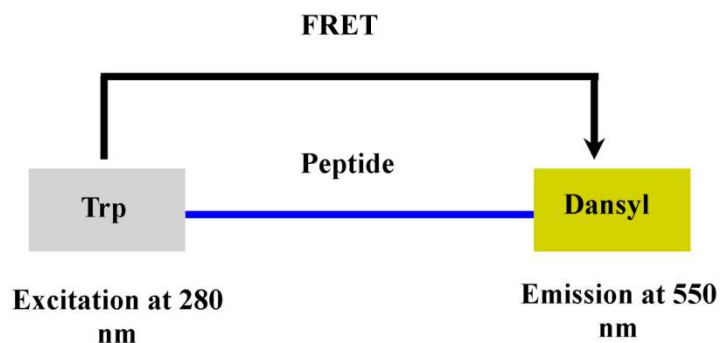
	$\phi$ (deg)	$\theta_1$ (deg)	$\theta_2$ (deg)	$\theta_3$ (deg)	$\Psi$ (deg)
Theoretical Calculation for $\delta$ -oligomer $H_{10}^a$	-98 $\pm$ 1	62.5 $\pm$ 1	68.4 $\pm$ 0.4	-168.7 $\pm$ 2	85.2 $\pm$ 2
Sharma $\alpha/\delta^5$ Hybrid <sup>b</sup>	138 $\pm$ 4	-72 $\pm$ 3	73 $\pm$ 1	56 $\pm$ 1	-135 $\pm$ 4
Balaram $\delta$ -Ava <sup>c</sup>	-67	-64	176	-59	-45
<b>P2<sup>c</sup></b>	-92.5	53	79	-158	7.12

<b>P4<sup>c</sup></b>	-107	61	80	-154	1.8
$\alpha/\delta^5$ from NMR calculation <sup>c</sup>	60±3	45±5	96±5	-80±10	60±5

<sup>a</sup>Theoretical calculation by Hofmann *et al.* [*J. Org. Chem.*, **2004**, *69*, 6214.] <sup>b</sup>Sharma *et al.* [*Chem. Eur. J.* **2009**, *15*, 5552.] <sup>d</sup>Balaram *et al.* *Biopolymers* **1996**, *39*, 769.] <sup>c</sup>Present Study.

### 3.4.5. Proteolytic Stability Studies of the Delta Amino Acids

The proteolytic stability of peptides composed of  $\beta$ - and  $\gamma$ - amino acids towards different proteases are well studied in the literature.<sup>21</sup> But the proteolytic stability of peptide composed of  $\delta$ -amino acids are not documented. As the  $\delta$ -amino acids resemble the dipeptides in the  $\alpha$ -peptides, it is worth examining the proteolytic stability of the peptides containing  $\delta$ -amino acids.



**Scheme 3.3:** Schematic representation of Trp-Dansyl FRET pair.

As the amide bond of dipeptide consisting of  $\alpha$ -amino acid is replaced by  $O^\beta-C^\gamma$  bond in  $\beta(O)-\delta^5$ -amino acid, so it can be proteolytically stable amino acid. In order to understand the proteolytic stability of  $\beta(O)-\delta^5$ -amino acid in peptides, we have synthesised peptide **P5** and **P6**. In peptide **P6**, Lys-Gly was replaced by  $\beta(O)-\delta^5$ -Lys. The C-terminal amino acid of the peptide was kept tryptophan as donor and N-terminal was coupled with DANSYL as acceptor and Fluorescence

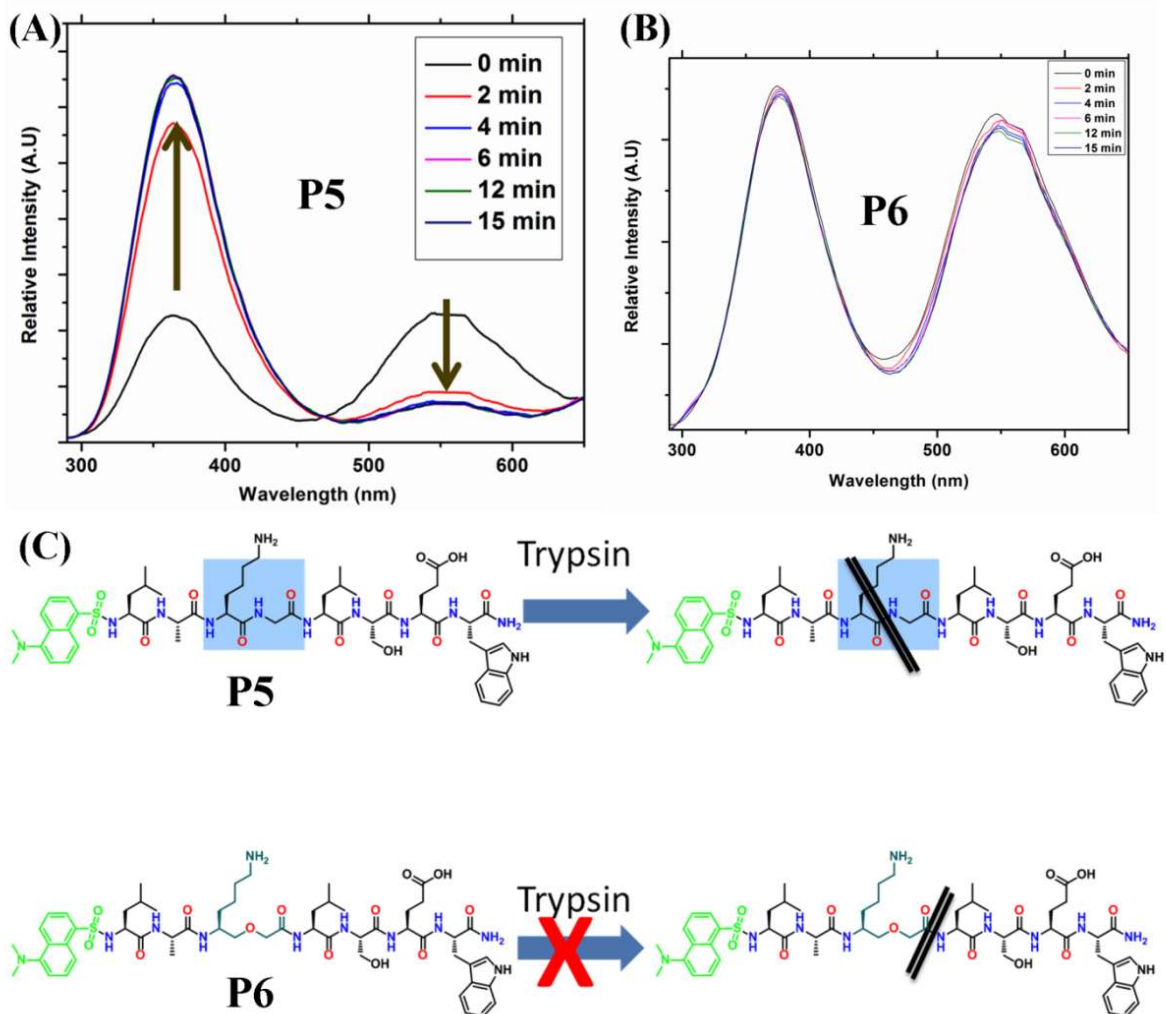


**Figure 3.14:** Time dependent fluorescence spectra of peptide (A) **P5** and (B) **P6** upon trypsin digestion. (C) Schematic representation of cleavage of peptide **P5** and **P6** by trypsin.

Resonance Energy Transfer (FRET) technique was used to study the proteolytic stability. Trypsin was used to study the cleavage process as it cleaved the C-terminal of Lys residue. Results of the peptides digestion with 0.2% Trypsin EDTA solution is shown in Figure 3.14. Results revealed that in case of peptide **P5**, with increase the time the fluorescence emission of DANSYL group is decreasing and emission intensity of tryptophan increases by excitation at 280 nm, indicating that the trypsin able to cleave the C-terminal of Lys residue and hence the FRET efficiency decreases with time. On the other hand, due to the insertion of the  $\beta(O)-\delta^5$ -Lys

residue, the fluorescence intensity of both tryptophan and DANSYL group remained same at excitation of 280 nm up to 15 min, revealing that the peptide **P6** is stable towards trypsin.

### 3.5. Conclusions

We have demonstrated the utilization of new  $\beta(\text{O})\text{-}\delta^5$ -amino acid for the construction of helices, where the amide bond in the dipeptide composed of  $\alpha$ -amino acid is replaced by the  $\text{O}^\beta\text{-C}^\gamma$  bond. The X-ray structure revealed that the replacement of the dipeptide in the  $\alpha$ -helix by  $\beta(\text{O})\text{-}\delta^5$ -amino acid residue are able to accommodate in helical structure however with fluctuations in the H-bonding pattern. Further, the replacement of  $\gamma^4$  residue by  $\beta(\text{O})\text{-}\delta^5$ -amino acid in  $\alpha,\gamma^4$  hybrid helices reveal that peptides is well accommodated  $\delta$ -amino acid in the hybrid helices without change in the hydrogen bonding pattern. This result further support the structural plasticity of the  $\alpha,\gamma$ -hybrid peptides. Furthermore, the two dimensional NMR studies of 1:1 hybrid peptide showed formation of 13/11 mixed helices in solution. This is quite surprising because  $\alpha/\delta$ -hybrid peptides adopt 13-helix conformation. In contrast,  $\alpha/\delta$ -hybrid peptide sequences adopted mixed 13/11-helix conformations. Finally, we have proved that the peptide composed of  $\beta(\text{O})\text{-}\delta^5$ -amino acids stable towards the proteases. This results reported in this chapter open new possibility for the design of proteolytically stable functional foldamers.

## 3.6. Experimental Section

### 3.6.1. Materials and Methods

All the reagents including amino acids were purchased from the commercial sources. DCM and MeOH were purchased from the commercial sources and distilled before to use. Column chromatography was performed on silica gel (120-200 mesh). Final peptides were purified by reverse phase HPLC.  $^1\text{H}$  (400 MHz) and  $^{13}\text{C}$  (100 MHz) NMR spectra were used to record the NMR spectra on respectively using the residual solvent signal as internal standards ( $\text{CDCl}_3$ ). Chemical shifts ( $\delta$ ) reported in parts per million (ppm) and coupling constants (J) reported in Hz. Mass of pure peptides was confirmed by MALDI-TOF /TOF.

### 3.6.2. NMR Spectroscopy

All NMR studies were carried out by using either 400 or 600 MHz spectrometer. Resonance assignments were obtained by TOCSY and ROESY analysis. All two-dimensional data were collected in phase-sensitive mode by using the time-proportional phase incrimination (TPPI) method. Sets of 1024 and 512 data points were used in the  $t_2$  and  $t_1$  dimensions respectively. For TOCSY and ROESY analysis, 32 and 72 transients were collected, respectively. A spectral width of 600MHz was used in both dimensions. A spin-lock time of 200 and 250 ms were used to obtain ROESY spectra. Zero-filling was carried out to finally yield a data set of  $2\text{ K} \times 1\text{ K}$ . A shifted square-sine-bell window was used before processing.

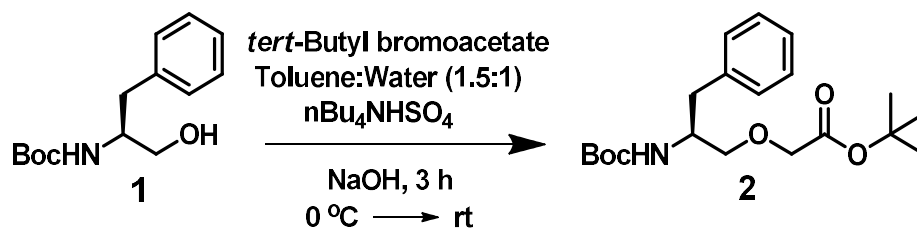
### 3.6.3. Synthetic Procedures

#### 3.6.3.1. Synthesis of *N*-Boc- $\beta(\text{O})$ - $\delta^5$ Phe- $\text{O}^t\text{Bu}$

*N*-Boc- $\beta(\text{O})$ - $\delta^5$ -Phe- $\text{O}^t\text{Bu}$  was synthesized by the reported protocol from *N*-Boc-amino alcohol.<sup>17</sup> Briefly, to the solution containing 10 mL of water and 10 mL of toluene, sodium hydroxide (10g, 250 mmol) was dissolved in ice-cold condition. Thereafter, *tert*-butyl bromoacetate (2.2 mL, 15 mmol) was added slowly to the biphasic reaction mixture at room temperature. After that, the solution containing *N*-Boc-Phenyl alanine alcohol (2.5 g, 10 mmol) in toluene (10 mL) was added slowly to the reaction mixture at 0 °C. The reaction mixture was stirred for about 3 h and allowed to come to room temperature. After completion of reaction (confirmed by TLC), the

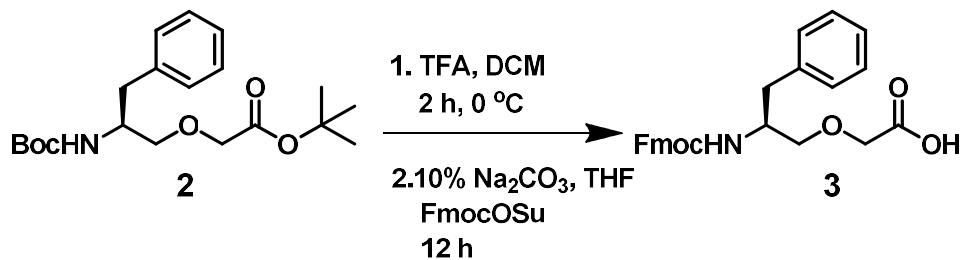


organic layer was extracted with diethyl ether (30 mL×2). The combined organic layer was washed with brine (30 mL×2) and dried over anhydrous sodium sulfate. The solvent was evaporated under reduced pressure to get white gummy product. The crude product of *N*-Boc- $\beta$ (O)- $\delta^5$ -Phe-O<sup>t</sup>Bu was purified by column chromatography using EtOAc/hexane solvent system.



### 3.6.3.2. Synthesis of *N*-Fmoc- $\beta$ (O)- $\delta^5$ Phe-OH

Compound 2 (3.65 g, 10 mmol) was dissolved in 15 mL of TFA/DCM (1:1) mixture at 0 °C. To this solution, 500 $\mu$ L of H<sub>2</sub>O was added. Then the reaction mixture was kept for about 2 h at RT. After completion of the reaction (confirmed by TLC), the TFA was evaporated completely under *vacuum*. Then the free amine was protected with Fmoc and used for the solid phase peptide synthesis.





### 3.6.4. Crystallographic Information of Peptide P1, P2 and P4

#### Peptide P1 (CCDC No 1919640):

Crystals of peptide **P1** were grown by slow evaporation of methanol/ water solution. A single crystal (0.22×0.17×0.13) was mounted on loop with a small amount of the paraffin oil. The X-ray data were collected at 100 K temperature on a Bruker AXS SMART APEX CCD diffractometer using Mo K $\alpha$  radiation ( $\lambda = 0.71073 \text{ \AA}$ ),  $\omega$ -scans ( $2\theta = 56.66$ ), for a total of 75166 independent reflections. Space group P1,  $a=10.2137$ ,  $b=16.143$ ,  $c=18.663 \text{ \AA}$ ;  $\alpha = 90$ ,  $\beta = 90$ ,  $\gamma = 102$ ;  $V = 3008.64 \text{ \AA}^3$ ; Triclinic,  $Z = 1$  for chemical formula  $C_{104} H_{177} N_{22} O_{24}$ ;  $\rho_{\text{calcd}} = 1.170 \text{ gcm}^{-3}$ ,  $\mu = 0.084 \text{ mm}^{-1}$ ,  $F(000) = 1147$ . The structure was obtained by direct methods using SHELXS-97.1. The final R value was 0.1105 ( $wR2 = 0.2662$ ) 26099 observed reflections ( $F0 \geq 4\sigma (|F0|)$ ) and 1385 variables,  $S = 1.145$ .

#### Peptide P2 (CCDC No 1919644):

Crystals of peptide **P2** were grown by slow evaporation of methanol/ water solution. A single crystal (0.2×0.19×0.13) was mounted on loop with a small amount of the paraffin oil. The X-ray data were collected at 100 K temperature on a Bruker AXS SMART APEX CCD diffractometer using Mo K $\alpha$  radiation ( $\lambda = 0.71073 \text{ \AA}$ ),  $\omega$ -scans ( $2\theta = 56.89$ ), for a total of 117916 independent reflections. Space group P2<sub>1</sub>,  $a=10.419$ ,  $b=30.242$ ,  $c=10.627 \text{ \AA}$ ;  $\alpha = 90$ ,  $\beta= 113.583$ ,  $\gamma= 90$ ;  $V = 3068.82 \text{ \AA}^3$ , Monoclinic,  $Z = 2$  for chemical formula  $C_{51} H_{86} N_{10} O_{14}$ ,  $\rho_{\text{calcd}} = 1.151 \text{ gcm}^{-3}$ ,  $\mu = 0.084 \text{ mm}^{-1}$ ,  $F(000) = 1148$ . The structure was obtained by direct methods using SHELXS-97.1. The final R value was 0.0811 ( $wR2 = 0.2107$ ) 15326 observed reflections ( $F0 \geq 4\sigma (|F0|)$ ) and 691 variables,  $S = 0.999$ .

#### Peptide P4 (CCDC No 1919641):

Crystals of peptide **P4** were grown by slow evaporation of methanol/ water solution. A single crystal (0.23×0.15×0.11) was mounted on loop with a small amount of the paraffin oil. The X-ray data were collected at 100 K temperature on a Bruker AXS SMART APEX CCD diffractometer using Mo K $\alpha$  radiation ( $\lambda = 0.71073 \text{ \AA}$ ),  $\omega$ -scans ( $2\theta = 43.20$ ), for a total of 6348 independent reflections. Space group P 2<sub>1</sub>,  $a=16.198$ ,  $b=17.843$ ,  $c=19.642 \text{ \AA}$ ;  $\alpha = 90$ ,  $\beta= 106.055$ ,  $\gamma= 90$ ;  $V =$

5455.53 Å<sup>3</sup>, Monoclinic, Z = 2 for chemical formula C<sub>104</sub> H<sub>152</sub> N<sub>16</sub>O<sub>21</sub>, ρ<sub>calcd</sub> = 1.194 gcm<sup>-3</sup>, μ = 0.084 mm<sup>-1</sup>, F(000) = 2112. The structure was obtained by direct methods using SHELXS-97.1. The final R value was 0.0678 (wR2 = 0.1878) 25616 observed reflections (F0 ≥ 4σ(|F0| )) and 1292 variables, S = 0.920.

### 3.6.5. Two Dimensional NMR Analysis of Peptide P3

Hydrogen bond constraints used for the structure calculation for peptide **P3**

NH(3)→CO(Acetyl)

NH(2)→CO(3)

NH(5)→CO(2)

NH(4)→CO(5)

NH(7)→CO(4)

NH(6)→CO(7)

Medium ≤ 4 Å

Weak ≤ 5 Å

Structure calculation was done using a simulated annealing protocol in vacuum using DESMOND and OPLS 2005 force field with NOE and hydrogen bonding constraints. A completely extended peptide molecule was kept in cubic simulation cell with an edge length of 46.55 Å. Upper limit for distance was kept at 4 Å and 5 Å for medium and weak NOEs respectively. All the lower distance limits were taken to be 1.8 Å. For Hydrogen bonding constraints, an upper bound of 2.5 Å and lower bound of 1.8 Å was used. A force constant of 1 Kcal/Mol and 2 Kcal/Mol were used for NOE and hydrogen bond constraints respectively. Potentials (appropriate for treating ambiguous NOE assignments) used are having the following form,

$$E_{\text{NOE}} = \text{fc} * (\text{lower} - d)^2, \text{ if } d < \text{lower};$$

$$E_{\text{NOE}} = 0, \text{ if } \text{lower} \leq d \leq \text{upper};$$

$$E_{\text{NOE}} = \text{fc} * (\text{upper} - d)^2, \text{ if } \text{upper} < d \leq \text{upper} + \text{sigma};$$

$$E_{\text{NOE}} = \text{fc} * (a + \text{beta} * (d - \text{upper}) + c / (d - \text{upper})), \text{ if } d > \text{upper} + \text{sigma};$$

where  $d$  is the distance and  $\text{fc}$  is the force constant.

Values of  $\text{sigma}$  and  $\text{beta}$  used in the calculation are 0.5 and 1.5 respectively. The values  $a$  and  $c$  are determined automatically such that potential is continuous and differential everywhere.

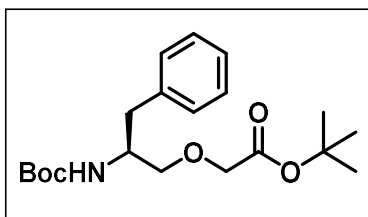
Before production run simulation, a default NVT relaxation was done as implemented in DESMOND. NVT ensemble was used for the production run simulation. Nose-Hoover Chain thermostat with a relaxation time of 1 ps was used. A RESPA integrator was used in which for all the bonded, near nonbonded and far nonbonded interaction a time step of 1 fs was used. A cutoff of 9 Å was used for short range electrostatic interactions. A smooth particle mesh ewald method was used for treating long range electrostatic interactions. Simulated annealing was done in 6 stages. First stage consist simulation for 30 ps at 10 K. In the second stage, temperature was linearly increased to 100 K till 100 ps. In the third stage, temperature was linearly increased to 300 K till 200 ps. In the fourth stage, temperature was linearly increased to 400 K till 300 ps. In the fifth stage, temperature was maintained at 400 k till 500 ps. In the sixth stage, temperature was linearly decreased to 300 K till 1000 ps and maintained at 300 k till 1200 ps. 10 minimum energy structures were taken from the trajectory between 1000 ps and 1200 ps.

### 3.6.6. Proteolytic Stability Studies of Peptides P5 and P6

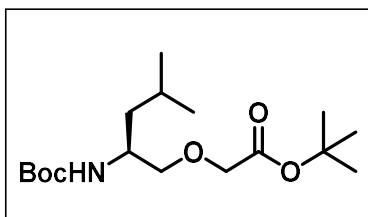
Proteolytic stability was carried out by FRET pair technique by reported protocol.<sup>22a</sup> Stock solution of peptide **P5** and **P6** was made in 50 mM Tris-buffer (pH 8.2) at a conc. of 1mM. In a clean quartz cuvette, 2 μL commercially available 0.05% trypsin EDTA solution was added to

400  $\mu\text{L}$  of 1mM peptide solution. Then time dependent fluorescence emission was monitored by excitation wavelength of  $\lambda_{\text{ex}} = 280 \text{ nm}$ .

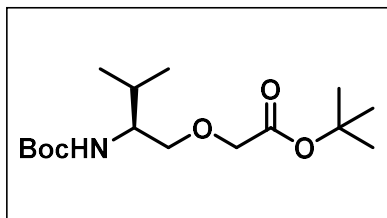
### 3. 7. Characterization of Compounds



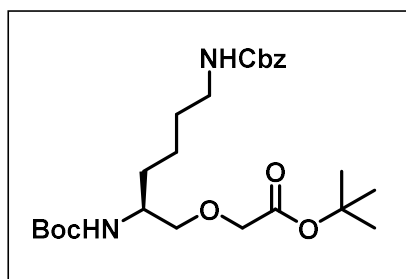
**$^1\text{H NMR}$**  (400 MHz, Chloroform-*d*)  $\delta$  7.30 – 7.18 (m, 5H), 5.17 (d,  $J = 8 \text{ Hz}$ , 1H), 3.96 – 3.89 (m, 3H), 3.45 – 3.44 (m, 2H), 2.95 (dd,  $J = 6.8 \text{ Hz}$ , 0H), 2.86 (dd,  $J = 12 \text{ Hz}$ , 4 Hz, 1H), 2.86 (dd,  $J = 12 \text{ Hz}$ , 8 Hz, 1H), 1.48 (s, 9H), 1.42 (s, 9H).  **$^{13}\text{C NMR}$**  (100 MHz, Chloroform-*d*)  $\delta$  169.73, 155.58, 138.40, 129.60, 128.49, 126.40, 81.96, 79.28, 71.70, 69.07, 51.96, 37.81, 28.51, 28.24. **HRMS**  $m/z$  calculated value for  $\text{C}_{20}\text{H}_{31}\text{NO}_5$  is  $[\text{M}+\text{Na}^+]$  388.2100 and observed 388.2100.



**$^1\text{H NMR}$**  (400 MHz, Chloroform-*d*)  $\delta$  4.85 (d,  $J = 8 \text{ Hz}$ , 1H), 3.92 (s, 2H), 3.74 (bs, 1H), 3.52-3.43 (m, 2H), 2.01 (bs, 1H), 1.64-1.59 (m, 2H), 1.44 (s, 9H), 1.40 (s, 9H), 0.88 (m, 6H).  **$^{13}\text{C NMR}$**  (100 MHz, Chloroform-*d*)  $\delta$  169.74, 155.69, 81.75, 79.05, 73.94, 69.14, 48.60, 41.10, 28.49, 28.19, 24.89, 23.0. **HRMS**  $m/z$  calculated value for  $\text{C}_{17}\text{H}_{23}\text{NO}_5$  is  $[\text{M}+\text{Na}^+]$  354.2256 and observed 354.2244.



**<sup>1</sup>H NMR** (400 MHz, Chloroform-*d*)  $\delta$  4.92 (d,  $J = 8$  Hz, 1H), 4.02 (s, 2H), 3.61-3.57 (m, 1H), 3.41 – 3.38 (m, 2H), 2.23 (bs, 1H), 1.40 (s, 9H), 1.36 (s, 9H), 0.86 (dd,  $J=8$  Hz, 4Hz, 7H). **<sup>13</sup>C NMR** (100 MHz, Chloroform-*d*)  $\delta$  169.65, 155.97, 81.79, 78.89, 71.82, 69.00, 55.55, 29.51, 28.40, 28.09, 19.47. **HRMS**  $m/z$  calculated value for C<sub>16</sub>H<sub>31</sub>NO<sub>5</sub> is [M+Na<sup>+</sup>] 340.2100 and observed 340.2085.



**<sup>1</sup>H NMR** (400 MHz, Chloroform-*d*)  $\delta$  7.35 – 7.30 (m, 5H), 5.08 (s, 0H), 5.01 (d,  $J=8$  Hz, 2H), 3.94 (s, 2H), 3.67 (bs, 1H), 3.56 (dd,  $J = 4, J = 4$  Hz, 1H), 3.48-3.45 (m, 1H), 3.22- 3.17 (m, 2H), 1.62 – 1.51 (m, 6H), 1.47 (s, 9H), 1.43 (s, 9H). **<sup>13</sup>C NMR** (100 MHz, Chloroform-*d*)  $\delta$  169.76, 156.59, 155.87, 136.81, 128.56, 128.20, 128.10, 81.90, 79.25, 73.32, 68.95, 66.61, 50.22, 40.82, 31.63, 29.59, 28.50, 28.21, 23.06. **HRMS**  $m/z$  calculated value for C<sub>25</sub>H<sub>40</sub>N<sub>2</sub>O<sub>7</sub> is [M+Na<sup>+</sup>] 503.2733 and observed 503.2716.

### 3.8. References

1. IUPAC-IUB Commission on Biochemical Nomenclature, *Biochemistry* **1970**, *9*, 3471.
2. Linderstrom-Lang, K. U.; Schellman, J. A. (1959), *The Enzymes*, (P. D. Boyer, Ed.), *Vol. 1*, 2<sup>nd</sup> ed. pp. 443-510. Academic Press, New York.
3. Ramachandran, G. N.; Ramakrishnan, C.; Sasi-sekharan, V. *J. Mol. Biol.* **1963**, *7*, 95.
4. a) Stewart, D. E.; Sarkar, A.; Wampler, J. E. *J. Mol. Biol.* **1990**, *214*, 253. b) Vasta, J. D.; Choudhary, A.; Jensen, K. H.; McGrath, N. A.; Raines, R. T. *Biochemistry* **2017**, *56*, 219.

5. a) Poduslo, J. F.; Curran, G. L.; Kumar, A.; Frangione, B.; Soto, C. *J. Neurobiol.* **1999**, *39*, 371. b) Adessi, C.; Soto, C. *Curr. Med. Chem.* **2002**, *9*, 963. c) Funke, S. A.; Willbold, D. *Curr. Pharm. Des.* **2012**, *18*, 755–767; d) Hruby, V. J. *Nat. Rev. Drug Discovery* **2002**, *1*, 847.
6. a) Qvit, N.; Rubin, S. J. S.; Urban, T. J.; Mochly-Rosen, D.; Gross, E. R. *Drug discovery today.* **2017**, *22*, 454. b) Lang, K.; Chin, J. W. *Chem. Rev.* **2014**, *114*, 4764. c) Young, T. S.; Young, D. D.; Ahmad, I.; Louis, J. M.; Benkovic, S. J.; Schultz, P. G. *Proc. Natl. Acad. Sci. USA* **2011**, *108*, 11052. d) Gentilucci, L.; De Macro, R.; Cerisoli, L. *Curr. Pharm Des.* **2010**, *16*, 3185.
7. a) Gellman, S. H. *Acc. Chem. Res.* **1998**, *31*, 173. b) Goodman, C. M.; Choi, S.; Shandler, S.; DeGrado, W. F. *Nat. Chem. Biol.* **2007**, *3*, 252. c) Cheng, R. P.; Gellman, S. H.; De Grado, W. F. *Chem. Rev.* **2001**, *101*, 3219. d) Venkatraman, J.; Shankaramma, S. C.; Balaram, P. *Chem. Rev.* **2001**, *101*, 3131. e) Seebach, D.; Beck, A. K.; Bierbaum, D. J. *Chem. Biodiversity* **2004**, *1*, 1111. f) Horne, W. S.; Gellman, S. H. *Acc. Chem. Res.* **2008**, *41*, 1399. g) Guichard, G.; Huc, I. *Chem. Commun.* **2011**, *47*, 5933. h) *Foldamers: Structure, Properties and Applications* (Eds.: S. Hecht, I. Huc), Wiley-VCH, Weinheim, **2007**.
8. a) Schmitt, A. M.; Weisblum, B.; Gellman, S. H. *J. Am. Chem. Soc.* **2004**, *126*, 6848. b) Sadowsky, J. D.; Schmitt, M. A.; Lee, H. S.; Umezawa, N.; Wang, S.; Tomita, Y.; Gellman, S. H. *J. Am. Chem. Soc.* **2005**, *127*, 11966. c) Horne, W. S.; Price, J. L.; Keck, J. L.; Gellman, S. H. *J. Am. Chem. Soc.* **2007**, *129*, 4178. d) Price, J. L.; Horne, W. S.; Gellman, S. H. *J. Am. Chem. Soc.* **2007**, *129*, 6376. e) Seebach, D.; Gardiner, J. *Acc. Chem. Res.* **2008**, *41*, 1366.
9. a) Hintermann, T.; Gademann, K.; Jaun, B.; Seebach, D. *Helv Chim Acta* **1998**, *81*, 983. b) Hanessian, S.; Luo, X. H.; Schaum, R.; Michnick, S. *J. Am. Chem. Soc.* **1998**, *120*, 8569. c) Hanessian, S.; Luo, X. H.; Schaum, R. *Tetrahedron Lett.* **1999**, *40*, 4925. d) Vasudev, P. G.; Shamala, N.; Ananda, K.; Balaram, P. *Angew. Chem. Int. Ed.* **2005**, *44*, 4972. e) Sharma, G. V. M.; Jayaprakash, P.; Narsimulu, K.; Sankar, A. R.; Reddy, K. R.; Krishna, P. R.; Kunwar, A. C. *Angew. Chem. Int. Ed.* **2006**, *45*, 2944. f) Szabo, L.; Smith, B. L.; McReynolds, K. D.; Parril, A. L.; Morris, E. R.; Gervay, J. *J. Org. Chem.* **1998**, *63*, 1074. g)

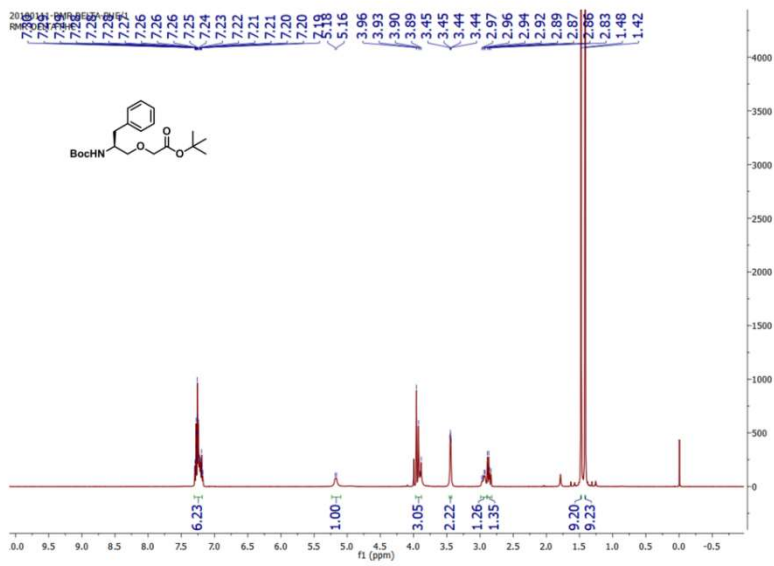
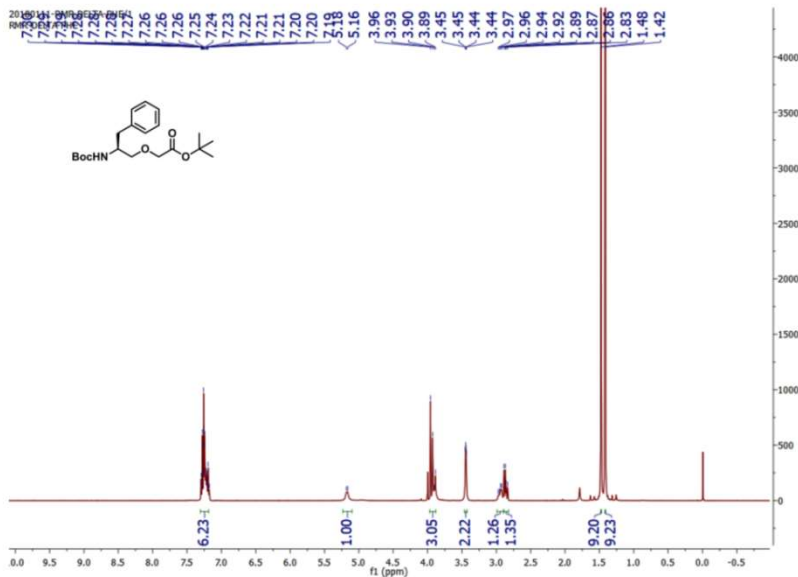


- Rai, R.; Vasudev, P. G.; Ananda, K.; Raghothama, S.; Shamala, N.; Karle, I. L.; Balaram, P. *Chem. Eur. J.* **2007**, *13*, 5917.
10. a) Hayen, A.; Schmitt, M. A.; Ngassa, F. N.; Thomasson, K. A.; Gellman, S. H. *Angew. Chem. Int. Ed.* **2004**, *43*, 505. b) De Pol, S.; Zorn, C.; Klein, C. D.; Zerbe, O.; Reiser, O. *Angew. Chem. Int. Ed.* **2004**, *43*, 511. c) Sharma, G. V. M.; Nagendar, P.; Jayaprakash, P.; Krishna, P. R.; Ramakrishna, K. V. S.; Kunwar, A. C. *Angew. Chem. Int. Ed.*, **2005**, *44*, 5878. d) Seebach, D.; Jaun, B.; Sebesta, R.; Mathad, R. I.; Floegel, O.; Limbach, M.; Sellner, H.; Cottens, S. *Helv Chim Acta* **2006**, *89*, 1801. e) Schmitt, M. A.; Choi, S. H.; Guzei, I. A.; Gellman, S. H. *J. Am. Chem. Soc.* **2005**, *127*, 13130. f) Srinivasulu, G.; Kumar, S. K.; Sharma, G. V. M.; Kunwar, A. C. *J. Org. Chem.* **2006**, *71*, 8395. g) Sharma, G. V. M.; Jadhav, V. B.; Ramakrishna, K. V. S.; Jayaprakash, P.; Narsimulu, K.; Subash, V.; Kunwar, A. C. *J. Am. Chem. Soc.* **2006**, *128*, 14657. h) Ananda, K.; Vasudev, P. G.; Sengupta, A.; Raja, K. M. P.; Shamala, N.; Balaram, P. *J. Am. Chem. Soc.* **2005**, *127*, 16668. i) Chatterjee, S.; Vasudev, P. G.; Ananda, K.; Raghothama, S.; Shamala, N.; Balaram, P. *J. Org. Chem.* **2008**, *73*, 6595. j) Chatterjee, S.; Vasudev, P. G.; Raghothama, S.; Ramakrishnan, C.; Shamala, N.; Balaram, P. *J. Am. Chem. Soc.* **2009**, *131*, 5956. k) Guo, L.; Almeida, A. M.; Zhang, W.; Reidenbach, A. G.; Choi, S. H.; Guzei, I. A.; Gellman, S. H. *J. Am. Chem. Soc.* **2010**, *132*, 7868. l) Grison, C. M.; Robin, S.; Aitken, D. J. *Chem. Commun.* **2016**, *52*, 7802. m) Grison, C. M.; Robin, S.; Aitken, D. J. *Chem. Commun.* **2015**, *51*, 16233.
11. Baldauf, C.; Gunther, R.; Hofmann, H.-J. *J. Org. Chem.* **2004**, *69*, 6214.
12. a) Chakraborty, T. K.; Roy, S.; Kumar, S. K.; Kunwar, A. C. *Tetrahedron Lett.* **2005**, *46*, 3065. b) Chakraborty, T. K.; Roy, S.; Koley, D.; Dutta, S. K.; Kunwar, A. C. *J. Org. Chem.* **2006**, *71*, 6240. c) Chakraborty, T. K.; Arora, A.; Roy, S.; Kumar, N.; Maiti, S. *J. Med. Chem.* **2007**, *50*, 5539. d) Siriwardena, A.; Pulukuri, K. K.; Kandiyal, P. S.; Roy, S.; Bande, O.; Ghosh, S.; Fernandez, J. M. G.; Martin, F. A.; Ghigo, J.-M.; Beloin, C.; Ito, K.; Woods, R. J.; Ampapathi, R. S.; Chakraborty, T. K. *Angew. Chem. Int. Ed.* **2013**, *52*, 10221.
13. Sharma, G. V. M.; Babu, B. S.; Ramakrishna, K. V. S.; Nagendar, P.; Kunwar, A. C.; Schramm, P.; Baldauf, C.; Hofmann, H.-J. *Chem. Eur. J.* **2009**, *15*, 5552.
14. Jiang, H.; Léger, J. M.; Huc, I. *J. Am. Chem. Soc.* **2003**, *125*, 3448.
15. Banerjee, A.; Pramanik, A.; Bhattacharjya, S.; Balaram, P. *Biopolymers* **1996**, *39*, 769.

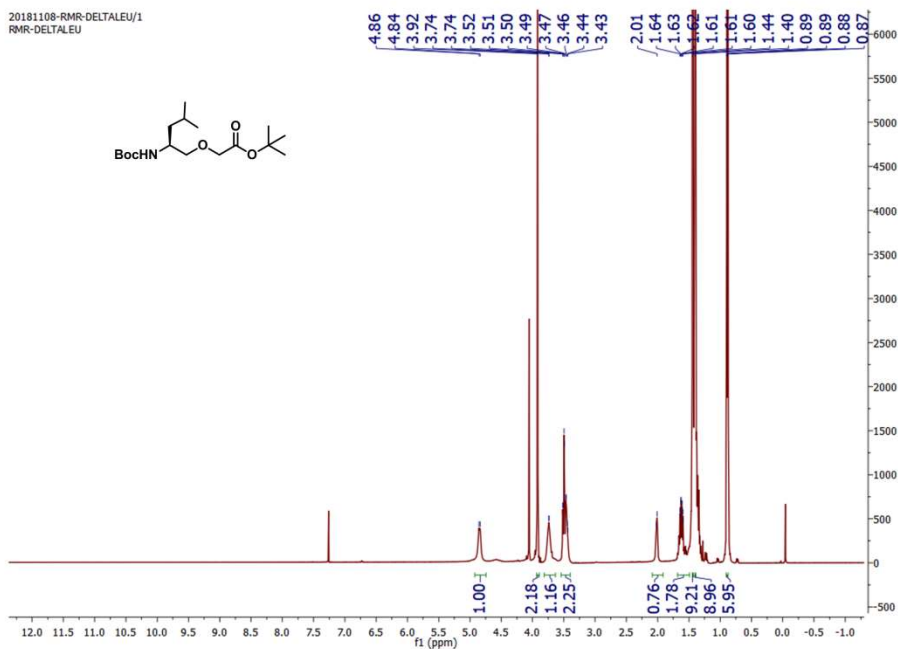
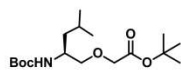
16. a) Jadhav, S. V.; Bandyopadhyay, A.; Gopi, H. N. *Org. Biomol. Chem.* **2013**, *11*, 509. b) Jadhav, S. V.; Misra, R.; Singh, S. K.; Gopi, H. N. *Chem. -Eur. J.* **2013**, *19*, 5955. c) Bandyopadhyay, A.; Gopi, H. N. *Org. Lett.*, **2012**, *14*, 2270. d) Kumar, M. G.; Thombare, V. J.; Katariya, M. M.; Veeresh, K.; Raja, K. M. P.; Gopi, H. N. *Angew. Chem. Int. Ed.* **2016**, *55*, 7847. e) Misra, R.; Dey, S.; Reja, R. M.; Gopi, H. N. *Angew. Chem. Int. Ed.* **2018**, *57*, 1057. f) Misra, R.; Saseendran, A.; George, G.; Veeresh, K.; Raja, K. M. P.; Raghothama, S.; Hofmann, H.-J.; Gopi, H. N. *Chem. Eur. J.* **2017**, *23*, 3764.
17. a) Yusof, Y.; Tan, D. T. C.; Arjomandi, O. K.; Schenk, G.; McGeary, R. P. *Bioorg. Med. Chem. Lett.* **2016**, *26*, 1589. b) Reja, R. M.; Patel, R.; Kumar, V.; Jha, A.; Gopi, H. N. *Biomacromolecules* **2019**, *20*, 1254.
18. Iqbal, M.; Balaram, P. *J. Am. Chem. Soc.* **1981**, *103*, 5548.
19. Baldauf, C.; Günther, R.; Hofmann, H. -J. *J. Org. Chem.* **2006**, *71*, 1200.
20. a) Sharma, G. V. M.; Jadhav, V. B.; Ramakrishna, K. V. S.; Jayaprakash, P.; Narsimulu, K.; Subash, V.; Kunwar, A. C. *J. Am. Chem. Soc.* **2006**, *128*, 14657. b) Fisher, B. F.; Guo, L.; Dolinar, B. S.; Guzei, I. A.; Gellman, S. H. *J. Am. Chem. Soc.* **2015**, *137*, 6484. c) Giuliano, M. W.; Maynard, S. J.; Almeida, A. M.; Guo, L.; Guzei, I. A.; Spencer, L. C.; Gellman, S. H. *J. Am. Chem. Soc.* **2014**, *136*, 15046. d) Srinivasulu, G.; Kumar, S. K.; Sharma, G. V. M.; Kunwar, A. C. *J. Org. Chem.* **2006**, *71*, 8395. e) Misra, R.; Raja, K. M. P.; Hofmann, H. -J.; Gopi, H. N. *Chem. Eur. J.* **2017**, *23*, 16644.
21. a) Gopi, H. N.; Ravindra, G.; Pal, P. P.; Pattanaik, P.; Balaram, H.; Balaram, P. *FEBS Lett.* **2003**, *535*, 175. b) Frackenpohl, J.; Arvidsson, P. I.; Schreiber, J. V.; Seebach, D. *ChemBioChem*, **2001**, *2*, 445. c) Hook, D. F.; Bindschädler, P.; Mahajan, Y. R.; Sebesta, R.; Kast, P.; Seebach, D. *Chem. Biodiversity* **2005**, *2*, 591.

### 3.9. Appendix III: Characterization Data of Synthesized Amino Acids and Peptides P1-P6

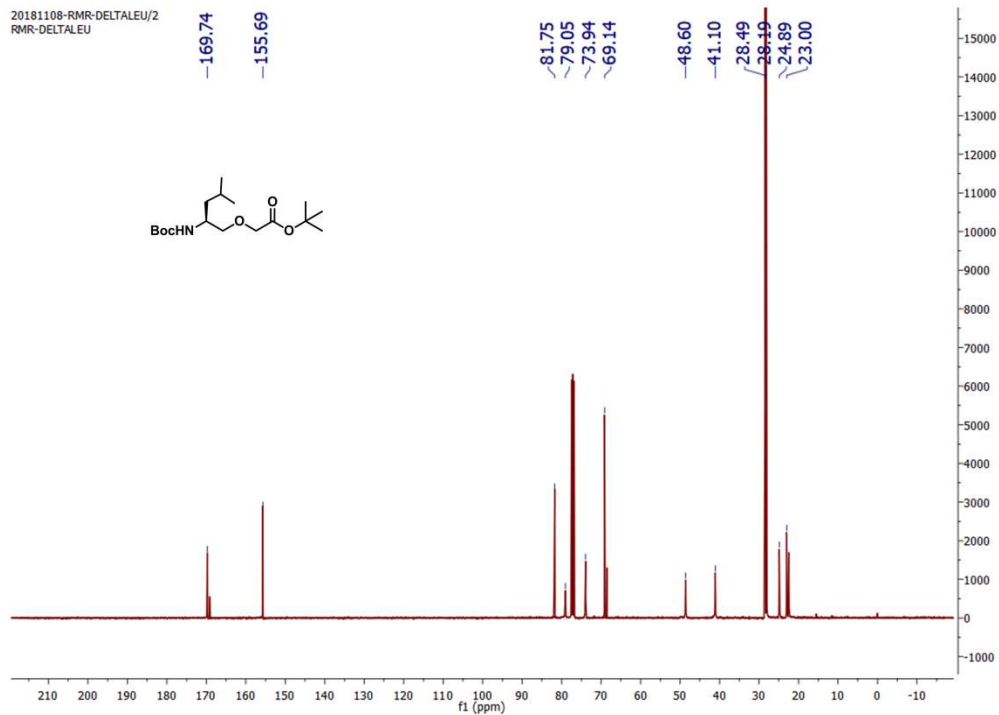
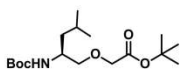
#### 3.9.1. $^1\text{H}$ and $^{13}\text{C}$ NMR Spectra of Compounds and Peptide P3



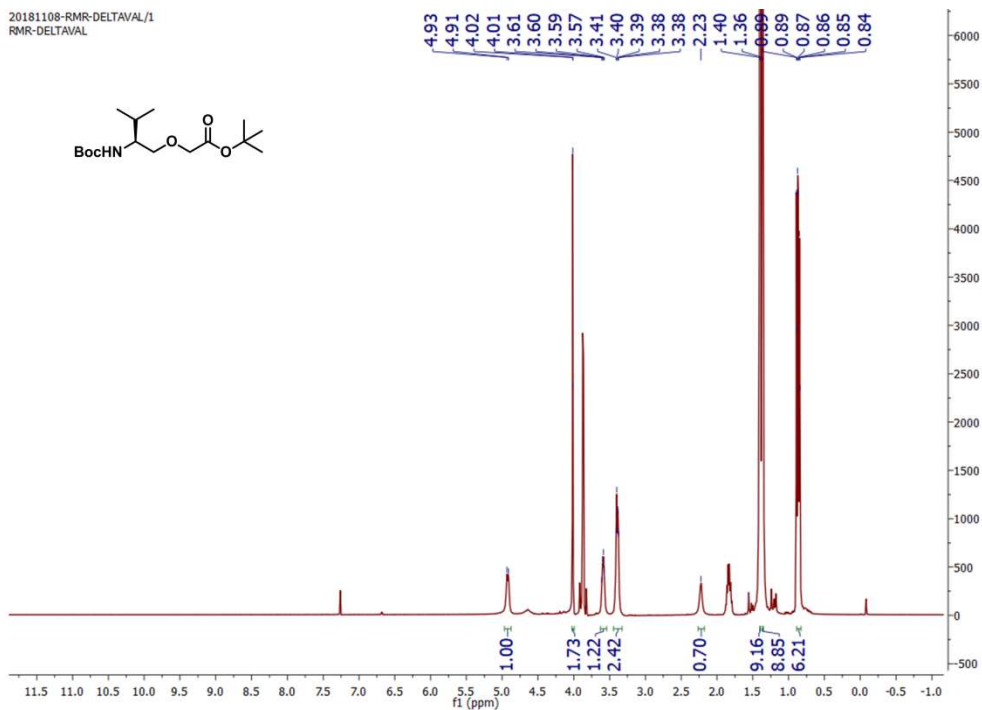
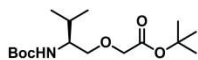
20181108-RMR-DELTALEU/1  
RMR-DELTALEU



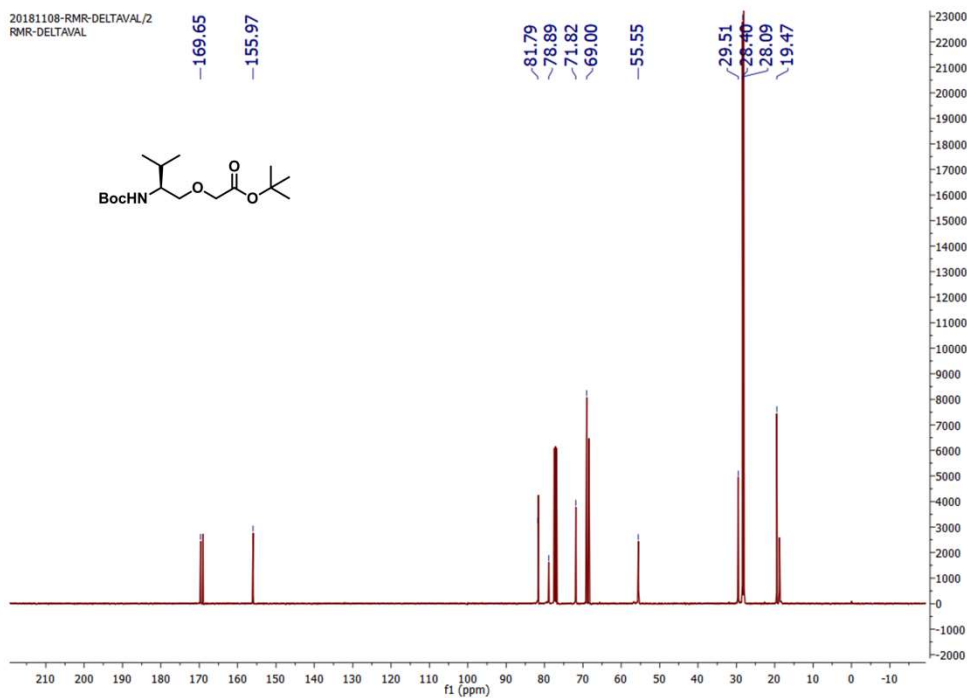
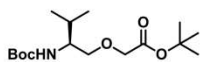
20181108-RMR-DELTALEU/2  
RMR-DELTALEU

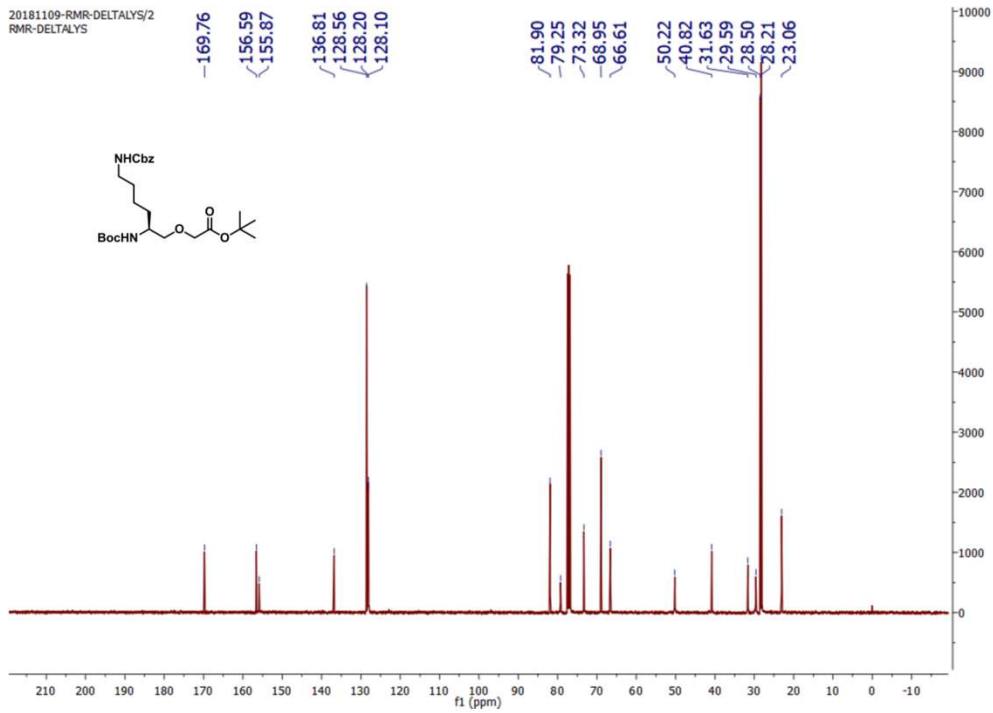
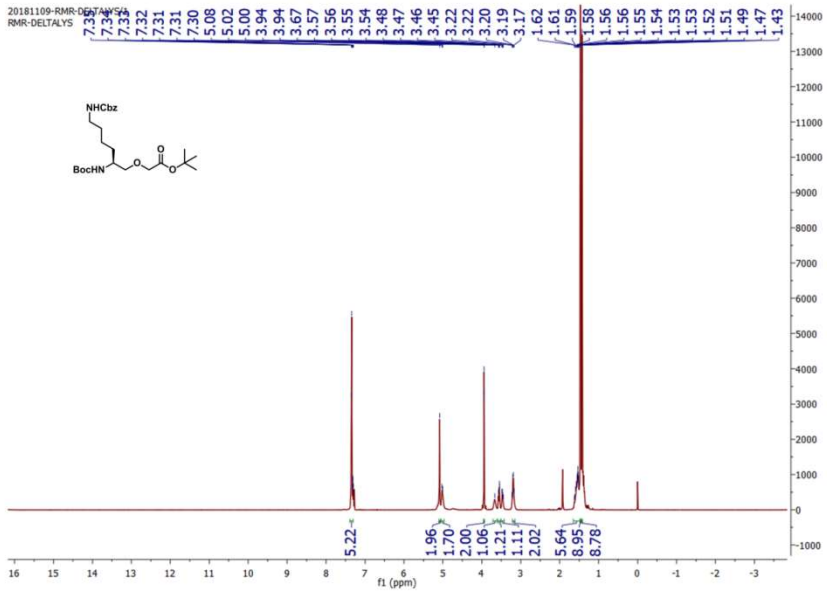


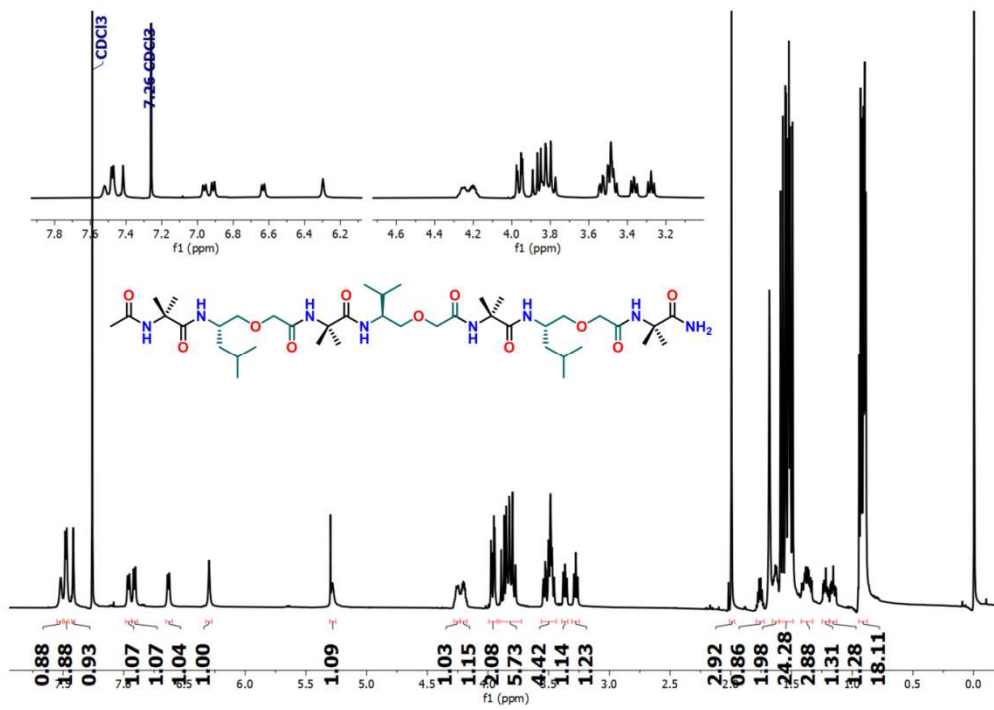
20181108-RMR-DELTAVAL/1  
RMR-DELTAVAL



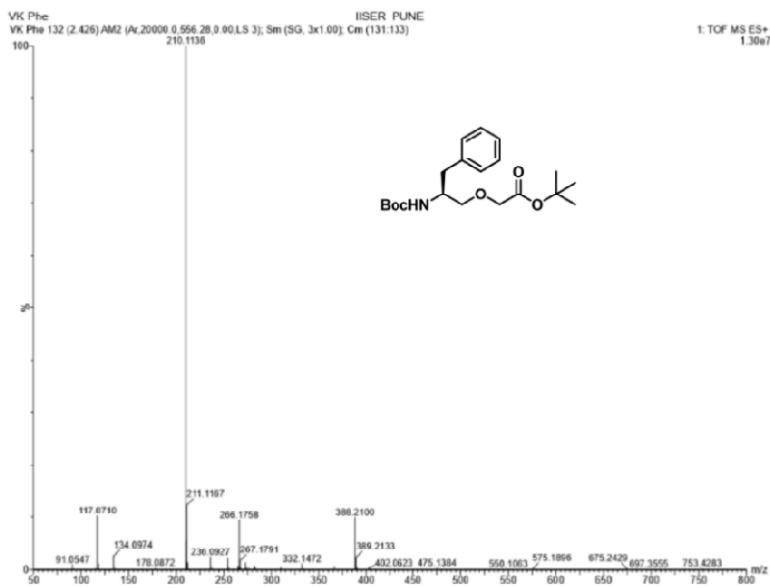
20181108-RMR-DELTAVAL/2  
RMR-DELTAVAL



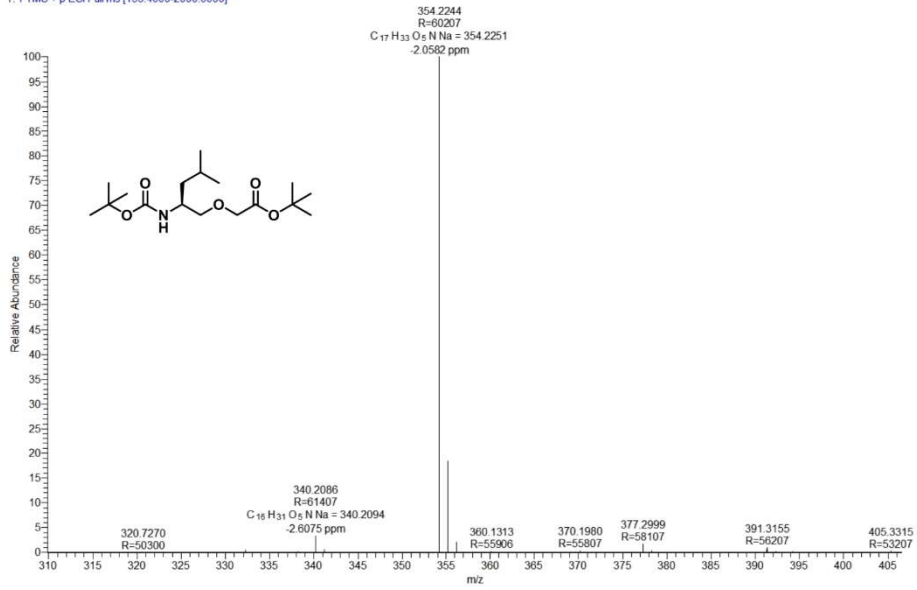




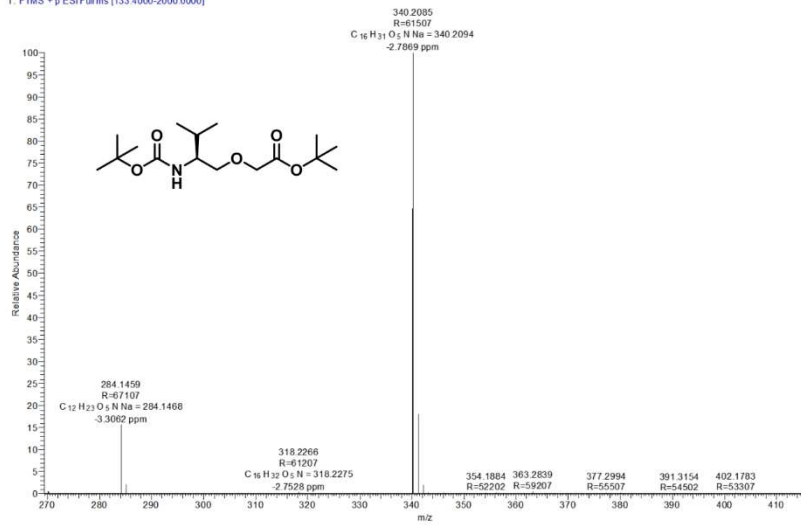
### 3. 9.2. High Resolution Mass Spectra (HRMS) of the Synthesized Amino Acids



RMR-4 #283 RT: 1.26 AV: 1 NL: 3.24E9  
T: FTMS + p ESI Full ms [133.4000-2000.0000]

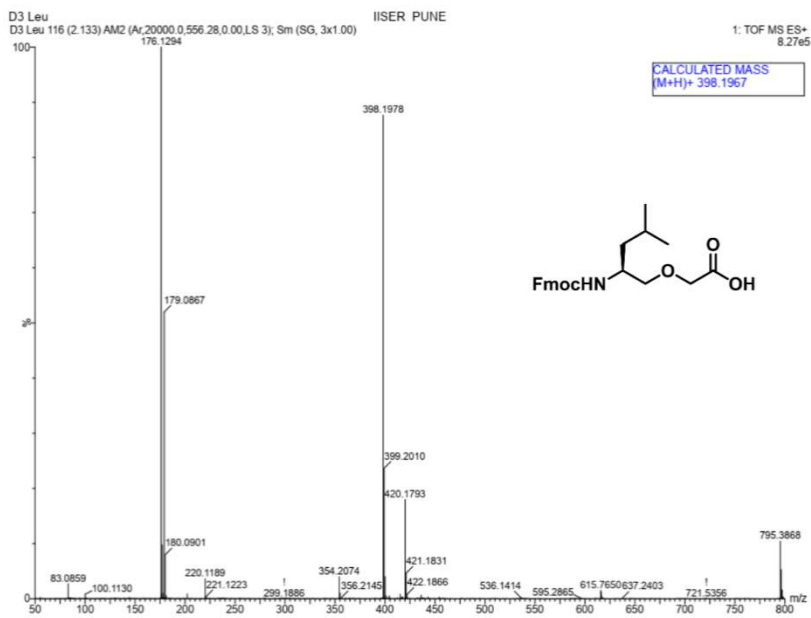
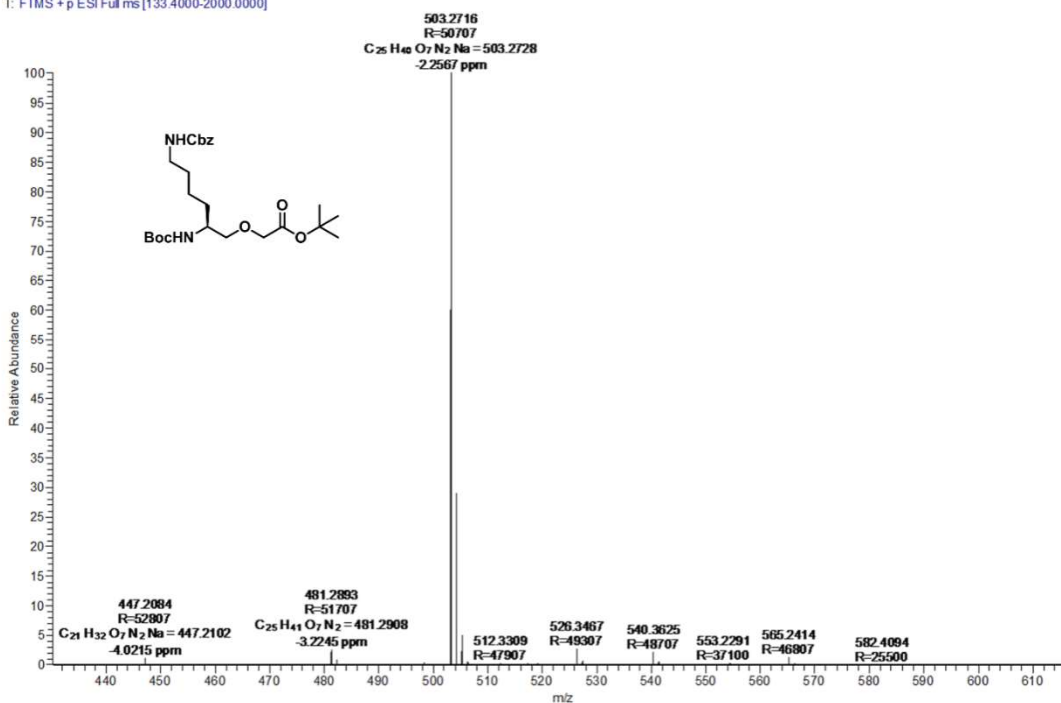


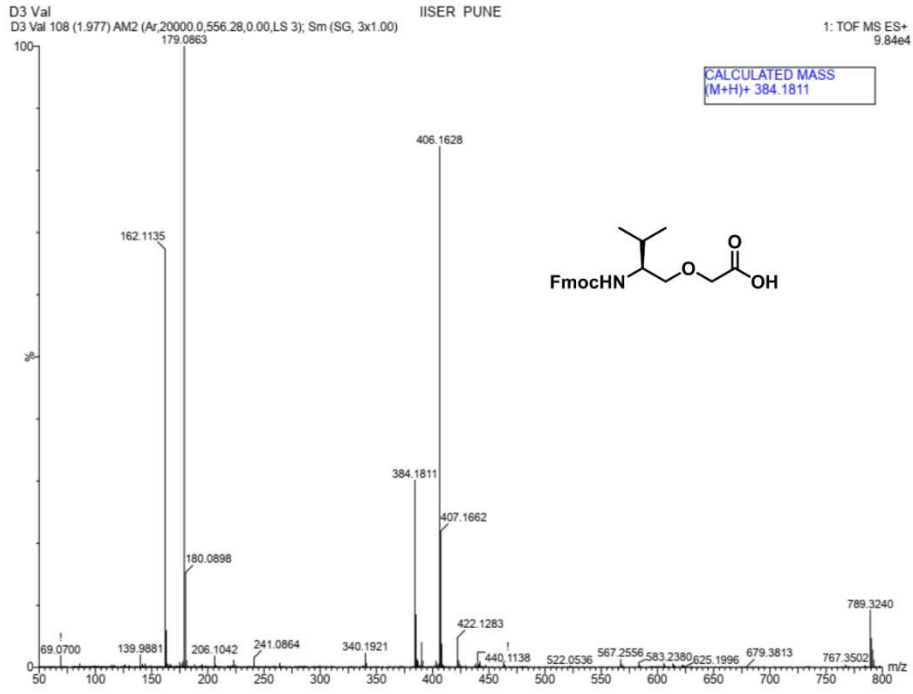
RMR-3 #274 RT: 1.23 AV: 1 NL: 4.89E9  
T: FTMS + p ESI Full ms [133.4000-2000.0000]



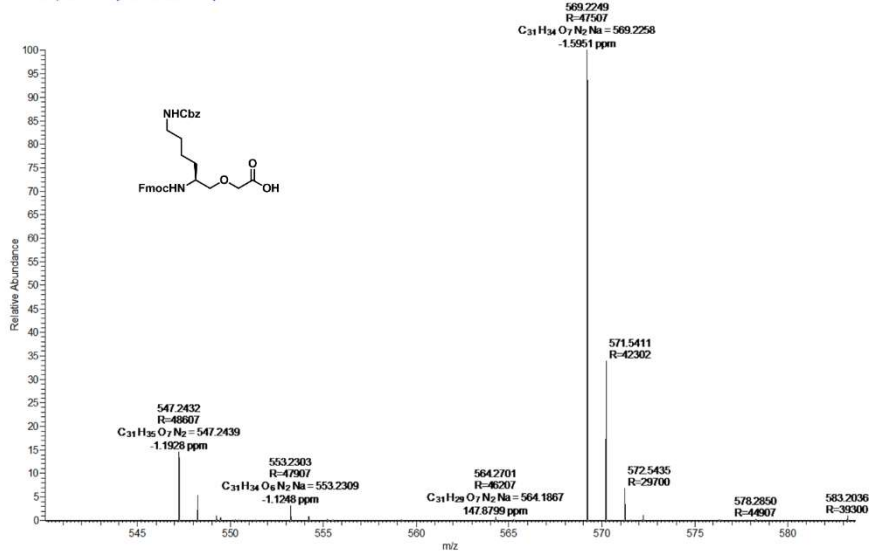


RMR-6 #276 RT: 1.23 AV: 1 NL: 3.51E9  
T: FTMS + p ESI Full ms [133.4000-2000.0000]





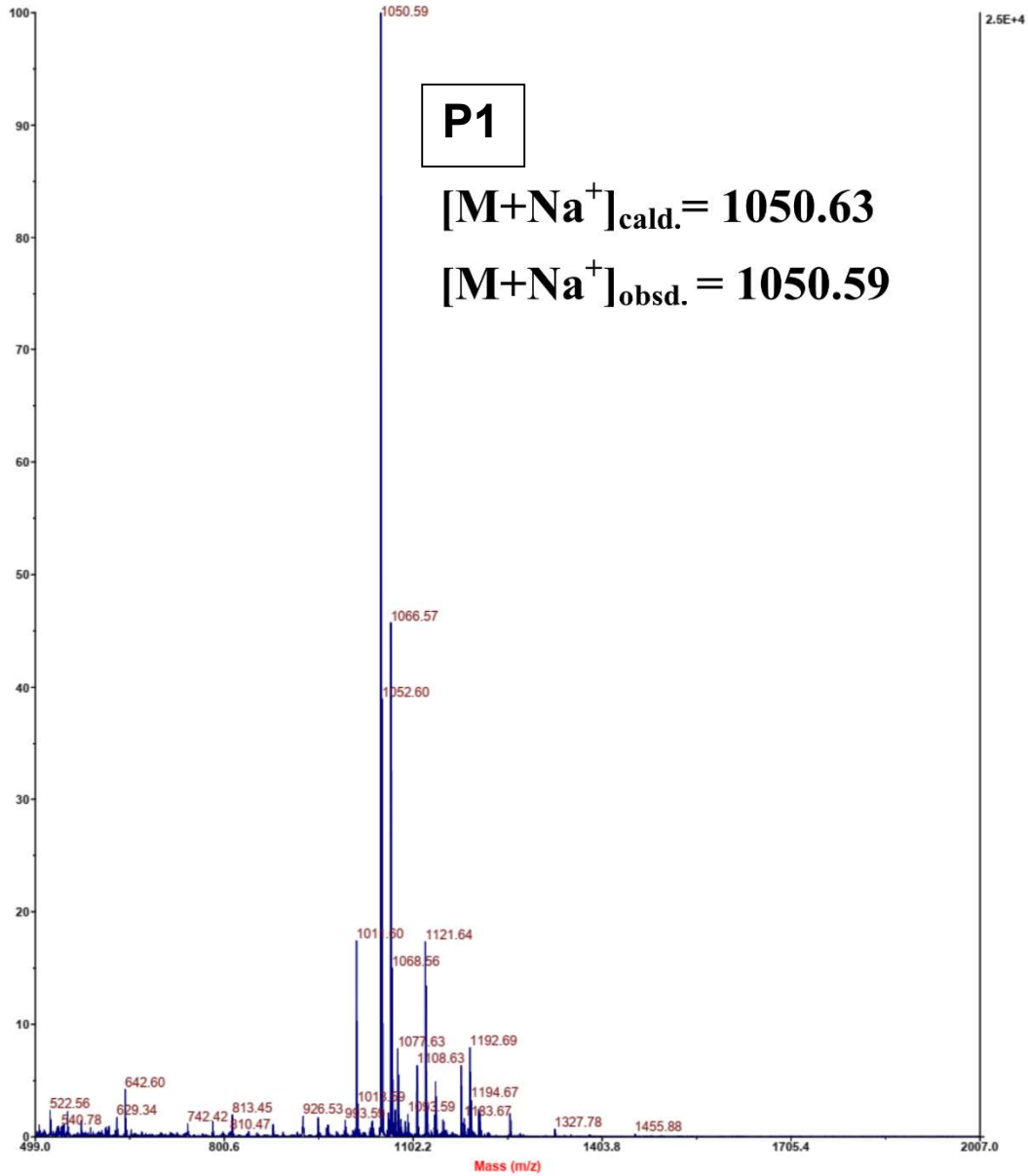
RMR-5 #271 RT: 1.21 AV: 1 NL: 260E8  
T: FTMS + p ESI Full ms [133.4000-2000.0000]



### 3.9.3. MALDI-TOF/TOF Spectra of the Peptides P1-P6

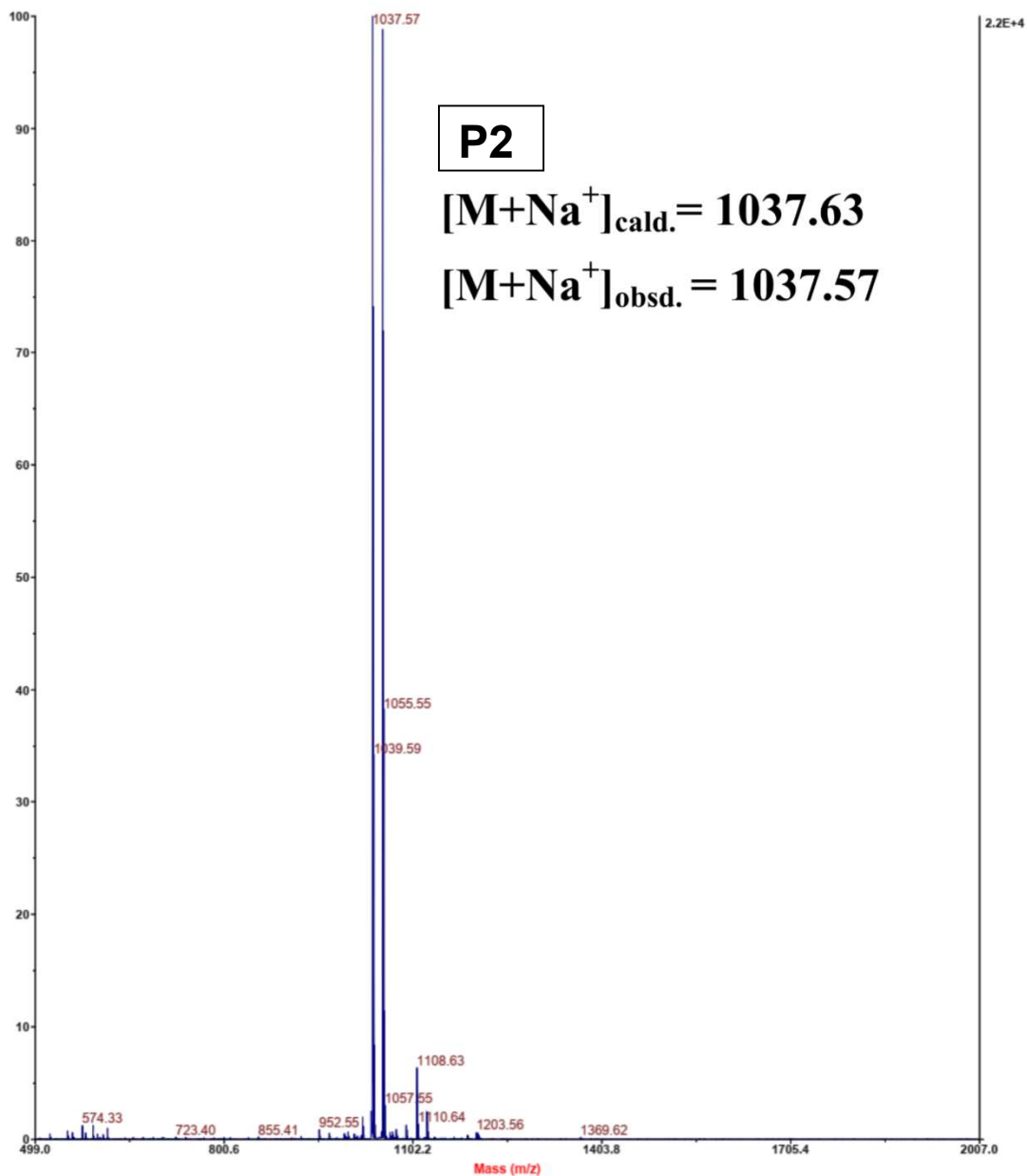
#### Spectrum Report

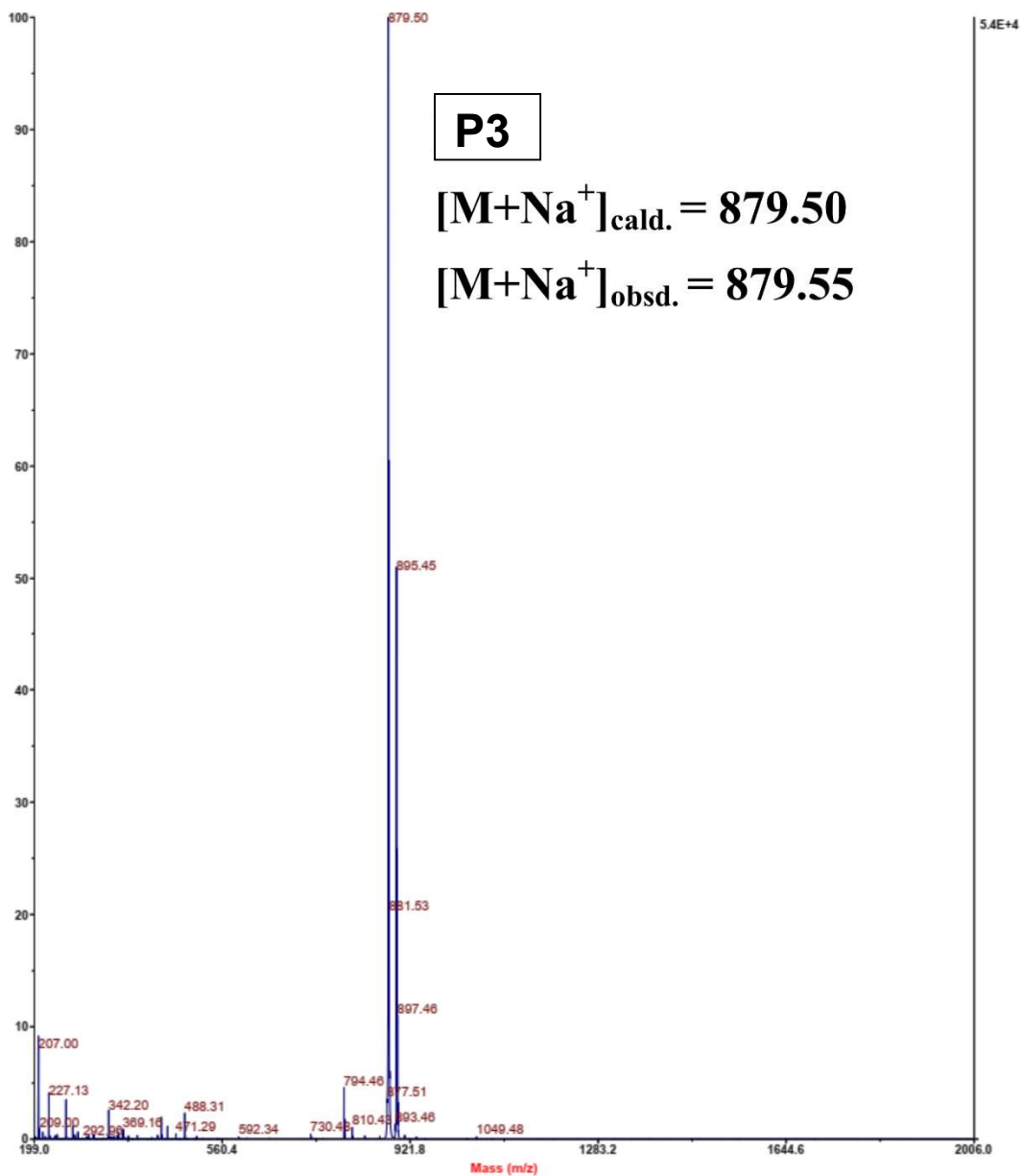
Final - Shots 500 - IISER-96-2-2018; Label G3



# spectrum report

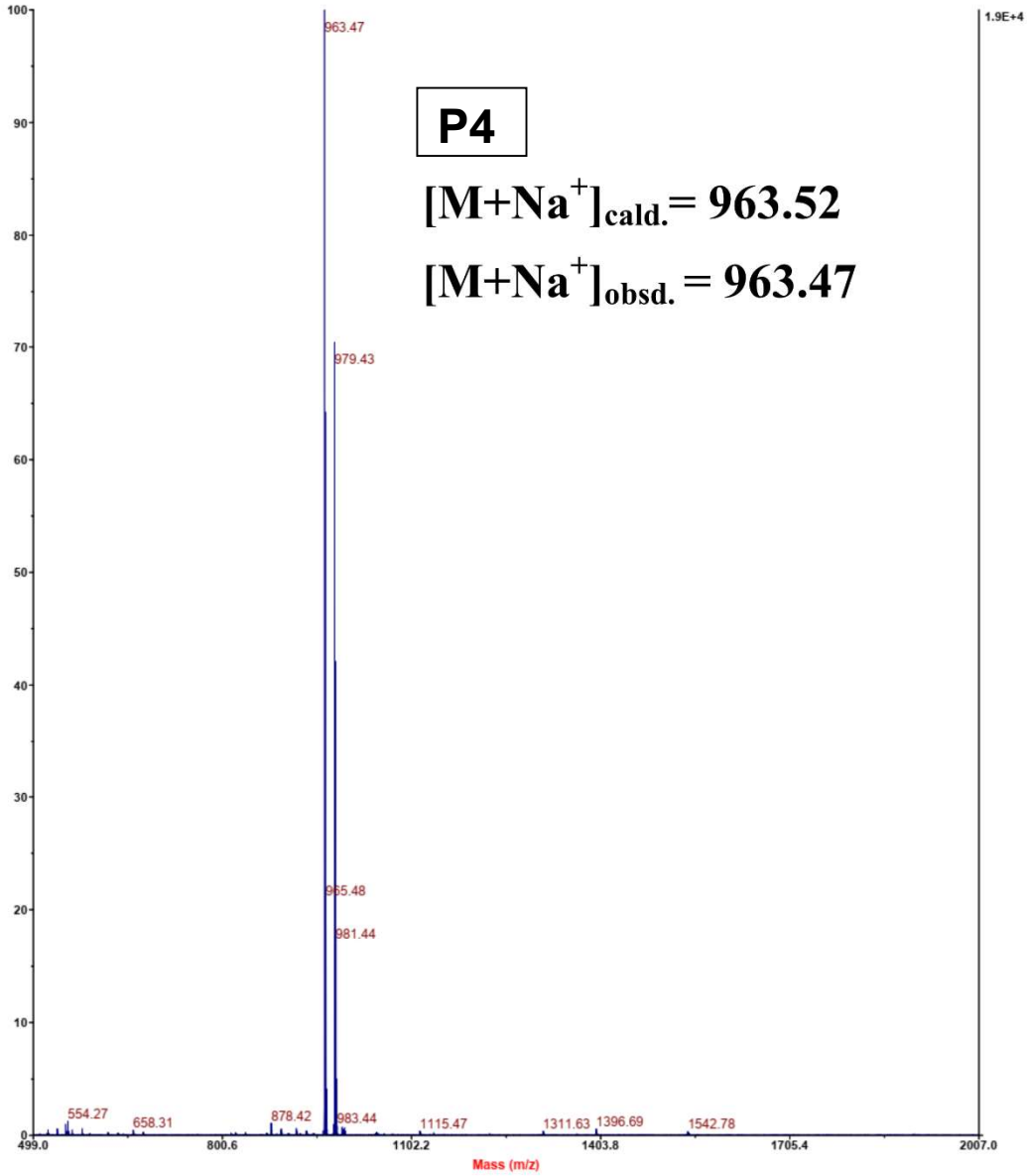
Final - Shots 500 - IISER-96-2-2018; Label G1





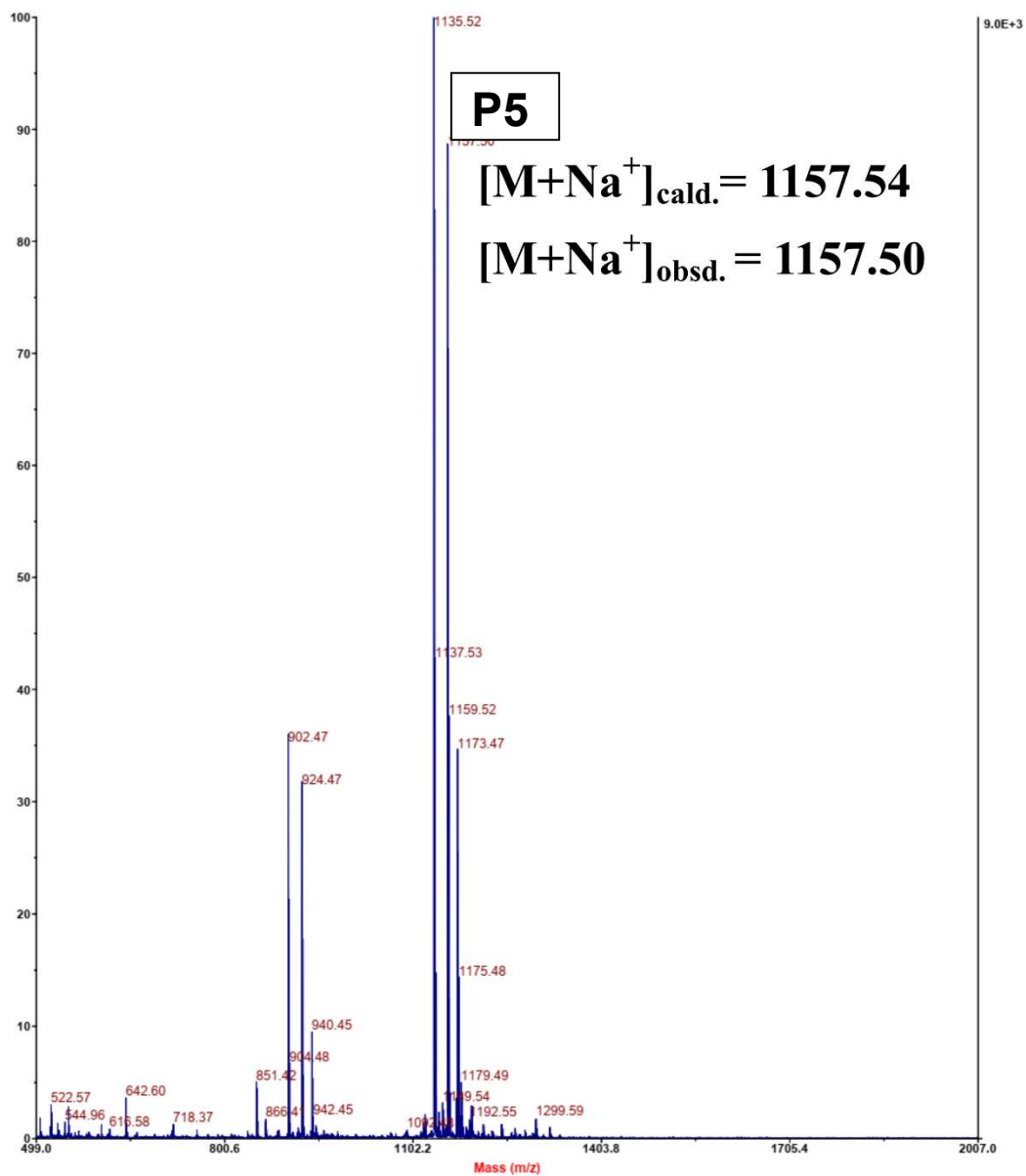
# Spectrum Report

Final - Shots 500 - IISER-96-2-2018; Label G2



# Spectrum Report

Final - Shots 500 - IISER-96-2-2018; Label G4



## *Chapter 4*

# **Divergent Supramolecular Gelation of Backbone Modified Short Hybrid $\delta$ -Peptides**



## **4. 1. Introduction**

The fundamental theme in the fields of nanoscience and nanotechnology is the formation of highly ordered self-assembled materials.<sup>1</sup> The fascinating properties showed by the nanostructures have attracted significant attention due to their widespread applications in energy technologies, biomedical, chemical biology and catalysis.<sup>2</sup> Along with the numerous types of nano-assemblies derived from the small organic molecules, the biomacromolecules such as lipids, proteins, carbohydrates and nucleic acids, often self-assembled into highly ordered supramolecular architectures.<sup>3</sup> The hierarchical supramolecular structures of biomacromolecules are stabilized by various types of non-covalent interactions such as H-bonding, salt bridge interactions, van der Waals interactions and aromatic pi-stacking.<sup>4</sup> Along with the biomacromolecules, short peptides have displayed a rich supramolecular diversity and have been serving as excellent tools to design various types of self-assembled biomaterials.<sup>5</sup> The finding of peptide nanotube from a Phe-Phe dipeptide by the Gazit and colleagues has opened new avenues in the generation of soft materials from the short peptides.<sup>6</sup> The dipeptide nanotubes have been explored as templates to cast silver nanowires, as drug delivery agents, light harvesting systems, energy storage materials and antimicrobial candidates etc.<sup>7</sup> In addition, the self-assembling properties of peptides have been finding applications in the fields of tissue engineering as well as nanoelectronics.<sup>8</sup> Thus the short peptide based self-assembled materials have attracted considerable attention in recent years.

## **4.2. Short Peptide Based Self Assembly**

The main advantages of peptide based soft materials are their chemical and structural diversity. This includes not only the 20 coded amino acids but different variations of non-coded and synthetic amino acids.<sup>9</sup> More over the peptide or protein based self-assembled materials are biocompatible and degradable.<sup>10</sup> Another advantage of these peptide based materials is that they can spontaneously self-assembled by their inherent non-covalent interactions. In their pioneering work, Ghadiri and co-worker discovered hollow nanotubular structure of alternating D- and L- amino acids self-assembled through intermolecular H-bonds between the cyclic peptides.<sup>11</sup> Further they utilized these nanotubular assembly for the transmembrane ion channels and anti-

microbial candidates.<sup>12</sup> In later on Zhang and co-workers utilized liner, surfactant like charge complementary peptide building blocks for the construction of different self-assembled nanostructures.<sup>13</sup> The group of Matsui and co-workers utilized amphiphilic bolaamphiphile peptides for the design of different functional nanotubes.<sup>14</sup> In addition, several amphiphilic peptides were developed by Stupp and colleagues by attaching a long hydrophobic fatty tail with hydrophilic peptides.<sup>15a-15d</sup>

### 4.3. Diphenyl Alanine Based Peptide Self Assembly

The work by Gazit and colleagues on Phe-Phe dipeptide derived from the core region of the Alzheimer's disease  $\beta$ -amyloid peptide has opened new avenues in the generation and design of soft materials and finding applications in various fields.<sup>16</sup> The group of Chen Beum Park reported light harvesting peptide nanotube system using Phe-Phe dipeptide motif.<sup>17a</sup> They showed Pt nanoparticle coated FF/THPP hybrid material exhibit same structure and electrochemical properties which is similar to the photo system I. Furthermore, they have also shown the formation of the semiconducting nanowire from the photo luminescent crystalline Phe-Phe in the vapor

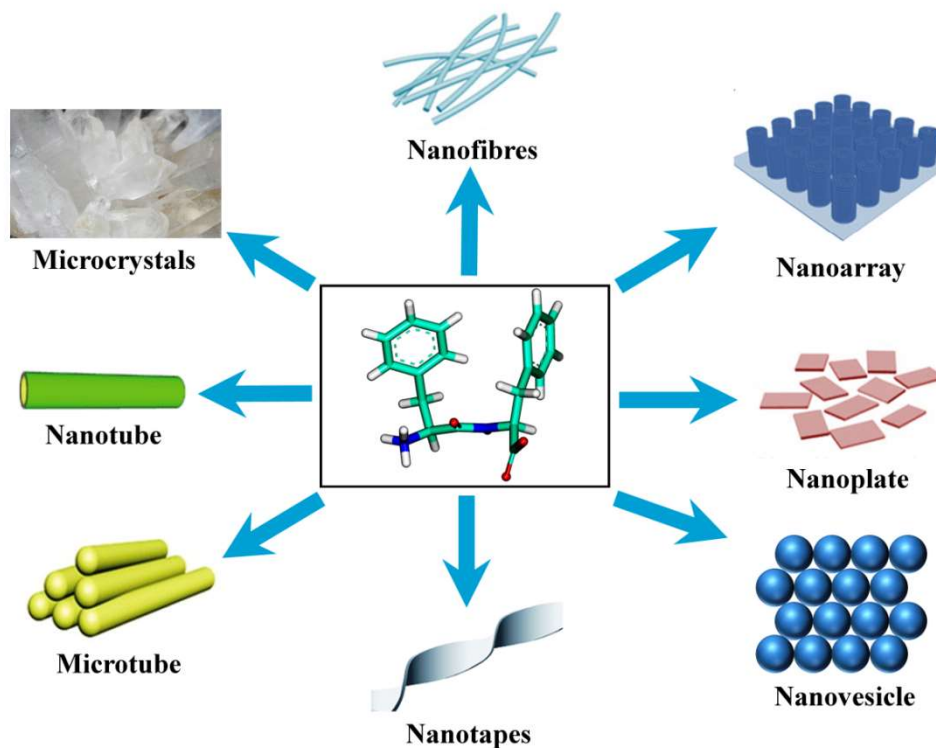


**Figure 4.1:** Different self -assembled nanoarchitechture from Phe-Phe dipeptide.

phase.<sup>17b</sup> In addition Phe-Phe have been also used as ferroelectric materials. The alignment of the dipoles due to the directional H-bonding and aromatic interactions help the Phe-Phe dipeptide as ferroelectric materials.<sup>18</sup> The group of J. Shen showed the light induced ferroelectricity from the Phe-Phe dipeptide nanotube.<sup>19</sup> Gazit and co-worker further reported the electrochemical biosensing approach from the diphenylalanine based peptide nanotube.<sup>20</sup> Furthermore recently it has been shown the strong piezoelectric effect from Phe-Phe nanotube. The effective piezoelectric coefficient value was  $60 \text{ pmV}^{-1}$  which is comparable to the lithium niobate ( $\text{LiNbO}_3$ ).<sup>21</sup> Apart from the formation of nanotubular assembly, Phe-Phe motif showed different self-assembled nano architectures such as vesicles, ribbons, spares, tapes, fibrous hydrogel etc.<sup>22</sup> The list of different morphology of the modified phe-phe dipeptides are shown in the Table 4.1. Among the different self-assembled nanostructure, Phe-Phe dipeptide having hydrogelation properties show various application ranging from tissue culture, drug delivery and biomaterials.<sup>23</sup> Ulijn and colleagues have shown remarkable hydrogelation properties from the Fmoc-Phe-Phe-OH. Furthermore, they utilized these hydrogels to grow the cells.<sup>24</sup> Banerjee and co-workers showed the utilization of fatty acid coupled dipeptide for the formation of different hydrogels.<sup>25</sup> They further utilized these hydrogels as antimicrobial agents and drug delivery platform.<sup>26</sup> Further, the diphenylalanine based hydrogels have also been used in different optoelectronics applications such as immobilization of QDs into the peptide hydrogel scaffold, conductive organogels.<sup>27</sup>

**Table 4.1:** List of the different nano-architectures from the self-assembled diphenylalanine peptide:

Peptide Sequence	Assembled Structure	Ref
H-Phe-Phe-OH	Nanotubes	<i>Science</i> <b>2003</b> , 300, 625
H-Phe-Phe-NH <sub>2</sub>	Nanotubes	<i>Angew. Chem. Int. Ed.</i> <b>2007</b> , 46, 2431
Ac-Phe-Phe-NH <sub>2</sub>	Nanotubes	<i>Isr. J. Chem.</i> <b>2005</b> , 45, 363
H-Cys-Phe-Phe-OH	Nanospheres	<i>Nano Lett.</i> <b>2004</b> , 4, 581

Boc-Phe-Phe-OH	Sphere, Tube	<i>Angew. Chem. Int. Ed.</i> <b>2010</b> , <i>49</i> , 9939
Cbz-Phe-Phe-OH	Amyloid like fibril	<i>Isr. J. Chem.</i> <b>2005</b> , <i>45</i> , 363
Fmoc-Phe-Phe-OH	Fibrous Hydrogel	<i>Adv. Mater.</i> <b>2006</b> , <i>18</i> , 611
Fmoc-Phe-Gly-OH/Fmoc-Gly-Phe-OH	Fibrous Hydrogel	<i>Langmuir</i> <b>2012</b> , <i>28</i> , 2015
Fmoc-Phe-Pro-OH	Sphere	<i>Langmuir</i> <b>2012</b> , <i>28</i> , 2015
H-Phe-Phe-OFm	Amyloid like fibril	<i>Langmuir</i> <b>2018</b> , <i>34</i> , 15551
Cyclo-Phe-Phe	Nanotube	<i>Nat. Nanotechnol.</i> <b>2009</b> , <i>4</i> , 849
H-Phe-Phe-Phe-OH	Nanoplates	<i>Biophys. J.</i> <b>2009</b> , <i>96</i> , 5020
BocNH- $\beta$ Phe- $\beta$ Phe-OH	Fibrous organogel	<i>Langmuir</i> <b>2017</b> , <i>33</i> , 7762
BocNH- $\gamma$ Phe- $\gamma$ Phe-OH	Fibrous organo and hydrogel	<i>Langmuir</i> <b>2017</b> , <i>33</i> , 7762
<b>BocNH-<math>\beta</math>(O)-<math>\delta^5</math>Phe-<math>\beta</math>(O)-<math>\delta^5</math>Phe-OH</b>	<b>Fibrous Hydrogel in 1<math>\times</math> PBS</b>	<b>Present Study</b>

#### 4.4. Short Peptide Based Assembly Composed of Different Non Canonical Amino Acids

Along with the  $\alpha$ -peptides, efforts have also been made in the literature to understand the molecular self-assemblies from the other non-canonical amino acids. Among them of  $\beta$ - and  $\gamma$ -peptides are well studied for the formation of different self-assembled nanostructures.<sup>28</sup> The advantage of  $\beta$ - and  $\gamma$ -peptides over the  $\alpha$ -peptides is that they are proteolytically stable and required short sequences to attain folded structures.<sup>29</sup> A variety of supramolecular architectures such as tapes, fibers, ribbons, polyhedrons, nanotubes and vesicles have also been derived from the supramolecular assemblies of  $\beta$ - and  $\gamma$ -peptides.<sup>30</sup> Bing Xu and colleagues showed the formation of stable hydrogels from the  $\beta$ -dipeptide coupled with N-terminal naphthyl group.<sup>31</sup> The group of Hamley and co-workers showed the effect of self-assembling properties of core sequence of amyloid beta A $\beta$ (16–20) containing  $\gamma$ - amino acids at the N-terminus.<sup>32</sup> Recently, Malhotra *et al.* demonstrated the antimicrobial properties of self-assembled  $\alpha,\gamma$ -hybrid peptides.<sup>33</sup> The group of Bianco and co-workers showed the self-assembly of the backbone homologated  $\gamma$ -dipeptide in combination with functionalized carbon naotube.<sup>28b</sup> Apart from the self-assembly of the backbone homologated peptides,  $\Delta$ Phe- $\Delta$ Phe peptide by Chauhan and

coworkers<sup>34</sup> and side-chain homologated Phe–Phe dipeptides by Gazit and co-workers<sup>35</sup> have also been investigated. In addition,  $\beta$ -Cyclobutane<sup>36</sup> and Oxatene<sup>37</sup> based amino acids have also been explored to design different self-assembled materials.

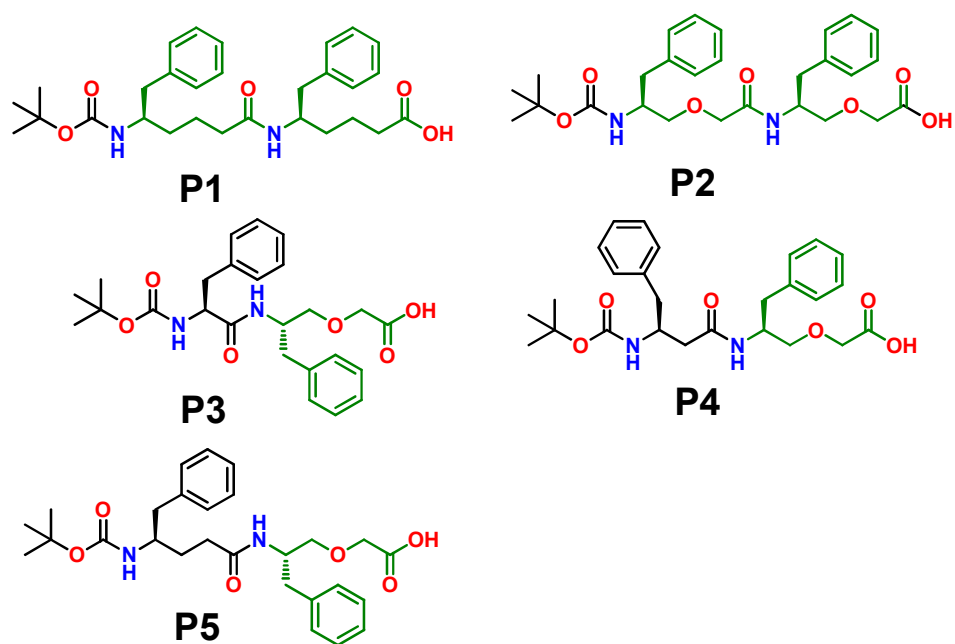
#### **4.5. Aim and Rationale of the Present Work**

We have been interested in understating the conformational and self-assembling properties of peptides composed of various types of non-natural  $\beta$ - and  $\gamma$ -amino acids.<sup>38</sup> In comparison to  $\beta$ - and  $\gamma$ -amino acids, structural and self-assembling properties of peptides composed of higher homologous amino acids such as  $\delta$ -amino acids<sup>39,40</sup> are scarcely examined in the literature. Recently, we have shown the spontaneous supramolecular gelation properties from  $\gamma^4$ Phe- $\gamma^4$ Phe dipeptide over the  $\beta^3$ Phe- $\beta^3$ Phe and Phe-Phe dipeptides.<sup>41</sup> As  $\gamma^4$ Phe- $\gamma^4$ Phe showed excellent gelation over the  $\beta$ - and  $\alpha$ -dipeptide counterparts, we have hypothesized that  $\delta^5$ Phe- $\delta^5$ Phe dipeptide motifs can be served as better hydrogelators than the  $\gamma$ -dipeptide counterpart. More importantly, as the length of the  $\delta^5$ -amino acids is equal to the length of an  $\alpha$ -dipeptide, they can be used as surrogates of  $\alpha$ -dipeptides to overcome the proteolytic cleavage. In this chapter, we have synthesized various peptides composed of  $\delta^5$ -amino acids and examined their gelation properties and their applications in oil spill recovery and 2D cell culture.

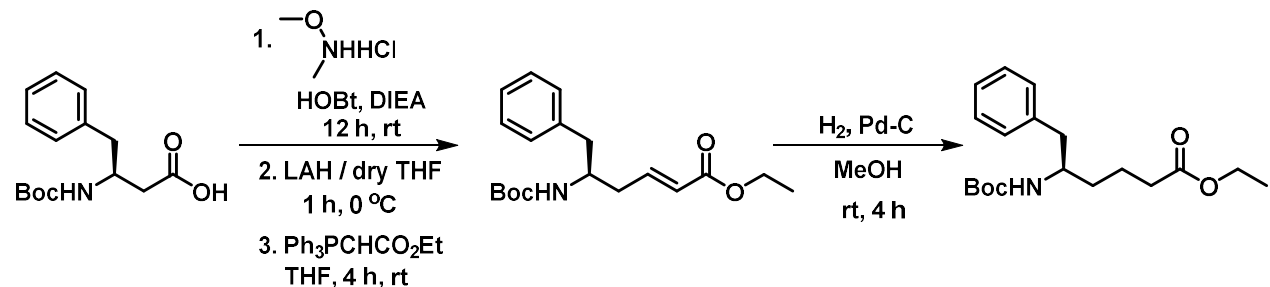
## 4. 6. Results and Discussion

### 4.6.1. Design and Synthesis of Peptide P1-P5

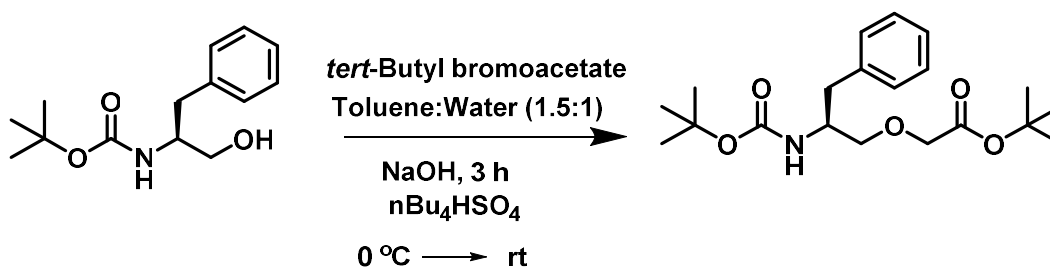
As a part of our investigation and to test our hypothesis, we have synthesized peptide **P1-P5**. The sequences of  $\delta$ - and hybrid  $\delta$ -peptides are given in the Scheme 4.1. The  $\beta^3$ - and  $\gamma^4$ -Phe were synthesized as reported earlier.<sup>42,38a</sup> The  $\delta^5$ -Phe was synthesized starting from the Boc- $\beta^3$ -Phe as shown in the Scheme 2. The new  $\beta(O)$ - $\delta^5$ -Phe was synthesized starting from  $\beta$ -amino alcohol as shown in the Scheme 3.<sup>43</sup>



**Scheme 4.1:** Sequences of the dipeptide under investigations.



**Scheme 4.2:** Synthesis of *N*-Boc- $\delta^5$ -Phe-OEt from *N*-Boc- $\beta^3$ -Phe-OH



**Scheme 4.3:** Synthesis of *N*-Boc- $\beta$ (O)- $\delta^5$ -Phe-O<sup>t</sup>Bu from *N*-Boc amino alcohol.

#### 4.6.2. Gelation Study of Peptides **P1**, **P2** and **P4**

To understand their ordered self-aggregation properties, the purified peptide **P1** was subjected to the gelation studies in 1× phosphate buffer saline (1×PBS) at pH=7.4 as well as in aromatic organic solvents. Peptide **P1** failed to give hydrogels in aqueous buffer however it gels various aromatic organic solvents. The organogels of **P1** in various aromatic solvents are shown in the Figure 4.3. In contrast, peptide **P2** gave stable gels in 1× PBS at pH 7.4 at the concentration of 10 mg/mL dissolved upon gently heating and standing for about 12 h. Inspired by the spontaneous hydrogelation of **P2**, we have systematically probed the gelation properties of hybrid dipeptides consisting Xxx- $\beta$ (O)- $\delta^5$ -Phe sequences (**P3-P5**, Scheme 4.1). Among the all hybrid peptides, **P4** has shown excellent gelation property in a variety of aromatic solvents such as toluene, benzene, xylene and mesitylene at the concentration of 10 mg/mL. Other peptides (**P3** and **P5**) were found to be either insoluble or not inducing the gelation in aromatic organic solvents. All hybrid peptides (**P3**, **P4** and **P5**) were found to be insoluble in 1× PBS and failed to give hydrogels. The gels derived from the peptides **P1**, **P2** and **P4** were found to be external stimuli responsive. The transition of gel to sol can be achieved by either mechanical forces or by increasing the temperature. In contrast to **P3** and **P5**, the hybrid peptide **P4** consisting of  $\beta$ - and  $\beta$ (O)- $\delta^5$ -Phe may be reached the threshold of hydrophobicity and hydrophilicity which probably responsible for the gelation of aromatic organic solvents.<sup>41</sup> Being side-chains were constant among all the peptides, the backbone conformational flexibility is probably responsible for the gelation properties of the peptides.<sup>41</sup>

**Table 4.2:** Details of the gelation property of peptides **P1-P5**

Solvent	P1	P2	P3	P4	P5
1× PBS at pH 7.4	Not dissolved <sup>#</sup>	Transparent Gel <sup>ψ</sup>	Sol	Not dissolved <sup>#</sup>	Not dissolved <sup>#</sup>
Toluene	Transparent Gel	Sol	Sol	Transparent Gel	Sol*
Benzene	Transparent Gel	Sol	Sol	Transparent Gel	Sol*
Xylene	Transparent Gel	Sol	Sol	Transparent Gel	Sol*
Mesitylene	Transparent Gel	Sol	Sol	Transparent Gel	Sol*
Gelation Time	~5 min	~12 h	----	~5 min	----

# Difficult to dissolve completely. \* Aggregating nature after 36 h. <sup>ψ</sup> keeping for longer time gel becomes opaque.

#### 4.6.3. Morphology Study

To understand supramolecular assembly formed by the peptides **P1**, **P2** and **P4**, the FE-SEM was carried out. As both **P3** and **P5** did not show any gelation properties, we have not subjected them for the morphology studies. Though the peptides **P1**, **P2** and **P4** displayed the fibrillar morphology however they are different from one another. Peptide **P1** and **P4** displayed densely packed fibrillar network compared to peptide **P2**.



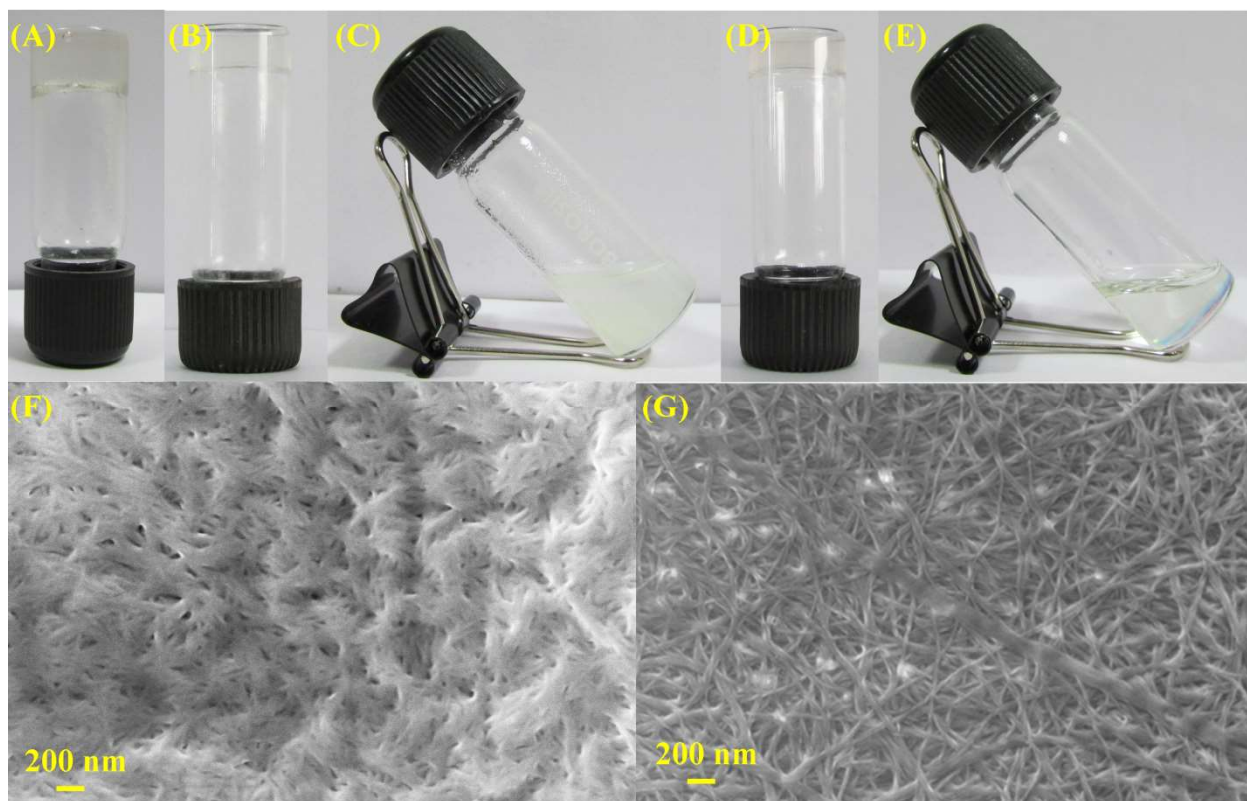


**Figure 4.2:** Examination for the formation of gel in (A) Peptide **P1** (conc. 10 mg/mL) in toluene (B) Peptide **P2** (conc. 10 mg/mL) in 1× PBS at pH 7.4. (C) Peptide **P3** (conc. 10 mg/mL) in toluene. (D) Peptide **P4** (conc. 10 mg/mL) in toluene. (E) Peptide **P5** (conc. 10 mg/mL) in toluene. (F) FE-SEM images of the organogel of peptide **P4** in toluene. (G) FE-SEM images of the hydrogel of peptide **P2** in 1× PBS.



**Figure 4.3:** (I) Solubility of peptide **P1** (10 mg/mL) in 1× PBS. Formation of organogel (10 mg/mL) of peptide **P1** in different aromatic solvent (II) Benzene (III) Toluene (IV) Xylene (V) Mesitylene.

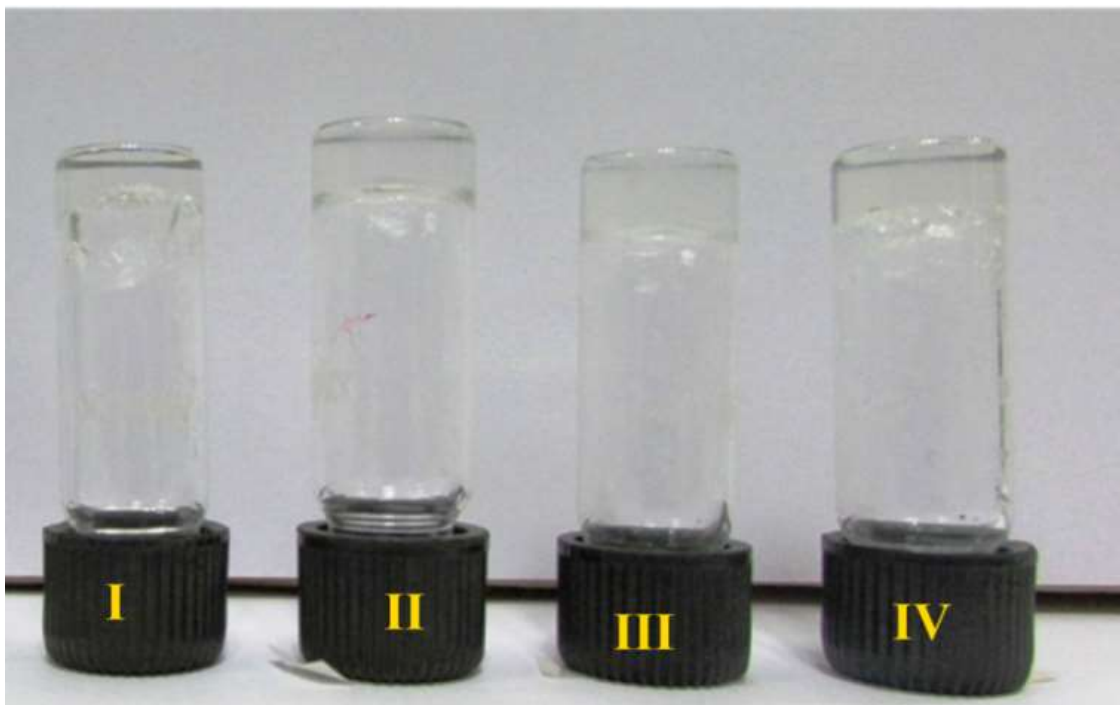


**Figure 4.4:** Formation of organogel (10 mg/mL) from peptide **P4** in different aromatic solvent (I) Toluene (II) Benzene (III) Xylene (IV) Mesitylene.

#### 4.6.4. Viscoelastic Property

To gain insight into the viscoelasticity and self-healing properties of organogels of **P1** and **P4** and hydrogels of **P2**, we carried out the rheological measurements. These results are shown in Figure 4.5. The larger value of the storage modulus ( $G'$ ) compared to the loss modulus ( $G''$ ) in the strain sweep experiment at constant angular frequency, signifying the elastic nature of both organogels (**P1** and **P4**) and hydrogels (**P2**). The constant values of  $G'$  and  $G''$  in a frequency sweep experiments further support the stable organic and hydrogels from these peptides.

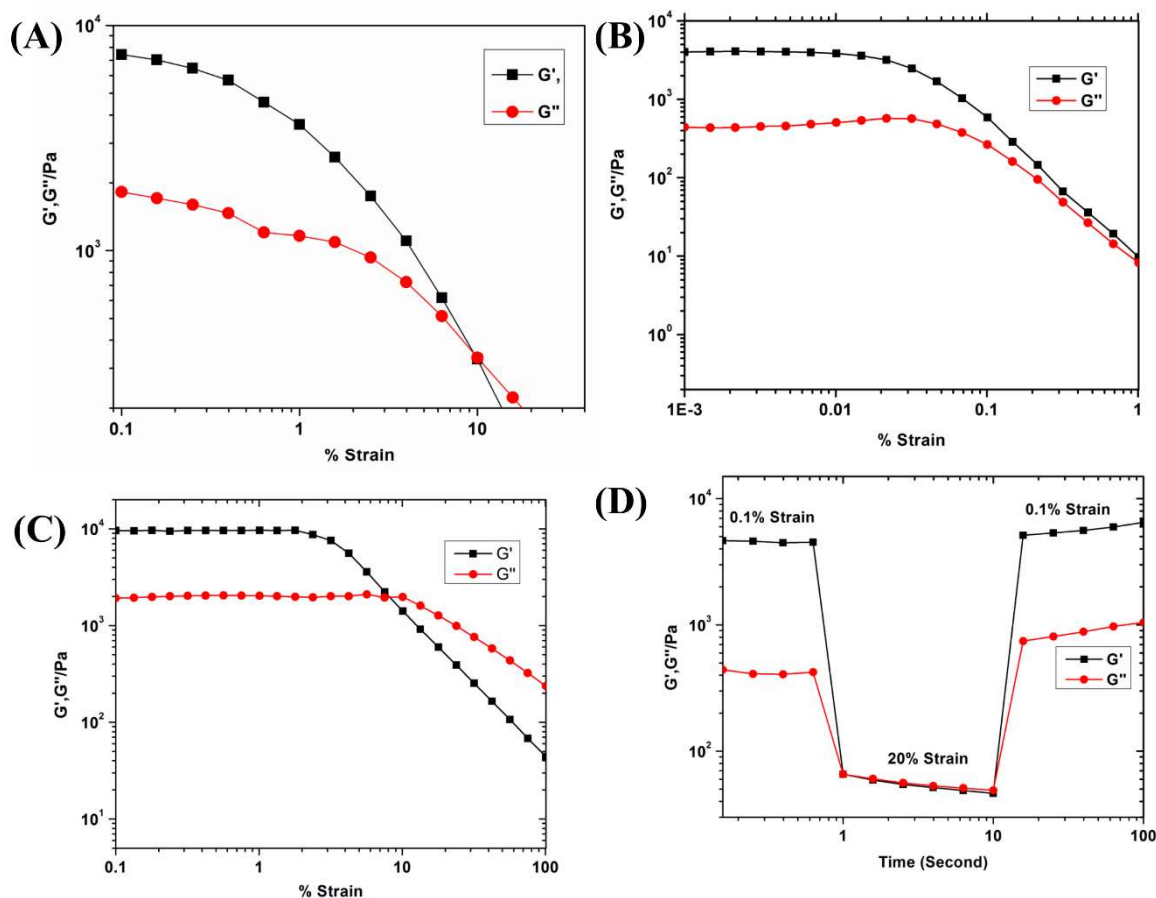


**Figure 4.5:** (A) Strain sweep rheological analysis of **P1**organogel in toluene (10 mg/mL) at constant angular frequency (1 rad/sec). (B) Strain sweep rheological analysis of the **P2**hydrogel in 1 ×PBS (10 mg/mL) at constant angular frequency (1 rad/Sec). (C) Strain sweep rheological analysis of **P4** organogel in toluene (10 mg/mL) at constant angular frequency (1 rad/Sec). (D) Step-strain rheology experiment of peptide **P2** hydrogel (10 mg/mL) at constant frequency (1rad/Sec).

#### 4.6.5. FT-IR Spectroscopy Study

Further, FT-IR spectroscopy was used to study the conformation of peptide **P1**, **P2** and **P4** in the xerogel state. The C=O stretching (amide I) and NH bending (amide II) frequencies around  $\sim 1650\text{ cm}^{-1}$  and  $\sim 1700\text{ cm}^{-1}$  respectively suggest the  $\beta$ -sheet character of peptides in the gel state.

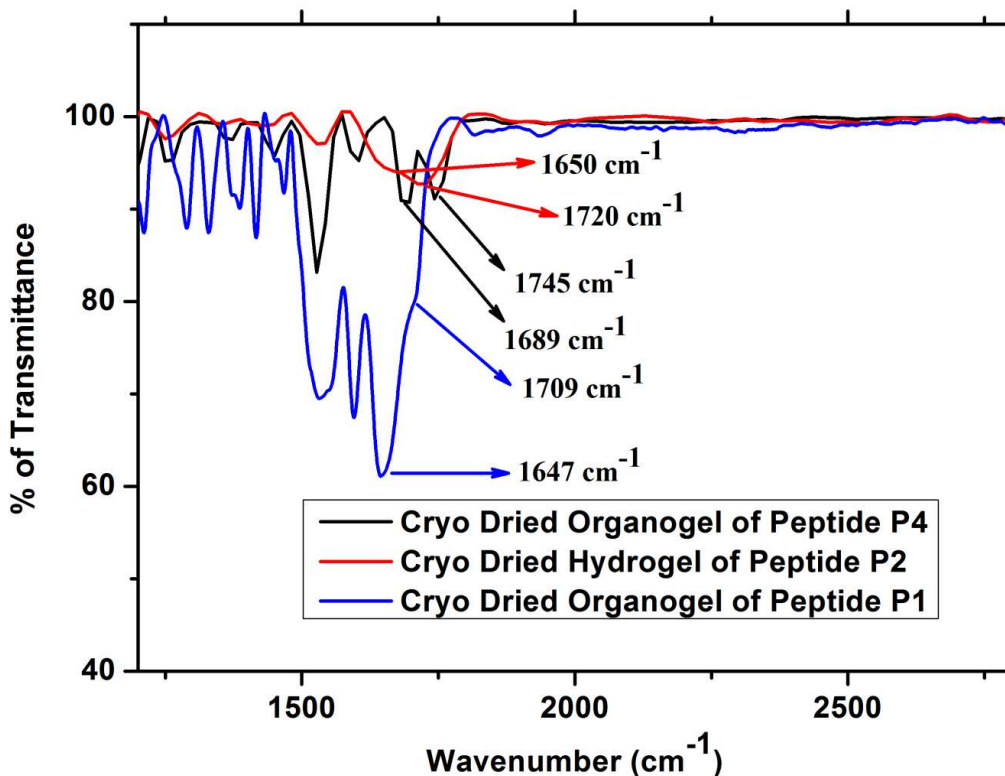


**Figure 4.6:** FT-IR spectra of the cryo dried gels from peptide **P1**, **P2** and **P4** at concentration of 10 mg/mL.

#### 4.6.7. Contact Angle Measurement

To gain more details in the hydrophobicity and hydrophilicity of the peptides **P1-P4**, we carried out the contact angle measurement experiment. Contact angle was measured by drop casting one drop of water on the surface of the solid samples. Image J software was used to calculate the contact angles. Results are shown in the Table 4.3. These results suggested that the peptide **P2** which has “O” atom in the backbone shows hydrophilic surface having contact angle value 45.17°. Other peptides show contact angle value more than 90° indicating the hydrophobic surface.

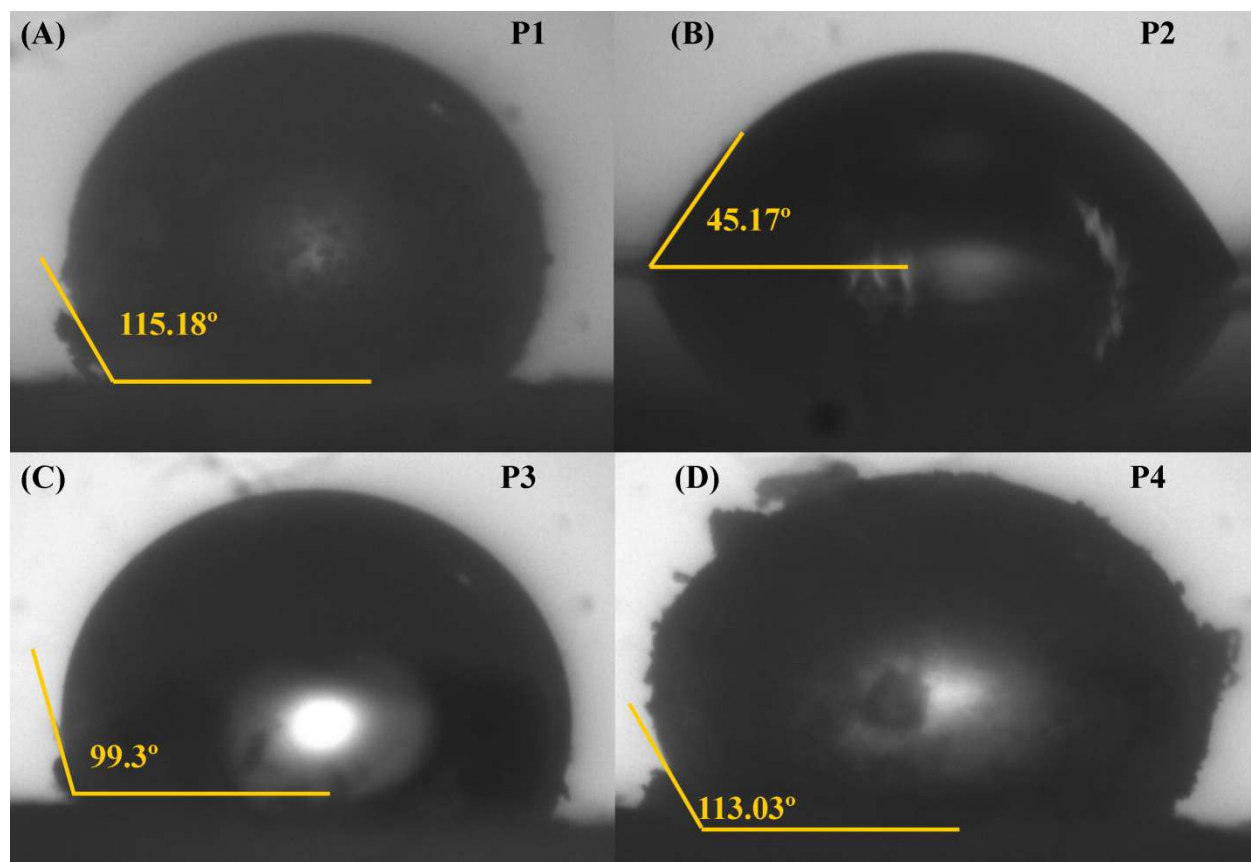


**Figure 4.7:** Contact angle measurement of the peptide (A) P1, (B) P2, (C) P3, (D) P4.

**Table 4.3:** Nature of the peptides P1-P4:<sup>44</sup>

Peptide	Contact Angle	Nature
P1	115.18°	Hydrophobic
P2	45.17 °	Hydrophilic
P3	99.3 °	Hydrophobic
P4	113.03 °	Hydrophobic
P5	Not Determined	Not Determined

#### 4.6.8. Stimuli Responsive Properties of Organo and Hydrogels

We further noticed that the organo gels of the peptides **P1** and **P4** and hydrogel of peptide **P2** were found to be external stimuli responsive. The transition from gel to sol can be achieved using either heat or mechanical shaking. Upon cooling and resting, the sol state slowly transformed into the gel state. By applying the mechanical strain, the hydrogel was transformed to sol and after removing the strain the sol slowly transformed again into the gel state. This thixotropic nature of the gels was further supported by the rheology experiments (Figure 8D). As these types of injectable hydrogels have been finding applications in the drug delivery, we have examined the potential of **P2** hydrogel as a drug delivery system. We encapsulated 500 $\mu$ L of 1mM proflavine solution in the gel matrix and 500  $\mu$ L of 1 $\times$  PBS was added on the top of the hydrogel matrix. Gradual increase in the intensity of the colour indicate the slow release of the dye from gel matrix to the solution.

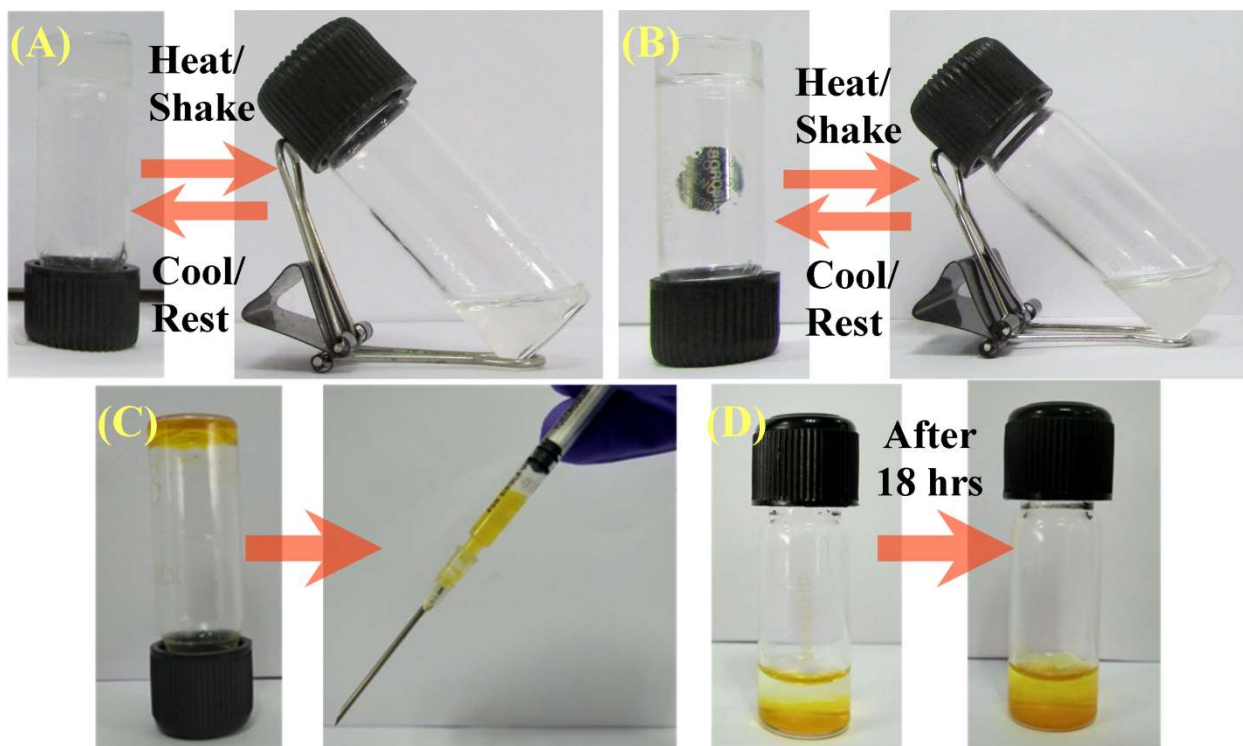


**Figure 4.8:** Stimuli responsive nature of the (A) organogel of peptide **P4** and (B) hydrogel of peptide **P2**. (C) Injectable nature of the hydrogel from peptide **P2**. (D) Slow release of the dye from hydrogel matrix to the 1 $\times$  PBS over about 18 h.

#### 4.6.9. Oil Spill Recovery by Organogel from Peptide P4

Inspired by the gelation of peptide **P4** in various aromatic solvents, we sought to investigate whether it can be used to selectively gelate the crude oil from the oil-water mixture. The large scale separation of oil from oil-water mixture has been one of the big challenges in worldwide due to the increasing release of oil contaminated waste water and marine oil spills to the seas which severely damage the marine eco-system.<sup>45</sup> There are numerous methods available for the oil-spill recovery, however peptide based amphiphiles attracted considerable attention in recent years in oil spill recovery.<sup>46</sup> Recently Basak *et al.* have demonstrated the oil spill recovery using

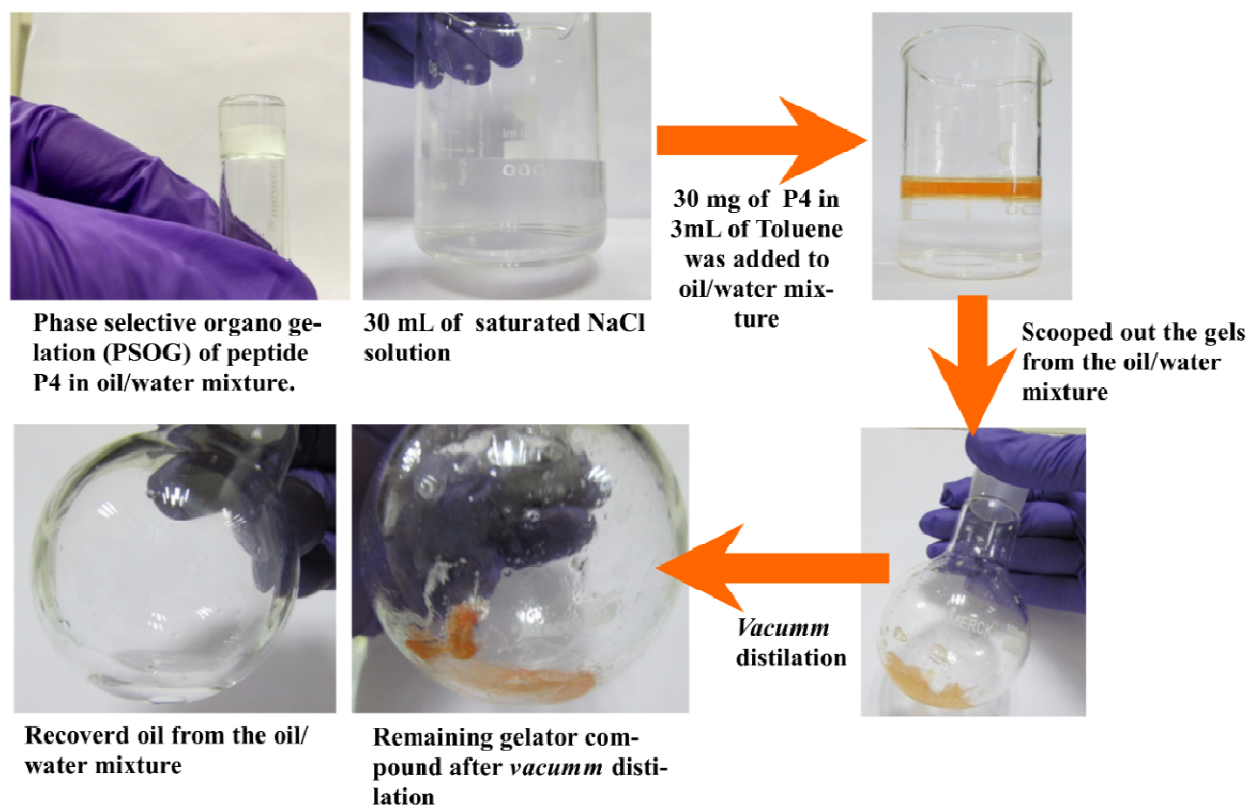


**Figure 4.9:** Phase selective gelation in oil/water mixture and oil spill recovery.

ethanolic solution of small peptides composed of aromatic amino acids.<sup>47</sup> The schematic process of oil spill recovery by the peptide **P4** is shown in the Figure 4.9. To understand the selective gelation of crude oil, the solution of peptide **P4** (30 mg in 3 mL) in toluene was added to the oil-water mixture composed of 10 mL of oil and 30 Ml of saturated NaCl solution. Instructively, upon treatment of the peptide solution, the oil transformed into gel in less than 5 min. The

peptide-oil gel was scooped out from the oil/water mixture and subjected for *vacuum* distillation. Through this process we have successfully recovered the oil from the oil-salt water mixture. Overall, the self-assembling nature of the dipeptide **P4** was found to be an excellent alternative for recovering the oil in oil spills.

#### 4.6.10. Biocompatibility Studies of the Peptide **P2** Hydrogel

As many thixotropic peptides based hydrogels have been using as a cell culture matrix, we sought to examine the biocompatibility of the peptide **P2** hydrogel and its utility as matrix in the 2D cell culture. To understand the biocompatibility, peptide gel was mixed with DMEM media at a ratio of 1:10 and the cells were grown over the gel matrix. We have examined biocompatibility of the **P2** hydrogel using both cancer cell line LN229 and normal cell line HEK293T. After 18h, the live cells were stained with calcein AM and imaged using fluorescence microscope. The difference in the growth of the cells over the gel matrix compared to the control experiment without peptide gel are shown in the Figure 4.10. These results suggest that hydrogel from  $\delta$ -peptide is biocompatible and this type of peptides can be used as matrix along with the culture media. As the  $\delta$ -amino acid can serve as a dipeptide mimetic, we have examined the proteolytic stability of peptide **P2** along with the control  $\alpha$ -dipeptide Boc-Phe-Phe-OH using the protease chymotrypsin. These results are shown in Figure 12. In contrast to  $\alpha$ -dipeptide, the HPLC analysis suggests that peptide **P2** was found to be stable to chymotrypsin.

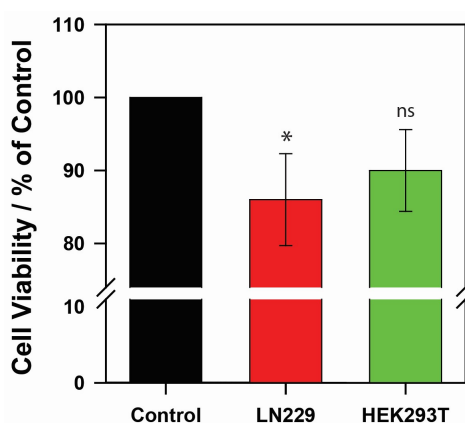


**Figure 4.10:** Effect of hydrogel from peptide **P2** on cell viability on cell lines LN229 and HEK293T.



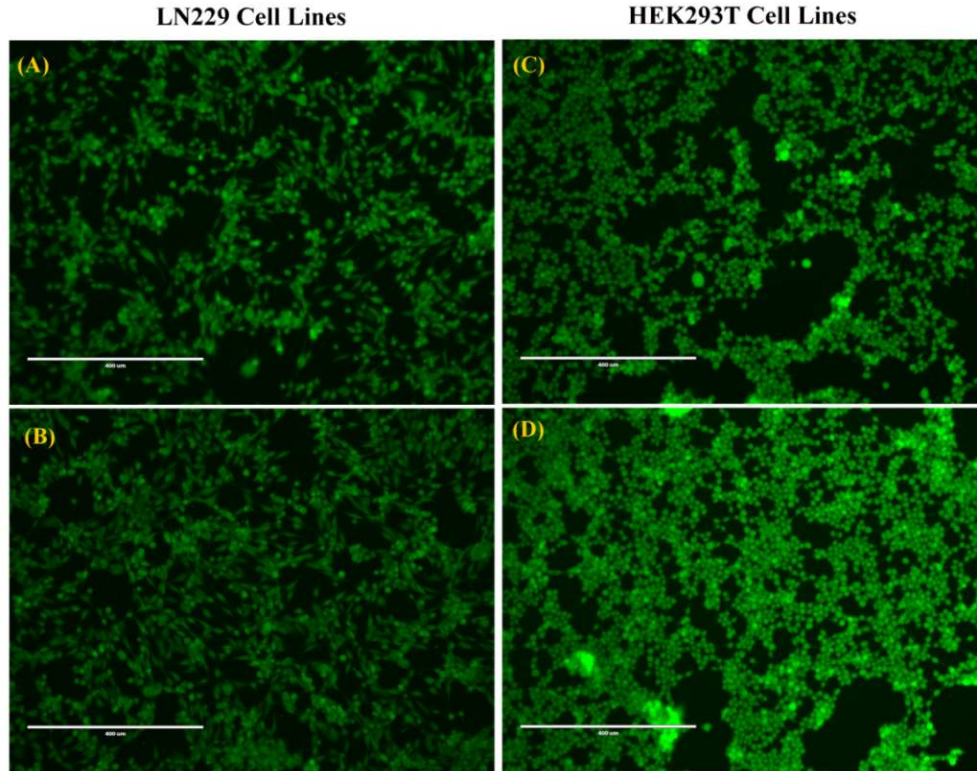


**Figure 4.11:** Growth of the cells over gel matrix after 18 h. (A) and (C) are the growth of the cells over gel matrix. (B) and (D) are the control experiment without any hydrogel. The viable cells are stained with calcein AM stain. (Scale bar for all images are 400  $\mu\text{m}$ )

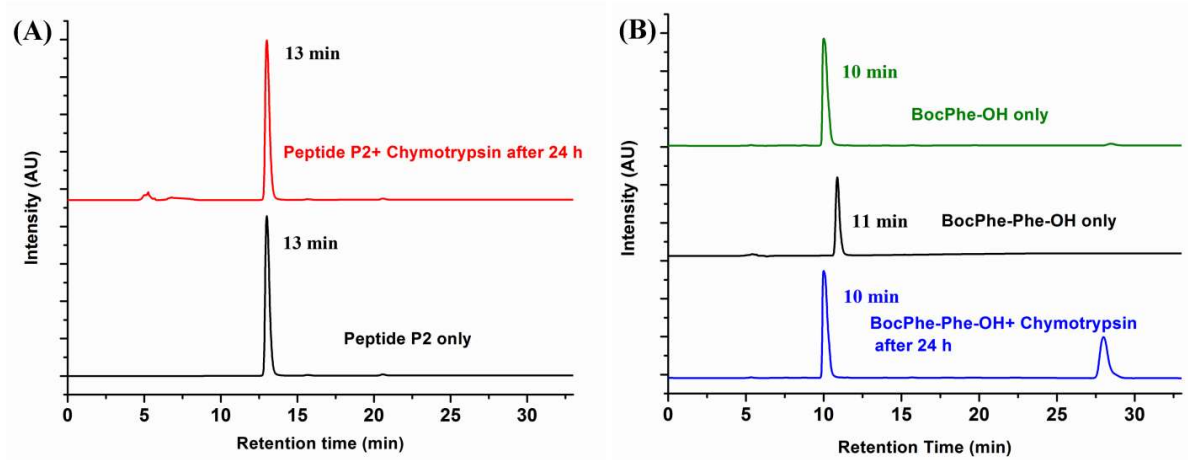


**Figure 4.12:** HPLC analysis depicting the stability of peptides (A) P2 and (B) control peptide Boc-Phe-Phe-OH against the protease chymotrypsin.

## 4.7. Conclusions

In conclusion, in this chapter, we have demonstrated the formation of self-assembled divergent gels from a new class of short peptides consisting of  $\delta$ -Phe. These  $\delta$ -amino acids may serve as surrogates of  $\alpha$ -dipeptide. The dipeptide (**P1**) composed of backbone homologated  $\delta^5$ -Phe was found to be insoluble in aqueous buffers, however gave stable gels in aromatic organic solvents. In contrast, the dipeptide composed  $\beta(\text{O})$ - $\delta^5$ -Phe showed remarkable, transparent, thixotropic hydrogels from the phosphate saline. Replacing backbone  $-\text{CH}_2-$  with “O” atom showed phenomenal change in their supramolecular gelation properties. The subtle change in the backbone leads to a drastic change in the molecular behavior of these peptides. Among the hybrid dipeptides **P3**, **P4** and **P5**, surprisingly only peptide **P4** ( $\beta^3/\beta(\text{O})$ - $\delta^5$ ) gave organogels in aromatic solvents. Further, we have demonstrated the utility of  $\beta^3/\beta(\text{O})$ - $\delta^5$ -hybrid peptide **P4** in the oil spill recovery through a phase selective gelation process. In addition, we have shown the potential applications of the dipeptide **P2** hydrogel as drug delivery system as well as matrix to grow the cells. Both **P2** and **P4** were found to be sensitive to the external heat as well as mechanical shaking. The biocompatibility, proteolytic stability and thixotropic nature of the new  $\delta$ -peptide may serve as potential alternatives to the existing peptide gels and it can be used as injectable and drug delivery agents. Overall, the study reported here can open new avenues for the design of biomaterials, injectable gels and drug delivery agents.

## 4.8. Experimental Section

### 4.8.1. Materials and Methods

All chemical and reagents including amino acids were purchased from commercial sources. Solvents ethyl acetate and petroleum ether (60–80 °C) were distilled before to use. Solvent tetrahydrofuran (THF) was dried by refluxing on sodium metal wire and distilled before to use. Silica gel 120–200 mesh was used to purify the protected amino acids and peptides in column chromatography. The  $^1\text{H}$  NMR spectra of protected amino acids and peptides were recorded on 400 MHz (or  $^{13}\text{C}$  on 100 MHz) in the solvent deuterated chloroform ( $\text{CDCl}_3$ ). The acid labile Boc and alkyl esters (ethyl or methyl esters) were used for the *N*- and *C*-terminus protections,

respectively. The Boc-(*S*)- $\beta^3$ -Phe was synthesized starting from Boc-Phe by the reported protocol.<sup>42</sup> The Boc-(*R*)- $\gamma^4$ -Phe was synthesized starting from Boc-(*S*)-Phe aldehyde through Wittig reaction followed by the reduction of double bonds using H<sub>2</sub>, Pd/C (10%). Finally, ethyl ester of Boc- $\gamma^4$ -Phe was subjected to saponification as reported earlier.<sup>38a</sup> The  $\beta$ (O)- $\delta^5$ -Phe was synthesized starting from Boc-protected amino alcohol using reported protocol.<sup>43</sup> The carbon analogous of  $\beta$ (O)- $\delta^5$ -Phe was synthesized from Boc-(*S*)- $\beta^3$ -Phe. All peptide couplings reactions were achieved using the coupling reagent *N*-ethyl-*N'*-(3-(dimethylaminopropyl)carbodiimide hydrochloride (EDC.HCl) and 1-hydroxybenzotriazole (HOBT) and *N,N*-diisopropylethylamine(DIEA). Finally, the pure peptides were characterized by <sup>1</sup>H and <sup>13</sup>C NMR spectroscopy and authenticated by high resolution mass spectroscopy (HRMS).

## 4.8.2. General Procedures for the Solution Phase Peptides (P1-P5) Synthesis

### 4.8.2.1. Synthesis of *N*-Boc- $\delta^5$ -Phe-OH

*N*-Boc- $\delta^5$ -Phe-OH was synthesized starting from *N*-Boc-(*S*)- $\beta^3$ -Phe-OH. Briefly, *N*-Boc-(*S*)- $\beta^3$ -Phe-Weinreb amide (1.6 gram, 5 mmol) was converted to aldehyde through the reduction of Weinreb amide using LAH (228 mg, 6 mmol) and subjected Wittig reaction to get *N*-Boc- $\alpha,\beta$ -unsaturated- $\delta^5$ -Phe-OEt. The Wittig product was purified using column chromatography by EtOAc/hexane solvent system. After that, the *N*-Boc- $\alpha,\beta$ -unsaturated- $\delta^5$ -Phe-OEt was reduced using H<sub>2</sub>/Pd-C to get *N*-Boc- $\delta^5$ -Phe-OEt. Further, the *N*-Boc- $\delta^5$ -Phe-OEt was subjected saponification using 1*N*NaOH in EtOH to obtain *N*-Boc- $\delta^5$ -Phe-OH and directly used for the peptides synthesis without purification.

### 4.8.2.2. Synthesis of *N*-Boc- $\beta$ (O)- $\delta^5$ -Phe-O<sup>t</sup>Bu

The *N*-Boc- $\beta$ (O)- $\delta$ -Phe was synthesized as reported earlier.<sup>43</sup> Briefly, *tetra*-butylammoniumhydrogensulfate (340 mg, 1 mmol) was dissolved in solution of sodium hydroxide (10 gram, 250 mmol in 10 mL of water and 15 mL of toluene). To this biphasic reaction mixture, *tert*-butylbromoacetate (2.2 mL, 15 mmol) was added slowly at room temperature. The reaction mixture was cooled to 0 °C, followed by slow addition of *N*-Boc-phenyl alanine alcohol (2.5 g, 10 mmol) in toluene (15 mL). The reaction was allowed to come

to room temperature and the stirring was continued for about 3 h. The organic phase was separated and aqueous phase. The aqueous solution was extracted with diethyl ether (30 mL ×2). The combined organic layer was washed with saturated sodium chloride solution (30 mL× 2), dried over anhydrous sodium sulfate and evaporated under reduced pressure. The crude product of *N*-Boc-β(O)-δ<sup>5</sup>-Phe-O<sup>t</sup>Bu was purified by column chromatography using EtOAc/hexane solvent system.

#### 4.8.2.3. Synthesis of Peptides P1-P5

All peptide (**P1-P5**) were synthesized through solution phase peptide chemistry as reported in the previous chapters.<sup>41</sup> In brief, 1 mmol of *N*-Boc-protected-amino acid was dissolved in 5 mL of DMF and the solution was cooled to 0 °C. Subsequently, 1mmol of 1EDC·HCl and 1mmol of HOBt and 2 mmol of DIEA were added reaction at 0 °C. Immediately, 1.1 mmol of methyl ester of amino acid to the reaction mixture and reaction was allowed to come to the room temperature. The reaction mixture was stirred for about 12 h. The reaction progress was monitored using TLC. After completion, 50 mL of ethyl acetate was added to the reaction mixture followed by 50 mL of saturated sodium chloride solution. The ethyl acetate layer was separated and the aqueous layer was extracted again with ethyl acetate (50mL ×3). The combined ethyl acetate layer was washed with 10% Na<sub>2</sub>CO<sub>3</sub> (20 mL× 3), 5% HCl (20 mL× 3 ), water (20 mL× 3), finally with saturated sodium chloride solution (30 mL× 2). The solution was dried over anhydrous sodium sulfate and evaporated under *vacuum* to obtain crude peptides. These crude peptides were purified using column chromatography with EtOAc/hexane solvent system. Finally, peptides were subjected to saponification in methanol solution using 1MNaOH. The peptide acids obtained after saponification were directly used gelation studies.

#### 4.8.3. Gelation Study of Peptides P1, P2 and P4

Peptides **P1** and **P4** (10 mg each) were placed in the separate sample vials. To each vial of peptides, 1 mL of toluene was added. The peptide solution in toluene was heated on a hot air gun to dissolve the peptides. The clear solution of peptides in toluene was cooled to room temperature and sonicated for about 10 min. The organo gelation property of peptide **P1** and **P4** was confirmed by the inverted sample vial experiment. For the hydrogelation, 10 mg of peptide

**P2** was dissolved in 1 mL of 1× PBS buffer at pH 7.4 and gently heated on a hot air gun to make it a clear solution and cooled to room temperature. Upon standing for about 12 h, the solution slowly transforms to gel state and the gelation property was further confirmed by the inverted sample vial experiment.

#### **4.8.4. Morphology Study of Peptide P1, P2 and P4**

FE-SEM experiment was carried out by drop casting 5 μL of gel on SiO<sub>2</sub>/Si substrate. The samples were dried at room temperature under *vacuum* and the samples on SiO<sub>2</sub>/Si substrate were again coated with gold. The images were taken using scanning electron microscope using tungsten filament as electron source operated at 10 kV.

#### **4.8.5. Rheology Experiment**

The rheology experiments were carried out on preformed gel samples of organogel (in toluene) and hydrogel (in 1× PBS) at a concentration of 10 mg/mL using rheometer. All experiments were carried out single time.

#### **4.8.6. Oil Spill Recovery Experiment**

Peptide **P4** shows phase selective gelation in hydrocarbon solvent. In a typical experiment the solution of peptide **P4** (30 mg in 3 mL) in toluene was added to the oil-water mixture composed of 10 mL of oil and 30 mL of saturated NaCl solution. To mimic the sea water saturated NaCl solution was used. Instructively, upon treatment of the peptide solution the oil transformed into gels in less than 5 min. The peptide-oil gel was scooped out from the oil/water mixture and subjected to *vacuum* distillation and the oil was recovered from the oil water mixture.

#### **4.8.7. Proteolytic Stability of Peptide P2**

Proteolytic stability of peptide **P2** was carried out using reported protocol.<sup>25</sup> The peptide **P2** (1 mM) was dissolved in 1 mL of HEPES buffer (pH 7.4) containing 5% DMSO. Then, 10 μL of 5 μM chymotrypsin enzyme was added to the peptide solution and incubated at 37 °C for about 24 h. After that, 50 μL from the above mentioned stock solution was injected in RP-HPLC. The

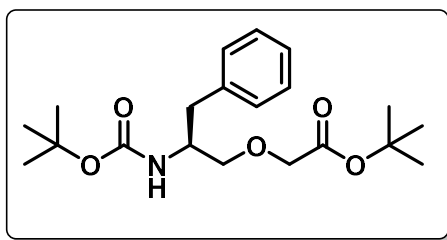
HPLC was carried out using ACN/H<sub>2</sub>O at flow rate of 1 mL/min. Same procedure was followed to understand the proteolytic stability of peptide Boc-Phe-Phe-OH.

#### 4.8.8. Effect of Hydrogel from Peptide P2 on Cell Viability

Cells were cultured in complete growth media (DMEM/F12) with 10% (v/v) (fetal bovine serum) FBS and 100 U/mL penicillin in humidified 5% (v/v) CO<sub>2</sub> at 37 °C. Gel was prepared by diluting peptide P2 dissolved in PBS to 10-fold using DMEM cell culture medium. This was coated on the 96-well cell culture plate and incubated further for about 3 h. Cells suspension in complete growth medium was pipetted into each well (pre-coated with gel) at a count of 10,000 cells/well. The plate was further incubated for 18 h at 37 °C under 5% of CO<sub>2</sub>. After 18 h of incubation complete growth media was removed and cells were washed with PBS. Cell viability assay was carried out after 18 h using calcein staining. Calcein AM stain at 2 μM final concentration was added to each cells and incubated for 45 min and then images were taken at 10× with fluorescence microscope. Experiments were performed as four independent replicates. The data represented in bar graph are further analyzed. Significance values indicated by \* for p < 0.05, ns ~ non-significant for p > 0.05; in comparison to the respective control cell samples.

#### 4.9. Characterization of Amino Acids and Peptides P1-P5

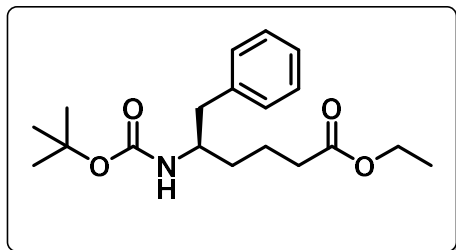
*N*-Boc-β(O)-δ<sup>5</sup>-Phe-O<sup>t</sup>Bu (*tert*-butyl(*S*)-2-(2-((*tert*-butoxycarbonyl)amino)-3 phenylpropoxy)acetate)



<sup>1</sup>H NMR (400 MHz, Chloroform-*d*) δ 7.30 – 7.18 (m, 5H), 5.17 (d, *J* = 8 Hz, 1H), 3.96 – 3.89 (m, 3H), 3.45 – 3.44 (m, 2H), 2.95 (dd, *J* = 6.8 Hz, 0H), 2.86 (dd, *J* = 12 Hz, 4 Hz, 1H), 2.86 (dd,

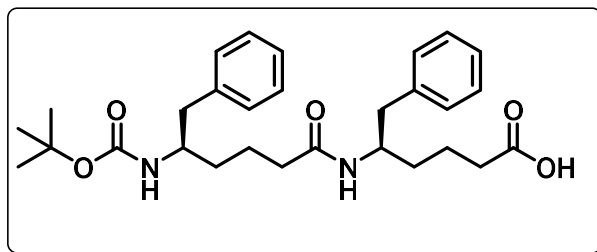
$J = 12$  Hz,  $8$  Hz,  $1$ H),  $1.48$  (s,  $9$ H),  $1.42$  (s,  $9$ H).  $^{13}\text{C}$  NMR (100 MHz, Chloroform- $d$ )  $\delta$  169.73, 155.58, 138.40, 129.60, 128.49, 126.40, 81.96, 79.28, 71.70, 69.07, 51.96, 37.81, 28.51, 28.24. HRMS  $m/z$  calculated value for  $\text{C}_{20}\text{H}_{31}\text{NO}_5$  is  $[\text{M}+\text{Na}^+]$  388.2100 and observed 388.2100.

***N*-Boc- $\delta^5$ -Phe-OEt (Ethyl (*R*)-5-((*tert*-butoxycarbonyl)amino)-6-phenylhexanoate**



$^1\text{H}$ NMR (400 MHz, Chloroform- $d$ )  $\delta$  7.30 – 7.26 (m,  $3$ H), 7.22 – 7.16 (m,  $2$ H), 4.35 (d,  $J = 8$  Hz,  $1$ H), 4.10 (q,  $J = 8$  Hz,  $2$ H), 3.82 (bs,  $1$ H), 2.83- 2.70 (m,  $J = 14.7$ ,  $6.4$  Hz,  $1$ H), 2.33 – 2.23 (m,  $2$ H), 1.68 – 1.49 (m,  $4$ H), 1.40 (s,  $9$ H), 1.23 (t,  $J = 8$  Hz,  $3$ H).  $^{13}\text{C}$ NMR (100 MHz, Chloroform- $d$ )  $\delta$  173.59, 155.61, 138.22, 129.60, 128.46, 126.44, 79.25, 60.41, 51.46, 41.53, 34.06, 33.60, 28.51, 21.58, 14.36. HRMS  $m/z$  calculated value for  $\text{C}_{19}\text{H}_{29}\text{NO}_4$  is  $[\text{M}+\text{Na}^+]$  358.1994 and observed 358.1988.

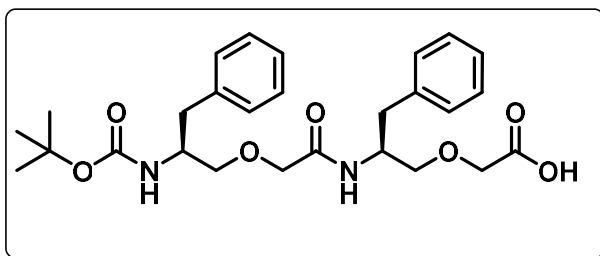
**Peptide P1 (((*R*)-5-((*R*)-5-((*tert*-butoxycarbonyl)amino)-6-phenylhexanamido)-6-phenylhexanoic acid)**



$^1\text{H}$  NMR (400 MHz, DMSO- $d_6$ )  $\delta$  11.96 (bs,  $1$ H), 7.58 (d,  $J = 8$  Hz,  $1$ H), 7.26 – 7.22 (m,  $5$ H), 7.17 – 7.14 (m,  $5$ H), 6.62 (d,  $J = 8$  Hz,  $1$ H), 3.91 – 3.84 (m,  $1$ H), 3.56 – 3.50 (m,  $1$ H), 2.64-2.57 (m,  $4$ H), 2.15 (q,  $J = 8$  Hz,  $2$ H), 1.95 (t,  $J = 8$  Hz,  $2$ H), 1.54 – 1.38 (m,  $8$ H), 1.31 (s,  $9$ H).  $^{13}\text{C}$

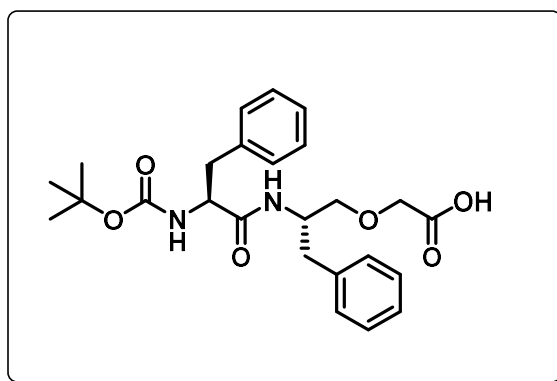
**NMR** (100 MHz, DMSO-*d*<sub>6</sub>)  $\delta$  174.32, 171.40, 155.21, 139.32, 139.07, 129.09, 127.99, 125.85, 125.76, 77.19, 51.45, 49.31, 40.81, 40.54, 35.41, 33.77, 33.48, 33.42, 28.26, 22.15, 21.14. **HRMS** *m/z* calculated value for C<sub>29</sub>H<sub>40</sub>N<sub>2</sub>O<sub>5</sub> is [M+Na<sup>+</sup>] 519.2835 and observed 519.2822.

**Peptide P2 ((6*S*,12*S*)-6,12-dibenzyl-2,2-dimethyl-4,10-dioxo-3,8,14-trioxa-5,11-diazahexadecan-16-oic acid)**



**<sup>1</sup>H NMR** (400 MHz, DMSO-*d*<sub>6</sub>)  $\delta$  7.58 (d, *J* = 8 Hz, 1H), 7.24 – 7.12 (m, 10 H), 6.82 (d, *J* = 8 Hz, 1H), 4.14 – 4.06 (m, 1H), 3.99 (s, 2H), 3.78 – 3.64 (m, 4H), 3.43 (d, *J* = 8 Hz, 2H), 2.86 (dd, *J* = 12 Hz, 4H, 2H), 2.76 – 2.69 (m, 2H), 2.63 – 2.58 (m, 1H), 1.29 (s, 9H). **<sup>13</sup>C NMR** (100 MHz, DMSO-*d*<sub>6</sub>)  $\delta$  171.75, 168.61, 155.14, 138.85, 138.63, 129.15, 128.12, 126.10, 125.98, 77.73, 72.32, 71.95, 70.00, 67.60, 51.33, 49.66, 36.94, 36.65, 28.25. **HRMS** *m/z* calculated value for C<sub>27</sub>H<sub>36</sub>N<sub>2</sub>O<sub>7</sub> is [M+H<sup>+</sup>] 501.2601 and observed 501.2603.

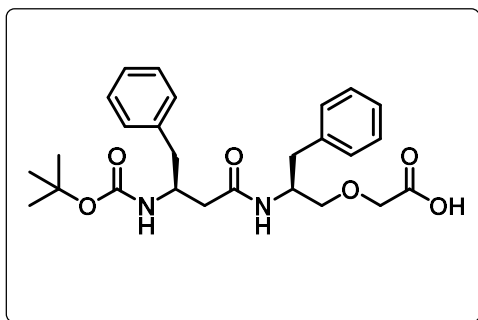
**Peptide P3 ((6*S*,9*S*)-6,9-dibenzyl-2,2-dimethyl-4,7-dioxo-3,11-dioxa-5,8-diazatridecan-13-oic acid)**





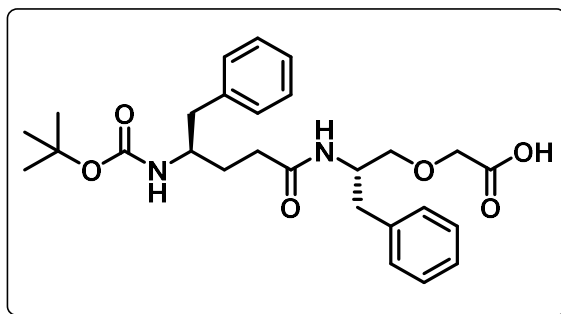
**<sup>1</sup>H NMR** (400 MHz, DMSO-*d*<sub>6</sub>) δ 7.85 (d, *J* = 8 Hz, 1H), 7.28 – 7.15 (m, 10H), 6.79 (d, *J* = 8 Hz, 1H), 4.11 – 4.08 (m, 1H), 4.00 (bs, 3H), 3.39-3.34 (m, 4H), 2.88-2.82 (m, 2H), 1.30 (s, 9H). **<sup>13</sup>C NMR** (100 MHz, DMSO-*d*<sub>6</sub>) δ 171.62, 171.17, 155.01, 138.58, 138.06, 129.18, 128.11, 127.95, 126.11, 126.02, 77.96, 71.75, 67.70, 55.79, 49.96, 37.73, 36.60, 28.12. **HRMS** *m/z* calculated value for C<sub>25</sub>H<sub>32</sub>N<sub>2</sub>O<sub>6</sub> is [M+H<sup>+</sup>] 457.2338 and observed 457.2346.

**Peptide P4 ((6*S*,10*S*)-6,10-dibenzyl-2,2-dimethyl-4,8-dioxo-3,12-dioxa-5,9-diazatetradecan-14-oic acid)**



**<sup>1</sup>H NMR** (400 MHz, DMSO-*d*<sub>6</sub>) δ 7.86 (d, *J* = 8 Hz, 1H), 7.25 – 7.06 (m, 10H), 6.59 (d, *J* = 8 Hz, 1H), 4.14 – 4.09 (m, 1H), 4.02 (s, 2H), 3.88 – 3.83 (m, 1H), 3.45 – 3.35 (m, 4H), 2.85 (dd, *J* = 16 Hz, 8 Hz, 1H), 2.64 (dd, *J* = 8 Hz, 4 Hz, 1H), 2.22 - 2.09 (m, 2H), 1.30 (s, 9H). **<sup>13</sup>C NMR** (100 MHz, DMSO-*d*<sub>6</sub>) δ 171.69, 169.62, 154.69, 138.92, 138.76, 129.16, 129.04, 128.04, 127.93, 125.95, 125.81, 77.42, 72.17, 67.76, 49.75, 49.22, 40.54, 36.74, 28.20. **HRMS** *m/z* calculated value for C<sub>26</sub>H<sub>34</sub>N<sub>2</sub>O<sub>6</sub> is [M+H<sup>+</sup>] 471.2495 and observed 471.2501.

**Peptide P5 ((6*R*,11*S*)-6,11-dibenzyl-2,2-dimethyl-4,9-dioxo-3,13-dioxa-5,10-diazapentadecan-15-oic acid)**



**<sup>1</sup>H NMR** (400 MHz, DMSO-*d*<sub>6</sub>) δ 12.66 (bs, 1H), 7.76 (d, *J* = 8 Hz, 1H), 7.28 – 7.13 (m, 10H), 6.66 (d, *J* = 8 Hz, 1H), 4.00 (bs, 3H), 3.55-3.50 (m, 1H), 3.42 – 3.26 (m, 1H), 2.82 (dd, *J* = 16 Hz, 4 Hz, 1H), 2.66 (bs, 1H), 2.08 – 1.95 (m, 2H), 1.59-1.40 (m, 2H), 1.32 (s, 9H). **<sup>13</sup>C NMR** (100 MHz, DMSO-*d*<sub>6</sub>) δ 171.68, 171.54, 155.22, 139.13, 138.81, 129.11, 129.06, 128.06, 128.01, 125.96, 125.83, 77.33, 72.08, 67.67, 51.49, 49.87, 40.59, 36.75, 32.45, 30.21, 28.25. **HRMS** *m/z* calculated value for C<sub>27</sub>H<sub>36</sub>N<sub>2</sub>O<sub>6</sub> is [M+H<sup>+</sup>] 485.2651 and observed 485.2660.

#### 4.10. References

1. Whitesides, G. M.; Mathias, J.; Seto, C. *Science* **1991**, *254*, 1312.
2. a) Zhang, S. *Nat. Biotechnol.* **2003**, *21*, 1171. b) Tseng, P.; Napier, B.; Zhao, S. W.; Mitropoulos, A. N.; Applegate, M. B.; Marelli, B.; Kaplan, D. L.; Omenetto, F. G. *Nat. Nanotechnol.* **2017**, *12*, 474. c) Chen, A.; Chatterjee, S. *Chem. Soc. Rev.* **2013**, *42*, 5425.
3. a) Douglas, S. M.; Dietz, H.; Liedl, T.; Högberg, B.; Graf, Franziska.; Shih, W. M. *Nature* **2009**, *459*, 414. b) Liu, Z.; Frasconi, M.; Lei, J.; Brown, Z. J.; Zhu, Z.; Cao, D.; Lehl, J.; Liu, G.; Fahrenbach, A. C.; Botros, Y. Y.; Farha, O. K.; Hupp, J. T.; Mirkin, C. A.; Stoddart, J. F. *Nat. Commun.* **2013**, *4*, 1855. c) Gazit, E. *Chem. Soc. Rev.* **2007**, *36*, 1263. d) Petka, W. A.; Harden, J. L.; MaGrath, K. P.; Wirtz, D.; Tirrell, D. A. *Science* **1998**, *281*, 389.
4. Chakraborty, P.; Gazit, E. *ChemNanoMat.* **2018**, *4*, 730.
5. a) Spicer, C. D.; Jumeaux, C.; Gupta, Bakul.; Stevens, M. M. *Chem. Soc. Rev.* **2018**, *47*, 3574. b) Gazit, E. *Annu. Rev. Biochem.* **2018**, *87*, 533. c) Habibi, N.; Kamaly, N.; Memicc, A.; Shafiee, H. *Nano Today* **2016**, *11*, 41.
6. Rechtes, M.; Gazit, E. *Science* **2003**, *300*, 625.
7. a) Gao, X.; Matsui, H. *Adv. Mater.* **2005**, *17*, 2037. b) Adler-Abramovich, L.; Gazit, E. *Chem. Soc. Rev.* **2014**, *43*, 6881. c) Tao, K.; Makam, P.; Aizen, R.; Gazit, E. *Science* **2017**, *358*, eaam9756. d) Schnaider, L.; Brahmachari, S.; Schmidt, N. W.; Mensa, B.; Shaham-Niv, S.; Bychenko, D.; Adler-Abramovich, L.; Shimon, L. J. W.; Kolusheva, S.; DeGrado, W. F.; Gazit, E. *Nat. Commun.* **2017**, *8*, 1365
8. a) Mahler, A.; Rechtes, M.; Rechter, M.; Cohen, S.; Gazit, E. *Adv. Mater.* **2006**, *18*, 1365.
9. Adler-Abramovich, L.; Gazit, E. *Chem. Soc. Rev.* **2014**, *43*, 6881.

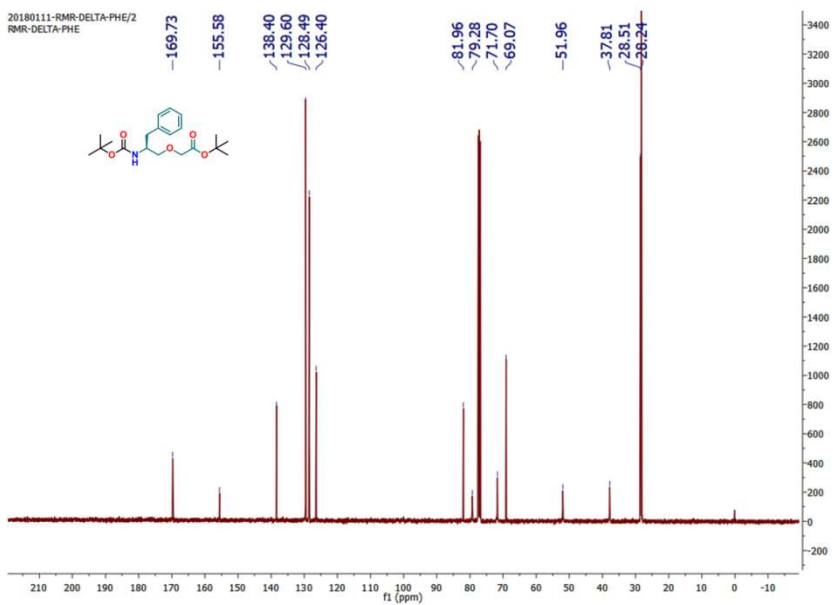
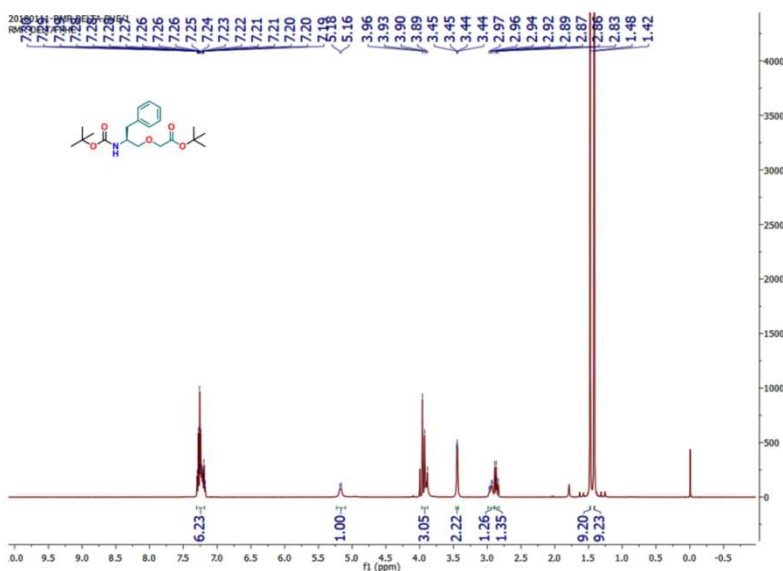
10. Ulijn, R. V.; Smith, A. M. *Chem. Soc. Rev.* **2008**, *37*, 664.
11. Ghadiri, M. R.; Granja, J. R.; Milligan, R. A.; McRee, D. E.; Khazanovich, N. *Nature* **1993**, *366*, 324.
12. a) Ghadiri, M. R.; Granja, J. R.; Buehler, L. K. *Nature* **1994**, *369*, 301. b) Fernandez-Lopez, S.; Kim, H.-S.; Choi, E. C.; Delgado, M.; Granja, J. R.; Khasanov, A.; Kraehenbuehl, K.; Long, G.; Weinberger, D. A.; Wilcoxon, K. M.; Ghadiri, M. R. *Nature* **2001**, *412*, 452.
13. a) Hauser, C. A. E.; Zhang, S. *Nature*, **2010**, *468*, 516. b) Zhang, S. *Nat. Biotechnol.* **2003**, *21*, 1171.
14. Ikezoe, Y.; Washino, G.; Uemura, T.; Kitagawa, S.; Matsui, H. *Nat. Mater.* **2012**, *11*, 1081.
15. a) Aida, T.; Meijer, E.W.; Stupp, S. I. *Science*, **2012**, *335*, 813. b) Hartgerink, J. D.; Beniash, E.; Stupp, S. I. *Science* **2001**, *294*, 1684. c) Hartgerink, J. D.; Beniash, E.; Stupp, S. I. *Proc. Natl. Acad. Sci. USA.* **2002**, *99*, 5133. d) Cui, H.; Webber, M. J.; Stupp, S. I. *Biopolymers* **2010**, *94*, 1.
16. Tao, K.; Makam, P.; Aizen, R.; Gazit, E. *Science* **2017**, *358*, eaam9756.
17. a) Kim, J. H.; Lee, M.; Lee, J. S.; Park, C. B. *Angew. Chem. Int. Ed.* **2012**, *51*, 517. b) Lee, J. S.; Yoon, I.; Kim, J.; Ihee, H.; Kim, B.; Park, C. B. *Angew. Chem. Int. Ed.* **2011**, *50*, 1164
18. Heredia, A.; Bdikin, I.; Kopyl, S.; Mishina, E.; Semin, S.; Sigov, A.; German, K.; Bystrov, V.; Gracio, J.; Kholkin, A. L. *J. Phys. D.* **2010**, *43*, 462001.
19. Gan, Z.; Wu, X.; Zhu, X.; Shen, J. *Angew. Chem. Int. Ed.* **2013**, *52*, 2055.
20. Yemini, M.; Reches, M.; Rishpon, J.; Gazit, E. *Nano Lett.* **2005**, *5*, 183.
21. Kholkin, A.; Amdursky, N.; Bdikin, I.; Gazit, E.; Rosenman, G. *ACS Nano* **2010**, *4*, 610.
22. Gazit, E. *Chem. Soc. Rev.* **2007**, *36*, 1263.
23. a) Gao, X.; Matsui, H. *Adv. Mater.* **2005**, *17*, 2037. b) Yan, X.; Zhu, P.; Li, J. *Chem. Soc. Rev.* **2010**, *39*, 1877. c) Adler-Abramovich, L.; Gazit, E. *Chem. Soc. Rev.* **2014**, *43*, 6881.
24. Jayawarna, V.; Ali, M.; Jowitt, T. A.; Miller, A. F.; Saiani, A.; Gough, J. E.; Ulijn, R. V. *Adv. Mater.* **2006**, *18*, 611-614.
25. Baral, A.; Roy, S.; Ghosh, S.; Hermida-Merino, D.; Hamley, I. W.; Banerjee, A. *Langmuir* **2016**, *32*, 1836.
26. Baral, A.; Roy, S.; Dehsorkhi, A.; Hamley, I. W.; Mohapatra, S.; Ghosh, S.; Banerjee, A. *Langmuir* **2014**, *30*, 929.

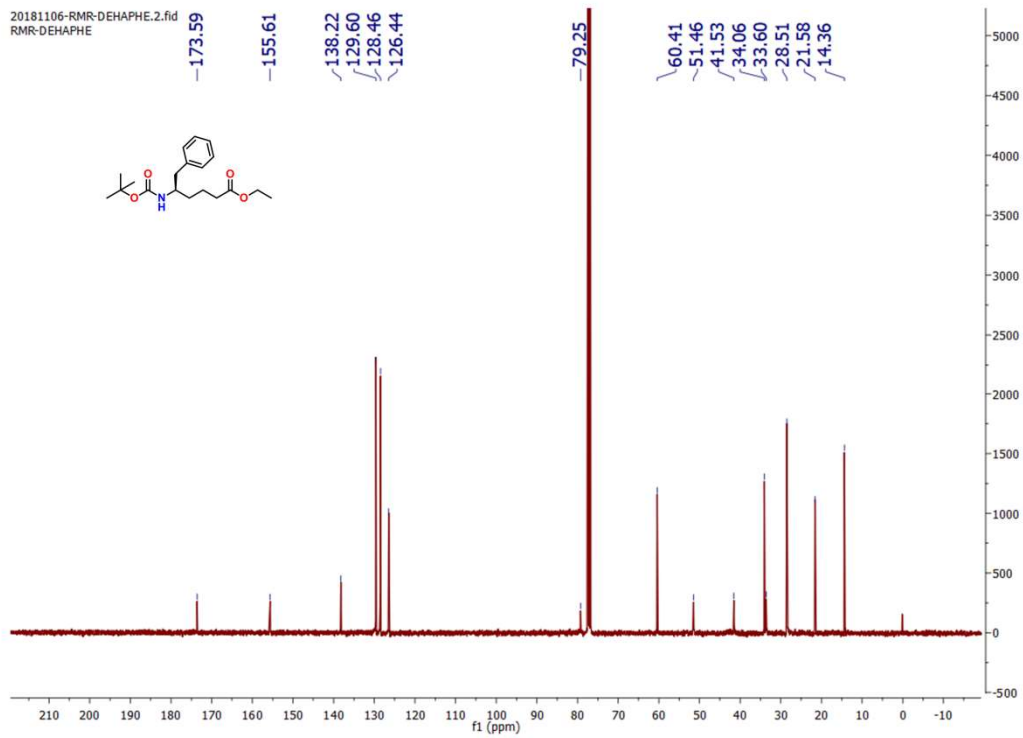
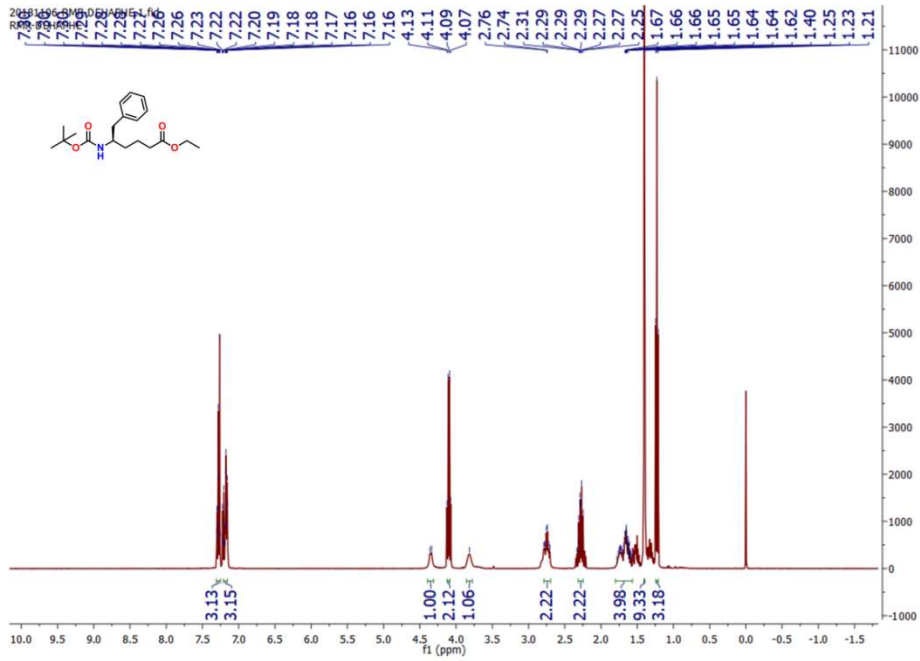
27. Nalluri, S. K. M.; Shivarova, N.; Kanibolotsky, A. L.; Zelzer, M.; Gupta, S.; Frederix, P. W. J. M.; Skabara, P. J.; Gleskova, H.; Ulijn, R. V. *Langmuir*, **2014**, *30*, 12429.
28. a) Rúa, F.; Boussert, S.; Parella, T.; Díez-Pérez, I.; Branchadell, V.; Giralt, E.; Ortuño, R. M. *Org. Lett.* **2007**, *9*, 3643. b) Dinesh, B.; Squillaci, M. A.; Ménard-Moyon, C.; Samorì, P.; Bianco, A. *Nanoscale* **2015**, *7*, 15873.
29. Gellman, S. H. *Acc. Chem. Res.* **1998**, *31*, 173.
30. a) Yoo, S. H.; Lee, H. S. *Acc. Chem. Res.* **2017**, *50*, 832. b) Kwon, S.; Kim, B. J.; Lim, H. K.; Kang, K.; Yoo, S. H.; Gong, J.; Yoon, E.; Lee, J.; Choi, I. S.; Kim, H.; Lee, H. S. *Nat. Commun.* **2015**, *6*, 8747. c) Misra, R.; Reja, R. M.; Narendra, L. V.; George, G.; Raghothama, S.; Gopi, H. N. *Chem. Commun.* **2016**, *52*, 9597.
31. Yang, Z.; Lianga, G.; Xu, B. *Chem. Commun.* **2006**, 738.
32. Castelletto, V.; Chengz, G.; Hamley, I. W. *Chem. Commun.* **2011**, *47*, 12470.
33. Malhotra, K.; Shankar, S.; Rai, R.; Singh, Y. *Biomacromolecules* **2018**, *19*, 782.
34. Panda, J. J.; Mishra, A.; Basu, A.; Chauhan, V. S. *Biomacromolecules* **2008**, *9*, 2244.
35. Pellach, M.; Mondal, S.; Shimon, L. J. W.; Adler-Abramovich, L.; Buzhansky, L.; Gazit, E. *Chem. Mater.* **2016**, *28*, 4341.
36. Celis, S.; Nolis, P.; Illa, O.; Branchadell, V.; Ortuno, R. M. *Org. Biomol. Chem.* **2013**, *11*, 2839.
37. McDougall, L.; Draper, E. R.; Beadle, J. D.; Shipman, M.; Raubo, P.; Jamieson, A. G.; Adams, D. J. *Chem. Commun.* **2018**, *54*, 1793-1796.
38. a) Jadhav, S. V.; Misra, R.; Singh, S. K.; Gopi, H. N. *Chem. -Eur. J.* **2013**, *19*, 16256. b) Jadhav, S. V.; Gopi, H. N. *Chem. Commun.* **2013**, *49*, 9179.
39. Baldauf, C.; Gunther, R.; Hofmann, H.-J. *J. Org. Chem.* **2004**, *69*, 6214.
40. a) Chakraborty, T. K.; Arora, A.; Roy, S.; Kumar, N.; Maiti, S. *J. Med. Chem.* **2007**, *50*, 5539. b) Sharma, G. V. M.; Babu, B. S.; Ramakrishna, K. V. S.; Nagendar, P.; Kunwar, A. C.; Schramm, P.; Baldauf, C.; Hofmann, H.-J. *Chem. Eur. J.* **2009**, *15*, 5552. c) Jiang, H.; Le'ger, J. M.; Huc, I. *J. Am. Chem. Soc.* **2003**, *125*, 3448. d) Banerjee, A.; Pramanik, A.; Bhattacharjya, S.; Balaram, P. *Biopolymers* **1996**, *39*, 769. e) Siriwardena, A.; Pulukuri, K. K.; Kandiyal, P. S.; Roy, S.; Bande, O.; Ghosh, S.; Fernandez, J. M. G.; Martin, F. A.; Ghigo, J.-M.; Beloin, C.; Ito, K.; Woods, R. J.; Ampapathi, R. S.; Chakraborty, T. K. *Angew. Chem. Int. Ed.* **2013**, *52*, 10221.

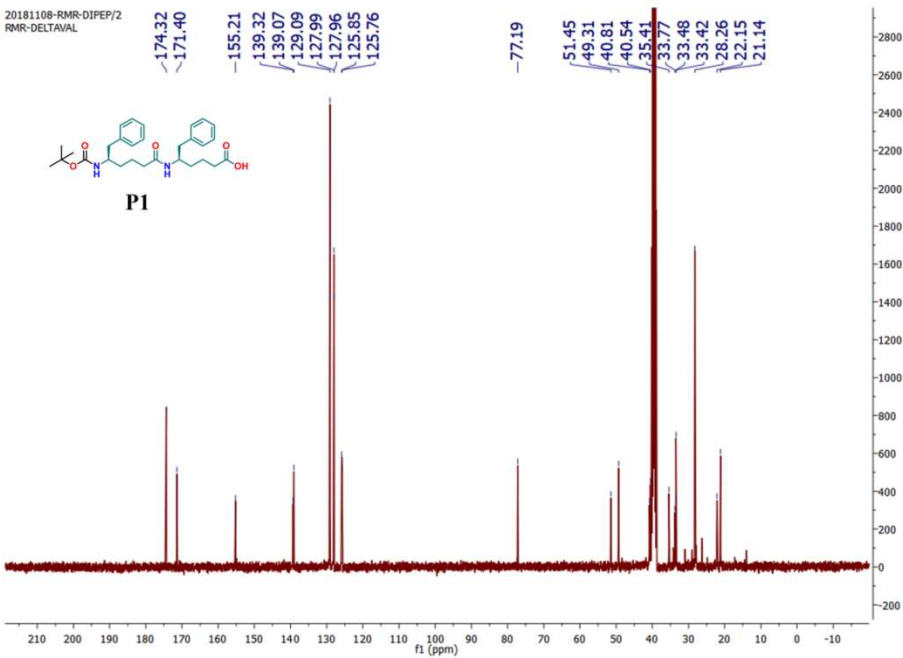
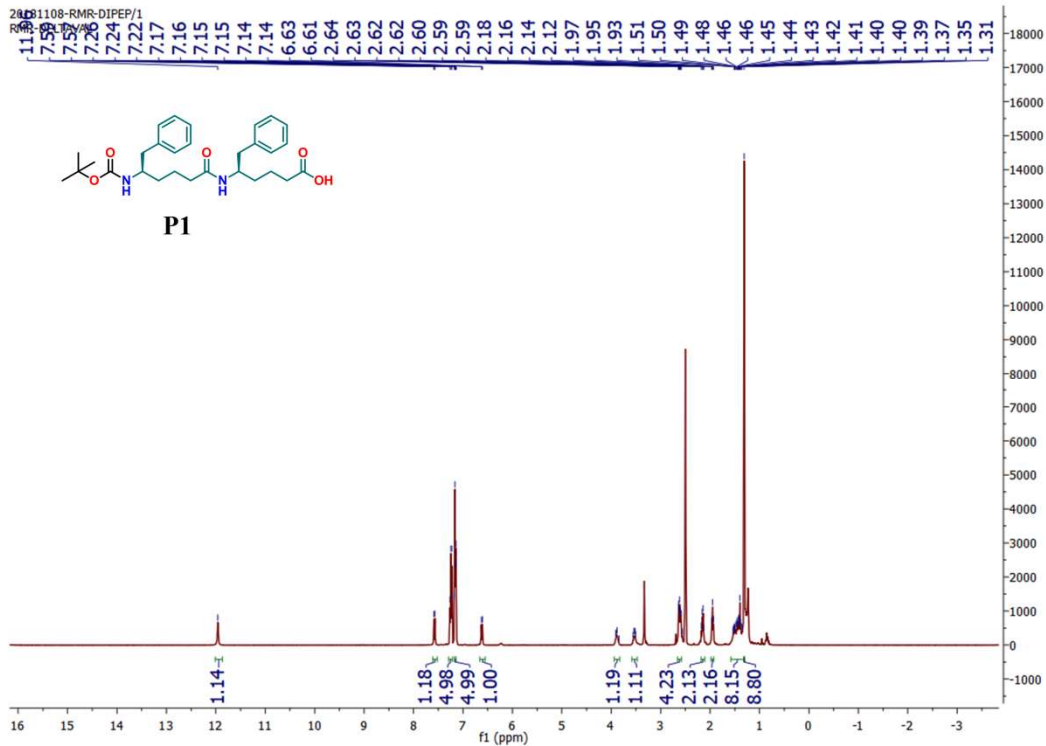
41. Misra, R.; Sharma, A.; Shiras, A.; Gopi, H. N. *Langmuir* **2017**, *33*, 7762.
42. Seebach, D.; Overhand, M.; Kühnle, F. N. M.; Martinoni, B.; Oberer, L.; Hommel, U.; Widmer, H. *Helv. Chim. Acta* **1996**, *79*, 913.
43. Yusof, Y.; Tan, D. T. C.; Arjomandi, O. K.; Schenk, G.; McGeary, R. P. *Bioorg. Med. Chem. Lett.* **2016**, *26*, 1589.
44. a) Law, K. W. *J. Phys. Chem. Lett.* **2014**, *5*, 686. b) Gao, L.; McCarthy, T. J. *Langmuir* **2008**, *24*, 9183.
45. a) Lessard, R. R.; Demarco, G. *Spill Sci. Technol. Bull.* **2000**, *6*, 59. b) Yuan, J.; Liu, X.; Akbulut, O.; Hu, J.; Suib, S. L.; Kong, J.; Stellacci, F. *Nat. Nanotechnol.* **2008**, *3*, 332.
46. Bhattacharya, S.; Krishnan-Ghosh, Y. *Chem. Commun.* **2001**, 185.
47. Basak, S.; Nanda, J.; Banerjee, A. *J. Mater. Chem.* **2012**, *22*, 11658.

## 4.11. Appendix IV: Characterization Data of Synthesized Amino Acids and Peptides P1-P5

### 4.11.1. $^1\text{H}$ and $^{13}\text{C}$ NMR Spectra

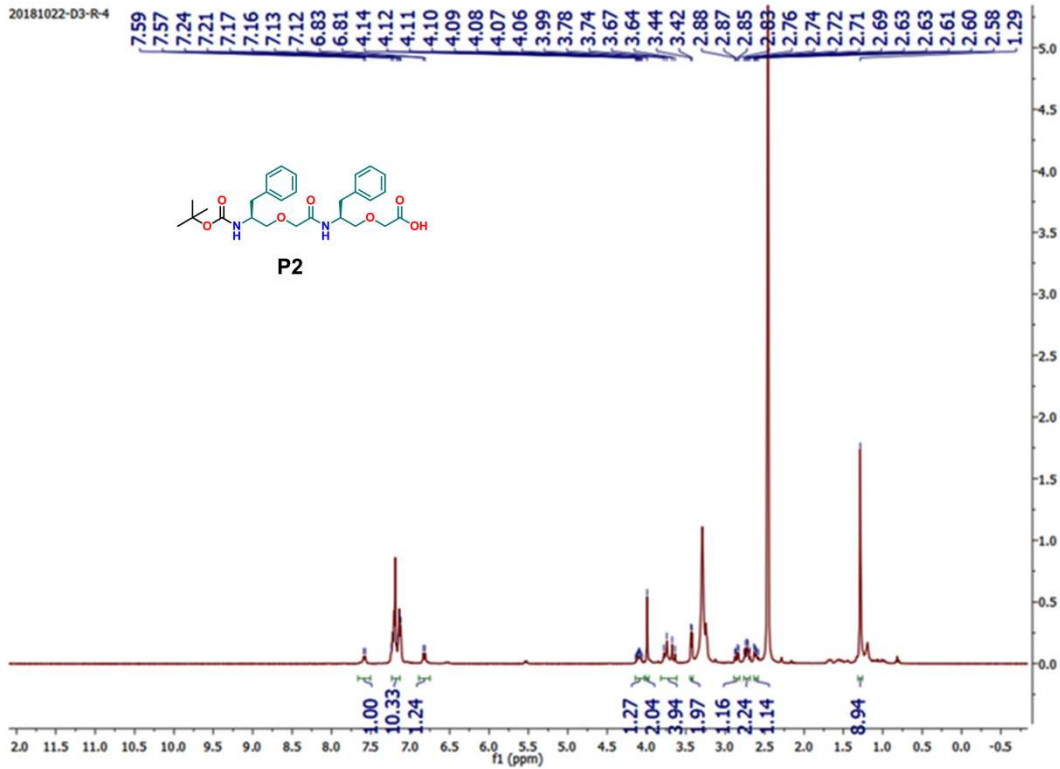




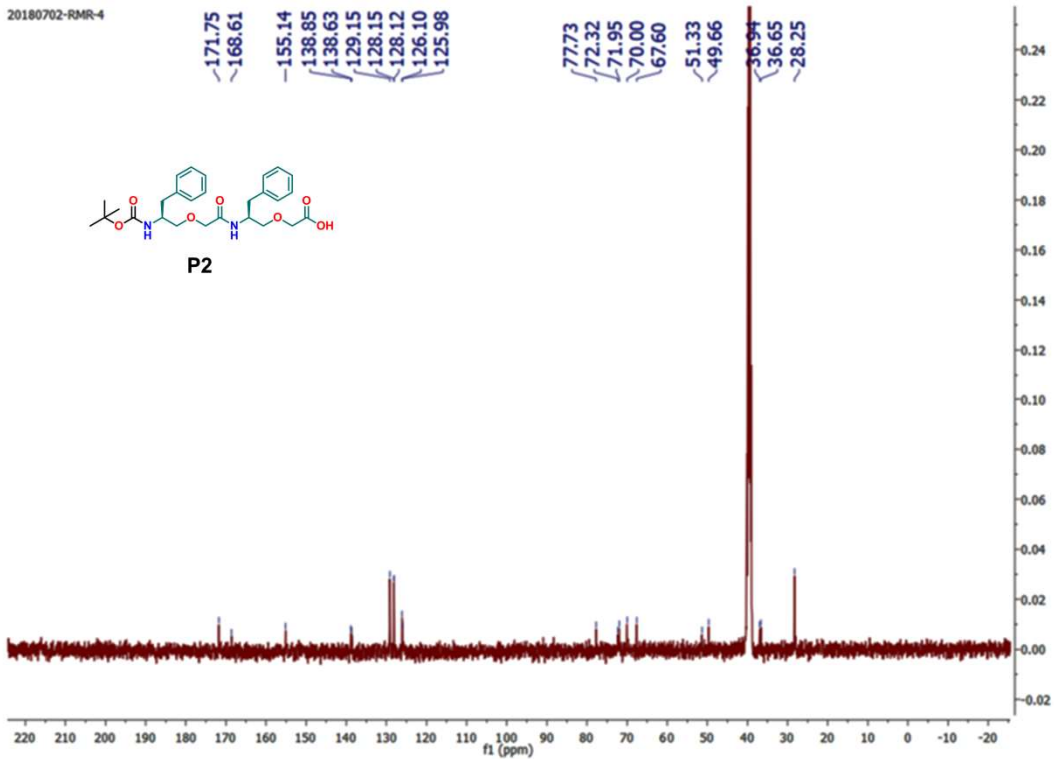


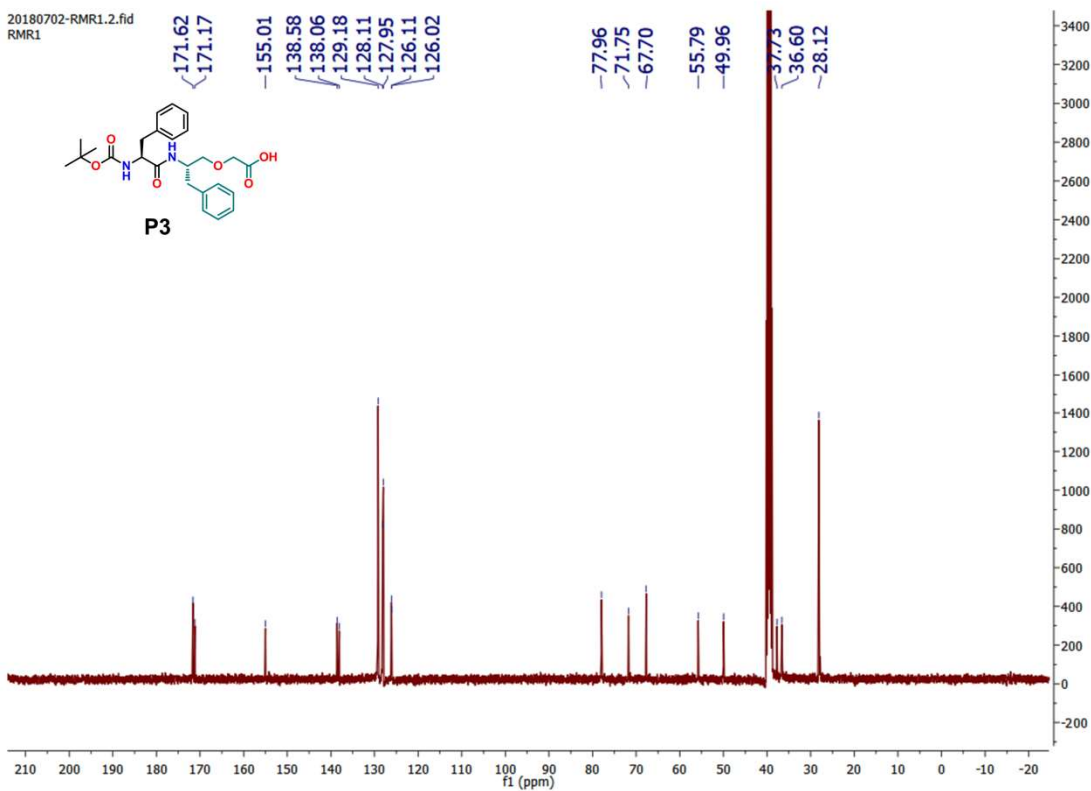
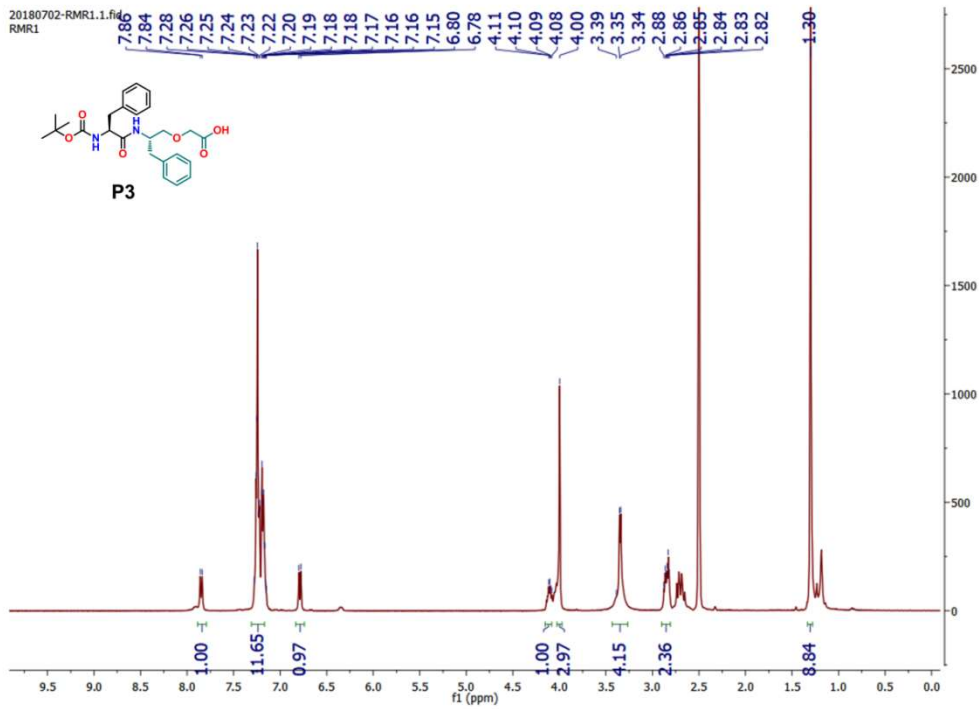


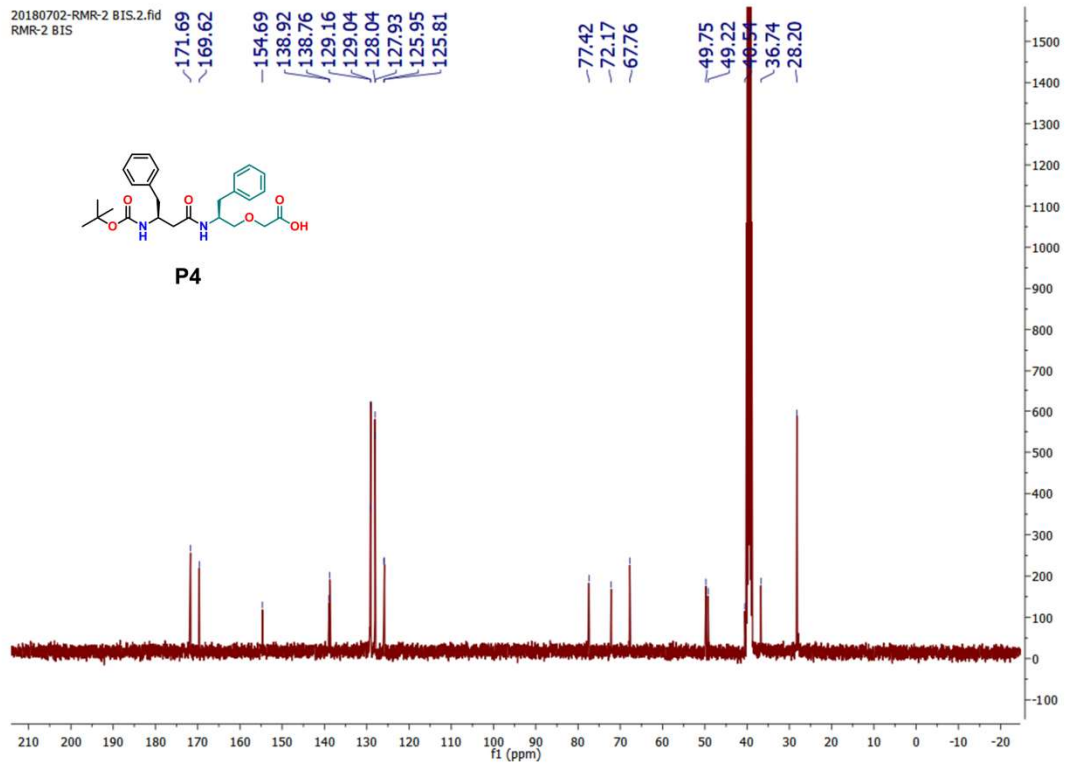
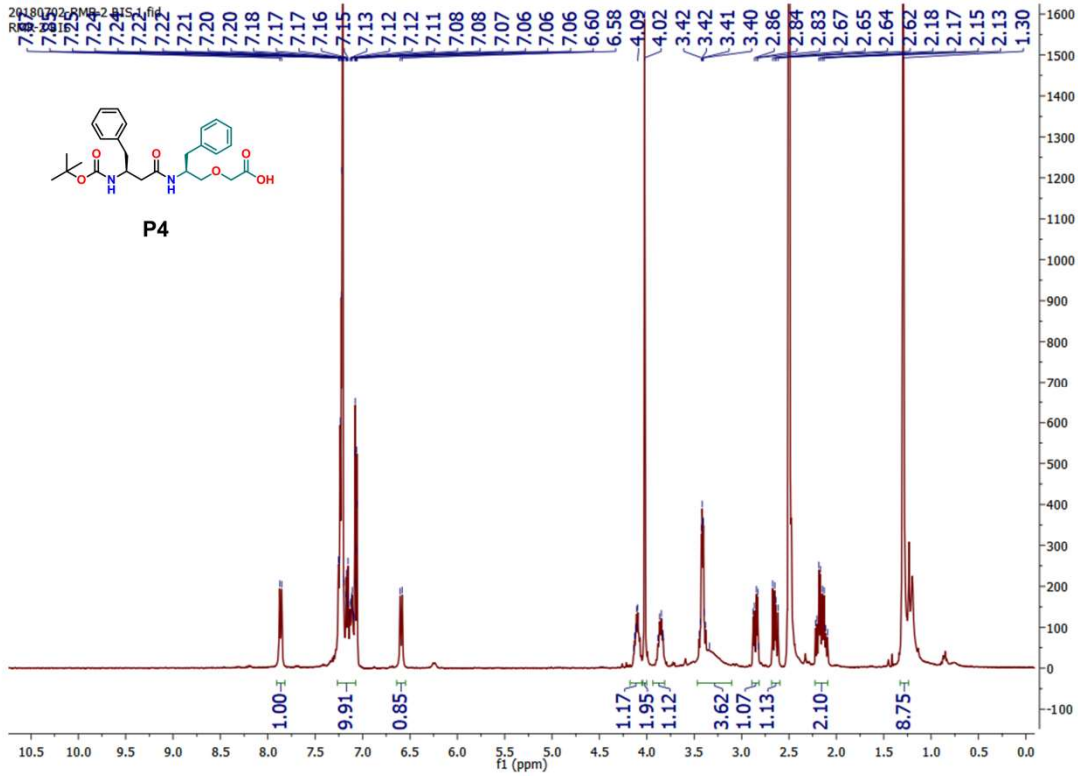
20181022-03-R-4



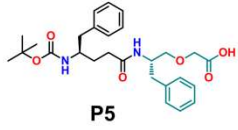
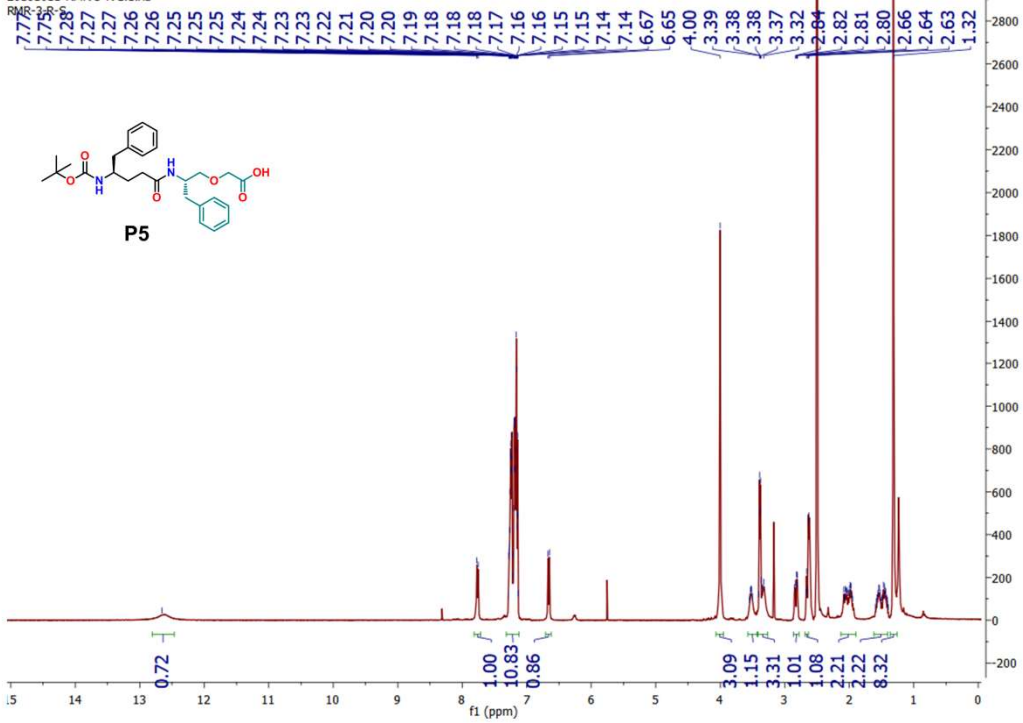
20180702-RMR-4



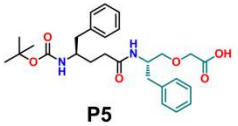
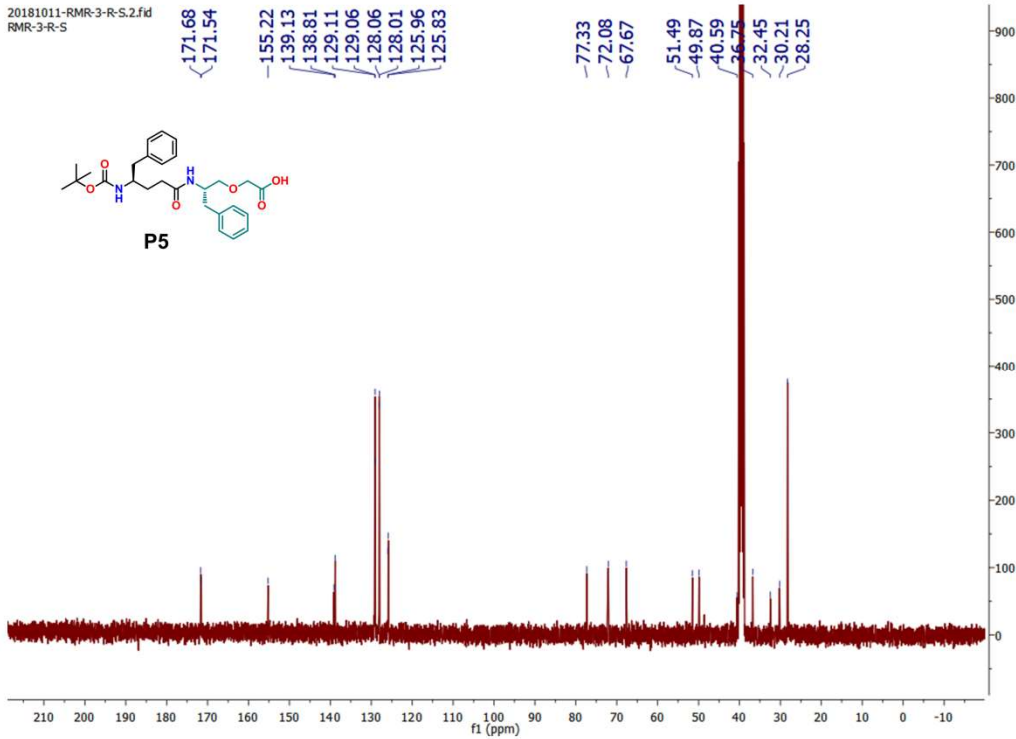




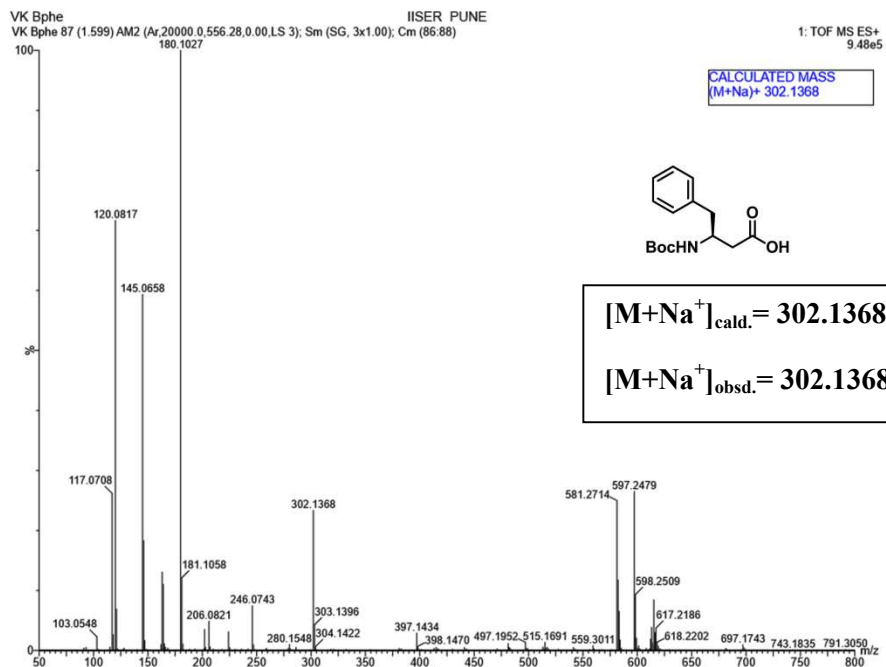
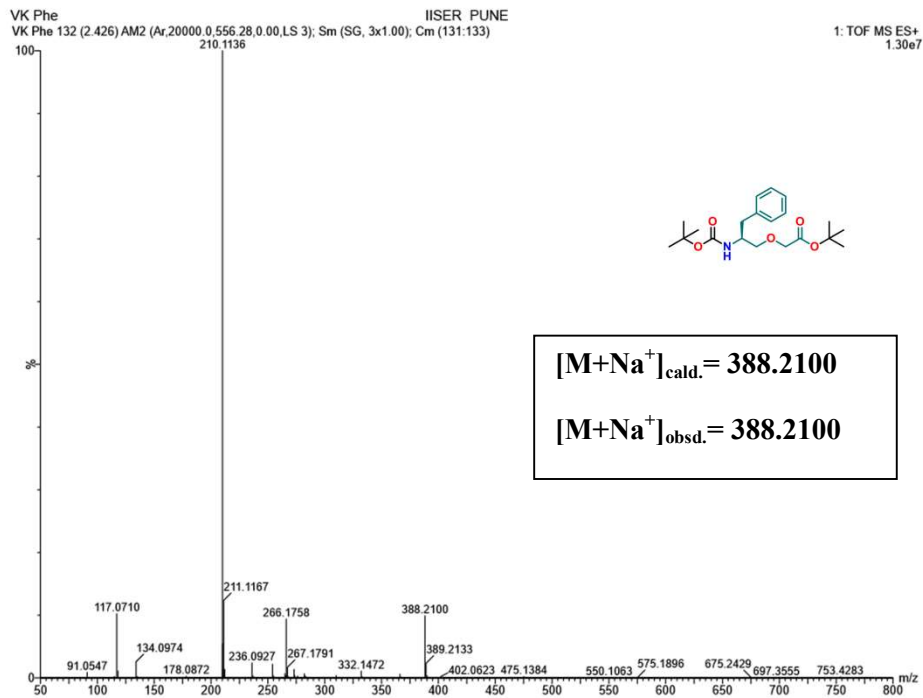
20181011-RMR-3-R-S.1.fid



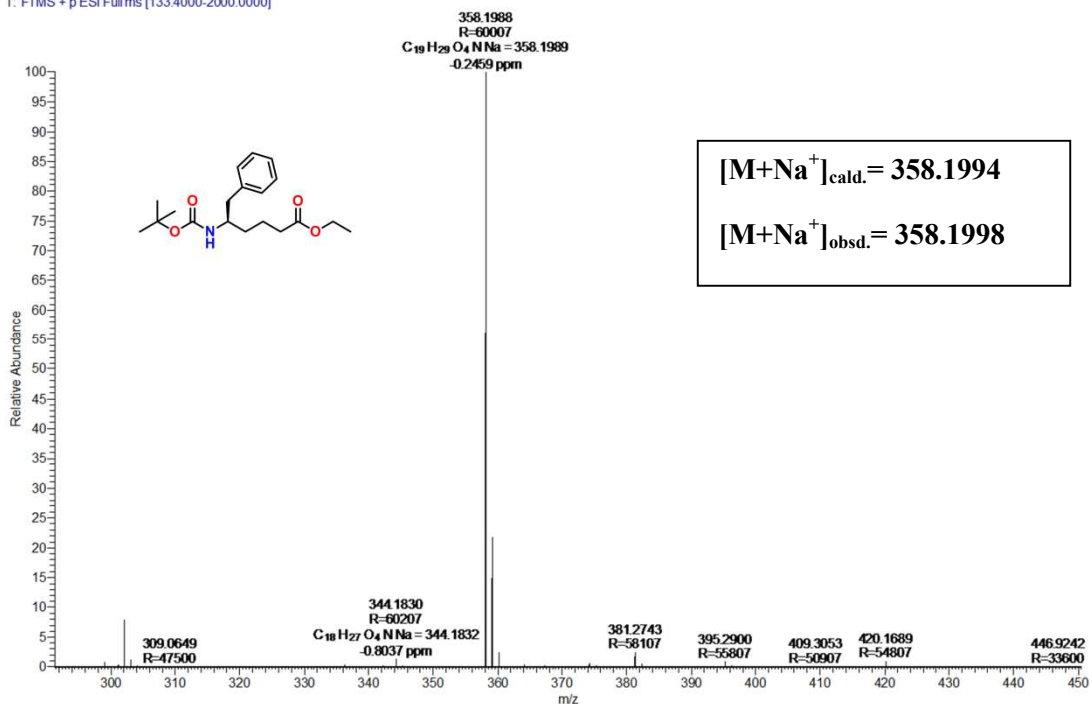
20181011-RMR-3-R-S.2.fid  
RMR-3-R-S



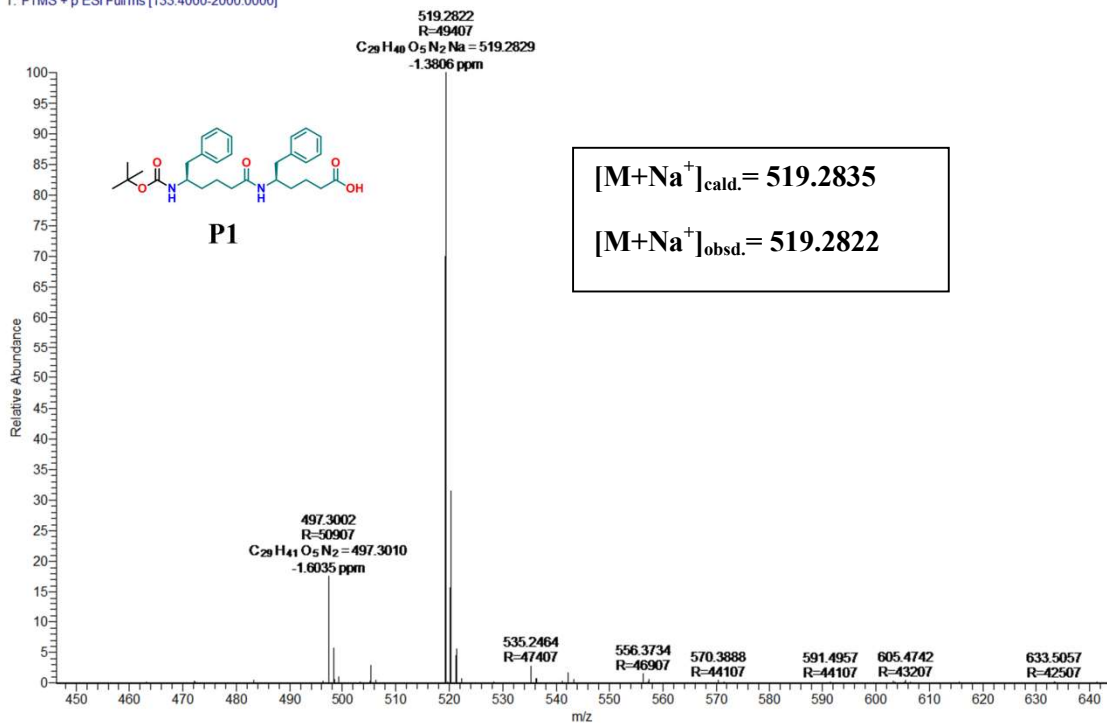
## 4.11.2. HRMS Spectra of Amino Acids and Peptides P1-P5

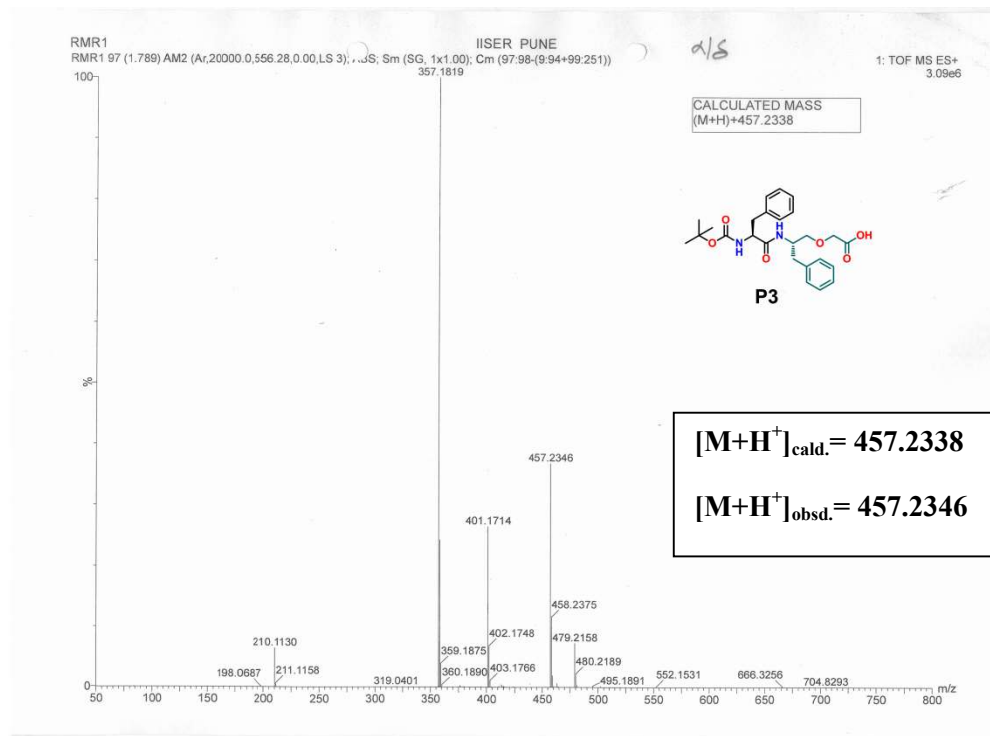
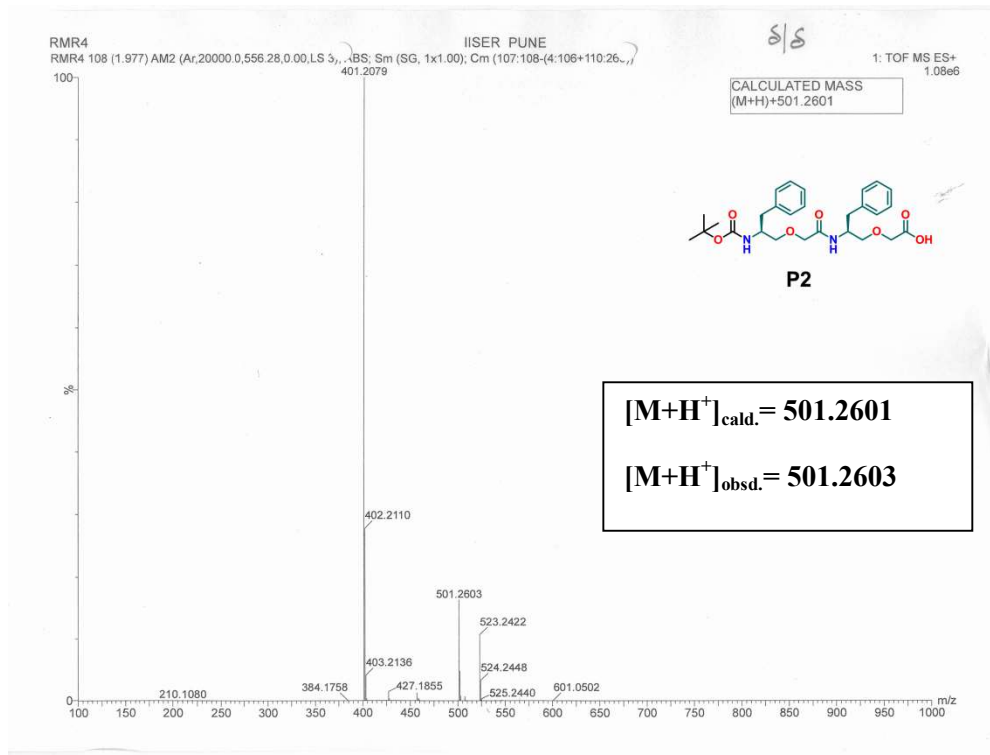


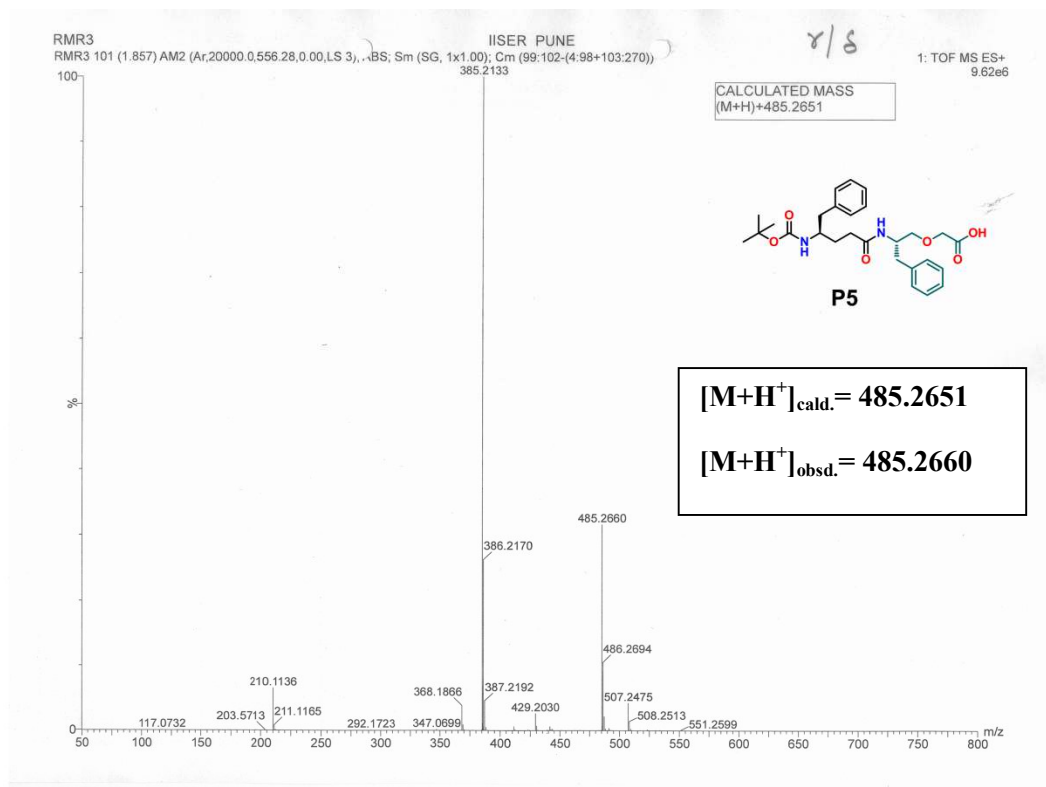
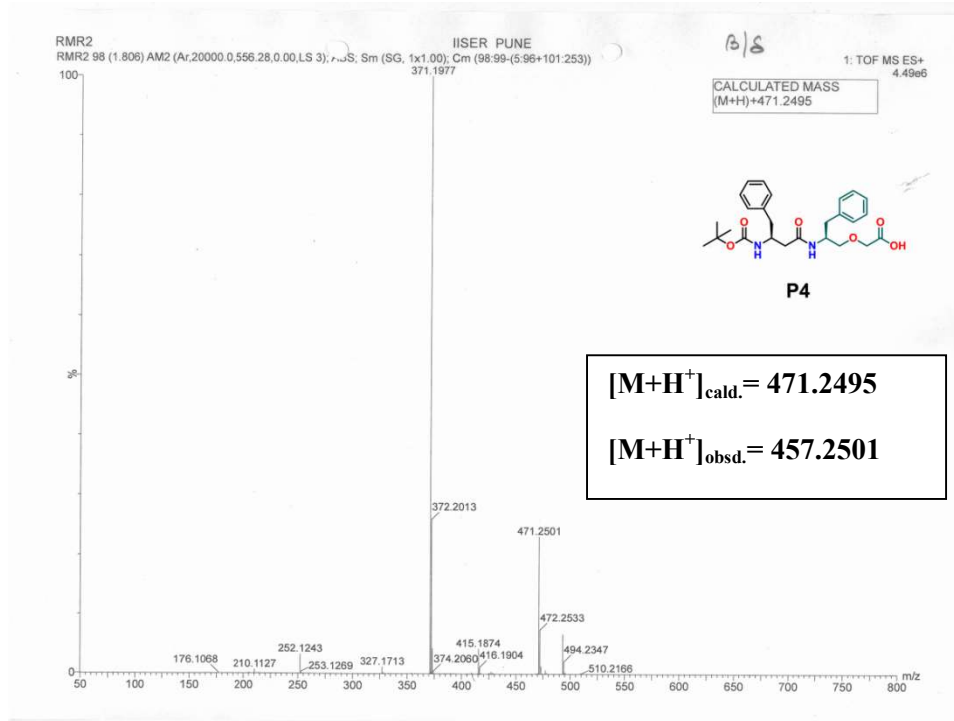
RMR-1 #273 RT: 1.22 AV: 1 NL: 1.69E9  
T: FTMS + p ESI Fullms [133.4000-2000.0000]



RMR-2 #265 RT: 1.18 AV: 1 NL: 3.93E8  
T: FTMS + p ESI Fullms [133.4000-2000.0000]









## *Chapter 5*

# **Design and Synthesis of Novel Parallel $\delta$ - Peptide Macrocycles for Transmembrane Ion Channels**

## 5.1. Introduction

The central theme concern with the nanotechnology is mainly preparation and characterisation of structures at nanoscale level and utilisation of these nanoscale materials for the design of functional molecules and devices.<sup>1</sup> Among the different nanostructure, nanotubes are one of the promising candidate because of its diversity applications such as transport, molecular separation, catalysis, optics, electronics, antimicrobial candidate, drug delivery agent etc.<sup>2</sup> In this regards, different nanotubular structures have been designed from the graphite, inorganic complexes, cyclodextrin and lipids.<sup>3</sup> From the last few decades, great advances were made in the field of the covalently

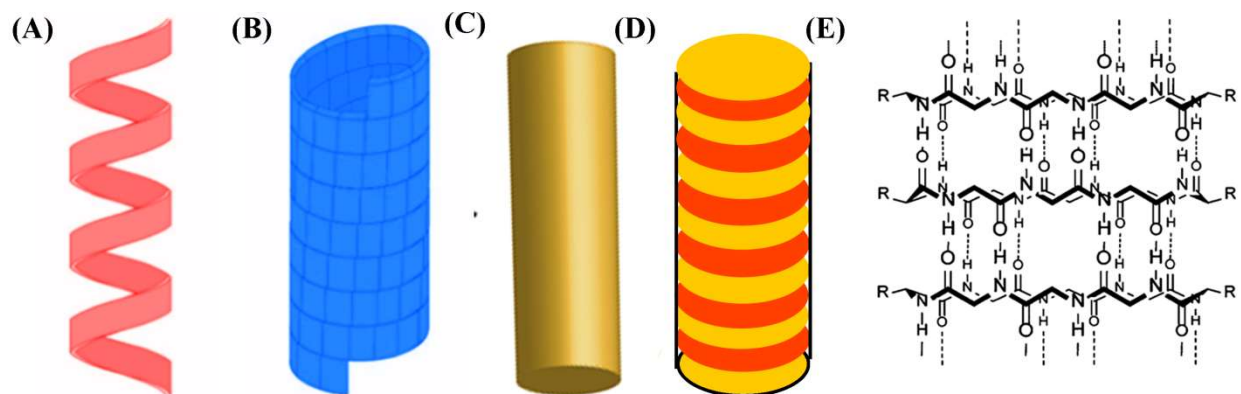


**Figure 5.1:** Different peptide base self assembled structure (A) coiling of helical structure (B) assembly of sector molecule (C) nanotubular structure (D) nanotubular structure derived from stacking of macrocycles (E) self-assembled peptide based nanotube formation from D,L- $\alpha$ -peptide.

bonded nanostructure. Recently, this field moves toward the nanostructure derived from the non-covalent interactions.<sup>4</sup> Several non-covalent approaches were investigated to derive self-assembled nanostructures such as, hollow rodlike structures, stacked rings, helically juxtapositioned truncated wedges etc.<sup>3</sup> Among the various structures, the stacked rings are particularly more attractive due to the control over the nanotube diameter which can be made by different size of the building blocks. In addition to the various nanotubular structures, cyclic peptides attracted considerable attention due to their spontaneous self-assembling ability. The cyclic peptides can be self-assembled into nanotubes (SPNs) through the stacking and the hydrogen bonding interactions.<sup>5</sup> To adopt a nanotubular architecture, the cyclic peptides must

adopt a flat conformation with all the side chains of the amino acids are projected outwards from ring and the amide backbone oriented perpendicular to the ring.<sup>5</sup> The diameter of the cyclic peptide and subsequent nanotubes can be easily controlled by the number of the amino acids involved in the cyclization process. Thus, cyclic peptides have attracted considerable attention in the construction of different nanotubes for specific functions.<sup>5</sup>

## 5.2. Design of the Cyclic Peptide Nanotubes (CPNs) form $\alpha$ -Amino Acids

In 1974, De Santis *et al* proposed through theoretical calculation that peptides composed of an even number of alternating conformationally equivalent  $\beta$ -type dihedral angles of D- and L- amino acid residues would be able to form closed a cyclic structure through backbone-backbone hydrogen bonding interactions.<sup>6</sup> Due to the poor solubility of these peptides, the experimental evidences were inconclusive.<sup>7</sup> After 20 years, in 1993 the group of Ghadiri and co-workers took the advantage of this theoretical proposal and showed the formation of the nanotubular structure by pH variation.<sup>8</sup> The first well documented and characterized CPNs were derived from the octapeptide *cyclo*-[(L-Gln-D-Ala-L-Glu-D-Ala)<sub>2</sub>]. The expected cyclic peptide nanotubular (CPNs) structure was further characterised by electron microscopy, FT-IR spectroscopy, electron diffraction and crystal structure modelling.<sup>8</sup> The self-assembling cyclic peptides (CPs) are arranged in an anti parallel  $\beta$ -sheet type arrangement. This is due to the flat conformation of the cyclic peptide rings. The internal diameters of the hollow nanotubular assemblies are 7.5 Å and distance between each CPs are approximate of 4.73 Å. In this conformation, all the amino acid side chains are projected outwards from the nanotubular structure. In this nanotubular structure the pore diameter and surface properties can be easily adjusted by the correct sequence of the CPs. Furthermore, this type of CPs can be easily synthesized by using solid phase peptide synthesis strategies. In continuation, Lambert and co-workers utilised pH controlled self-assembled nanotubular structure from cyclic D-,L- $\alpha$ -octa peptide containing two aspartic units.<sup>9</sup> In addition, Ghadiri's group also improved the design of the nanotubular assemblies using uncharged D,L- $\alpha$ -cyclic octapeptide and explored the effect of hydrophobicity on the crystallisation.<sup>10</sup> In recent studies, Unden's group showed the formation of heteromeric nanotube formation from the enantiomeric pairs of CPs. In this study, the presence of bulky amino acid *tert*-leucine (TLe) prevents one isomer to form self-assembled nanotube due to the steric effect,

whereas the another isomer readily formed self-assembling nanotubular structure.<sup>11</sup> Further, Ghadiri and co-workers showed the expansion of internal pore diameter of 13 Å using the dodecapeptide *cyclo*-[(L-Gln-D-Ala-L-Glu-D-Ala)<sub>3</sub>] CPNs.<sup>12</sup> This finding suggest that just varying the number of the amino acids in the CPs, it is possible to control the internal diameter of the self-assembled cyclic peptide nanotubes (CPNs).

### 5.3. Design of Cyclic Peptide Nanotubes (CPNs) from Non-Canonical Amino Acids

Apart from the D-,L- $\alpha$ -peptide, cyclic peptide nanotubes (CPNs) were also developed from the oligomer and the hybrid peptide form the  $\beta$ -, $\gamma$ -, $\delta$ - and  $\epsilon$ - amino acids.<sup>13</sup> The cyclic peptide nanotubes (CPNs) derived from the non-canonical amino acids can be utilized for finding application in different fields due to their backbone flexibility. The first nanotube formation of the cyclic peptide composed of  $\beta$ -amino acids was developed by Seebach and co-workers.<sup>14</sup>

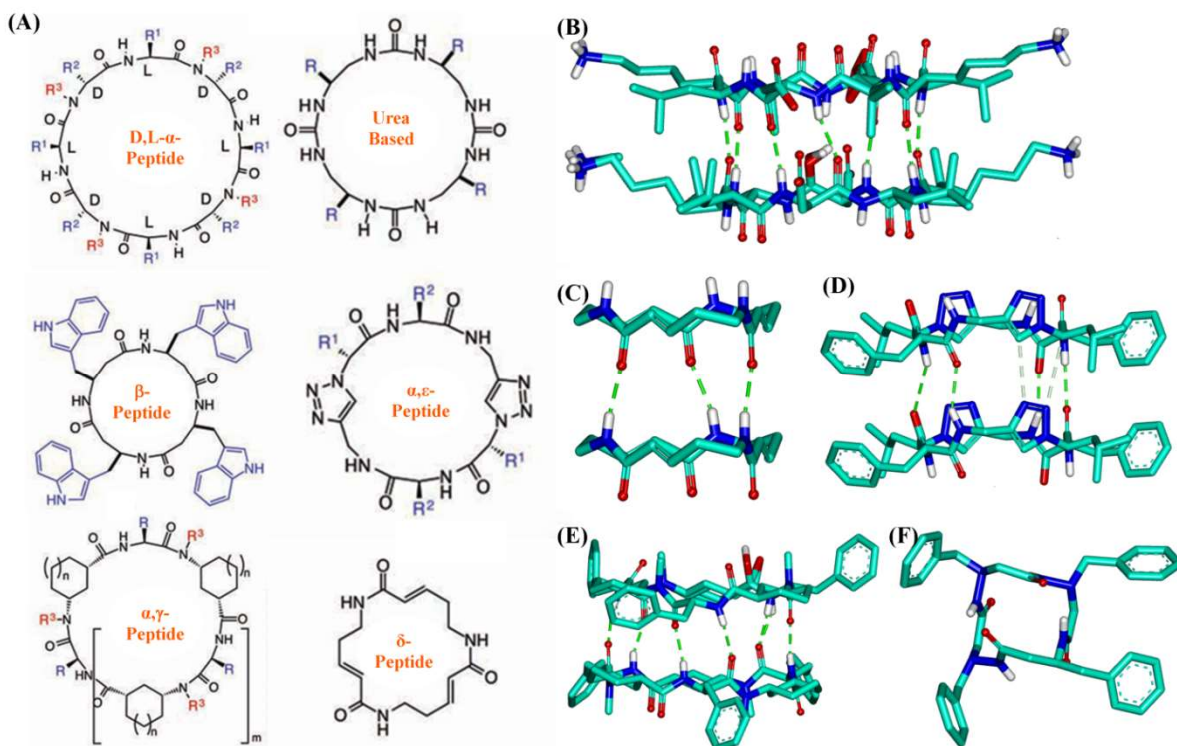


**Figure 5.2:** (A) Sequences of CPs derived from non canonical amino acids. Single crystal structure of the CPs from (B) D,L- $\alpha$ -peptide (CCDC No 1520675 ) (C)  $\delta$ -peptide (CCDC No 164581) (D)  $\alpha,$   $\epsilon$ -

peptide(E)  $\alpha$ ,  $\gamma$ - peptide(F) Aza- $\beta^3$ -peptide. Crystal structure of (D), (E) and (F) were generated from the CIFs in the ref no. 21, 17b and 14b respectively.

From the molecular modelling and X-ray structure analysis they showed that in solid state, cyclic peptide composed of chiral  $\beta^3$ -amino acid residues can stack each other to form self-assembled nanotubes similar to the earlier reported D,L- $\alpha$ -cyclic peptide.<sup>8</sup> The CPs are stacked over each other by the four unidirectional polar hydrogen bonding. Extensive studies suggested that *cyclo*-[( $\beta^3$ -HAla)<sub>4</sub>] adopts a flat conformation and each cyclic peptide stack over each other by four hydrogen bonding interactions.<sup>14</sup> The resulted pore diameter of the CPNs was approximate of 2.6 Å. Furthermore Kimura and co-workers reported formation of CPNs from the novel class of CPs constituted from sugar  $\beta$ -amino acids.<sup>15</sup> In addition Ghadiri and co-workers reported efficient ion channels formation from the CPNs form the  $\beta^3$ -amino acids.<sup>16</sup> Apart from the CPNs formation from the  $\beta$ -amino acids, new class of self-assembling nanotubular structure was reported by the Granja and co-workers.<sup>17</sup> The structure was mainly based on the  $\alpha$ - and cyclic  $\gamma$ - amino acids. Furthermore, the Granja and co-workers further modified the inner surface of the cavity for the construction of different supramolecular capsules.<sup>18</sup> Efforts have been also made for the construction of CPNs from different novel amino acids. In this regards, Dory and colleagues reported cyclic tripeptide from the  $\alpha,\beta$ -unsaturated  $\delta$ -amino acid residue with *trans* geometry of the vinyl group.<sup>19</sup> Due to the presence of the even number of atoms in the peptide backbone, all the NHs and carbonyl groups are projected in the same direction. In recent studies by Granja and co-workers reported self-assembled nanotubular structure with large cavity from  $\alpha,\delta$  hybrid peptide and these large cavity was further used for encapsulation of C<sub>60</sub>.<sup>20</sup> Apart from the nanotubes constructed from the cyclic and acyclic amino acids, Ghadiri's group reported design and synthesis and characterisation of novel class of peptide macrocycles form 1, 2, 3-triazole as  $\epsilon$ -amino acids.<sup>21</sup>

#### **5. 4. Application of Self-Assembled Cyclic Peptide Nanotubes (CPNs)**

The nanotube resulted from the self-assembling cyclic peptide have been utilising as a promising candidate in the fields of nanotechnology and material sciences due to ease in control in the pore diameter and outer surface functionalization. The self-assembled cyclic peptide nanotube which are internally hydrophilic and external surface with appropriate characteristics can certainly

mimic the transmembrane ion channels. In 1994, the first cyclic peptide  $\text{cyclo-[L-Gln-(D-Leu-L-Trp)}_3\text{-D-Leu]}$  which can self-assemble in the lipid bilayer was reported by Ghadiri and

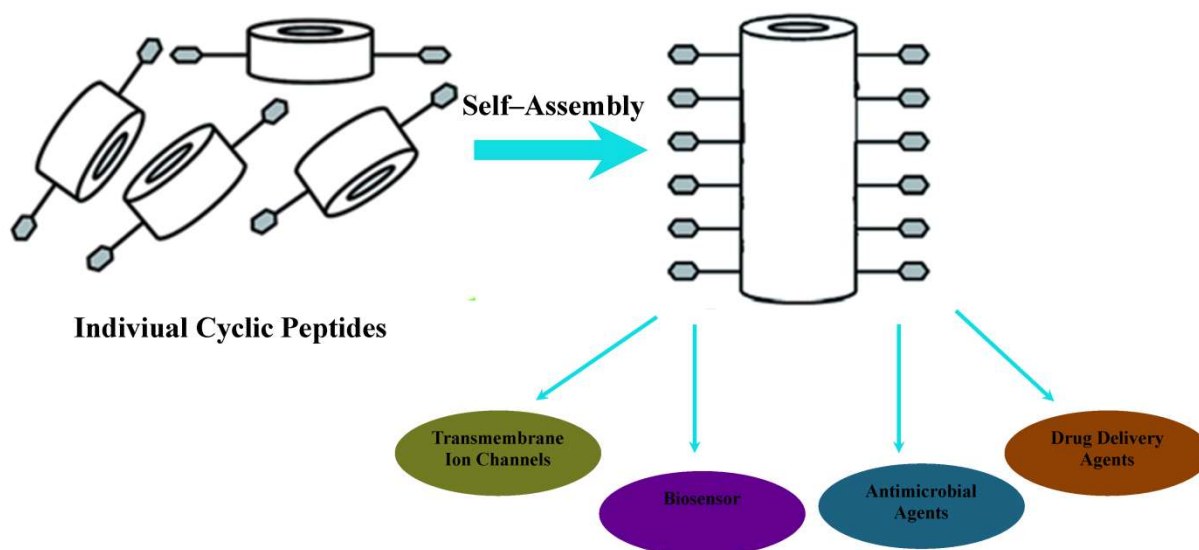


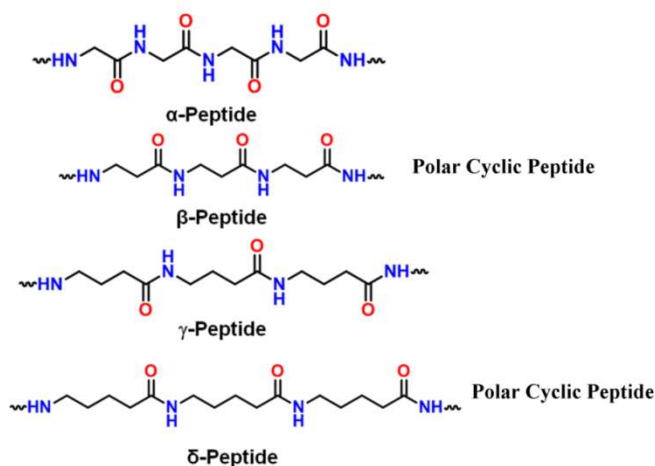
**Figure 5.3:** Application of the self-assembled cyclic peptide nanotubes (CPNs)

colleagues.<sup>22</sup> This cyclic peptide nanotube displayed transport activities for  $\text{K}^+$  and  $\text{Na}^+$ . Furthermore, they reported transport of glucose and glutamic acid from the decapeptide  $\text{cyclo [L-Gln-(D-Leu-L-Trp)}_4\text{-D-Leu]}$ . In addition, like D,L- $\alpha$ -counterparts, cyclic peptide from  $\beta$ -amino acids such as  $\text{cyclo-}[(\text{Trp})_4]$  and  $\text{cyclo-}[(\beta^3\text{-Trp-}\beta^3\text{-Leu-})_2]$  were also explored for transmembrane ion channel activity.<sup>23</sup> Apart from the ion channel activity, amphipathic D, L- $\alpha$ -CPs have been explored as antimicrobial candidates.<sup>24</sup> Ghadiri and co-workers showed that the CPs are assembled like nanotubular structure on the bacterial membrane at an angle of  $20^\circ$ . In this assembled structure all the hydrophobic side chains are projected into the lipid part of the cell membrane and hydrophilic side chains are projected in the hydrophilic part of the cell membrane. Thus the CPNs showed significant broad spectrum antimicrobial activity which also included methicillin-resistant *Staphylococcus aureus* (MRSA) by carpet type mechanism. These CPNs also have been finding promising candidate in various applications in material sciences. Guldi and colleagues reported artificial photosystem mimic form the Me-blocked heterodimeric nanotube form  $\alpha,\gamma$ - hybrid peptide through exTTF as donar and  $\text{C}_{60}$  acceptor molecule.<sup>25</sup> Recently the group of Granja and co-workers reported biosensors from the novel multi

components network of pyrene and dapoxy-derivatized  $\alpha,\gamma$ -CPs.<sup>26</sup> Further the self-assembled CPNs were also explored for the finding application in nanoelectronics.<sup>27</sup> In this regards, Ashkenasy *et al* reported electronically delocalized peptide nanotube from eight residue D, L- $\alpha$ -CPs which contain redox active 1,4,5,8-naphthalenetetracarboxylic diimide (NDI) as in the side chain of the amino acid residues.<sup>28</sup> In recent studies, Kimuras laboratory reported the formation of CPNs and metal complexation from novel cyclic tri  $\beta$ -peptide containing terpyridine ligands.<sup>29</sup> Such assembles show both high conductivity and large dipole and finding promising application in the field of organic electronics.

### 5.5. Aim and Rationale of the Present Work

Most of the reported CPNs from the non-canonical amino acids are anti parallel  $\beta$ -sheet type structure.<sup>13</sup> These CPNs are non-polar in nature because of their projection of the hydrogen bonds between the stacks. But polar CPNs are not well explored in the literature. The polar CPNs are finding great applications in the organic nano-electronics, however it is difficult to access the polar nanotubes except through cyclic  $\beta$ -peptides.<sup>29</sup> The CPNs derived from homooligomers of  $\beta$ - amino acids are not well explored in the literature may be due to the solubility of the cyclic  $\beta$ -peptides. As  $\delta$ -amino acids are higher homologues of  $\beta$ -amino acids and also contains even number of backbone atoms, it is expected that cyclic peptides composed of  $\delta$ -amino acids may adopt polar



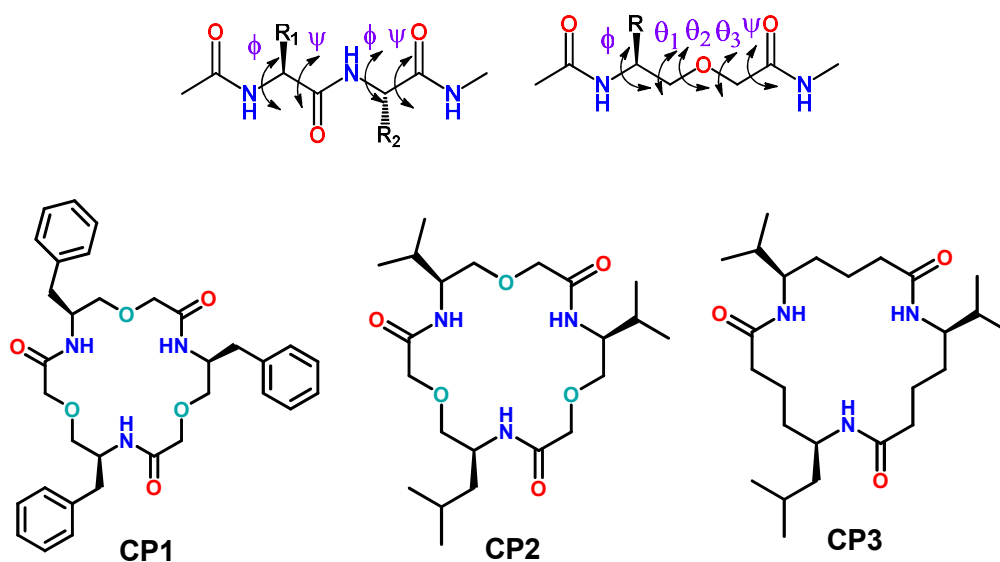
**Scheme 5.1:** H-bond projection of oligomers from  $\alpha \rightarrow \delta$  amino acids.

cyclic peptide nanotubes by projecting amide NH groups at face of the cyclic peptide and carbonyl groups on the other side. However, CPNs containing  $\delta$ - amino acids are not well explored due to the difficulties in the synthesis of  $\delta$ - amino acids. Schematic representation of the alternating projection of amide bonds in  $\alpha$ - and  $\gamma$ -peptides and same side projection of the all carbonyl groups and amide NH groups in the peptides containing  $\beta$ -and  $\delta$ -amino acids are shown in the Scheme 5.1. Nevertheless, Chakraborty and co-workers reported of the design and synthesis of cyclic peptide from the furan based  $\delta$ -amino acids. Further they utilized these CPs to target G-Quadruplex.<sup>30</sup> In the previous chapter, we have demonstrated the various gelation properties of the  $\beta(O)$ - $\delta^5$ -amino acids, in this chapter we sought to investigate, whether  $\beta(O)$ - $\delta^5$ -amino acids can be used to design self-assembling cyclic peptides. It is also interesting to note that cyclic peptides of  $\beta(O)$ - $\delta^5$ -amino acids are the hybrids of crown ether and regular cyclic peptides.

## 5.6. Results and Discussion

### 5.6.1. Design and Synthesis

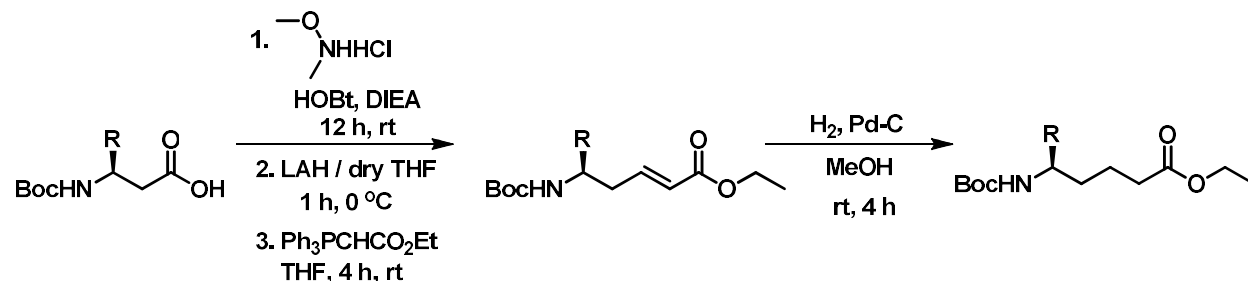
In order to understand whether or not the cyclic peptides composed of  $\beta(O)$ - $\delta^5$ -amino acids can polar self-assembled tubular structures, we have designed three different cyclic peptides. The



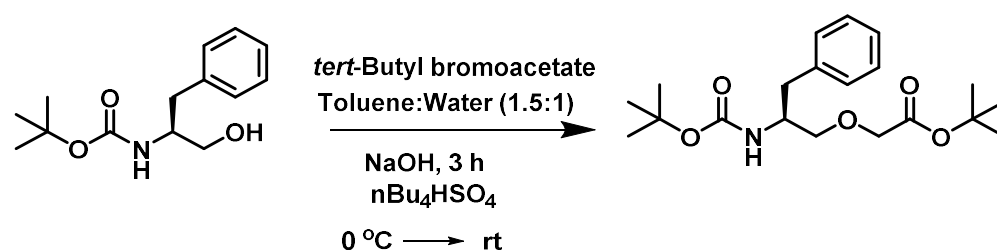
**Scheme 5.2:** Sequences of cyclic peptides under investigations.



sequences of CPs are shown in Scheme 5.2. The schematic representation of the synthesis of  $\beta(O)\text{-}\delta^5$ -amino acid is shown in the Scheme 5.3. As mentioned in the previous chapters  $\beta(O)\text{-}\delta^5$ -amino



**Scheme 5.3:** Synthesis of ethyl ester of *N*-Boc- $\delta^5$ -Amino Acid from *N*-Boc- $\beta^3$ -Amino acid.



**Scheme 5.4:** Synthesis of *N*-Boc- $\beta(O)\text{-}\delta^5$ -Phe- $O^t$ Bu from *N*-Boc amino alcohol.

acids were synthesized starting from Boc protected amino alcohol.<sup>31</sup> The carbon analogous of  $\beta(O)\text{-}\delta^5$ -amino acids were synthesized from the corresponding Boc- $\beta^3$ -amino acids.<sup>31b</sup> The Schematic representation of the synthesis of the  $\delta^5$ -amino acids is shown in the Scheme 5.3. First, all the linear peptides were synthesized by the conventional solution phase condensation strategy and macrocyclisation was carried out by using high dilution methodology. The schematic representation of the macrocyclization is shown in the experimental section. The crude peptide macrocycles were purified by RP-HPLC using MeOH/H<sub>2</sub>O gradient system. Along with cyclic peptides **CP1** and **CP2** composed of  $\beta\text{-O-}\delta^5$ -amino acids, cyclic peptide composed of  $\delta^5$ -amino acids with complete carbon backbone **CP3** was also synthesized to understand their relative properties. We studied the self-assembly properties of these CPs in solid state as well as solution state. Along with structural properties we have also studied transmembrane activity of **CP1** and **CP2** through vesicle leakage assay.

## 5. 6.2. ORTEP Diagram of BocNH- $\beta$ (O)- $\delta^5$ -Val-- $\beta$ (O)- $\delta^5$ -Leu-OH and Peptide CP1

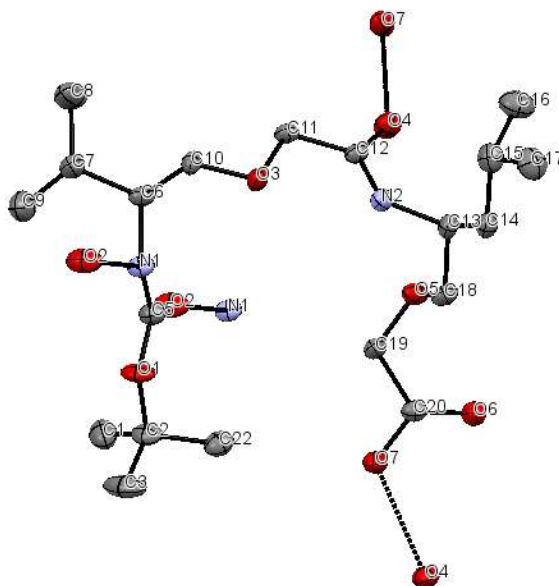


**Figure 5.4:** ORTEP diagram of peptide BocNH- $\beta$ (O)- $\delta^5$ -Val-- $\beta$ (O)- $\delta^5$ -Leu-OH. H-bonds are shown in dotted lines. H-atoms are omitted for clarity. Ellipsoids are drawn at 50% probability. (CCDC No. 1950175)

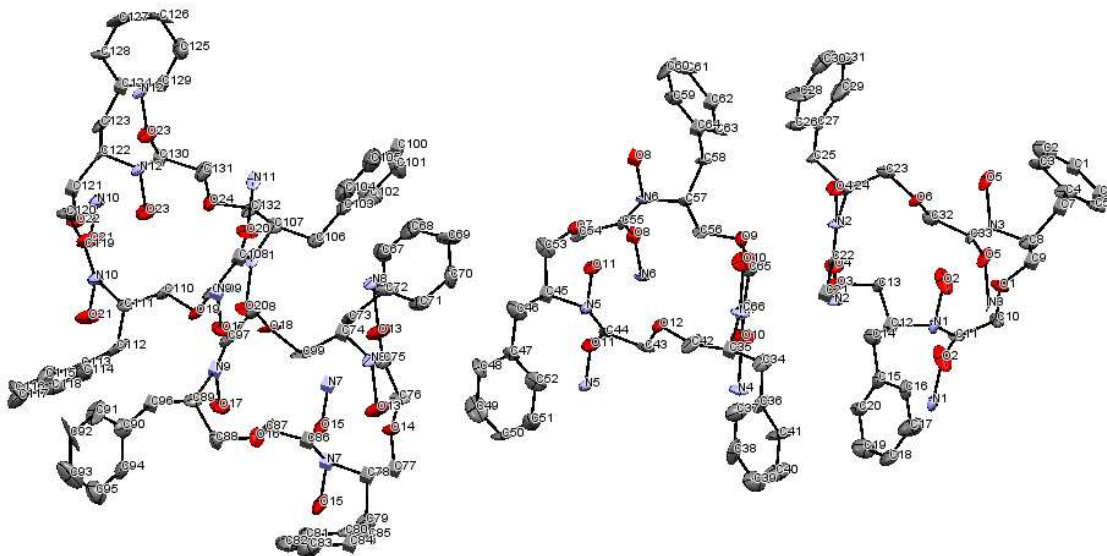


**Figure 5.5:** ORTEP diagram of peptide CP1. H-bonds are shown in dotted lines. H-atoms are omitted for clarity. Ellipsoids are drawn at 50% probability. (CCDC No 1950174)

### 5.6.3. Conformational Analysis of Peptides CP1-CP3

As single crystal structures provide unambiguous structural information, we subjected all cyclic peptides for crystallization in various solvent combinations. Among the three cyclic peptides, **CP1** gave X-ray quality single crystals from slow evaporation of peptide solution in toluene/ $\text{CHCl}_3$ . Even after several attempts, **CP2** did not give the X-diffraction quality single crystals and **CP3** was found to be insoluble in organic solvent solvents. The X-ray diffraction structure **CP1** is shown in the Figure 5.6A. Four molecules of **CP1** were found in the asymmetric unit. The crystal structure analysis revealed that the cyclic peptide **CP1** adopts a  $C_3$  symmetric molecule and average pore diameter of  $\sim 5.25$  Å. Instructively, the CPs is a hybrid of both the crown ether and peptide macrocycles. More importantly, the CPs are assembled into tubular assembly through the

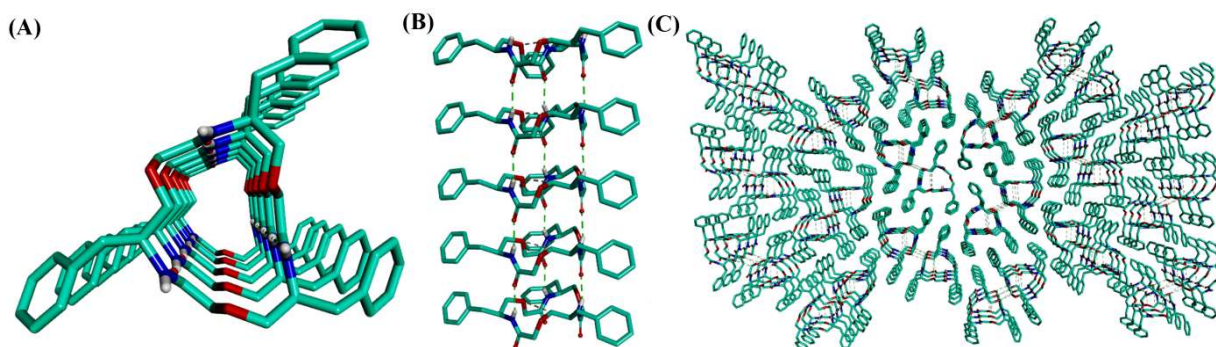


**Figure 5.6:** (A) Top view of the self-assembled nanotubular structure form **CP1** (B) Parallel  $\beta$ -sheet type hydrogen bonding of the self-assembled **CP1** (C) Overall packing and top view of the self-assembled nanotubes from peptide **CP1**.

intermolecular hydrogen bonding in a parallel  $\beta$ -sheet type of assembly. As anticipated, the direction of the hydrogen bonding is along one direction in the tubular structure, representing the polar tubular assembly of **CP1**. The tubular assembly of cyclic peptide **CP1** is shown Figure 5.6B. The conformation of  $\beta(\text{O})$ - $\delta^5$ -amino acid in the cyclic peptide can be represented by the backbone torsion angles  $\phi(\text{N}-\text{C}^\delta)$ ,  $\theta_1(\text{C}^\delta-\text{C}^\gamma)$ ,  $\theta_2(\text{C}^\gamma-\text{O}^\beta)$ ,  $\theta_3(\text{O}^\beta-\text{C}^\alpha)$  and  $\psi(\text{C}^\alpha-\text{C}=\text{O})$  (Scheme 5.2). The torsion angle parameters of cyclic  $\beta(\text{O})$ - $\delta^5$ -peptide **CP1** are tabulated in the Table 5.1. The intermolecular H-bond parameters are tabulated in the Table 5.2. The average inter distance of the each stacked cyclic peptides is around 5.16 Å. Furthermore, each CPs are also stabilized

through the CH---O interaction between O<sup>β</sup> with C<sup>α</sup>H of another molecule of CP by laterally. The overall crystal packing of the **CP1** was shown in Figure 5.6C. As **CP2** did not give X-ray quality single crystals, we studied its conformation in the solution using NMR spectroscopy. The <sup>1</sup>H NMR of the peptide **CP2** in CDCl<sub>3</sub> (3 mM) revealed the well dispersed NH and C<sup>δ</sup>H in solution. The two dimensional ROESY spectrum of **CP2** is shown in Figure 5.7A and 5.7B. The amino acid type and sequential connectivity of the residues were established using ROESY and TOCSY spectra. The observed key NOEs are shown in Figure 5.7C. The assigned

**Table 5.1:** Backbone torsion angle parameters of peptide **CP1**:

Peptide CP1	φ(deg)	θ <sub>1</sub> (deg)	θ <sub>2</sub> (deg)	θ <sub>3</sub> (deg)	Ψ (deg)
<b>Molecule A</b>					
β(O)-δ <sup>5</sup> -Phe 1	-128.32	42.86	64.47	-161.47	-17.44
β(O)-δ <sup>5</sup> -Phe 2	-91.86	170.74	-90.35	-79.42	-16.71
β(O)-δ <sup>5</sup> -Phe 3	-120.43	49.38	64.12	161.85	-12.66
<b>Molecule B</b>					
β(O)-δ <sup>5</sup> -Phe 1	-129.20	42.93	60.91	-160.95	-16.33
β(O)-δ <sup>5</sup> -Phe 2	-92.08	173.48	-89.46	-80.85	-13.68
β(O)-δ <sup>5</sup> -Phe 3	-119.63	46.73	65.33	162.78	-13.53
<b>Molecule C</b>					
β(O)-δ <sup>5</sup> -Phe 1	-132.50	44.87	64.64	-162.20	-14.60
β(O)-δ <sup>5</sup> -Phe 2	-91.97	173.12	-93.19	-76.64	-18.10
β(O)-δ <sup>5</sup> -Phe 3	-120.07	47.25	67.18	160.77	-11.78

<b>Molecule D</b>					
$\beta(\text{O})\text{-}\delta^5\text{-Phe 1}$	-129.84	41.37	62.96	-161.42	-15.04
$\beta(\text{O})\text{-}\delta^5\text{-Phe 2}$	-95.15	172.33	-91.07	-78.18	-16.91
$\beta(\text{O})\text{-}\delta^5\text{-Phe 3}$	-118.85	45.32	68.31	160.51	-31.21

**Table 5.2:** Hydrogen bonding parameters of peptide **CP1**

Intermolecular H-Bond Parameters

<b>Donor(D)</b>	<b>Acceptor(A)</b>	<b>D...A(Å)</b>	<b>DH...A(Å)</b>	<b>NH...O(deg)</b>
<b>Molecule A</b>				
N1	O2	2.916	2.160	146.75
N2	O4	2.925	2.142	150.85
N3	O5	2.924	2.173	145.49
<b>Molecule B</b>				
N4	O10	2.952	2.166	151.52
N5	O11	2.915	2.168	144.99
N6	O8	2.893	2.150	144.62
<b>Molecule C</b>				
N7	O15	2.902	2.159	144.31
N8	O13	2.960	2.189	148.61
N9	O17	2.946	2.163	151.09

Molecule D				
N10	O21	2.928	2.156	149.36
N11	O20	2.938	2.155	151.41
N12	O23	2.882	2.141	143.97

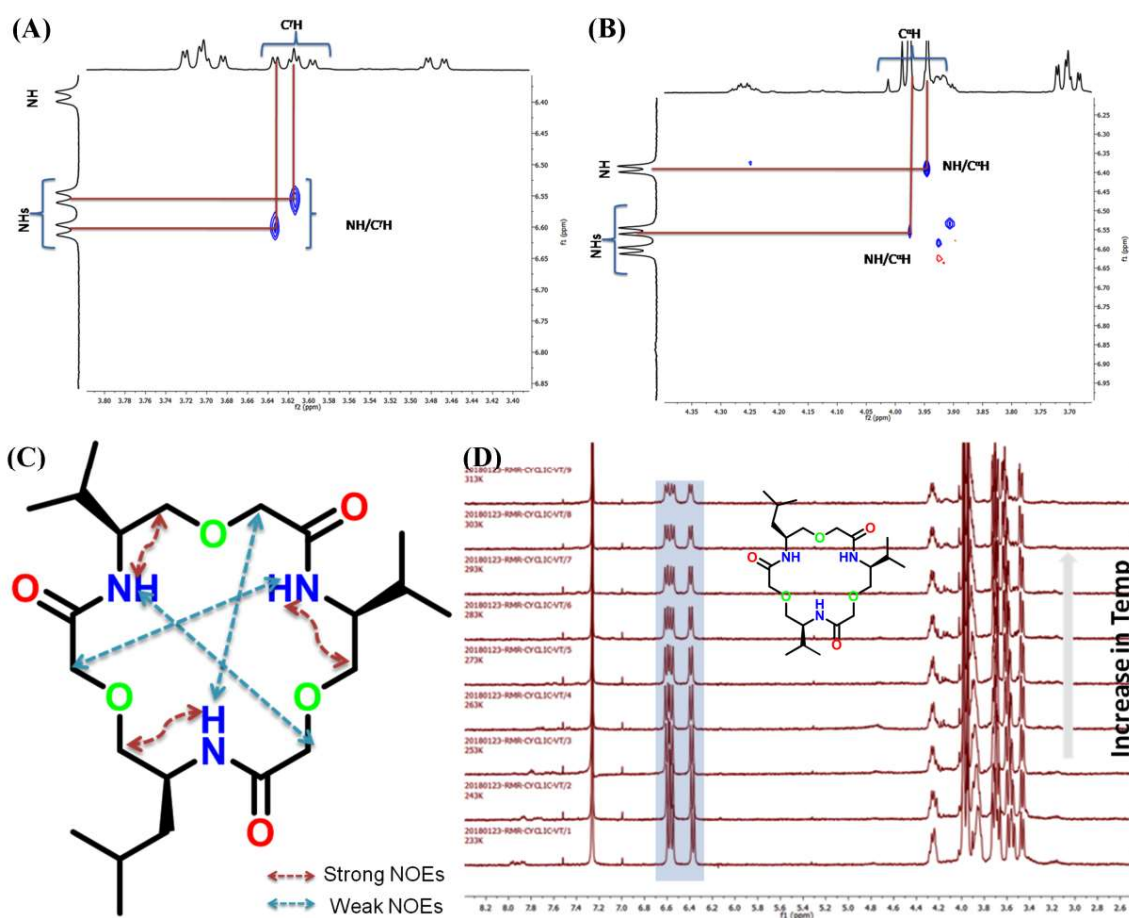


**Figure 5.7:** NMR characterization of peptide **CP1**. 2D ROESY spectra showing (A) NH ↔ C<sup>γ</sup>H (B) NH ↔ C<sup>α</sup>H interaction. (C) Key NOEs observed in peptide **CP1** (D) Temperature dependent <sup>1</sup>H NMR of peptide **CP1** in CDCl<sub>3</sub>.

spectra suggested that the strong NOEs was observed between  $\text{NH}(i) \leftrightarrow \text{C}^{\gamma}\text{H}(i)$  and weak NOEs observed between  $\text{NH}(i) \leftrightarrow \text{C}^{\alpha}\text{H}(i)$  residue. Further the temp dependent NMR (Figure 5.7D) suggested that there is no significant change of the chemical shift value ( $\delta_{ppm}$ ) of NHs. Which indicate that the peptide **CP2** was also retaining its conformation with increase in the temperature. As **CP3** did not soluble in any of the polar protic or aprotic solvent we did not further pursue with **CP3**. These results suggested huge influence of backbone ‘‘O’’ towards the increased solubility of the macrocycles compared to the  $\delta^5$ -amino acids with complete carbon backbone.

#### 5.6.4. Vesicle Leakage Assay for the Study of Transmembrane Activity of the Peptides CP1 and CP2

As many cyclic peptides showed transmembrane ion channel activity,<sup>22</sup> we sought to investigate ion channel activity of these polar cyclic peptides **CP1** and **CP2**. The activity was carried out by the vesicle leakage assay using pH sensitive HPTS (8-Hydroxypyrene-1,3,6-Trisulfonic Acid) dye. The schematic representation of the vesicular leakage assay is shown in the Figure 5.8. The large unilamellar vesicles (LUVs) formed from the EYPC lipid was loaded with HPTS dye. A pH gradient, ( $\text{pH}_{\text{out}} = 7.8$  and  $\text{pH}_{\text{in}} = 7.0$ ) across the bilayer of large unilamellar vesicles (LUVs) was

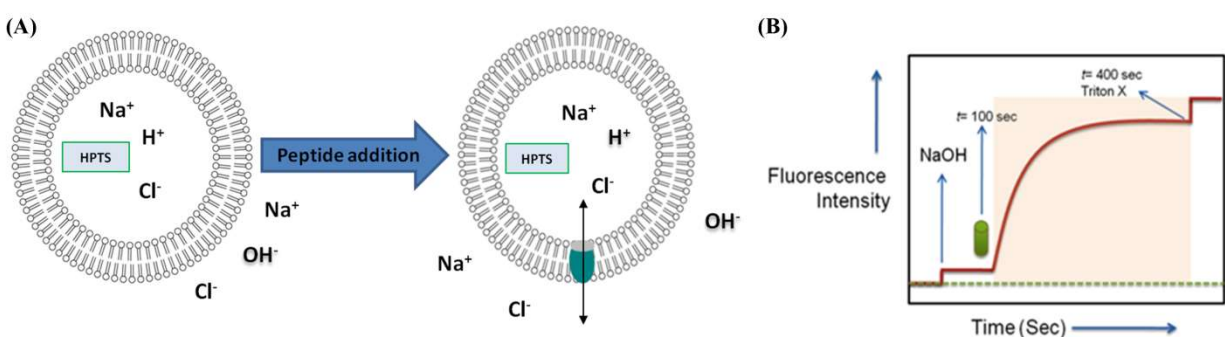


**Figure 5.8:** Schematic representation of (A) vesicle leakage assay (B) HPTS dye based fluorescence assay.

created by the addition of NaOH. After that upon the addition of a cyclic peptide **CP1** and **CP2** in DMSO, an increase in the internal pH of the vesicles due to the the pH gradientcollapse. This progress of the vesicle leakage was monitored by a change in

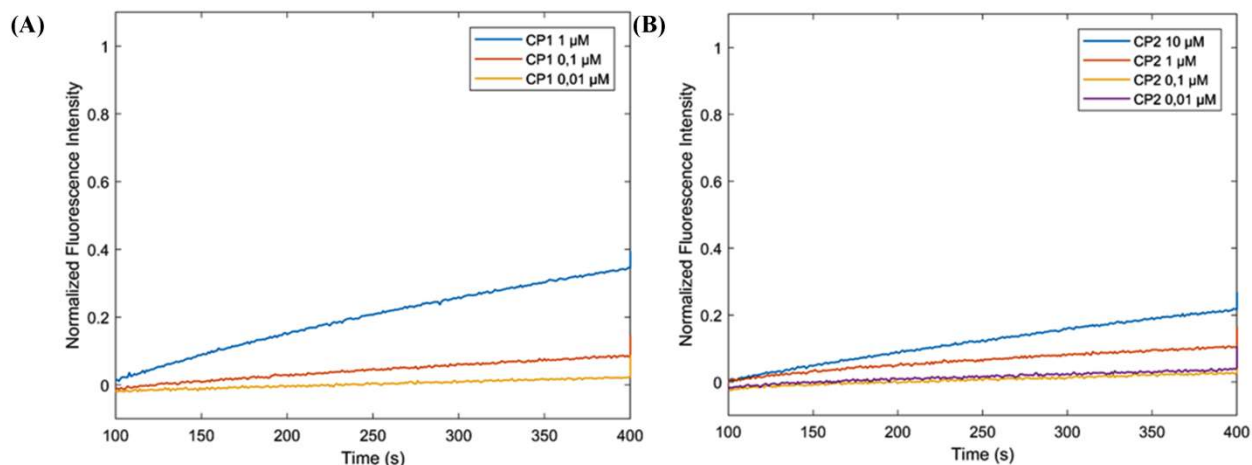


**Figure 5.9:** Increase in the fluorescence intensity of HPTS dye over the time in the vesicle leakage experiment by different concentration of peptide (A) **CP1** and (B) **CP2**.

the fluorescence intensity of HPTS with time. Complete collapse of the LUVs was achieved by addition of 10% Triton X-100 to the solution containing LUVs. The change of HPTS emission at  $\lambda = 510$  nm was monitored with excitation at 450 nm ( $\lambda_{\text{ex}} = 450$  nm) with time and normalized with the DMSO solvent without any cyclic peptides. The results are shown in Figure 5.9. These results suggested that with increase in the conc. of the cyclic peptides **CP1** and **CP2**, there is an increase in the normalized fluorescence intensity, indicating that the cyclic peptides **CP1** and **CP2** are self-assembled into a tubular fashion in the lipid bilayer and act as a synthetic transmembrane ion channels.

## 5.7. Conclusions

In conclusion, we are first time reporting the cyclic peptide from the  $\beta(\text{O})\text{-}\delta^5$ -amino acid mimicking as hybrid of crown ether and peptide macrocycles. Results showed that the cyclic tripeptide from the oligomer of  $\beta(\text{O})\text{-}\delta^5$ -amino acid was self-assembled to form the hollow tubular structure with pore diameter of  $\sim 5.25$  Å. These tubular structures are stabilized intermolecular H-bonds. In contrast to the cyclic peptides from  $\alpha$ -amino acids, the cyclic peptides from  $\beta(\text{O})\text{-}\delta^5$ -amino acid are stabilized by the unidirectional H-bonds. Further NMR



analysis suggested existence of tubular assembly of peptides in solution. Further, the cyclic peptide composed of carbon analogous of  $\beta(\text{O})\text{-}\delta^5$ -amino acid was found to be insoluble in most of the organic solvent. The insertion of “O”atom in backbone has a huge influence on the solubility of the cyclic peptide derived from the  $\delta$ -amino acids. From the vesicle leakage assay, it is evident that these cyclic peptides further assembled into tubular structure in the lipid bilayer and act as synthetic transmembrane ion channels. The electrophysiological studies of these CPs are under progress. Thus the newly designed polar crown ether peptide macrocycles can open up new directions in the design of cyclic peptide based biomaterials and transmembrane ion channels.

## **5.8. Experimental Section**

### **5.8.1. Materials and Methods**

All the reagents including amino acids were purchased from the commercial sources. DCM and MeOH were purchased from the commercial sources and distilled before to use. Column chromatography was performed on silica gel (120-200 mesh). Final peptides were purified by reverse phase HPLC.  $^1\text{H}$  (400 MHz) and  $^{13}\text{C}$  (100 MHz) NMR spectra were used to record the NMR spectra on respectively using the residual solvent signal as internal standards ( $\text{CDCl}_3$ ). Chemical shifts ( $\delta$ ) reported in parts per million (ppm) and coupling constants (J) reported in Hz. Mass of pure peptides was confirmed by MALDI-TOF /TOF.

### **5.8.2. NMR Spectroscopy**

All NMR studies were carried out by using either 400 or 600 MHz spectrometer. Resonance assignments were obtained by TOCSY and ROESY analysis. All two-dimensional data were collected in phase-sensitive mode by using the time-proportional phase incrimination (TPPI) method. Sets of 1024 and 512 data points were used in the  $t_2$  and  $t_1$  dimensions respectively. For TOCSY and ROESY analysis, 32 and 72 transients were collected, respectively. A spectral width of 600MHz was used in both dimensions. A spin-lock time of 200 and 250 ms were used to obtain ROESY spectra. Zero-filling was carried out to finally yield a data set of  $2\text{ K} \times 1\text{ K}$ . A shifted square-sine-bell window was used before processing.

### 5.8.3. General Procedure for the Solution Phase Peptides (CP1-CP3) Synthesis

#### 5.8.3.1. Synthesis of *N*-Boc- $\delta^5$ -Leu-OH

*N*-Boc- $\delta^5$ -Leu-OH was synthesized starting from *N*-Boc-(*S*)- $\beta^3$ -Leu-OH by reported protocol.<sup>31b</sup> Briefly, *N*-Boc-(*S*)- $\beta^3$ -Leu-Weinreb amide (1.4 g, 5 mmol) was converted to aldehyde through the reduction of the corresponding Weinreb amide using LAH (228 mg, 6 mmol). After that the aldehyde was subjected for Wittig reaction to get *N*-Boc- $\alpha,\beta$ -unsaturated- $\delta^5$ -Leu-OEt. Then, the crude Wittig product was purified using column chromatography by EtOAc/hexane solvent system. After that, the *N*-Boc- $\alpha,\beta$ -unsaturated- $\delta^5$ -Leu-OEt was reduced using H<sub>2</sub>/Pd-C to get *N*-Boc- $\delta^5$ -Leu-OEt. Further, the *N*-Boc- $\delta^5$ -Leu-OEt was subjected for ester hydrolysis using 1M NaOH in EtOH to obtain *N*-Boc- $\delta^5$ -Leu-OH and directly used for the peptides synthesis without purification. Same procedure was followed for the synthesis of *N*-Boc- $\delta^5$ -Val-OH.

#### 5.8.3.2. Synthesis of *N*-Boc- $\beta$ (O)- $\delta^5$ -Phe-O<sup>t</sup>Bu

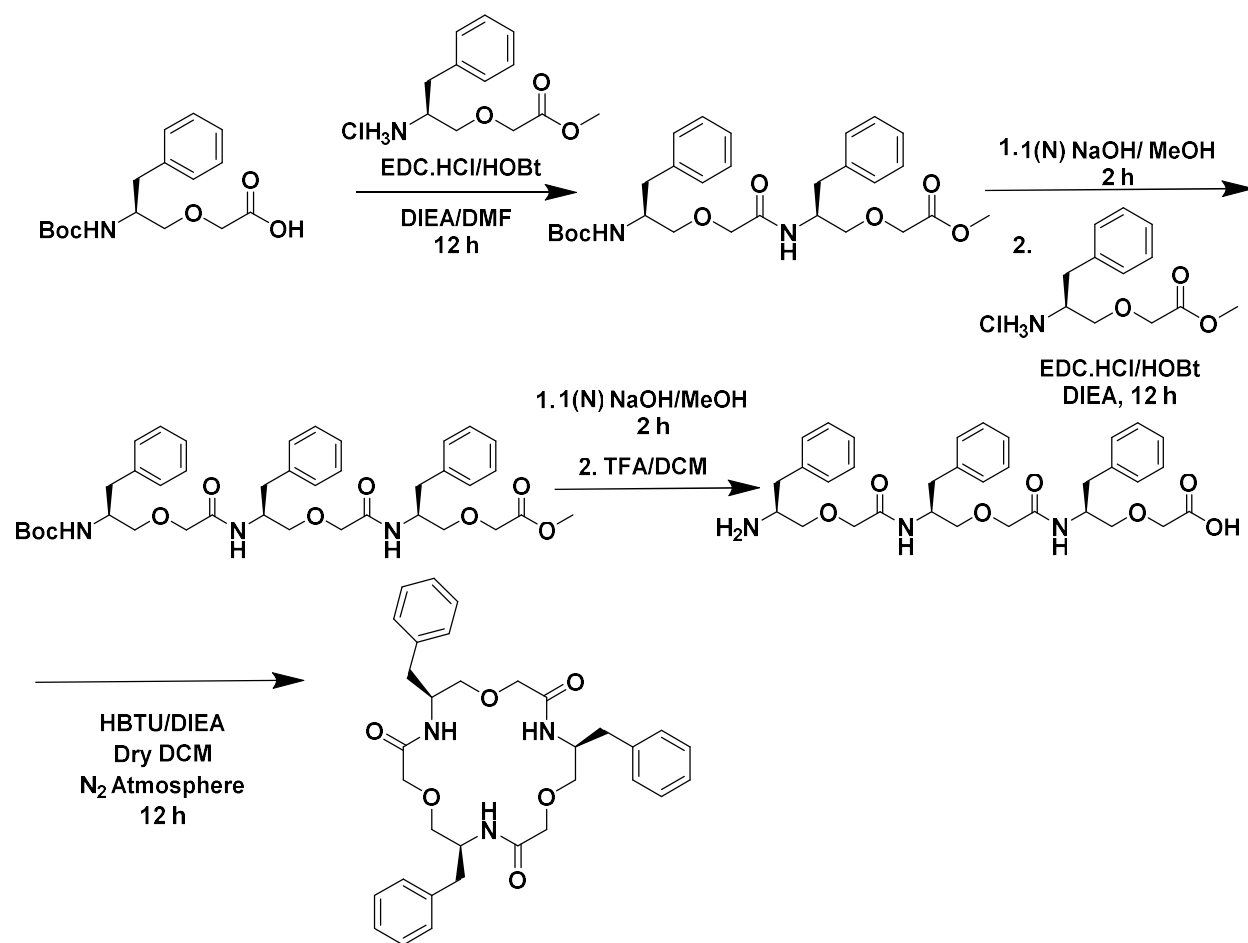
The *N*-Boc- $\beta$ (O)- $\delta^5$ -Phe was synthesized as reported previous chapters.<sup>31</sup> *N*-Boc- $\beta$ (O)- $\delta^5$ -Phe-O<sup>t</sup>Bu was synthesized by the reported protocol from *N*-Boc-amino alcohol.<sup>17</sup> Briefly, to the solution containing 10 mL of water and 10 mL of toluene, sodium hydroxide (10g, 250 mmol) was dissolved in ice-cold condition. Thereafter, *tert*-butyl bromoacetate (2.2 mL, 15 mmol) was added slowly to the biphasic reaction mixture at room temperature. After that, the solution containing *N*-Boc-Phenyl alanine alcohol (2.5 g, 10 mmol) in toluene (10 mL) was added slowly to the reaction mixture at 0 °C. The reaction mixture was stirred for about 3 h and allowed to come to room temperature. After completion of reaction (confirmed by TLC), the organic layer was extracted with diethyl ether (30 mL $\times$ 2). The combined organic layer was washed with brine (30 mL $\times$ 2) and dried over anhydrous sodium sulfate. The solvent was evaporated under reduced pressure to get white gummy product. The crude product of *N*-Boc- $\beta$ (O)- $\delta^5$ -Phe-O<sup>t</sup>Bu was purified by column chromatography using EtOAc/hexane solvent system. Same procedure was followed for the synthesis of *N*-Boc- $\beta$ (O)- $\delta^5$ -Leu and *N*-Boc- $\beta$ (O)- $\delta^5$ -Val.

### 5.8.3.3. Synthesis of Cyclic Peptides CP1-CP3

#### Synthesis of CP1

*N*-Boc- $\beta$ (O)- $\delta^5$ -Phe-OH (1.54 g, 5 mmol) was dissolved in 3 mL of DMF under N<sub>2</sub> atmosphere. To this solution EDC.HCl (960 mg, 5 mmol), HOBT (675 mg, 5 mmol) and DIEA (1.74 mL, 10 mmol) was added at 0 °C. Then the reaction mixture was stirred for about 15 min. After that ClH<sub>3</sub>N- $\beta$ (O)- $\delta^5$ -Phe-OMe (1.42 g, 5.5 mmol) was added to the reaction mixture and stirred for about 12 h. After completion of the reaction (confirmed by TLC), 15 mL of brine solution was added to the reaction mixture and the compound was extracted with EtOAc (3 × 20 mL). The combined organic layer was washed with 10% HCl (3 × 20 mL), 10% Na<sub>2</sub>CO<sub>3</sub> (3 × 20 mL) and brine (3 × 20 mL) respectively. Then the combined organic layer was dried over anhydrous Na<sub>2</sub>SO<sub>4</sub>. After that the combined organic layer was evaporated under reduced pressure to get the dipeptide BocNH- $\beta$ (O)- $\delta^5$ -Phe-  $\beta$ (O)- $\delta^5$ -Phe-OMe. After that the dipeptide was hydrolysed using 1*N* NaOH in MeOH. Then the dipeptide acid BocNH- $\beta$ (O)- $\delta^5$ -Phe- $\beta$ (O)- $\delta^5$ -Phe-OH (1.5 g, 3 mmol) was dissolved in 3 mL of DMF under N<sub>2</sub> atmosphere. To this solution EDC.HCl (576 mg, 3 mmol), HOBT (405 mg, 3 mmol) and DIEA (1mL, 6 mmol) was added at 0 °C. Then the reaction mixture was stirred for about 15 min. After that ClH<sub>3</sub>N- $\beta$ (O)- $\delta^5$ -Phe-OMe (854 mg, 3.3 mmol) was added to the reaction mixture and stirred for about 12 h. After completion of the reaction, 15 mL of brine solution was added to the reaction mixture and the compound was extracted with EtOAc (3 × 20 mL). The combined organic layer was washed with 10% HCl (3 × 20 mL), 10% Na<sub>2</sub>CO<sub>3</sub> (3 × 20 mL) and brine (3 × 20 mL) respectively. Then the combined organic layer was dried over anhydrous Na<sub>2</sub>SO<sub>4</sub>. After that the combined organic layer was evaporated under reduced pressure to get the Tripeptide BocNH- $\beta$ (O)- $\delta^5$ -Phe- $\beta$ (O)- $\delta^5$ -Phe-  $\beta$ (O)- $\delta^5$ -Phe-OMe. After that the tripeptide BocNH- $\beta$ (O)- $\delta^5$ -Phe- $\beta$ (O)- $\delta^5$ -Phe-  $\beta$ (O)- $\delta^5$ -Phe-OMe. (700 mg, 1 mmol) was dissolved in 10 mL of MeOH. To this solution 5 mL of 1*N* NaOH was added. Then the reaction mixture was stirred for 1 h. After completion of the reaction (confirmed by TLC), MeOH was evaporated under *vacuum*. Then it was acidified with 10% HCl and extracted with EtOAc (3 × 20 mL). The combined organic layer was brine (3 × 20 mL). Then the combined organic layer was dried over anhydrous Na<sub>2</sub>SO<sub>4</sub>. After that the combined organic layer was evaporated under reduced pressure to get the tripeptide BocNH- $\beta$ (O)- $\delta^5$ -Phe- $\beta$ (O)- $\delta^5$ -Phe- $\beta$ (O)- $\delta^5$ -Phe-OH. After that the Boc group was deprotected using TFA/DCM mixture. After

completion of the reaction, the TFA was evaporated under reduced pressure to get  $\text{H}_2\text{N}-\beta(\text{O})-\delta^5$ -Phe- $\beta(\text{O})-\delta^5$ -Phe- $\beta(\text{O})-\delta^5$ -Phe-OH and subjected for the macrocyclisation. The macrocyclisation of the linear peptide was carried out using high dilution technique. The both side deprotected peptide at 1mg/10mL concentration was dissolved in dry DCM under  $\text{N}_2$  atmosphere and cooled to  $0^\circ\text{C}$ . To the reaction mixture, HBTU (3 equivalent) and DIEA (10 equivalent) was added at  $0^\circ\text{C}$ . The reaction mixture was stirred for about 12 h. After completion of the reaction, DCM was evaporated under reduced pressure. Then the compound was extracted with EtOAc ( $3 \times 20$  mL). The combined organic layer was washed with 10% HCl ( $3 \times 20$  mL), 10%  $\text{Na}_2\text{CO}_3$  ( $3 \times 20$  mL) and brine ( $3 \times 20$  mL) respectively. Then the combined organic layer was dried over anhydrous  $\text{Na}_2\text{SO}_4$ . After that the combined organic layer was evaporated under reduced pressure to get the crude cyclic peptide **CP1**. Then the crude peptide **CP1** was dissolved in MeOH and purified by RP-HPLC on C18 column using MeOH/ $\text{H}_2\text{O}$  gradient solvent system. Same procedure was followed for the synthesis of **CP2** and **CP3**.



#### 5. 8.4. Crystallographic Information

##### **BocNH-β(O)-δ<sup>5</sup>-Val--β(O)-δ<sup>5</sup>-Leu-OMe (CCDC No 1950175)**

Crystals of compound BocNH-β(O)-δ<sup>5</sup>-Val--β(O)-δ<sup>5</sup>-Leu-OMe were grown by slow evaporation of methanol/ water solution. A single crystal (0.2×0.17×0.11) was mounted on loop with a small amount of the paraffin oil. The X-ray data were collected at 100 K temperature on a Bruker AXS SMART APEX CCD diffractometer using Mo Kα radiation ( $\lambda = 0.71073 \text{ \AA}$ ),  $\omega$ -scans ( $2\theta = 56.74$ ), for a total of 5846 independent reflections. Space group P2<sub>1</sub>,  $a = 5.1479$ ,  $b = 16.817$ ,  $c = 13.622 \text{ \AA}$ ;  $\alpha = 90$ ,  $\beta = 91.546$ ,  $\gamma = 90$ ;  $V = 1178.86 \text{ \AA}^3$ , Monoclinic,  $Z = 2$  for chemical formula C<sub>20</sub> H<sub>38</sub> N<sub>2</sub> O<sub>7</sub>,  $\rho_{\text{calcd}} = 1.179 \text{ g cm}^{-3}$ ,  $\mu = 0.088 \text{ mm}^{-1}$ ,  $F(000) = 456$ . The structure was obtained by direct methods using SHELXS-97.1. The final R value was 0.0614 ( $wR2 = 0.1751$ ) 5846 observed reflections ( $F0 \geq 4\sigma(|F0|)$ ) and 270 variables,  $S = 0.839$ .

##### **Peptide CP1 (CCDC No 1950174)**

Crystals of compound CP1 were grown by slow evaporation of CHCl<sub>3</sub>/ Toluene solution. A single crystal (0.15×0.16×0.13) was mounted on loop with a small amount of the paraffin oil. The X-ray data were collected at 100 K temperature on a Bruker AXS SMART APEX CCD diffractometer using Mo Kα radiation ( $\lambda = 0.71073 \text{ \AA}$ ),  $\omega$ -scans ( $2\theta = 56.73$ ), for a total of 14483 independent reflections. Space group P1,  $a = 5.1638$ ,  $b = 17.305$ ,  $c = 33.407 \text{ \AA}$ ;  $\alpha = 89.858$ ,  $\beta = 89.994$ ,  $\gamma = 89.989$ ;  $V = 2985.23 \text{ \AA}^3$ , Triclinic,  $Z = 2$  for chemical formula C<sub>33</sub> H<sub>39</sub> N<sub>3</sub> O<sub>6</sub>,  $\rho_{\text{calcd}} = 1.276 \text{ g cm}^{-3}$ ,  $\mu = 0.088 \text{ mm}^{-1}$ ,  $F(000) = 1224.0$ . The structure was obtained by direct methods using SHELXS-97.1. The final R value was 0.1052 ( $wR2 = 0.2469$ ) 14483 observed reflections ( $F0 \geq 4\sigma(|F0|)$ ) and 1513 variables,  $S = 0.946$ .

#### 5.8.5. Preparation of Large Unilamellar Vesicles (LUVs)

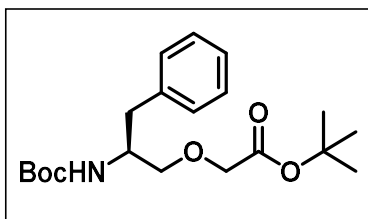
Large unilamellar vesicle was prepared by the reported protocol.<sup>32</sup> Briefly, 25 mg Egg yolk phosphatidylcholine (EYPC) was dissolved in 1 mL of CHCl<sub>3</sub>. Then the transparent thin layer of lipid was formed by purging of nitrogen and continuous rotation in a clean and dry small round bottomed flask. After that the all trace of CHCl<sub>3</sub> was removed by applying vacuum for 8 h. Then

films were hydrated with 1 mL buffer (1 mM HPTS, 10 mM HEPES, 100 mM NaCl, pH = 7.0) for 1 h with 4-5 times vortexing occasionally and it was subjected to freeze-thaw cycle ( $\geq 19$  times). Extrusions were done by a Mini-extruder with a polycarbonate membrane pore size 100 nm. Extravesicular dyes were removed by gel filtration (Sephadex G-25) with buffer (10 mM HEPES, pH = 7.0) and diluted to 6 mL to get the liposome having EYPC  $\sim 5.0$  mM EYPC, inside: 1 mM HPTS, 10 mM HEPES, 100 mM NaCl, pH = 7.0, outside: 10 mM HEPES, pH = 7.0.

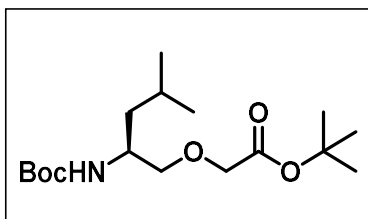
#### **5.8.6. Procedure for the Vesicle Leakage Assay**

Vesicle leakage assay was carried out by the reported protocol.<sup>32</sup> Briefly, To a clean and dry fluorescence cuvette 1975  $\mu\text{L}$  of HEPES buffer (10 mM HEPES, 100 mM NaCl, pH = 7.0) was added followed by addition of 25  $\mu\text{L}$  HPTS dye encapsulated liposome. Then the cuvette was kept in slowly stirring condition in fluorescence instrument (at  $t = 0$ ). The time course of HPTS fluorescence emission intensity,  $F_t$  was observed at  $\lambda_{\text{em}} = 510$  nm upon excitation at 450 nm ( $\lambda_{\text{ex}} = 450$  nm). 20  $\mu\text{L}$  of 0.5 M NaOH was added to the cuvette at  $t = 20$  s to make the pH gradient between the intra and extra vesicular system. Channel forming peptide were added at  $t = 100$  s and at  $t = 400$  s, of 10% Triton X-100 (25  $\mu\text{L}$ ) was added to lyse vesicles for complete destruction of pH gradient. For the data analysis Y axis (fluorescence intensity) was normalised with the blank fluorescence coming from only the solution.

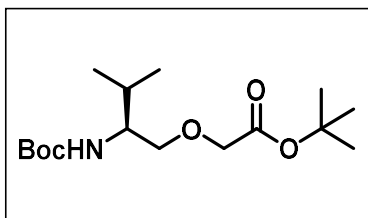
## 5.9. Characterization of Synthesized Amino Acids and Peptides CP1-CP3



**<sup>1</sup>H NMR** (400 MHz, Chloroform-*d*)  $\delta$  7.30 – 7.18 (m, 5H), 5.17 (d,  $J$  = 8 Hz, 1H), 3.96 – 3.89 (m, 3H), 3.45 – 3.44 (m, 2H), 2.95 (dd,  $J$  = 6.8 Hz, 0H), 2.86 (dd,  $J$  = 12 Hz, 4 Hz, 1H), 2.86 (dd,  $J$  = 12 Hz, 8 Hz, 1H), 1.48 (s, 9H), 1.42 (s, 9H). **<sup>13</sup>C NMR** (100 MHz, Chloroform-*d*)  $\delta$  169.73, 155.58, 138.40, 129.60, 128.49, 126.40, 81.96, 79.28, 71.70, 69.07, 51.96, 37.81, 28.51, 28.24. **HRMS**  $m/z$  calculated value for C<sub>20</sub>H<sub>31</sub>NO<sub>5</sub> is [M+Na<sup>+</sup>] 388.2100 and observed 388.2100.

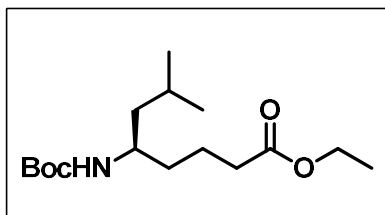


**<sup>1</sup>H NMR** (400 MHz, Chloroform-*d*)  $\delta$  4.85 (d,  $J$  = 8 Hz, 1H), 3.92 (s, 2H), 3.74 (bs, 1H), 3.52-3.43 (m, 2H), 2.01 (bs, 1H), 1.64-1.59 (m, 2H), 1.44 (s, 9H), 1.40 (s, 9H), 0.88 (m, 6H). **<sup>13</sup>C NMR** (100 MHz, Chloroform-*d*)  $\delta$  169.74, 155.69, 81.75, 79.05, 73.94, 69.14, 48.60, 41.10, 28.49, 28.19, 24.89, 23.0. **HRMS**  $m/z$  calculated value for C<sub>17</sub>H<sub>23</sub>NO<sub>5</sub> is [M+Na<sup>+</sup>] 354.2256 and observed 354.2244.

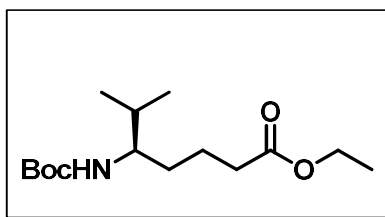


**<sup>1</sup>H NMR** (400 MHz, Chloroform-*d*)  $\delta$  4.92 (d,  $J$  = 8 Hz, 1H), 4.02 (s, 2H), 3.61-3.57 (m, 1H), 3.41 – 3.38 (m, 2H), 2.23 (bs, 1H), 1.40 (s, 9H), 1.36 (s, 9H), 0.86 (dd,  $J$ =8 Hz, 4Hz, 7H). **<sup>13</sup>C NMR**(100 MHz, Chloroform-*d*)  $\delta$  169.65, 155.97, 81.79, 78.89, 71.82, 69.00, 55.55, 29.51,

28.40, 28.09, 19.47. **HRMS**  $m/z$  calculated value for  $C_{16}H_{31}NO_5$  is  $[M+Na^+]$  340.2100 and observed 340.2085.

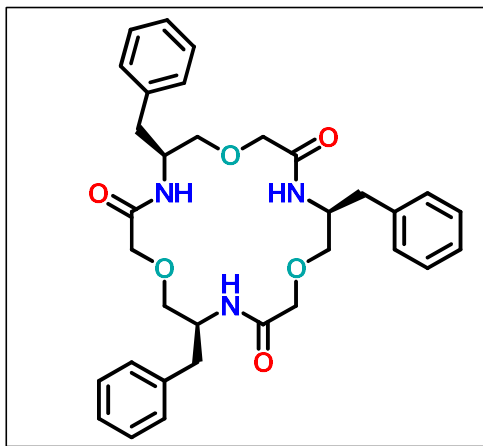


$^1H$  NMR (400 MHz, Chloroform-*d*)  $\delta$  4.55 (d,  $J = 8$ Hz, 1H), 4.12 (q,  $J = 8$ Hz, 2H), 3.69-3.58 (m, 1H), 2.38 - 2.25 (m, 3H), 1.72 - 1.59 (m, 4H), 2.14 (bs, 2H), 1.43 (s, 9H), 1.25 (t,  $J = 8$ Hz, 3H), 0.92- 0.89 (m, 6H).  $^{13}C$  NMR (100 MHz, Chloroform-*d*)  $\delta$  173.38, 155.56, 78.49, 60.00, 48.19, 44.74, 35.30, 33.90, 28.26, 24.73, 22.98, 22.09, 21.07, 14.08. **HRMS**  $m/z$  calculated value for  $C_{16}H_{31}NO_4$  is  $[M+Na^+]$  324.2151 and observed 324.2145.

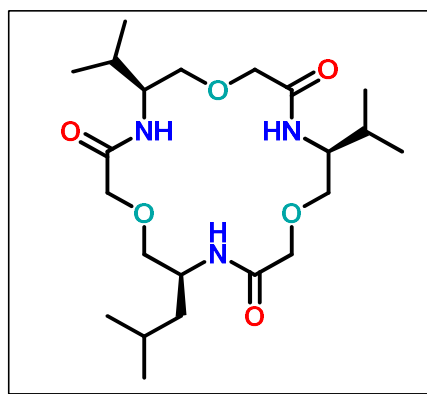


$^1H$  NMR (400 MHz, Chloroform-*d*)  $\delta$  4.56 (d,  $J = 12$  Hz, 1H), 4.12 (q,  $J = 8$ Hz, 2H), 3.47 - 3.39 (m, 1H), 2.37 - 2.25 (m, 3H), 1.76 - 1.59 (m, 4H), 1.44 (s, 9H), 1.25 (t,  $J = 8$ Hz, 3H), 0.91 - 0.86 (m, 6H).  $^{13}C$  NMR (100 MHz, Chloroform-*d*)  $\delta$  173.33, 155.92, 78.51, 59.99, 55.07, 33.85, 32.05, 31.61, 28.25, 21.55, 18.96, 17.57, 14.07. **HRMS**  $m/z$  calculated value for  $C_{15}H_{29}NO_4$  is  $[M+Na^+]$  310.1994 and observed 310.2001





**<sup>1</sup>H NMR** (400 MHz, Chloroform-*d*)  $\delta$  7.35 – 7.18 (m, 15H), 6.69 (d,  $J$  = 8 Hz, 3H), 4.48 – 4.42 (m, 3H), 3.94 (s, 2H), 3.60 (dd,  $J$  = 8 Hz, 4Hz, 3H), 3.40 (dd,  $J$  = 8, 4 Hz, 3H), 3.0 (dd,  $J$  = 8 Hz, 4Hz, 3H), 2.90 (dd,  $J$  = 8 Hz, 4Hz, 3H). **MALDI-TOF/TOF**  $m/z$  calculated value for C<sub>33</sub>H<sub>39</sub>N<sub>3</sub>O<sub>6</sub> is [M+Na<sup>+</sup>] 596.27 and observed 596.23.



**<sup>1</sup>H NMR** (400 MHz, Chloroform-*d*)  $\delta$  6.61 (d,  $J$  = 12 Hz, 1H), 6.55 (d,  $J$  = 12 Hz, 1H), 6.39 (d,  $J$  = 8 Hz, 1H), 4.29 – 4.23 (m, 1H), 3.99 – 3.92 (m, 8H), 3.70 (dd,  $J$  = 8 Hz, 4 Hz, 3H), 3.61 (dd,  $J$  = 8 Hz, 4 Hz, 2H), 3.47 (dd,  $J$  = 8 Hz, 4 Hz, 1H), 1.98 – 1.87 (m, 4H), 1.47 – 1.38 (m, 3H), 1.02 – 0.94 (m, 18H). **MALDI-TOF/TOF**  $m/z$  calculated value for C<sub>22</sub>H<sub>41</sub>N<sub>3</sub>O<sub>6</sub> is [M+Na<sup>+</sup>] 466.28 and observed 466.52.

## 5.10. References

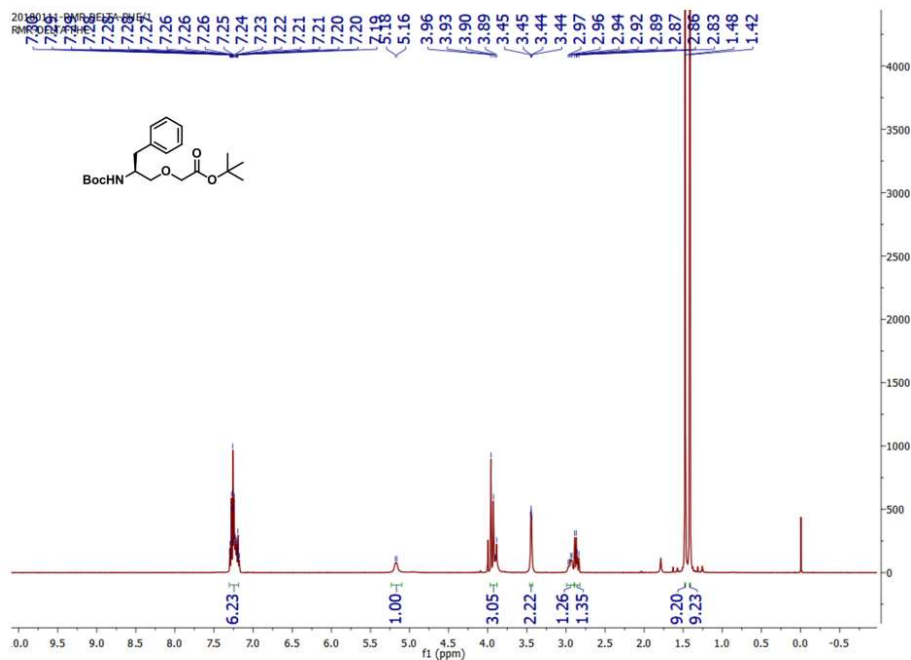
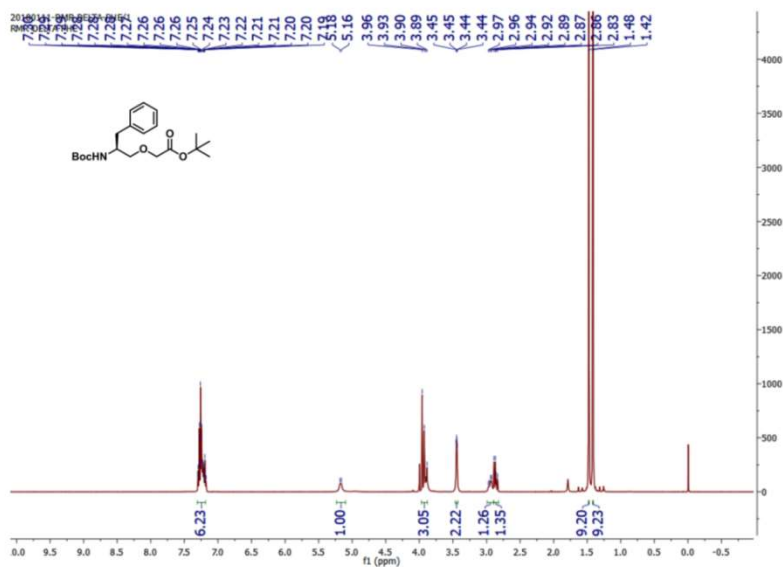
1. a) Whitesides, G. M.; Mathias, J.; Seto, C. *Science* **1991**, *254*, 1312. b) Mirkin, C. A. *Small* **2005**, *1*, 14.
2. a) Martin, C. R.; Kohli, P. *Nat. Rev. Drug Discovery*. **2003**, *2*, 29. b) Gazit, E. *Chem. Soc. Rev.* **2007**, *36*, 1263.
3. a) Casini, A.; Woods, B.; Wenzel, M. *Inorg. Chem.* **2017**, *56*, 14715. b) Bong, D. T.; Clark, T. D.; Granja, J. R.; Ghadiri, M. R. *Angew. Chem. Int. Ed.* **2001**, *40*, 988. c) Rui Qiao, R.; Ke, P. C. *J. Am. Chem. Soc.* **2006**, *128*, 13656.
4. Special issue on supramolecular chemistry and self-assembly, *Science* **2002**, *295*, 2395.
5. a) Brea, R. J.; Granja, J. R. *Dekker Encyclopedia of Nanoscience and Nanotechnology*, Marcel Dekker Inc. New York (USA), **2004**, 3439. b) Brea, R. J.; Reiriz, C.; Granja, J. R. *Chem. Soc. Rev.* **2010**, *39*, 1448.
6. De Santis, P.; Morosetti, S.; Rizzo, R. *Macromolecules*, **1974**, *7*, 52.
7. Tomasic, L.; Lorenzi, G. P. *Helv. Chim. Acta*, **1987**, *70*, 1012.
8. Ghadiri, M. R.; Granja, J. R.; Milligan, R. A.; McRee, D. E.; Khazanovich, N. *Nature*, **1993**, *366*, 324.
9. Polaskova, M. E.; Ede, N. J.; Lambert, J. N. *Aust. J. Chem.* **1998**, *51*, 535.
10. Hartgerink, J.; Granja, J. R.; Milligan, R. A.; Ghadiri, M. R. *J. Am. Chem. Soc.* **1996**, *118*, 43.
11. Rosenthal, K.; Svensson, G.; Undén, A. *J. Am. Chem. Soc.* **2004**, *126*, 3372.
12. Khazanovich, N.; Granja, J. R.; Milligan, R. A.; McRee, D. E.; Ghadiri, M. R. *J. Am. Chem. Soc.* **1994**, *116*, 6011.
13. Chapman, R.; Danial, M.; Koh, M. L.; Jolliffe, K. A.; Perrier, S. *Chem. Soc. Rev.* **2012**, *41*, 6023.
14. a) Seebach, D.; Mathews, J. L.; Meden, A.; Wessels, T.; Baerlocher, C.; McCusker, L. B. *Helv. Chim. Acta* **1997**, *80*, 173. b) Mocquet, C.; Salaün, A.; Claudon, P.; Grel, B. L.; Potel, M.; Guichard, G.; Jamart-Grégoire, B.; Grel, P. L. *J. Am. Chem. Soc.* **2009**, *131*, 14521.
15. Fujimura, F.; Horikawa, Y.; Morita, T.; Sugiyama, J.; Kimura, S. *Biomacromolecules*, **2007**, *8*, 611.
16. Clark, T. D.; Buehler, K. L.; Ghadiri, M. R. *J. Am. Chem. Soc.* **1998**, *120*, 651.

17. a) Reiriz, C.; Brea, R. J.; Arranz, R.; Carrascosa, J. L.; Garibotti, A.; Manning, B.; Valpuesta, J. M.; Eritja, R.; Castedo, L.; Granja, J. R. *J. Am. Chem. Soc.* **2009**, *131*, 11335. b) Amorín, M.; Castedo, L.; Granja, J. R. *J. Am. Chem. Soc.* **2003**, *125*, 2844. c) Amorín, M.; Castedo, L.; Granja, J. R. *Chem. Eur. J.* **2005**, *11*, 6543. d) Montenegro, J.; Vazquez-Vazquez, C.; Kalinin, A.; Geckeler, K. E.; Granja, J. R. *J. Am. Chem. Soc.* **2014**, *136*, 2484. e) Brea, R. J.; Amorín, M.; Castedo, L.; Granja, J. R. *Angew. Chem. Int. Ed.* **2005**, *44*, 5710. f) Rodríguez-Vázquez, N.; Amorín, M.; Granja, J. R. *Org. Biomol. Chem.* **2017**, *15*, 4490.
18. a) Rodríguez-Vázquez, N.; García-Fandino, R.; Amorín, M.; Granja, J. R. *Chem. Sci.* **2016**, *7*, 183. b) Rodríguez-Vázquez, N.; Amorín, M.; Alfonso, I.; Granja, J. R. *Angew. Chem. Int. Ed.* **2016**, *55*, 4504.
19. Gauthier, D.; Baillargeon, P.; Drouin, M.; Dory, Y. L. *Angew. Chem. Int. Ed.* **2001**, *40*, 4635
20. Lamas, A.; Guerra, A.; Amorín, M.; Granja, J. R. *Chem. Sci.* **2018**, *9*, 8228.
21. Horne, W. S.; Stout, C. D.; Ghadiri, M. R. *J. Am. Chem. Soc.* **2003**, *125*, 9372.
22. a) Ghadiri, M. R.; Granja, J. R.; Buehler, L. K. *Nature* **1994**, *369*, 301. b) Montenegro, J.; Ghadiri, M. R.; Granja, J. R. *Acc. Chem. Res.* **2013**, *46*, 2955.
23. a) Granja, J. R.; Ghadiri, M. R. *J. Am. Chem. Soc.* **1994**, *116*, 10785. b) Sánchez-Quesada, J.; Kim, H. S.; Ghadiri, M. R. *Angew. Chem. Int. Ed.* **2001**, *40*, 2503.
24. a) Fernández-López, S.; Kim, S. H.; Choi, E. C.; Delgado, M.; Granja, J. R.; Khasanov, A.; Kraehenbuehl, K.; Long, G.; Weinberger, D. A.; Wilcoxon, K. M.; Ghadiri, M. R. *Nature* **2001**, *412*, 452. b) Fletcher, J. T.; Finlay, J. A.; Callow, M. E.; Callow, J. A.; Ghadiri, M. R. *Chem.–Eur. J.* **2007**, *13*, 4008.
25. Brea, R. J.; Herranz, M. A.; Sánchez, L.; Castedo, L.; Seitz, W.; Guldi, D. M.; Martín, N.; Granja, J. R. *Proc. Natl. Acad. Sci. U. S. A.* **2007**, *104*, 5291.
26. Brea, R. J.; Vázquez, M. E.; Mosquera, M.; Castedo, L.; Granja, J. R. *J. Am. Chem. Soc.* **2007**, *129*, 1653.
27. Shimizu, T.; Masuda, M.; Minamikawa, H. *Chem. Rev.* **2005**, *105*, 1401.
28. Ashkenasy, N.; Horne, W. S.; Ghadiri, M. R. *Small* **2006**, *2*, 99.
29. Fujimura, F.; Kimura, S. *Org. Lett.* **2007**, *9*, 793.
30. Chakraborty, T. K.; Arora, A.; Roy, S.; Kumar, N.; Maiti, S. *J. Med. Chem.* **2007**, *50*, 5539.

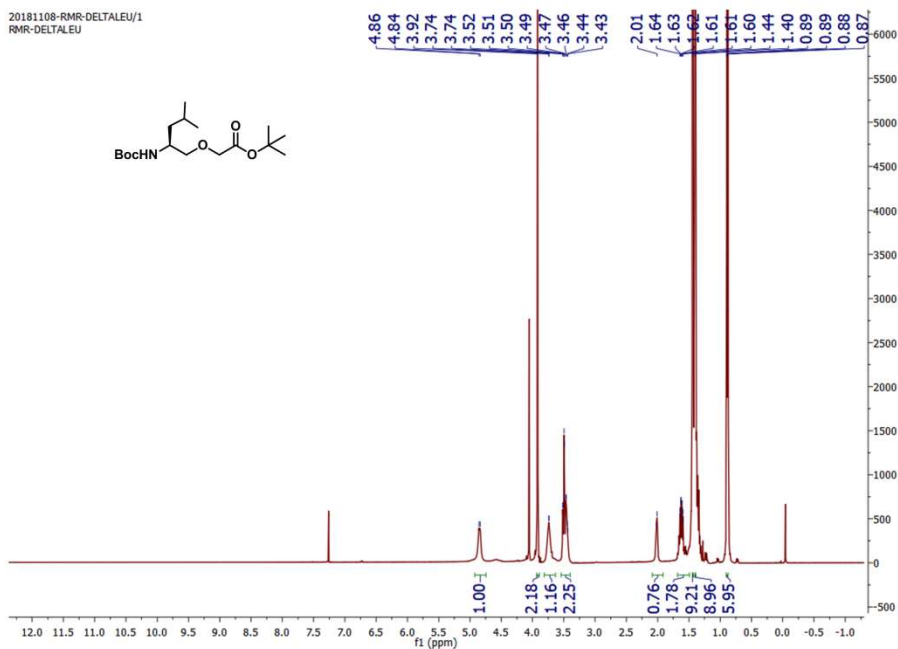
31. a) Yusof, Y.; Tan, D. T. C.; Arjomandi, O. K.; Schenk, G.; McGeary, R. P. *Bioorg. Med. Chem. Lett.* **2016**, *26*, 1589. b) Reja, R. M.; Patel, R.; Kumar, V.; Jha, A.; Gopi, H. N. *Biomacromolecules* **2019**, *20*, 1254.
32. a) Weiss, L. A.; Sakai, N.; Ghebremariam, B.; Ni, C.; Matile, S. *J. Am. Chem. Soc.* **1997**, *119*, 12142. b) Gorteau, V.; Bollot, G.; Mareda, J.; Perez-Velasco, A.; Matile, S. *J. Am. Chem. Soc.* **2006**, *128*, 14788.

## 5.11. Appendix V: Characterization Data of Synthesized Amino Acids and Peptides CP1-CP3

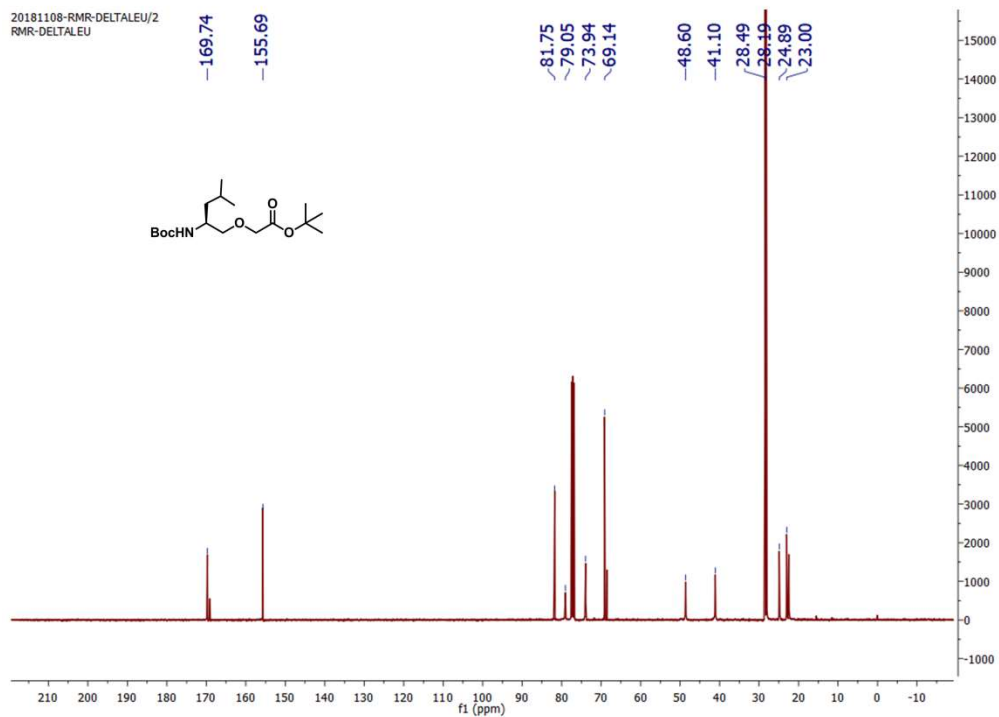
### 5.11.1. $^1\text{H}$ and $^{13}\text{C}$ NMR Spectra of Compounds



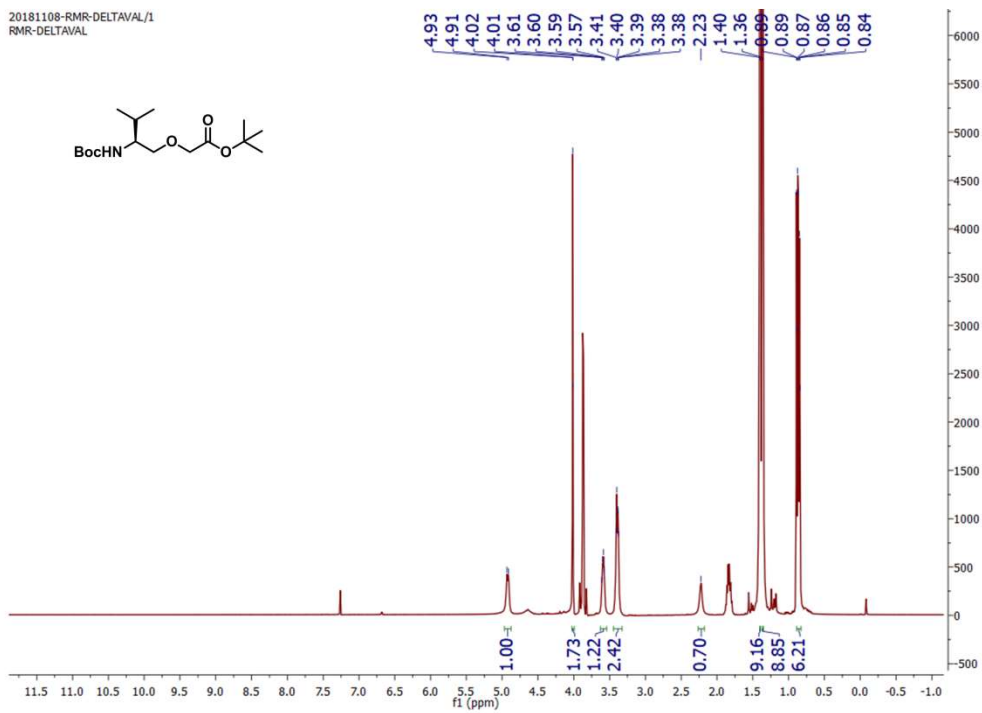
20181108-RMR-DELTALEU/1  
RMR-DELTALEU



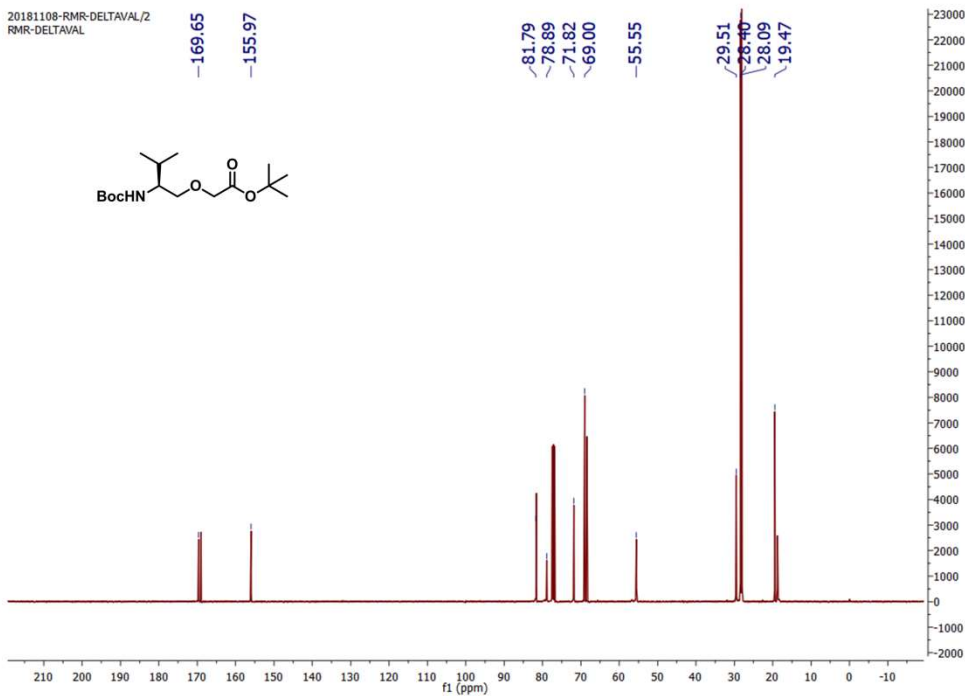
20181108-RMR-DELTALEU/2  
RMR-DELTALEU

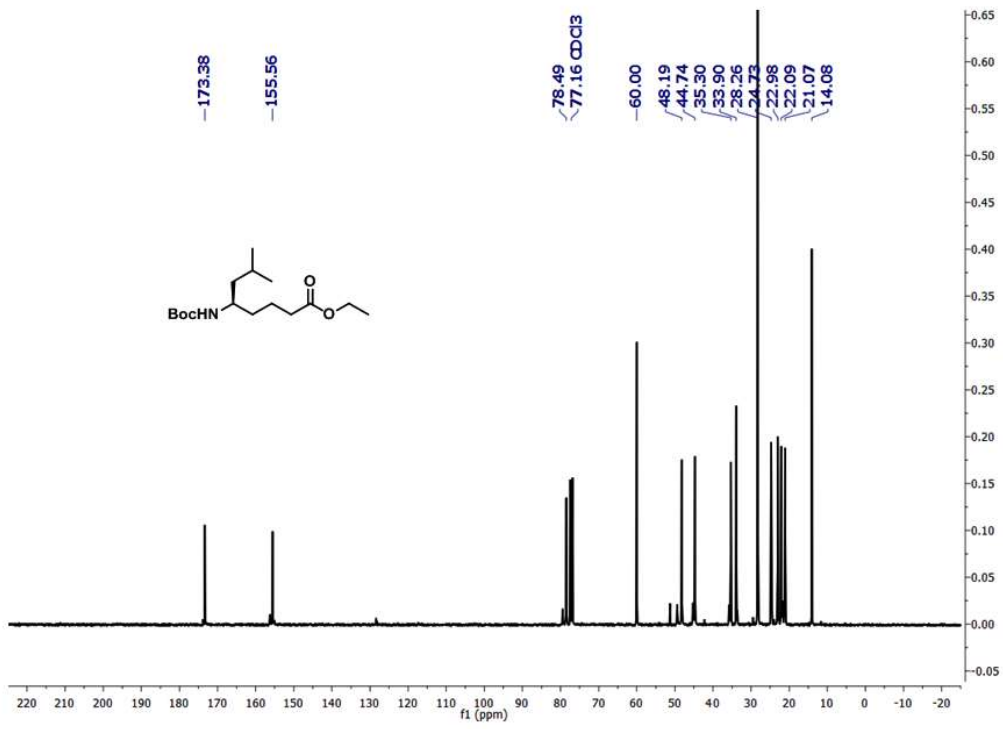
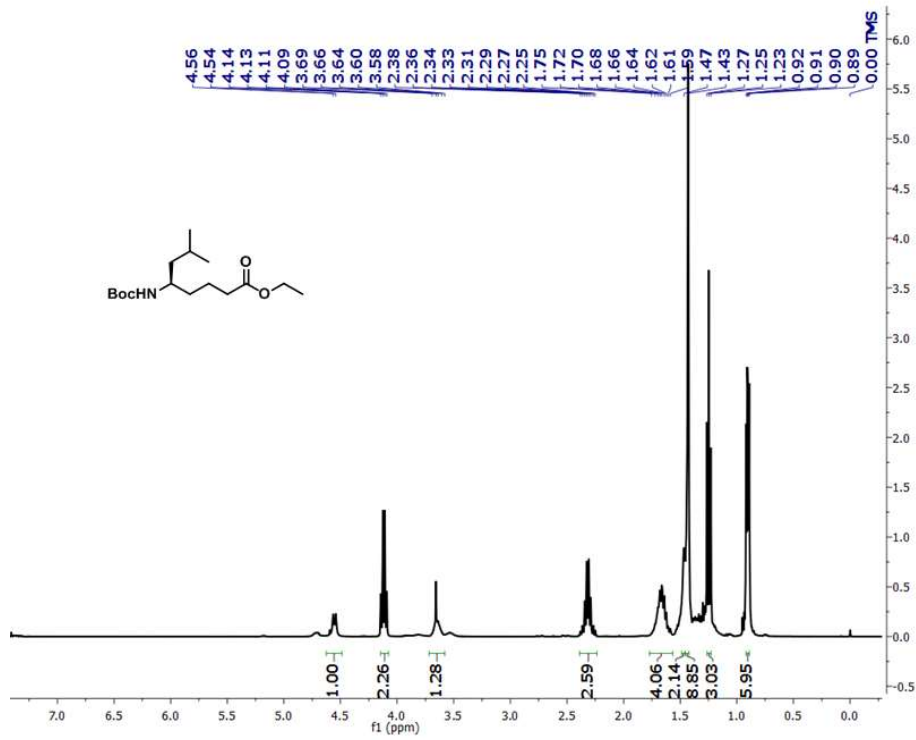


20181108-RMR-DELTAVAL/1  
RMR-DELTAVAL

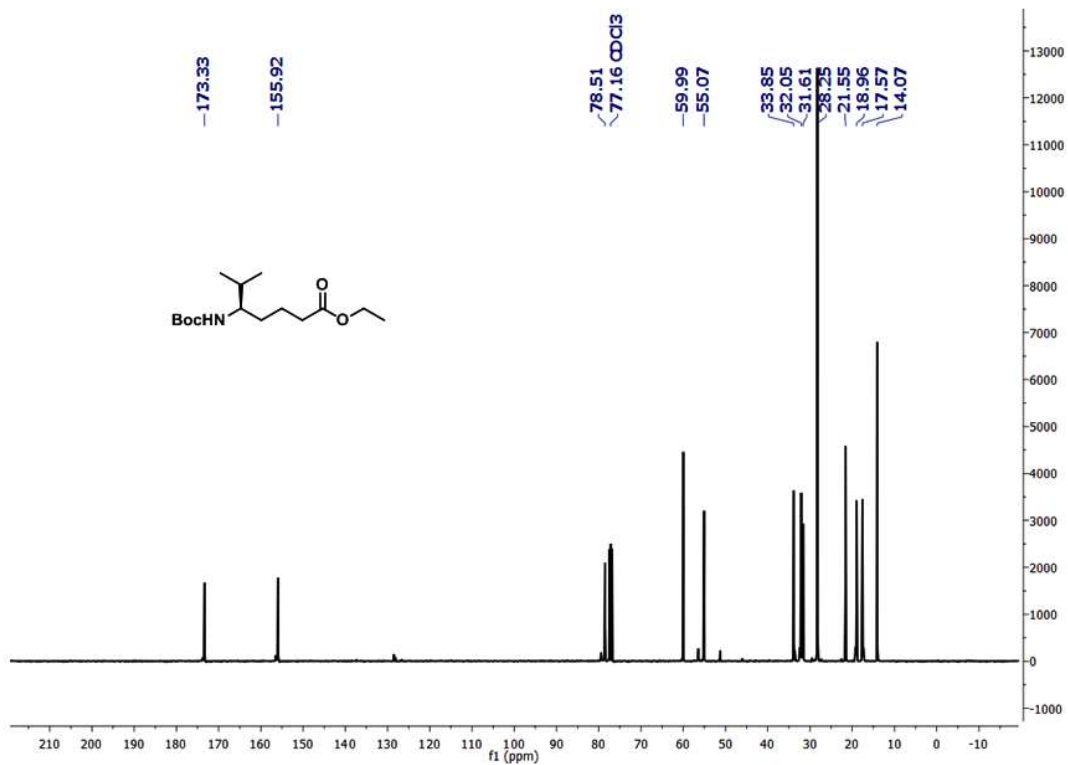
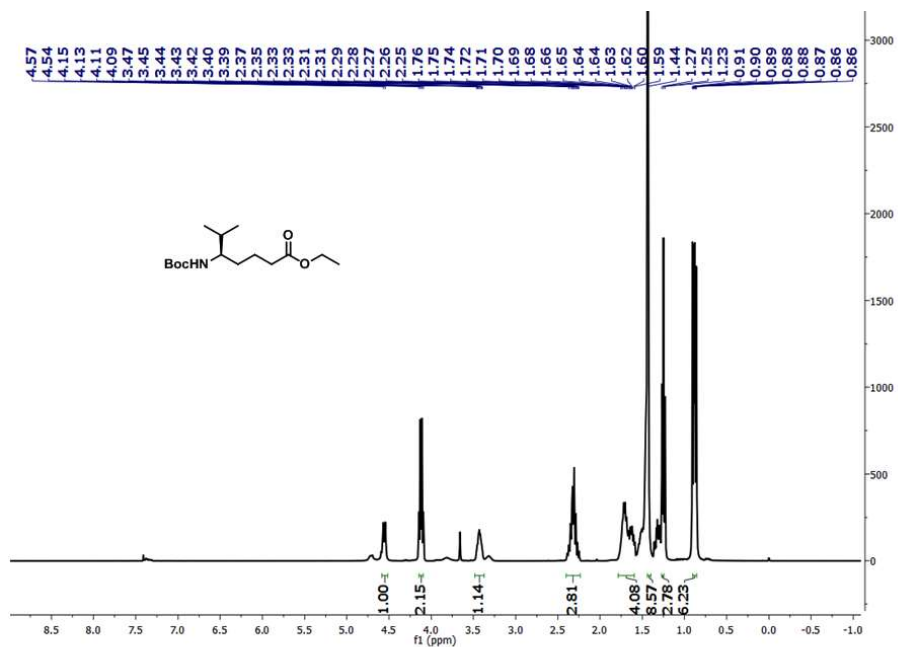


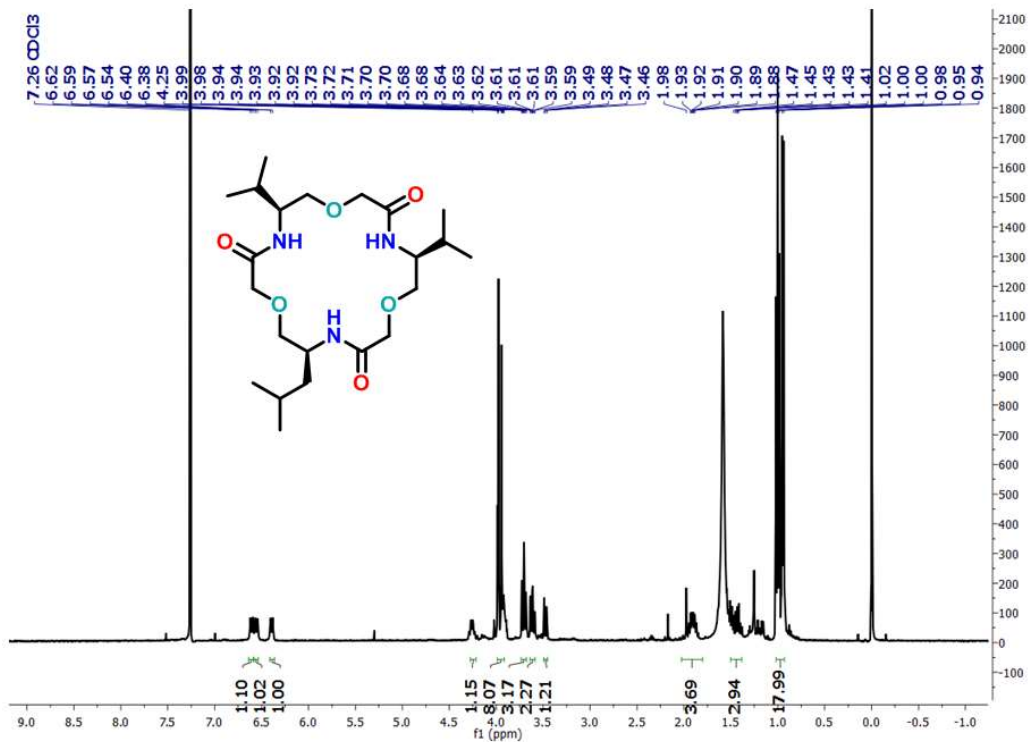
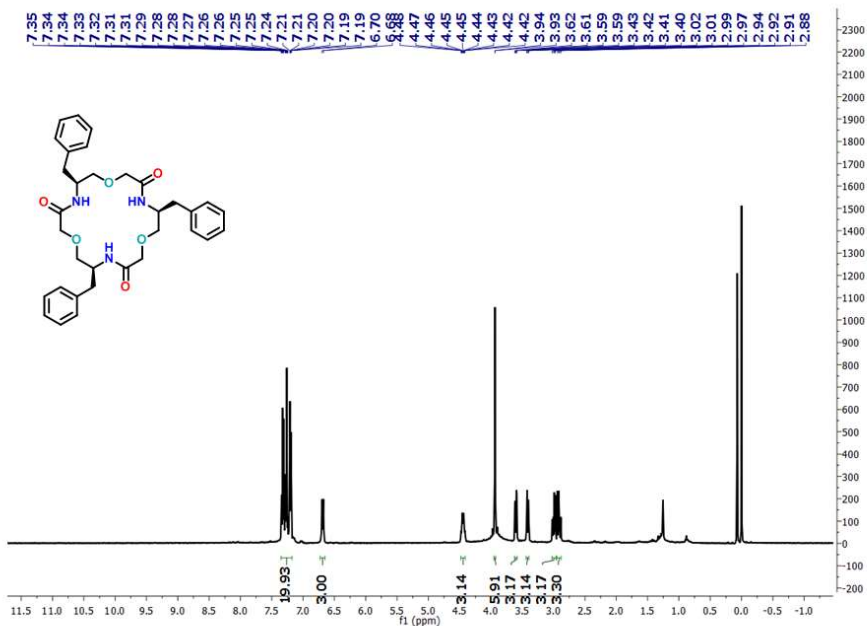
20181108-RMR-DELTAVAL/2  
RMR-DELTAVAL



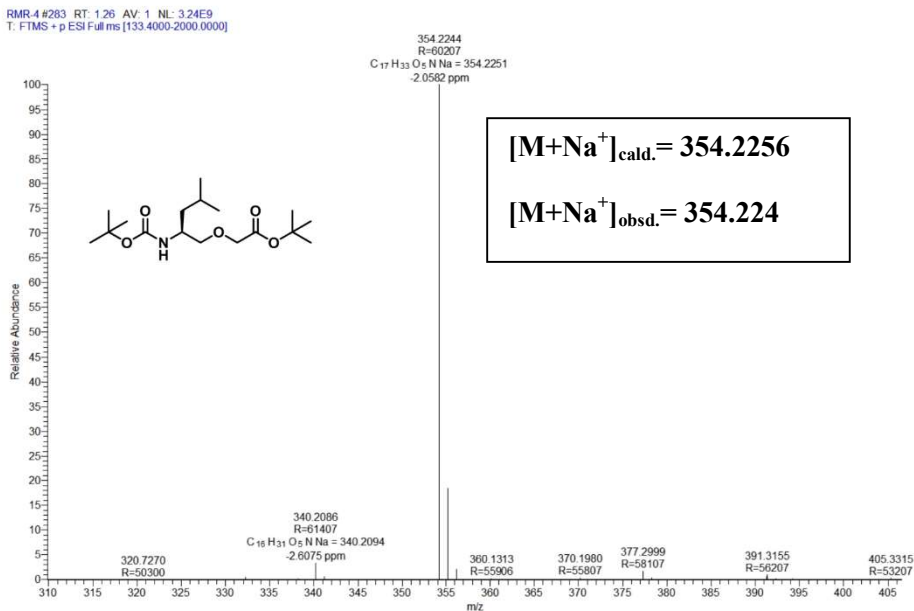
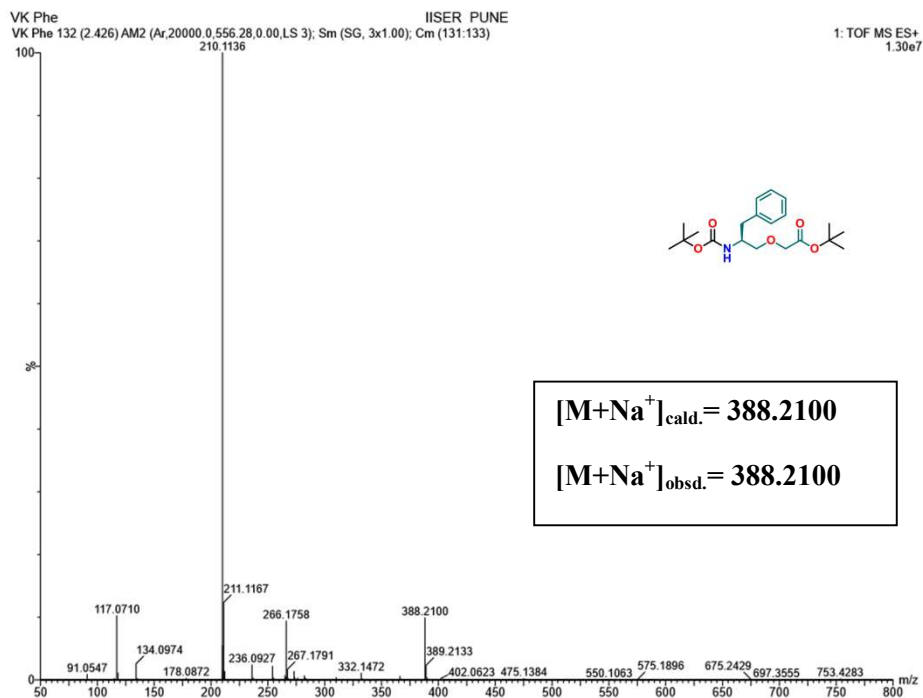




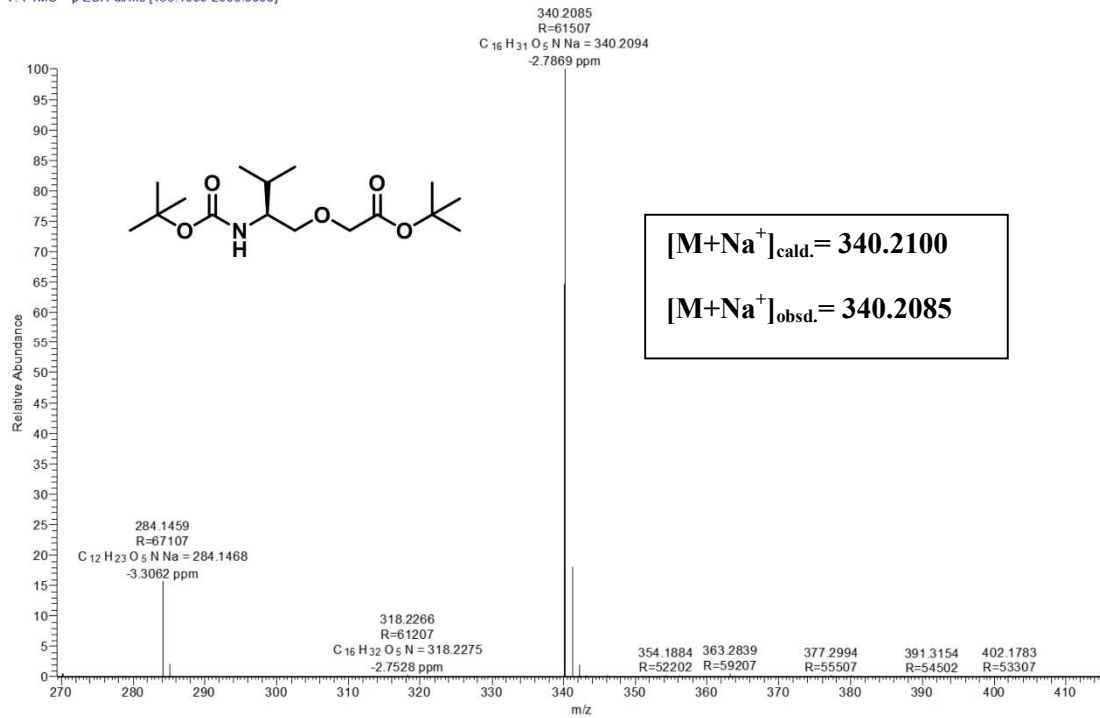




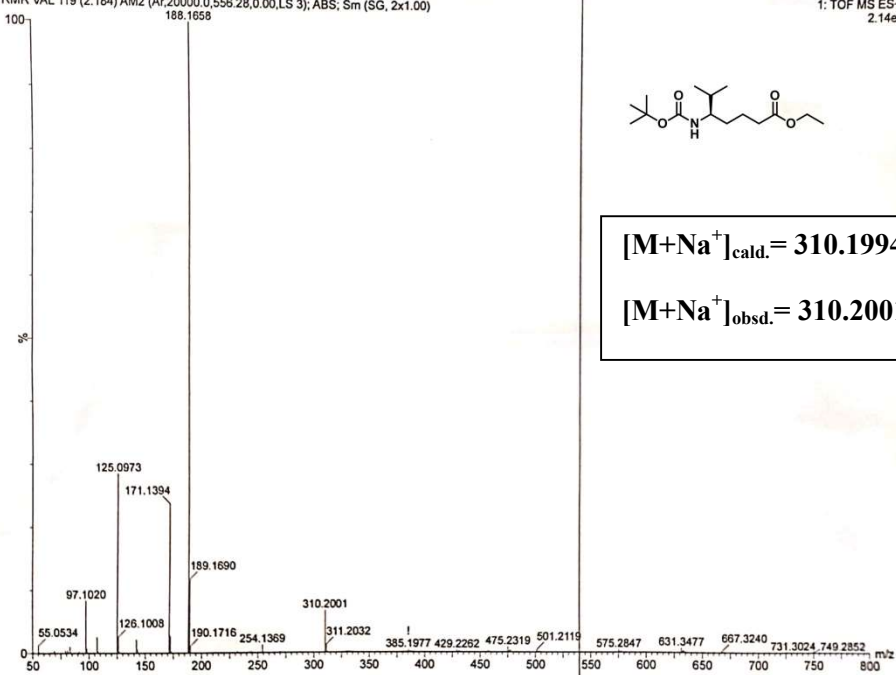
## 5.11.2. HRMS and MALDI-TOF/TOF Spectra of Amino Acids and Peptides CP1-CP3



RMR-3 #274 RT: 1.23 AV: 1 NL: 4.90E9  
T: FTMS + p ESI Full ms [133.4000-2000.0000]



HMR VAL  
RMR VAL 119 (2.184) AM2 (Ar,20000,0.556,28,0.00,LS 3); ABS; Sm (SG, 2x1.00) IISER PUNE

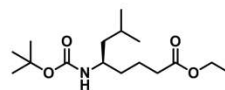
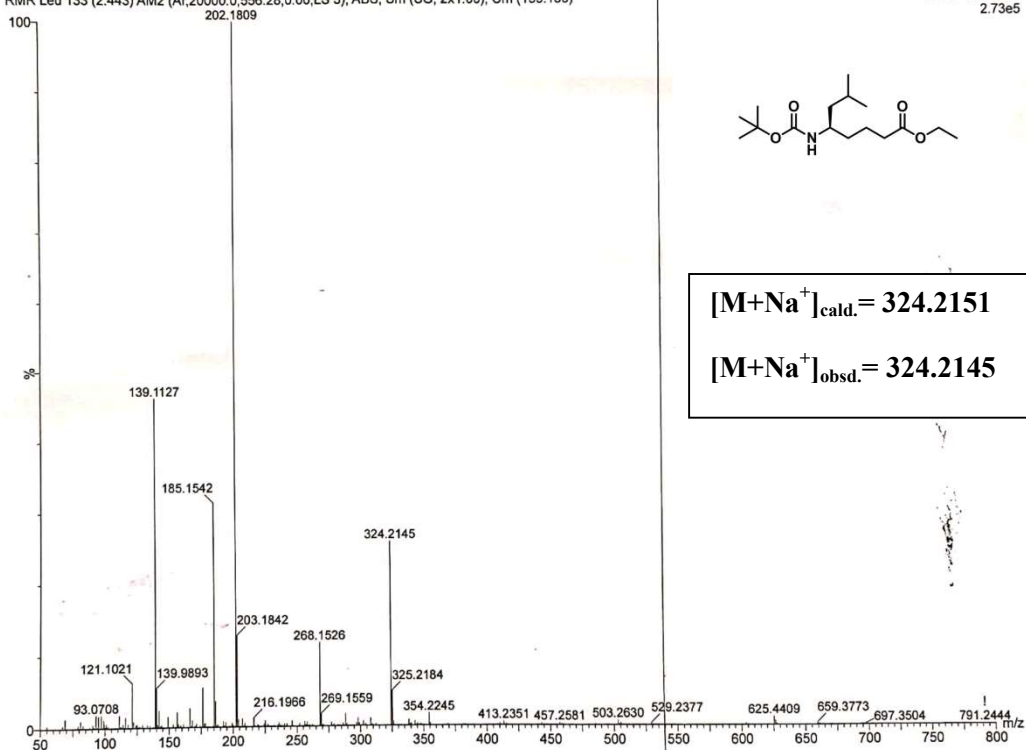


$[M+Na^+]_{\text{cald.}} = 310.1994$   
 $[M+Na^+]_{\text{obsd.}} = 310.2001$

RMR Leu  
RMR Leu 133 (2.443) AM2 (Ar,20000.0,556.28,0.00,LS 3); ABS; Sm (SG, 2x1.00); Cm (133:135)

IISER PUNE

1: TOF MS ES+  
2.73e5



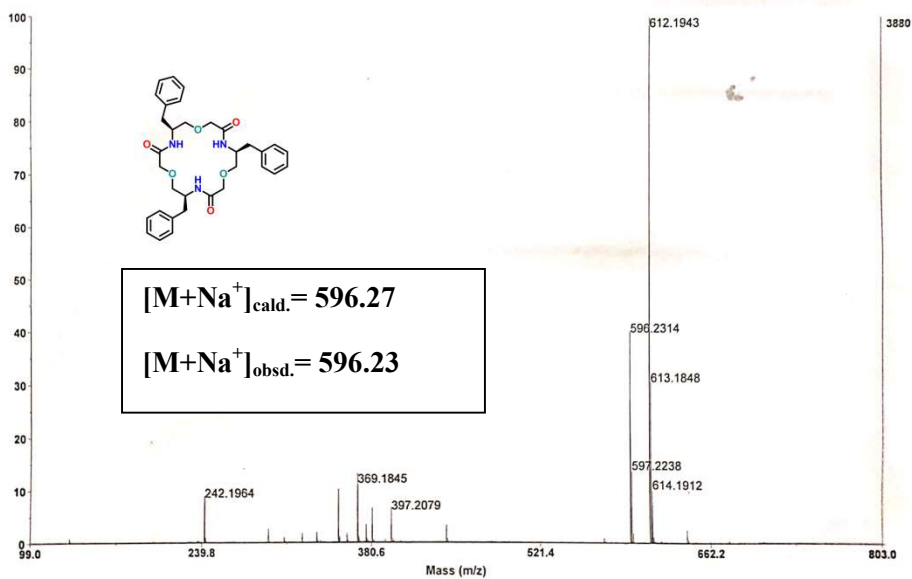
$[M+Na^+]_{\text{cald.}} = 324.2151$

$[M+Na^+]_{\text{obsd.}} = 324.2145$

Spectrum Report

*Rabi*

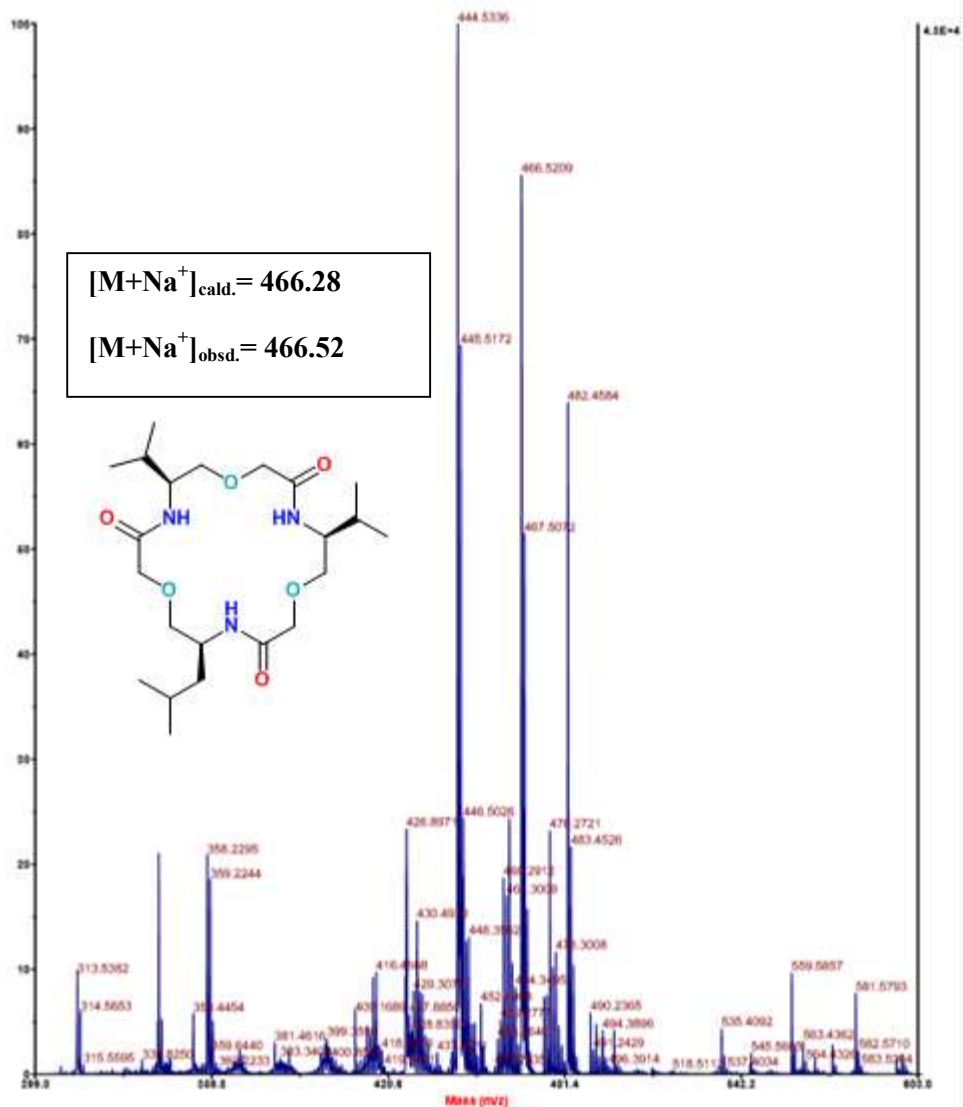
Final - Shots 500 - IISER-96-2-2018; Label A7



$[M+Na^+]_{\text{cald.}} = 596.27$

$[M+Na^+]_{\text{obsd.}} = 596.23$

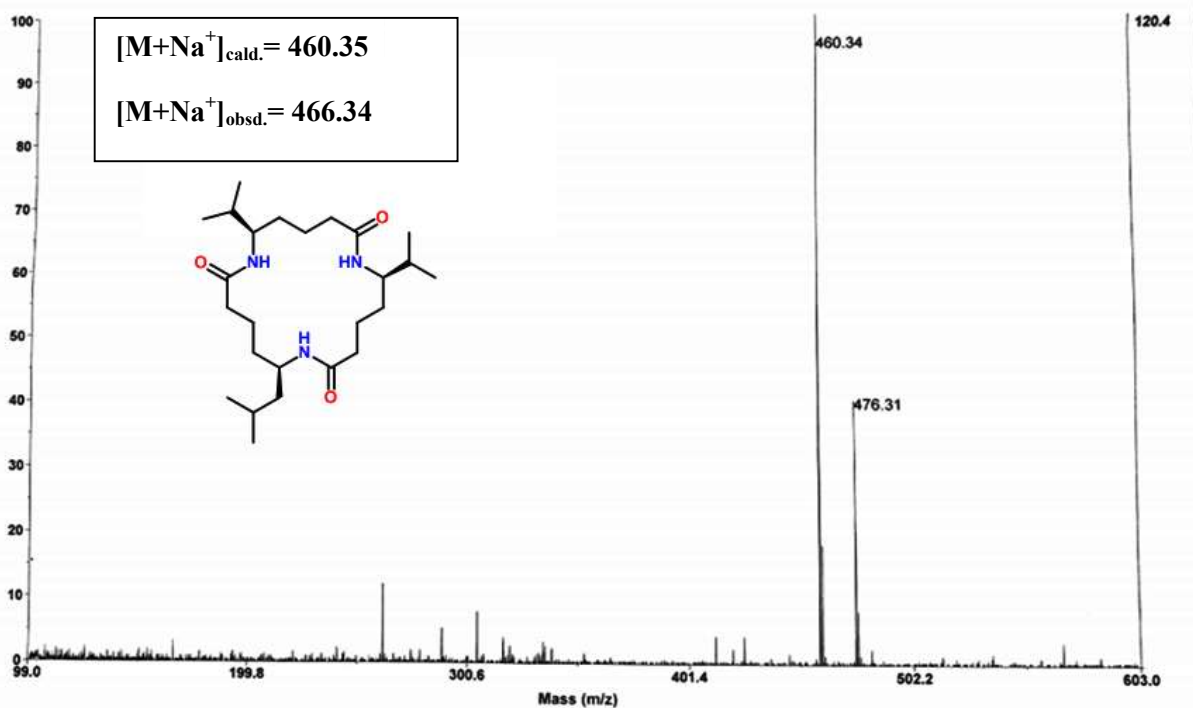
Final - Shot# 400 - 8/23/2019 Label E1



10198SER-06-2-2019 Label E1 Run # 234

Page 1

8/23/2019 4:27:47 PM





## **Permission for Reuse of Figures from Journals**



# RightsLink®

[Home](#)[Account Info](#)[Help](#)

**Title:**  $\beta$ -Hairpin Peptidomimetics: Design, Structures and Biological Activities  
**Author:** John A. Robinson  
**Publication:** Accounts of Chemical Research  
**Publisher:** American Chemical Society  
**Date:** Oct 1, 2008  
Copyright © 2008, American Chemical Society

Logged in as:  
Rahi Reja  
Account #:  
3001504219

[LOGOUT](#)

## PERMISSION/LICENSE IS GRANTED FOR YOUR ORDER AT NO CHARGE

This type of permission/license, instead of the standard Terms & Conditions, is sent to you because no fee is being charged for your order. Please note the following:

- Permission is granted for your request in both print and electronic formats, and translations.
- If figures and/or tables were requested, they may be adapted or used in part.
- Please print this page for your records and send a copy of it to your publisher/graduate school.
- Appropriate credit for the requested material should be given as follows: "Reprinted (adapted) with permission from (COMPLETE REFERENCE CITATION). Copyright (YEAR) American Chemical Society." Insert appropriate information in place of the capitalized words.
- One-time permission is granted only for the use specified in your request. No additional uses are granted (such as derivative works or other editions). For any other uses, please submit a new request.

If credit is given to another source for the material you requested, permission must be obtained from that source.

[BACK](#)[CLOSE WINDOW](#)

Copyright © 2019 [Copyright Clearance Center, Inc.](#) All Rights Reserved. [Privacy statement.](#) [Terms and Conditions.](#)  
Comments? We would like to hear from you. E-mail us at [customercare@copyright.com](mailto:customercare@copyright.com)



# RightsLink®

[Home](#)[Account Info](#)[Help](#)

**Title:**  $\delta$ -Peptides and  $\delta$ -Amino Acids as Tools for Peptide Structure DesignA Theoretical Study

Logged in as:  
Rahi Reja

[LOGOUT](#)

**Author:** Carsten Baldauf, Robert Günther, Hans-Jörg Hofmann

**Publication:** The Journal of Organic Chemistry

**Publisher:** American Chemical Society

**Date:** Sep 1, 2004

Copyright © 2004, American Chemical Society

## PERMISSION/LICENSE IS GRANTED FOR YOUR ORDER AT NO CHARGE

This type of permission/license, instead of the standard Terms & Conditions, is sent to you because no fee is being charged for your order. Please note the following:

- Permission is granted for your request in both print and electronic formats, and translations.
- If figures and/or tables were requested, they may be adapted or used in part.
- Please print this page for your records and send a copy of it to your publisher/graduate school.
- Appropriate credit for the requested material should be given as follows: "Reprinted (adapted) with permission from (COMPLETE REFERENCE CITATION). Copyright (YEAR) American Chemical Society." Insert appropriate information in place of the capitalized words.
- One-time permission is granted only for the use specified in your request. No additional uses are granted (such as derivative works or other editions). For any other uses, please submit a new request.

If credit is given to another source for the material you requested, permission must be obtained from that source.

[BACK](#)[CLOSE WINDOW](#)

Copyright © 2019 [Copyright Clearance Center, Inc.](#) All Rights Reserved. [Privacy statement.](#) [Terms and Conditions.](#) Comments? We would like to hear from you. E-mail us at [customer-care@copyright.com](mailto:customer-care@copyright.com)



# RightsLink®

[Home](#)[Account Info](#)[Help](#)

**Title:** A Peptide Hairpin Inhibitor of Amyloid  $\beta$ -Protein Oligomerization and Fibrillogenesis

Logged in as:

Rahi Reja

Account #:  
3001504219

**Author:** Ghiam Yamin, Piotr Ruchala, David B. Teplow

[LOGOUT](#)

**Publication:** Biochemistry

**Publisher:** American Chemical Society

**Date:** Dec 1, 2009

Copyright © 2009, American Chemical Society

## PERMISSION/LICENSE IS GRANTED FOR YOUR ORDER AT NO CHARGE

This type of permission/license, instead of the standard Terms & Conditions, is sent to you because no fee is being charged for your order. Please note the following:

- Permission is granted for your request in both print and electronic formats, and translations.
- If figures and/or tables were requested, they may be adapted or used in part.
- Please print this page for your records and send a copy of it to your publisher/graduate school.
- Appropriate credit for the requested material should be given as follows: "Reprinted (adapted) with permission from (COMPLETE REFERENCE CITATION). Copyright (YEAR) American Chemical Society." Insert appropriate information in place of the capitalized words.
- One-time permission is granted only for the use specified in your request. No additional uses are granted (such as derivative works or other editions). For any other uses, please submit a new request.

[BACK](#)[CLOSE WINDOW](#)

Copyright © 2019 [Copyright Clearance Center, Inc.](#) All Rights Reserved. [Privacy statement.](#) [Terms and Conditions.](#) Comments? We would like to hear from you. E-mail us at [customer@copyright.com](mailto:customer@copyright.com)



# RightsLink®

[Home](#)[Account Info](#)[Help](#)

**Title:**  $\alpha$ -Helix Mimetics as Modulators of A $\beta$  Self-Assembly

**Author:** Sunil Kumar, Andrew D. Hamilton

**Publication:** Journal of the American Chemical Society

**Publisher:** American Chemical Society

**Date:** Apr 1, 2017

Copyright © 2017, American Chemical Society

Logged in as:

Rahi Reja

Account #:  
3001504219

[LOGOUT](#)

## PERMISSION/LICENSE IS GRANTED FOR YOUR ORDER AT NO CHARGE

This type of permission/license, instead of the standard Terms & Conditions, is sent to you because no fee is being charged for your order. Please note the following:

- Permission is granted for your request in both print and electronic formats, and translations.
- If figures and/or tables were requested, they may be adapted or used in part.
- Please print this page for your records and send a copy of it to your publisher/graduate school.
- Appropriate credit for the requested material should be given as follows: "Reprinted (adapted) with permission from (COMPLETE REFERENCE CITATION). Copyright (YEAR) American Chemical Society." Insert appropriate information in place of the capitalized words.
- One-time permission is granted only for the use specified in your request. No additional uses are granted (such as derivative works or other editions). For any other uses, please submit a new request.

[BACK](#)[CLOSE WINDOW](#)

Copyright © 2019 [Copyright Clearance Center, Inc.](#) All Rights Reserved. [Privacy statement.](#) [Terms and Conditions.](#) Comments? We would like to hear from you. E-mail us at [customercare@copyright.com](mailto:customercare@copyright.com)



# RightsLink®

[Home](#)[Account Info](#)[Help](#)

**Title:** Inhibition of  $\beta$ -Amyloid Aggregation through a Designed  $\beta$ -Hairpin Peptide

**Author:** Anjali Jha, Mothukuri Ganesh Kumar, Hosahudya N. Gopi, et al

**Publication:** Langmuir

**Publisher:** American Chemical Society

**Date:** Jan 1, 2018

Copyright © 2018, American Chemical Society

Logged in as:

Rahi Reja

Account #:  
3001504219

[LOGOUT](#)

## PERMISSION/LICENSE IS GRANTED FOR YOUR ORDER AT NO CHARGE

This type of permission/license, instead of the standard Terms & Conditions, is sent to you because no fee is being charged for your order. Please note the following:

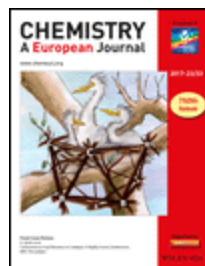
- Permission is granted for your request in both print and electronic formats, and translations.
- If figures and/or tables were requested, they may be adapted or used in part.
- Please print this page for your records and send a copy of it to your publisher/graduate school.
- Appropriate credit for the requested material should be given as follows: "Reprinted (adapted) with permission from (COMPLETE REFERENCE CITATION). Copyright (YEAR) American Chemical Society." Insert appropriate information in place of the capitalized words.
- One-time permission is granted only for the use specified in your request. No additional uses are granted (such as derivative works or other editions). For any other uses, please submit a new request.

[BACK](#)[CLOSE WINDOW](#)

Copyright © 2019 [Copyright Clearance Center, Inc.](#) All Rights Reserved. [Privacy statement.](#) [Terms and Conditions.](#) Comments? We would like to hear from you. E-mail us at [customer@copyright.com](mailto:customer@copyright.com)



# RightsLink®

[Home](#)
[Account Info](#)
[Help](#)


**Title:** Synthesis and Structure of  $\alpha/\delta$ -Hybrid Peptides—Access to Novel Helix Patterns in Foldamers

**Author:** Hans-Jörg Hofmann, Carsten Baldauf, Peter Schramm, et al

**Publication:** Chemistry - A European Journal

**Publisher:** John Wiley and Sons

**Date:** May 19, 2009

Copyright © 2009 WILEY-VCH Verlag GmbH & Co. KGaA, Weinheim

Logged in as:

Rahi Reja

[LOGOUT](#)

## Order Completed

Thank you for your order.

This Agreement between Mr. Rahi Reja ("You") and John Wiley and Sons ("John Wiley and Sons") consists of your license details and the terms and conditions provided by John Wiley and Sons and Copyright Clearance Center.

Your confirmation email will contain your order number for future reference.

### [printable details](#)

License Number	4653160034443
License date	Aug 20, 2019
Licensed Content Publisher	John Wiley and Sons
Licensed Content Publication	Chemistry - A European Journal
Licensed Content Title	Synthesis and Structure of $\alpha/\delta$ -Hybrid Peptides—Access to Novel Helix Patterns in Foldamers
Licensed Content Author	Hans-Jörg Hofmann, Carsten Baldauf, Peter Schramm, et al
Licensed Content Date	May 19, 2009
Licensed Content Volume	15
Licensed Content Issue	22
Licensed Content Pages	15
Type of use	Dissertation/Thesis
Requestor type	University/Academic
Format	Print and electronic
Portion	Abstract
Will you be translating?	Yes, including English rights
Number of languages	1
Languages	English
Title of your thesis / dissertation	Exploring Delta Amino Acids in the Design of New Peptide Foldamers and Biomaterials
Expected completion date	Aug 2020
Expected size (number of pages)	200
Requestor Location	Mr. Rahi Reja Dept. of Chemistry IISER -Pune Dr. Homi Bhabha Raod, Pashan Pune, Maharashtra 411008 India Attn: Mr. Rahi Reja
Publisher Tax ID	EU826007151
Total	0.00 USD

**Would you like to purchase the full text of this article? If so, please continue on to the content ordering system located here: [Purchase PDF](#)**

**If you click on the buttons below or close this window, you will not be able to return to the content ordering system.**

**ORDER MORE**

**CLOSE WINDOW**

Copyright © 2019 [Copyright Clearance Center, Inc.](#) All Rights Reserved. [Privacy statement.](#) [Terms and Conditions.](#)  
Comments? We would like to hear from you. E-mail us at [customercare@copyright.com](mailto:customercare@copyright.com)





rahi reja &lt;rahi.reja@students.iiserpune.ac.in&gt;

---

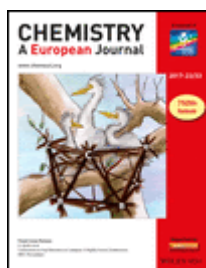
## Thank you for your order with RightsLink / John Wiley and Sons

1 message

---

no-reply@copyright.com <no-reply@copyright.com>  
To: rahi.reja@students.iiserpune.ac.in

Tue, Apr 21, 2020 at 10:32 PM



### Thank you for your order!

Dear Mr. Rahi Reja,

Thank you for placing your order through Copyright Clearance Center's RightsLink® service.

#### Order Summary

Licensee: Mr. Rahi Reja  
Order Date: Apr 21, 2020  
Order Number: 4813960823427  
Publication: Chemistry - A European Journal  
Title: Structural Investigation of Hybrid Peptide Foldamers Composed of  $\alpha$ -Dipeptide Equivalent  $\beta$ -Oxy- $\delta$ 5-amino Acids  
Type of Use: Dissertation/Thesis  
Order Total: 0.00 USD

View or print complete [details](#) of your order and the publisher's terms and conditions.

Sincerely,

Copyright Clearance Center

Tel: +1-855-239-3415 / +1-978-646-2777  
customer@copyright.com  
<https://myaccount.copyright.com>



RightsLink®

4/21/2020

IISER, Pune Mail - Thank you for your order with RightsLink / John Wiley and Sons

This message (including attachments) is confidential, unless marked otherwise. It is intended for the addressee(s) only. If you are not an intended recipient, please delete it without further distribution and reply to the sender that you have received the message in error.



# RightsLink®

[Home](#)[Account Info](#)[Help](#)

**Title:** Divergent Supramolecular Gelation of Backbone Modified Short Hybrid  $\delta$ -Peptides

**Author:** Rahi M. Reja, Rajat Patel, Vivek Kumar, et al

**Publication:** Biomacromolecules

**Publisher:** American Chemical Society

**Date:** Mar 1, 2019

Copyright © 2019, American Chemical Society

Logged in as:  
Rahi Reja

[LOGOUT](#)

## PERMISSION/LICENSE IS GRANTED FOR YOUR ORDER AT NO CHARGE

This type of permission/license, instead of the standard Terms & Conditions, is sent to you because no fee is being charged for your order. Please note the following:

- Permission is granted for your request in both print and electronic formats, and translations.
- If figures and/or tables were requested, they may be adapted or used in part.
- Please print this page for your records and send a copy of it to your publisher/graduate school.
- Appropriate credit for the requested material should be given as follows: "Reprinted (adapted) with permission from (COMPLETE REFERENCE CITATION). Copyright (YEAR) American Chemical Society." Insert appropriate information in place of the capitalized words.
- One-time permission is granted only for the use specified in your request. No additional uses are granted (such as derivative works or other editions). For any other uses, please submit a new request.

[BACK](#)[CLOSE WINDOW](#)

Copyright © 2019 [Copyright Clearance Center, Inc.](#) All Rights Reserved. [Privacy statement.](#) [Terms and Conditions.](#) Comments? We would like to hear from you. E-mail us at [customercare@copyright.com](mailto:customercare@copyright.com)